

Department of Chemical Engineering

**Ryan-Holmes and Modified Ryan-Holmes
Processes for LNG Production**

Fonny Lastari

**This thesis is presented for the Degree of
Doctor of Philosophy
of
Curtin University of Technology**

December 2009

DECLARATION

To the best of my knowledge and belief this thesis contains no material previously published by any other person except where due acknowledgement has been made.

This thesis contains no material which has been accepted for the award of any other degree or diploma in any university.

Signature:

Date:

SUMMARY

The objective of this research was to evaluate various process alternatives for the production LNG (Liquefied Natural Gas) from natural gas feeds with significant CO₂ levels, typical of some of the Australian gas reserves. It is believed that the conventional amine process which is commonly utilized for treating sour natural gas may be energy-intensive, particularly if CO₂ produced must be sequestered. Consequently, two different alternatives to the amine process were investigated, which were based on the Ryan-Holmes (RH) process with one of them also using membrane in addition to distillation columns.

The key point of the RH process is the extractive distillation used to both avoid CO₂ freeze up and split the CO₂/C₂ azeotrope. The RH process operates at low temperatures, which simultaneously produces methane which is subsequently condensed to LNG, CO₂ for geological sequestration, and NGL (Natural Gas Liquids). In the past, the RH process has been used for processing high CO₂ natural gases from Enhanced Oil Recovery (EOR) fields.

Two different natural gas feed compositions were examined in this research. The first feed was a representative of Australia's largest natural gas reserve, the Gorgon field. A richer natural gas feed with relatively lower acid gas composition was the second feed, which was investigated to explore the hydrocarbon recovery potential and associated economics. The objective was to assess the optimum alternative for both feeds. A global optimization on the design variables in terms of the overall energy consumption and capital cost was performed to analyse the economic feasibility using a discounted cash flow (DCF) concept.

An overall economic evaluation of the process alternatives for treating the two feed gas conditions indicated that the amine process was the most optimum option for treating the lean Gorgon gas feed; however, the RH process was superior for treating the richer natural gas feed (i.e. the feed having more ethane, propane etc.). It was

observed that the capital cost for the amine process was lower for treating the high CO₂ Gorgon gas although the heating duty for amine regeneration was considerable. In contrast, the RH process proved to be a better option for the rich natural gas feed not only because of simultaneous removal of acid gas and LPG but also because of its inherent synergies with the liquefaction process. It was also observed that the HRH process was the most fuel efficient alternative; however, the additional capital cost due to the membrane system prevailed over this advantage.

The optimization of design variables and minimum approach temperature had a significant effect on the overall energy consumption and capital cost of the process. The design variables that significantly affected the overall energy demand and capital cost (e.g., DEC1 and azeo column pressures) also had stronger effect on the DCF. One of the key design parameters for optimizing the extractive distillation process was the solvent amount, which was a function of the feed composition, solvent composition, and feed and solvent inlet stages.

In summary, this thesis has for the first time provided an original analysis of the RH and HRH processes as alternatives to the conventional amine process for LNG production for reducing the CO₂ emissions from a high CO₂ natural gas feed. The strengths and weaknesses of each alternative were assessed by conducting a thorough sensitivity analysis on various process variables. This study is likely to have even bigger impact in future after the proposed emissions trading scheme (ETS) is implemented.

BRIEF BIOGRAPHY OF THE AUTHOR

Fonny Lastari graduated in Chemical Engineering from Parahyangan Catholic University, Indonesia in 2001. She worked three years in a professional capacity as a planning and analysis staff at PT. Astra Daihatsu Motor, Jakarta, Indonesia. She commenced her PhD work in March 2006 and had a Western Australia, Energy Research Alliance (WA:ERA) Scholarship for her studies. She was also a teaching assistant in Process Simulation and Process Synthesis and Design units during the period of 2006-2009.

Publications written in support of this thesis

Lastari, F., Pareek, V., Trebble, M., Tade, M.O., Chinn, D., Tsai, N.C., and Chan, K.I., “*Simulation and Optimization of Extractive Distillation for CO₂-Ethane Separation*”, in the 8th World Congress of Chemical Engineering, Montreal, Canada, 23-27 August 2009.

Lastari, F., Pareek, V., Trebble, M., Tade, M.O., Chinn, D., Tsai, N.C., and Chan, K.I., “Extractive Distillation for CO₂-Ethane Separation”, manuscript submitted to the Chemical Engineering and Processing, 2010.

ACKNOWLEDGEMENT

This thesis has been accomplished with the advice, support, and help from many people whom I would like to express my sincere appreciation. First of all, I would like to thank my supervisor Associate Professor Vishnu Pareek and co-supervisors Professor Mark Trebble and Professor Moses O. Tade for their invaluable guidance and continuous advice and support which made this study possible. I would also like to thank Chevron's representatives Dr. Daniel Chinn, Ms. Nancy Tsai, and Ms. Kaman Ida Chan, for their constant support and advice throughout this study. The financial support from the Chevron Energy Technology Company through the Western Australia Energy Research Alliance (WA:ERA) Gas Research Program was greatly acknowledged.

I would also like to extend my sincere thanks to the former Chevron Relationship Manager at Curtin University of Technology, Professor Robert Johnson as well as to the former professional members of the Chevron Energy Technology Company Dr. Paul Bryan and Dr. Tony Eaton. My thanks also go to the current staff of Chevron Energy Technology Company, Ms. Malika Nayar.

Thanks are also due to my officemates: Monica Gumulya, Yuli Setiyorini, Yenny Rojaz, Nina Darmawan, Deepak Jaganattha, and Chao Li with whom I have shared treasured moments. I greatly appreciate the assistance from Jann Bolton, Naomi Tokisue and all the staff and ex-staff of the Department of Chemical Engineering.

Finally, I would also like to thank my family and my extended family for their continuous support and love during my study. Last but not the least, thanks to my husband, Dr. Johan Utomo, for his constant love, advice, and understanding. This thesis is also dedicated to our first son, Jonas.

TABLE OF CONTENTS

DECLARATION	i
SUMMARY	ii
BRIEF BIOGRAPHY OF THE AUTHOR	iv
ACKNOWLEDGEMENT	v
TABLE OF CONTENTS.....	vi
LIST OF FIGURES	viii
LIST OF TABLES.....	xi
1. INTRODUCTION AND RESEARCH OVERVIEW	1
1.1 Background.....	1
1.2 Ryan-Holmes (RH) Process.....	2
1.3 Hybrid Membrane Ryan-Holmes Process	3
1.4 Research Methodology	5
1.5 Significance of Research.....	6
1.6 Research Objectives and Contributions	6
1.7 Thesis Overview	7
2. REVIEW OF PROCESS ALTERNATIVES.....	10
2.1. Amine Process	12
2.2. Ryan-Holmes (RH) Process.....	18
2.3. Hybrid Membrane Ryan-Holmes (HRH) Process	23
2.4. Utilities and Heat Integration System.....	30
2.4.1. Air Cooling	30
2.4.2. Refrigeration System	30
2.4.3. Hot Oil	31
2.4.4. Heat Integration System.....	31
3. SIMULATION AND OPTIMIZATION OF PROCESS ALTERNATIVES.....	33
3.1. Simulation Setup and Constraints.....	33
3.1.1. Capital Cost Estimation	35
3.1.2. Operational Cost Estimation.....	36
3.2. Optimization Objective.....	38
3.3. Sensitivity Analysis of Process Variables.....	41
3.3.1. Optimization and Sensitivity Analysis of the Amine Process	43

3.3.2. Optimization and Sensitivity Analysis of the RH Process.....	46
3.3.3. Optimization and Sensitivity Analysis of the HRH Process.....	53
3.3.4. Column Pressure and Solvent Properties.....	57
3.4. Effect of Minimum Approach Temperature	66
3.5. Heuristics for Optimization.....	74
3.6. Conclusions.....	78
5. EXTRACTIVE DISTILLATION and SOLVENT COMPOSITION.....	80
4.1. Extractive Distillation	80
4.2. Solvent Composition.....	88
4.3. Conclusions.....	93
5. ANALYSIS of BASE CASE SCENARIOS.....	95
5.1. Energy Comparison and Economic Evaluation.....	96
5.2. Comparison between process alternatives	104
5.3. Analysis of Process Alternatives with Various CO ₂ Range.....	105
5.4. Conclusions.....	110
6. CONCLUSIONS AND RECOMMENDATIONS	113
6.1. Guidelines for securing the Ryan-Holmes process and the hybrid membrane Ryan-Holmes process	113
6.2. Conclusions.....	114
6.3. Recommendations for future work	116
Appendix A. Dehydration System Calculation.....	123
Appendix B-1. Amine1 process.....	128
Appendix B-2. Amine2 process	128
Appendix C-1. RH1 process	128
Appendix C-2. RH2 process	128
Appendix D-1. HRH1 process	128
Appendix D-2. HRH2 process	128
Appendix E. Calculation of Equivalent Fuel	160
Appendix F. List of Equipment	163
Appendix G. DCF Calculation (RH1 Process).....	166
Appendix H. H ₂ S Removal Facility Calculation	167

LIST OF FIGURES

Figure 1-1. Thesis structure.	9
Figure 2-1. Molecular-sieve dehydrator twin tower system (GPSA 2004).	11
Figure 2-2. Typical gas sweetening with amine process (GPSA 2004).	13
Figure 2-3. Solubility data of CO ₂ in 50%-w MDEA (Jou, Mather, and Otto 1982)..	14
Figure 2-4. Simplified flowsheet of the amine1 process	17
Figure 2-5. Simplified flowsheet of the amine2 process	17
Figure 2-6. A 3-column Ryan-Holmes process.	19
Figure 2-7. Ryan-Holmes process flowsheet for Feed2 gas.	19
Figure 2-8. Pressure-temperature diagram for CO ₂ -methane system (Katz et al. 1959).	20
Figure 2-9. Hybrid Membrane Ryan-Holmes Feed1 process.	24
Figure 2-10. Hybrid Membrane Ryan-Holmes Feed2 process.	24
Figure 2-11. Two-stage membrane system in the HRH process.	28
Figure 3-1. Expander outlet pressure effect on IRR for amine2 process.	45
Figure 3-2. Stripper column setup for Feed2 gas.	49
Figure 3-3. Optimization of the stripper inlet temperature.	49
Figure 3-4. Optimization of the stripper column pressure.	50
Figure 3-5. Optimization of the number of ideal stages in the stripper.	50
Figure 3-6. Optimization of C2 specification at the azeo column overhead of RH1...52	52
Figure 3-7. Sensitivity of C3 spec in azeo overhead on IRR for HRH1 process.....55	55
Figure 3-8. Effect of DEC1 column pressure on reflux ratio and solvent demand58	58
Figure 3-9. Effect of DEC1 column pressure on reflux ratio and solvent demand (ΔT Freeze \pm 5.5°C) – HRH2 Process.....59	59
Figure 3-10. Optimization of azeo column pressure - HRH2 process.....60	60
Figure 3-11. Effect of solvent inlet stage for RH2 process.....62	62
Figure 3-12. Effect of solvent inlet stage on IRR for RH2 process.....62	62
Figure 3-13. Effect of DEC1 solvent temperature on IRR and DEC1 reflux ratio - HRH1.....63	63
Figure 3-14. Effect of azeo solvent temperature on IRR and azeo reflux ratio - RH2 process.....64	64

Figure 3-15. Effect of solvent flow on reflux ratio and CO ₂ purity in the overhead of the azeo column.	65
Figure 3-16. Interaction between solvent temperature and solvent amount in the azeo column improved IRR.....	66
Figure 3-17. Schematic diagram of the cascade refrigeration system.	67
Figure 3-18. Schematic diagram of the propane refrigeration cycle – RH1 process...	70
Figure 3-19. Cost estimation of the BEM type heat exchanger.....	71
Figure 3-20. Cost estimation of the NKN type heat exchanger.....	71
Figure 3-21. Optimization of refrigeration temperature level and minimum temperature approach of the 1st stage of propane refrigerant.....	72
Figure 3-22. Minimum approach temperature effect on IRR in the azeo and SR condensers.....	73
Figure 3-23. Minimum approach temperature effect on IRR –	73
Figure 3-24. Sensitivity of DEC1 solvent temperature on IRR – RH1 process.	76
Figure 3-25. Sensitivity of DEC1 column pressure on IRR – RH1 process.....	77
Figure 3-26. Sensitivity of DEC1 column pressure on IRR - HRH1 process.....	77
Figure 3-27. Sensitivity of C4 fraction in the overhead of SR column on IRR.....	78
Figure 5-1. Effect of an excessive reflux ratio in an extractive distillation process....	82
Figure 5-2. Schematic diagram of an extractive distillation column and a solvent recovery column.....	82
Figure 5-3. Minimum solvent amount and reflux ratio effects on CO ₂ purity in the overhead.....	83
Figure 5-4. Optimum azeo solvent amount in terms of energy demand.....	84
Figure 5-5. Optimum azeo solvent amount in terms of total capital and energy costs – RH1 process.....	85
Figure 5-6. Reflux ratio and minimum solvent amount as a function of feed inlet stage.	85
Figure 5-7. Effect of solvent inlet stage.....	86
Figure 5-8. Composition profiles as a function of solvent amount (=liquid profile; = vapor profile with minimum solvent 10,636 kgmole/h; =liquid profile; =vapor profile with solvent 12,475 kgmole/h; =liquid profile;.....	87
Figure 5-9. Effect of C3 fraction in solvent on azeo reflux ratio.....	88
Figure 5-10. Effect of C3 fraction in solvent on CO ₂ purity in the overhead.....	88

Figure 5-11. Effect of solvent composition on minimum ΔT to CO ₂ freezing point in DEC1.....	89
Figure 5-12. Phase equilibrium of CO ₂ -ethane mixture as a function of nC5 additive.	90
Figure 5-13. Mole fraction of the solvent required to break CO ₂ -ethane azeotrope....	90
Figure 5-14. Minimum solvent amount required for different solvent compositions..	91
Figure 5-15. Effect of the solvent composition on the reflux ratio.....	92
Figure 5-16. Total energy requirement as a function the solvent composition.	92
Figure 5-1. Comparison of installed equipment costs.	98
Figure 5-2. Cooling duties distribution in each process alternatives.	99
Figure 5-3. Feed flow rate reduction with membrane utilization in HRH process....	103
Figure 5-4. Solvent demand in DEC1 as a function of CO ₂ variation in the feed.	106
Figure 5-5. Reflux ratio and minimum solvent amount with variation of CO ₂ content in the feed.....	107
Figure 5-6. Lever-arm rule for calculating solvent demand in a residue curve.	107
Figure 5-7. Minimum solvent amount in DEC1 as a function of CO ₂ fraction in the feed.....	108
Figure 5-8. Solvent amount in azeo column as a function of CO ₂ fraction in the feed.	109
Figure 5-9. %DCF as a function of CO ₂ fraction in the feed.....	109
Figure 5-10. Solvent flow as a function of CO ₂ variations in Feed1.....	110
Figure 5-11. Solvent flow as a function of CO ₂ variations in Feed2.....	110

LIST OF TABLES

Table 1-1. Feed gas conditions.	2
Table 2-1. Summary of dehydration process in RH/HRH and amine processes.	12
Table 2-2. Amine simulation result.	15
Table 2-3. Component permeability constants and membrane properties.....	26
Table 2-4. Separation performance with one single stage membrane – HRH1.....	27
Table 2-5. Two-stage membrane-RH simulation result.....	29
Table 2-6. Estimation of number of membrane modules for HRH Feed1 process.....	29
Table 3-1. Product Specification Requirement.....	34
Table 3-2. Detailed economic presentation of the project.	39
Table 3-3. Optimization of number of ideal stages (N) and feed inlet location (Nf) in the azeo column – RH1 process.....	41
Table 3-4. Effect of the number of ideal stage in the scrub column on IRR.	44
Table 3-5. Summary of column specifications (%-mole) for amine process.	45
Table 3-6. Effect of number of ideal stage and feed inlet location on IRR - amine2 process.....	46
Table 3-7. Optimization of C1 specification for DEC1 bottom product – RH1.....	48
Table 3-8. Effect of C3 and C4 specs in SR column on IRR – RH1 process.....	53
Table 3-9. Summary of column specifications (%-mole) for RH process.....	53
Table 3-10. Effect of C3 fraction in the azeo overhead on solvent composition and C3 Loss – HRH1 Process.	54
Table 3-11. Optimization of C3 fraction in the overhead of azeo column –	55
Table 3-12. Summary of column specifications (%-mole) for HRH process.....	57
Table 3-13. Summary of column pressure.....	60
Table 3-14. Number of ideal stages and feed inlet location.	61
Table 3-15. Cooling temperature range in the cascade refrigeration cycle.	66
Table 3-16. Example of the minimum approach temperature optimization for the propane refrigerant stage1 – RH1 process.....	67
Table 3-17. Refrigeration utilization in process flowsheet.....	69
Table 3-18. Refrigerant temperature level and minimum approach optimization result.	74

Table 5-1. Ratio of optimum solvent to the minimum solvent for single component solvents.	91
Table 5-2. CO ₂ recovery column overhead product	93
Table 5-1. Product generation from optimized simulation.	95
Table 5-2. Comparison of the energy consumption and economic evaluation.....	97
Table 5-3. The majority of the refrigeration distribution.....	101
Table 5-4. Comparison of PV values.....	104
Table 5-5. Summary of comparative benefits and drawbacks of process alternatives.	111

1. INTRODUCTION AND RESEARCH OVERVIEW

1.1 Background

This research examined three different alternatives to process natural gas feeds with significant CO₂ levels. The objective was to produce LNG (Liquefied Natural Gas) as well as to sequester the CO₂ impurity in order to lower the CO₂ emissions. The conventional amine process generally becomes more energy intensive with higher CO₂ levels. Therefore, various alternatives to generate a low cost LNG process were investigated.

Two natural gas feeds were examined. The first feed was a representative of Australia's largest natural gas reserve, the Gorgon field. It contains approximately 12-15%-vol CO₂ which will require considerable processing costs to produce a typical natural gas specification (Stacey 2005). A richer natural gas with relatively lower acid gas composition was the second feed investigated to explore the hydrocarbon recovery potential and its inherent economics. The Gorgon gas is denoted as "Feed1" and the richer natural gas feed as "Feed2" throughout the discussion. Table 1-1 displays these feed conditions.

The objective of this research was to assess several low temperature separation schemes as an alternative to amine treating for the separation of natural gas feed to a LNG plant which requires CO₂ to be reduced to a maximum of 100 ppm and to recover the CO₂ for geological sequestration to reduce CO₂ emissions at minimum production costs. The alternatives were the Ryan-Holmes (RH) and the hybrid membrane Ryan-Holmes (HRH). The option for the hydrocarbon recovery was also studied to potentially increase the overall revenue from the plant.

Table 1-1. Feed gas conditions.

	Feed1	Feed2
Flow Rate (MMSCFD)	1200	
Temperature (°C)	7	
Pressure (kPa)	8800	
Composition (mole fraction)		
C1 (Methane)	0.7775	0.7782
C2 (Ethane)	0.0323	0.0540
C3 (Propane)	0.0089	0.0195
iC4 (i-Butane)	0.0015	0.0040
nC4 (n-Butane)	0.0015	0.0047
iC5 (i-Pentane)	0.0013	0.0022
nC5 (n-Pentane)	0	0.0016
n-C6 (n-Hexane)	0	0.0020
n-C7 (n-Heptane)	0	0.0035
n-C8 (n-Octane)	0	0.0035
n-C9 (n-Nonane)	0	0.0030
n-C10 (n-Decane)	0	0.0030
CO ₂ (Carbon Dioxide)	0.1470	0.1160
N ₂ (Nitrogen)	0.0300	0.0050
H ₂ S (Hydrogen Sulfide)	0.000030	0.000030

1.2 Ryan-Holmes (RH) Process

The Ryan-Holmes process was originally developed for processing sour gases from Enhanced Oil Recovery (EOR) fields (Carmody 2006; Holmes et al. 1982; Inc. 2006; Price and Gregg 1983; Ryan and Schaffert 1984; Schaffert and Ryan 1985; Wood, O'Brien, and Schaffert 1986). The problem for separating CO₂ from light hydrocarbon is complicated by two factors – the CO₂/C2 azeotrope and the relatively high freezing point of CO₂. The fundamental feature of the RH process solves these problems by the addition of the extractive recycle to avoid CO₂ freeze up and break the CO₂/C2 azeotrope. This process is a series of distillation columns operating at low temperatures to separate the feed gas components into relatively pure methane and

CO₂, and ethane and propane plus products. The Ryan-Holmes process has been reported to be superior to other processes in treating high CO₂ natural gas from EOR operations. There are several natural gas processing plants using the RH technology and the list includes the Seminole Unit, operated by Amerada Hess Company, the Willard Unit, operated by ARCO oil and gas company, the GMK South Field, operated by Mobil Oil Corporation, and the Wasson Denver Unit, operated by Shell Oil Company (Holmes et al. 1982; Price and Gregg 1983; Ryan and O'Brien 1986; Ryan and Schaffert 1984; Schaffert and Ryan 1985; Wood, O'Brien, and Schaffert 1986). In addition, the RH process has the advantage of lower dehydration requirement relative to the amine process, non-corrosiveness, NGL-based solvent usage, and high pressure of the rejected acid gas product (Denton and Rule 1985). Another benefit offered by the RH process is the high hydrocarbon liquid recovery, which is essential for EOR operations, in order to increase the revenue of the plant due to the decreasing methane content. Moreover, with the Ryan-Holmes process, a high pressure CO₂ stream is produced which is more suitable for CO₂ injection and it also offers significant synergies between the separation, fractionation trains, and liquefaction processes.

1.3 Hybrid Membrane Ryan-Holmes Process

The idea to combine the membrane process with the Ryan-Holmes process was to potentially reduce the processing costs. Membrane technology uses the partial pressure as the driving force for the separation and therefore a concentrated CO₂ feed gas would be suitable for a membrane application.

Industrial applications of membranes for the separation of sour natural gases have been widely reported in the open literature either as a stand-alone membrane system, hybrid membrane-amine, hybrid membrane-hot pot (hot potassium carbonate), or hybrid membrane Ryan-Holmes process. Some of these applications include the EOR projects for CO₂ removal, for example: Cynara membranes in the Mallet CO₂-removal facility in Texas and SACROC CO₂-removal from the EOR project unit in Texas, Separex membrane for CO₂ removal in the Qadirpur and Kadanwari natural gas plants, Pakistan, a hybrid UOP SeparexTM membrane-cryogenic distillation process to recover ethane from an increasing CO₂ content feed at Karsto plant in

Norway (Bhide, Voskericyan, and Stern 1998; Blizzard, Parro, and Hornback 2005; Cook and Losin 1995; Dortmund and Doshi 1999; Echt 2002; Friedman, Wissbaum, and Anderson 2004; McKee, Changela, and Reading 1991; Nordstad, Kristiansen, and Dortmund 2003; Russell and Coady 1982; Schendel 1982; Schendel and Seymour 1985). As a stand-alone application, the membranes can be arranged in a one-stage or two-stage configuration depending on the purity requirement and the economics of the process. A primary advantage of this approach is the ability to stage capital as needed. The gas flow from EOR operation is difficult to predict and may require substantial time to break through after initiation of CO₂ injection. The hydrocarbon flow changes relatively less the CO₂ flow – so the tools required to recover and purify hydrocarbon can be sized and built with capacity for CO₂ removal added as needed. Two-stage membrane processes are able to produce a higher purity CO₂ product; however, it normally happens at the expense of the additional capital and recompression costs. In the hybrid membrane-amine system, the membrane is usually located upstream of the process for a bulk removal followed by the amine process for a final cleanup to a specific CO₂ level. The upfront installation of membranes requires adequate pre-treatment processes to prevent any membrane impairment. Membranes can also be combined with the Ryan-Holmes process in a similar manner, in an upstream location for a bulk removal. However, since the base case in this study involved high flow rates and high methane contents, and the membrane is more cost effective for low flow rate applications (McKee, Changela, and Reading 1991; Spillman 1989), the use of membranes for bulk removal was not considered in this research. On the other hand, there is another method for combining the membrane with the Ryan-Holmes process. The membranes can be placed in the overhead of the CO₂ stripper column, after the propane and heavier components are separated from the CO₂-ethane azeotrope mixture, which aids in breaking the CO₂-ethane azeotrope. The overhead of the CO₂ stripper column contains significant CO₂ after the methane is removed and this stream is suitable for the separation with membranes. A hybrid membrane-distillation process patented by Fluor, resulted in a reduction of cost by 20% for the utilities and 25% in the capital compared to a stand alone extractive distillation process for treating sour natural gas (Schendel 1984; Schendel and Selleck 1981).

1.4 Research Methodology

This research involved a purely computer-simulation study using Aspen HYSYS version 2004.2 platform. This software includes models for commonly used unit operations as well as comprehensive component, thermodynamic, and property libraries. The Ryan-Holmes, the hybrid membrane Ryan-Holmes, and the amine dehydration and liquefaction train were simulated using the Peng-Robinson property package available in the HYSYS database.

An independent study on the validation of CO₂-ethane azeotrope prediction with the Peng-Robinson property package in HYSYS to the experimental data was also conducted. The result showed that the prediction of CO₂-ethane azeotrope in the range of 0.6-0.7 CO₂ mole fraction match quite well with the experimental data and the average absolute deviation of vapor pressure ($|\Delta P|$) and percent vapor fraction ($|\Delta y \times 100|$) was 0.295 in the temperature range of -50°C to 20°C (Lastari and Maeda 2008).

The membrane implementation in HYSYS was carried out by utilizing a membrane key available from the Chevron in-house program suite. The amine acid gas removal unit was simulated utilizing the Bryan Research and Engineering (BR&E) Promax software. The economic calculation of the capital and operating costs of the process alternatives is embedded in the HYSYS spreadsheet based on cost line information adopted from several literatures (Garrett 1989; Peters, Timmerhaus, and West 2003; Walas 1990).

Information on the feed conditions, some of the design criteria and equipment parameters were based on the inputs from Chevron and other verified internal sources. The design parameters were optimized within a certain range and the optimization objective was economic in nature which included the capital and operating costs. The optimized processes were then compared with the more mature amine process.

1.5 Significance of Research

The choice of a process for the production of LNG is related to many aspects such as feed flow rate, feed composition, plant location, objective of separation, market drivers, economic aspects, management policy, and government regulation. These factors determine the preferred route for the LNG process. Although LNG processes are mature, there are still significant challenges in processing the feed gas containing high levels of CO₂. The investigation of the Ryan-Holmes process and the modified Ryan-Holmes for potentially producing a low cost LNG alternate for treating the Australian high CO₂ natural gas is deemed to be valuable for practical LNG process development.

In addition, this research is the first initiative to directly compare the Ryan-Holmes and hybrid membrane Ryan-Holmes processes with the mature amine process for LNG production. Although it is realised that each application is suitable for certain feed conditions and several other factors, it is worthwhile to understand the strengths and weaknesses of each of the process alternative in handling sour natural gas to simultaneously produce the LNG, high pressure CO₂ for injection, and hydrocarbon liquids.

1.6 Research Objectives and Contributions

The specific objective of this research was to explore the benefits of the Ryan-Holmes process and the hybrid membrane Ryan-Holmes for treating the high CO₂ natural gases. These two process alternatives were then compared with the conventional amine process. An in-depth analysis of these process alternatives has made a significant scientific contribution under the following broad areas:

1. Development of a fully heat integrated simulation model for an LNG facility which includes the capability of costing both capital and operating expenses allowing a single model for optimizing the overall plant costs.
2. Development of heuristics for choosing process alternatives for LNG production (for example comparing the Ryan-Holmes and hybrid membrane Ryan-Holmes processes with the amine process) as a function of CO₂ impurity and feed conditions.

3. Development of an economic-based optimization strategy of the process alternatives using a parametric sensitivity.
4. Design and optimization strategy for an extractive distillation column to break the CO₂-ethane azeotrope, as well as the effect of solvent composition on the separation.

1.7 Thesis Overview

Chapter 1 describes in brief the background information for the research project. The motives for examining the Ryan-Holmes and hybrid membrane-Ryan Holmes processes are presented.

Chapter 2 reviews the process alternatives examined in this research, namely: the Ryan-Holmes, modified Ryan-Holmes, and amine processes. The strategies for utility minimization and heat integration have also been discussed.

In chapter 3, the simulation constraints and the optimization objectives are defined. Operating variables were perturbed within a certain range to study the sensitivity of the process variables. The effect of the minimum temperature approach on the overall economic objective function was also investigated.

Chapter 4 explores the fundamental behaviour of an extractive distillation column for the separation of CO₂-ethane azeotrope. The effect of solvent composition on the separation in both the demethanizer and the extractive distillation columns was also examined.

Chapter 5 presents a comparative study of process alternatives. The economic assessment and operability comparison between the process alternatives is also presented. The variations in feed composition were also simulated in the optimized flowsheets to observe the plant performance with various CO₂ ranges.

Chapter 6 provides the conclusions and recommendations for future work and also formulates general guidelines for choosing the process alternatives investigated in this study.

Appendices provide supplementary information for the economic calculation used in this research. The thesis structure is shown in Figure 1-1.

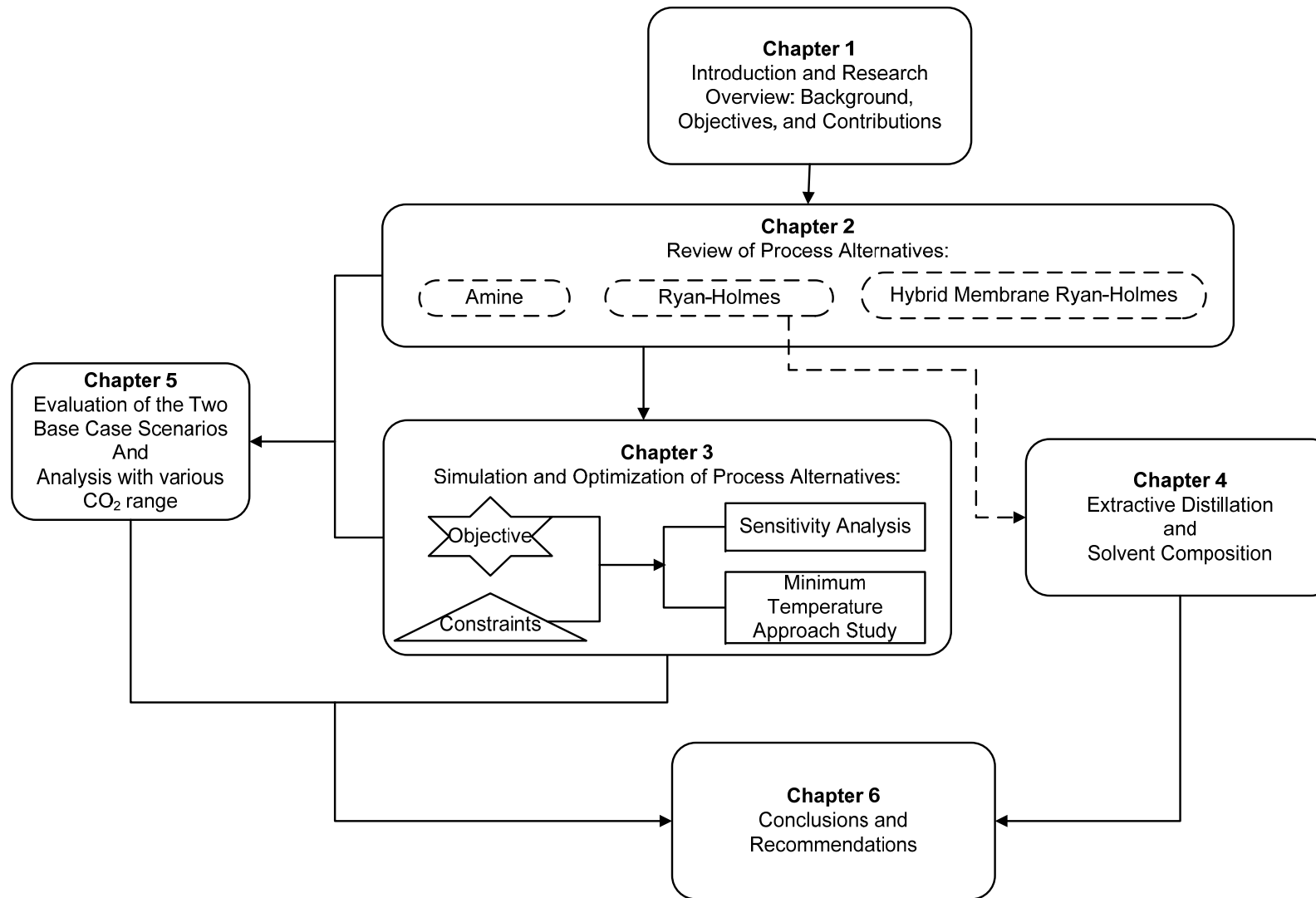


Figure 1-1. Thesis structure.

2. REVIEW OF PROCESS ALTERNATIVES

A slug catcher outlet condition was defined as the feed inlet for all of the process simulations. The conditions of this stream were 7°C and 8,800 kPa. This stream contained MEG (*Mono Ethylene Glycol*) to prevent the hydrate formation at high pressure and thus it was assumed to be water saturated. This water should be removed before entering the low temperature processes to prevent the formation of ice and hydrates.

In the Ryan-Holmes (RH) and the hybrid membrane Ryan-Holmes (HRH) processes, the wet feed stream was first sent to the dehydration system prior to entering the low temperature distillation process. In contrast, the dehydration system for the amine process was installed after the acid gas removal unit because the gas from the amine contactor will be H₂O-saturated. Dehydration with molecular sieve is required to obtain extremely low water contents in the gas for cryogenic processing (GPSA 2004). Application of molecular sieve dehydration in a continuous process requires two (or more) columns for the process. In the simplest application, one is operated to remove the water and the other is regenerated with the hot dry gas. These columns are equipped with valves to switch the dehydration process from one column to another. The wet gas enters the dehydration column from the top and flows through the sieve bed. This allows high velocity flow without the possibility of fluidizing the bed. In the column that is being regenerated, the sieve is dried by passing a heated regeneration gas from the bottom through the column. In this way, any water left in the sieves will be in the top of the column and will not affect the effluent dewpoint when the adsorption process is resumed. The schematic diagram of the dehydration process is depicted in Figure 2-1.

From the dehydration process point of view, the RH and HRH processes hold a distinct advantage compared to the amine process. This is because these processes need only to remove the original water content in the feed stream from the production separator while the amine process requires bigger capacity and regeneration energy to handle the saturated stream from the absorption column after coming in contact with the hotter amine aqueous solution.

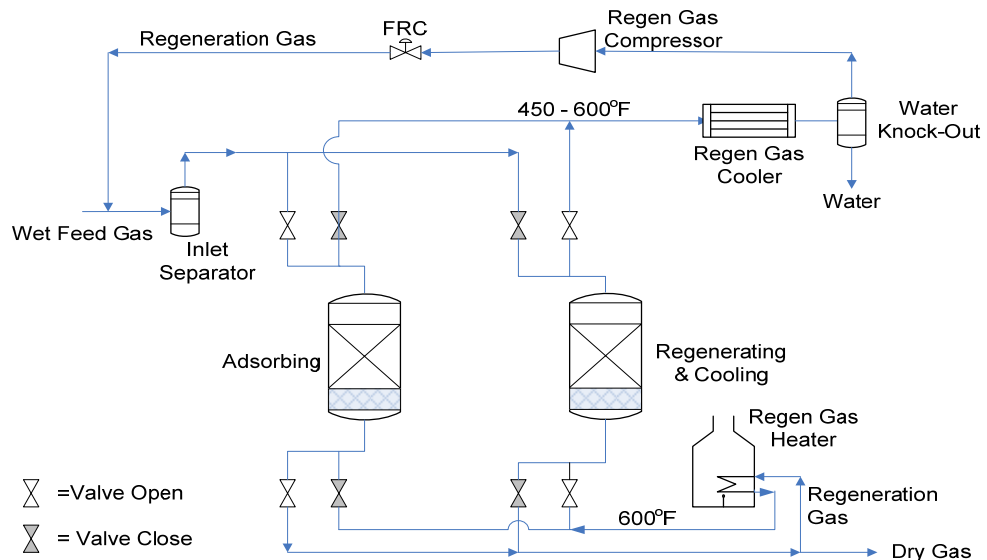


Figure 2-1. Molecular-sieve dehydrator twin tower system (GPSA 2004).

The water content in the feed stream was adjusted to obtain a H₂O-saturated condition. Therefore, the amount of water in Feed1 and Feed2 was different. The amount of water in Feed1 and Feed 2 were 253 kg/h and 316 kg/h respectively. The amount of water to be removed in the dehydration process was different between RH/HRH and the amine process. The saturated Feed1 gas entering into the dehydration process in the RH/HRH processes contains 253 kg/h water at 7°C while the saturated Feed1 in the amine process contains 1,854 kg/h water at the air cooling temperature (49°C). The result shows that dehydration for the amine system requires higher energy and capital costs than the RH/HRH dehydration process because of the higher water content and hotter temperature of the process stream. A comparison between the stream operating conditions going into the dehydration process and the design specifications for the dehydration system in both RH/HRH and the amine process for Feed1 and Feed2 is presented in Table 2-1. Detailed calculations of the dehydration system are presented in Appendix A.

In the amine case, the stream from the dehydration process is free from the acid gases and thus it can be sent directly to low temperature processes to generate LNG or fractionation columns. While in the RH and HRH processes, after passing through the dehydration system, the stream was sent to the low temperature distillation process to remove the acid gases and separate the hydrocarbon components.

Table 2-1. Summary of dehydration process in RH/HRH and amine processes.

Dehydration Process	Feed1		Feed2	
	RH/HRH	Amine	RH/HRH	Amine
Inlet feed from	Slug catcher outlet	Absorber column	Stripper overhead	Absorber column
Feed temperature (°C)	7	49	6	49
Water contents (kg/h)	253	1,854	230	2,550
Saturated gas flow rate (ACT_m3/h)	11,735	17,761	11,313	17,682
Operating adsorbing vessel	3	3	3	3
Operating regenerating vessel	3	3	3	3
Total number of vessel	6	6	6	6
Vessel design pressure (kPag)	9,425	7,480	9,300	7,480
Vessel diameter (m)	2.3	2.9	2.6	3
L/D	3.2	2.3	2.6	2.6
Molecular sieve weight (kg)	107,383	149,510	121,830	204,360
Heat for regeneration (kJ/h)	1.173×10^7	8.814×10^7	1.135×10^7	1.123×10^8
Regeneration gas rate (kg/h)	15,040	126,920	13,500	185,625
Regeneration gas temp (°C)	315	315	315	315
Cycle time (hours)	48	8	60	8

2.1. Amine Process

The amine process is a mature and well-proven technology for natural gas sweetening treatment. In fact, 95% of the total natural gas sweetening applications in the USA utilizes the amine method (Association 2004; GPSA 2004). It involves absorption and chemical reactions of the CO₂ and H₂S sour gas with solvents of the alkanolamines family, such as MEA (*Monoethanolamine*), DEA (*Diethanolamine*), DGA (*Diglycolamine*), and MDEA (*Methyl-diethanolamine*). This process is performed in an absorption column consisting of trays or packed beds and followed by a stripping column to remove the CO₂ and H₂S from the solvent. A typical amine process design is presented in Figure 2-2.

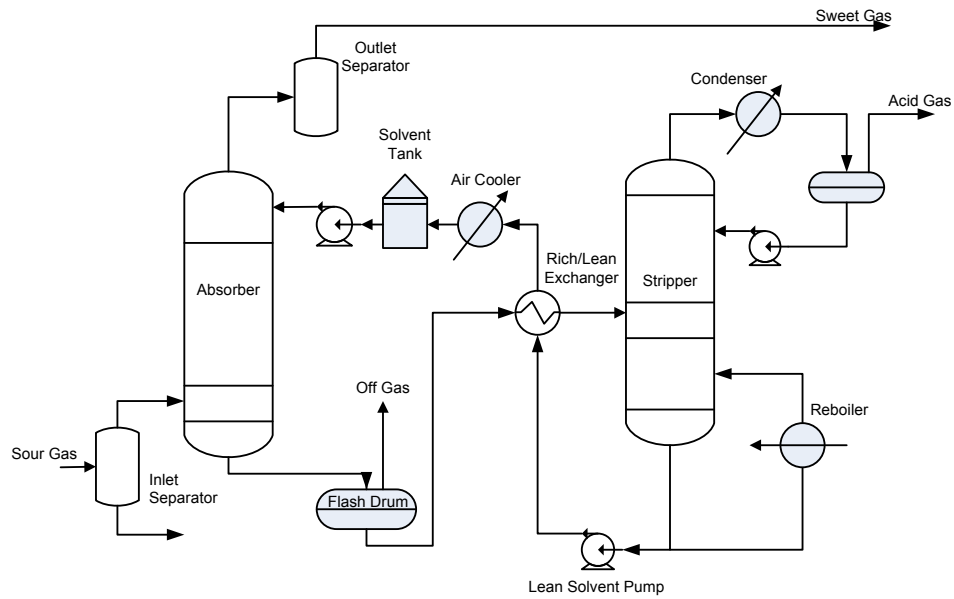
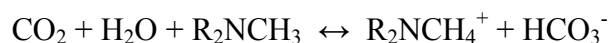


Figure 2-2. Typical gas sweetening with amine process (GPSA 2004).

The sour gas from the slug catcher outlet passed through a gas pre-heater and a pressure letdown then entered the amine process at specified conditions of 20°C and 7000 kPa. The heat source for the pre-heater was supplied from the propane refrigerant sub-cooling. The pre-heater increased the stream temperature from 7°C to 28°C and the propane refrigerant temperature decreased from 44°C to 39.5°C. In Figure 2-2, the heated sour gas was first sent to an inlet separator to remove any free liquids that would cause trouble in the downstream processing. The sour gas was then contacted with the MDEA solvent in the absorber. The solvent contains 48% by weight solution of MDEA with the balance consisting of treated water. The conditions of the MDEA solvent were at 49°C and 6900 kPa. The sweet gas outlet was specified to contain less than 100 ppm-mole CO₂.

The activated MDEA solvent was selected mainly because of the lower energy consumption. Theoretically, it allows for higher CO₂ pick-up (1 mole CO₂/mole amine) compared to the primary and secondary amines following the reaction (MacKenzie et al. 1987):



Furthermore, experience has shown that MDEA is suitable for CO₂ removal applications due to several reasons: high solution concentration (up to 50-55%-w), low corrosion, slow degradation rates, lower heats of reaction, and low vapor

pressure and solution losses (Bullin, Polasek, and Donnelly 1990; Kohl and Nielsen 1997; Polasek, Iglesias-Silva, and Bullin 1992). Although it is also known that the reaction of tertiary amine such as MDEA with CO₂ is slow, because it requires the formation of bicarbonate ion first which then reacts with the amine in the acid-base reaction, however, developments of the activated MDEA by the addition of proprietary activators has been found to enhance CO₂ pick up efficiency. Activators are usually primary or secondary amines that are added to enhance the hydrolysis of carbamate and hydration of CO₂. Several studies on the mixture of MDEA combined with MEA and DEA solvent to improve sour gas pick up have also been presented (Kohl and Nielsen 1997; Lunsford and Bullin 1996; Spears et al. 1996).

The other important design variable for the amine system is the solvent circulation rate. The solvent amount is mainly determined by the quantity of acid gas to be removed and the acid gas loading. High acid gas content in the sour gas requires a higher solvent circulation rate and a higher acid gas loading requires less solvent circulation rate. Experimental data on the CO₂ solubility in 50%-w MDEA in Figure 2-3 shows that the equilibrium acid gas loading in amine solvents is determined by the partial pressure and the absorption temperature. Higher partial pressures and lower temperatures result in higher acid gas loading in the amine solvents (Kohl and Nielsen 1997; Younger 2004).

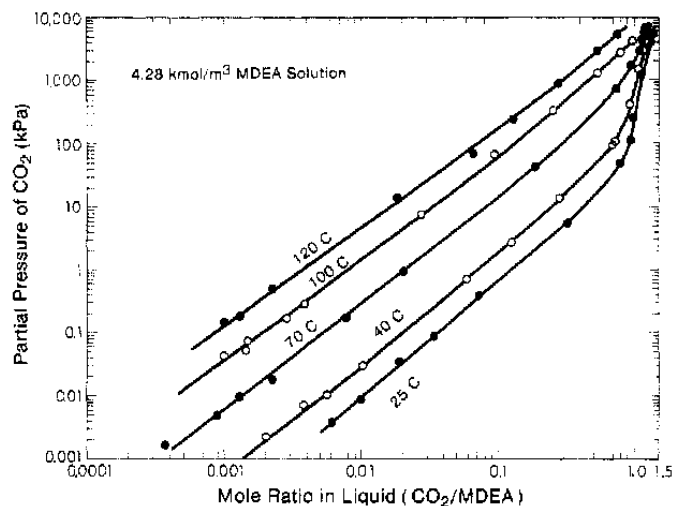


Figure 2-3. Solubility data of CO₂ in 50%-w MDEA (Jou, Mather, and Otto 1982)

In this study, the acid gas concentration in the lean amine was calculated from a comparison with internal data provided by Chevron for similar feed condition (Chan 2008). The comparison was necessary so that the amine process simulation can be evaluated against an empirical figure for the scale of feed given in this research. The regeneration operation from the simulation and the data given from Chevron was compared using the lean loading and reboiler duty specifications. We also compared the lean loading figure to the range in the literature. With specified amine molar flow rate and temperature, heat duty in the stripper's reboiler, and CO₂ impurity level in the sweet gas, it was calculated in the Promax program that the lean amine loading capacity was 0.0137. The Promax calculated the VLE in the absorption and stripper columns with the assumption that the contactor stages were at equilibrium. Then, using the calculated lean amine loading value, the solvent circulation rates for Feed1 and Feed2 were manipulated until the purity in the sweet gas was achieved. Solvent circulation rates of 9,200 USGPM and 7,700 USGPM were obtained for Feed1 and Feed2, respectively. These results were obtained utilizing 2-trains of acid gas removal unit similar to the in-house reference. The results are within the typical operational range and are shown in Table 2-2.

Table 2-2. Amine simulation result.

	Feed1	Feed2	General range
Lean amine loading, mole acid gas/mol amine	0.0136687	0.0136687	0.01 – 0.04*
Rich amine loading, mole acid gas/mol amine	0.5122	0.4932	0.5 – 0.6*
Acid gas pick-up, mole acid gas/mol amine	0.4985	0.4795	0.2 – 0.8
Reboiler temperature, °C	126	126	110 – 132
Heat reboiler duty (kJ/gal amine)	807.7	807.8	± 805.5*

*Target range provided by Chevron, others from GPSA Electronic Databook (GPSA 2004)

The sweetened gas came out at the top of the absorber and was then sent into the outlet separator to recover any solvent carried over in the sweetened gas. This stream was saturated with water; and therefore, it was necessary to send the stream into the

dehydration process prior to fractionation and liquefaction. The dehydration system, fractionation columns, and the liquefaction system were simulated in HYSYS.

The rich solvent from the bottom of absorber contained acid gases. It was sent to the flash drum to remove dissolved hydrocarbons in an off-gas stream. This stream was sent to the fuel system and was accounted for to meet the fuel requirement. Next, this stream was heated by passing through a heat exchanger and taking the heat from the lean amine coming from the bottom of the stripper. The rich/lean heat exchanger minimum temperature approach was set at 3°C following the internal data reference (Chan 2008). The heated stream was then sent to the stripper where the CO₂ and H₂S were stripped off the solution to the column overhead while the lean amine exited at the bottom of the column. The overhead of the stripper was sent to a condenser and then separated to recover water which was sent back into the stripper as reflux. The lean amine was recycled back into the absorption column. From the process description above, it is recognized that the amine process is more advantageous given that it removes the CO₂ and H₂S gases altogether, whereas in the RH and HRH processes, the sour gases are removed individually thus an additional H₂S removal facility is required. If the H₂S amount is not considerable, simple scavenger processes such as the iron-sponge process or PuraSpec could be easily utilized (GPSA 2004); however, when the amount of acid gas is significant, the amine process is usually the most cost effective option (Fleming, Spears, and Bullin 1988). In addition, if the amine process was used for H₂S removal from the ethane stream, the H₂O-saturated ethane stream from the amine process should be water dehydrated if this stream was to be sent to low temperature liquefaction process. Nevertheless, the requirement of treating only a small amount of ethane stream instead of the entire feed in the amine process for H₂S removal is beneficial to reduce the costs of the process.

The condenser was set at 210 kPa to allow condensing the overhead stream with cooling water. The specifications used in the stripper column were the overhead condensing temperature of 49°C and the calculated lean amine loading of 0.0137. The rejected acid gases in the overhead stream were then sent to several compression stages to achieve a 215 bar discharge pressure for geological injection.

After the acid gas was removed from the process stream, the sweet gas passed through the dehydration system. Following the dehydration system, the downstream flowsheet setup was quite different for Feed1 and Feed2. Figure 2-4 and Figure 2-5 shows the simplified flowsheet of the amine1 and amine2 respectively.

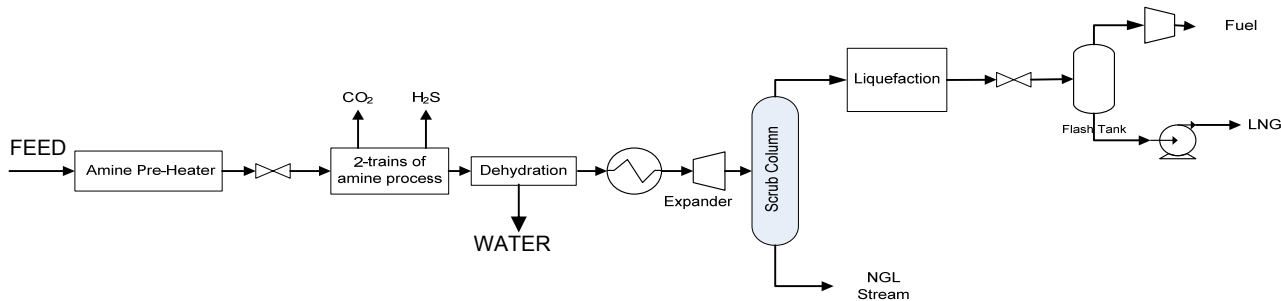


Figure 2-4. Simplified flowsheet of the amine1 process

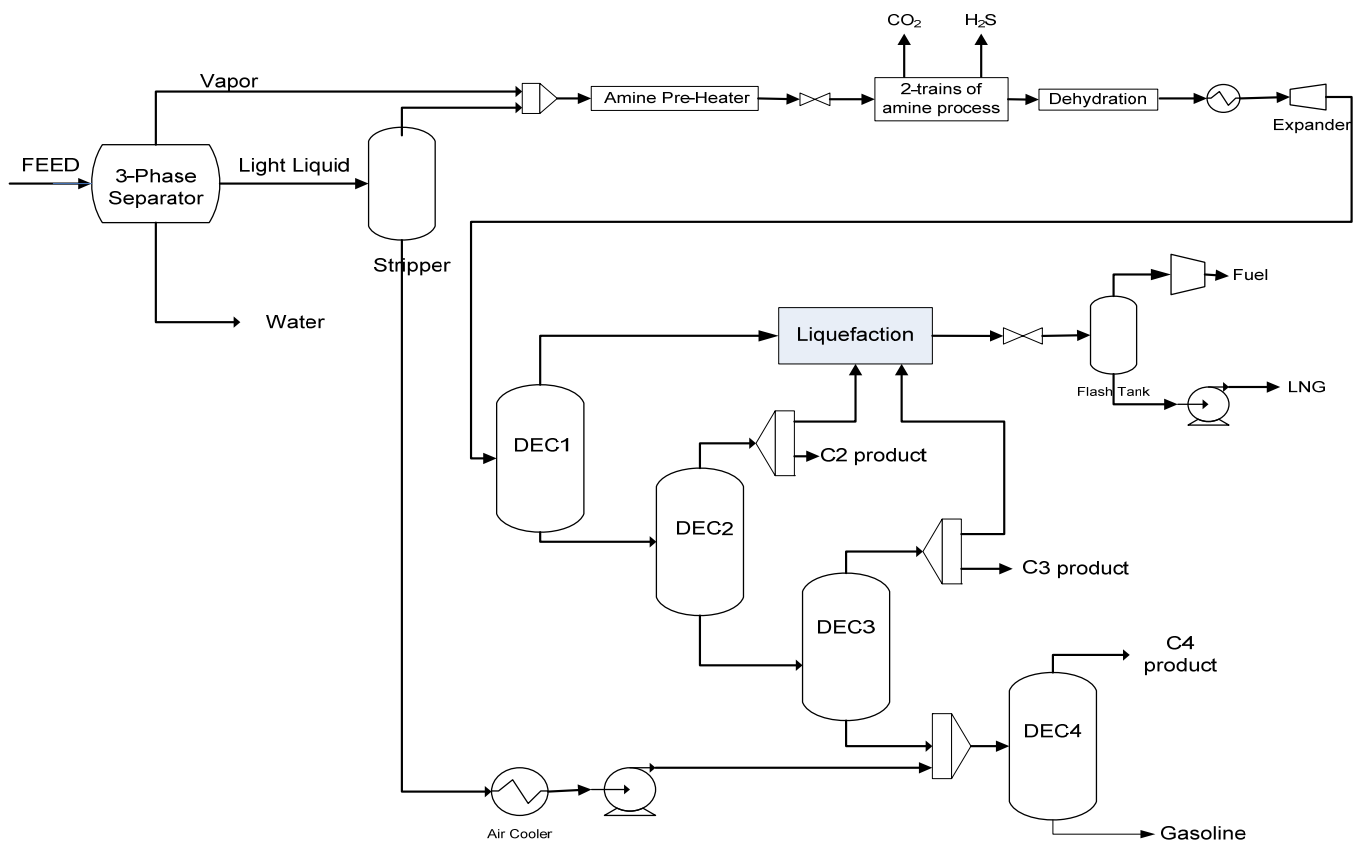


Figure 2-5. Simplified flowsheet of the amine2 process

It is shown that the amine2 process is more complex than amine1 process. Amine2 process requires more fractionation columns to generate the differentiated hydrocarbon products. However, with amine1 process, it is necessary to mix the

lighter hydrocarbon with C1 to generate LNG with the required heating value while the heavier hydrocarbon is removed in the scrub column.

As shown in Figure 2-4 the stream from the dehydration system in the amine1 process was sent through the turbo expander to assist in lowering the stream's temperature as well as recovering some of the power for compression. A 2758 kPa expander outlet pressure was obtained from the optimization process. Then, the stream was sent to a scrub column to remove the heavy components prior to the liquefaction process. The overhead stream from the scrub column was sent for further liquefaction while the bottom product, with most of the heavy components, was generated as a sellable product. The C3 specification at the bottom stream leaving the scrub column was adjusted to make a sufficient heating value in the LNG product. The commercial LNG Btu value of approximately 39.5 MJ/Sm³ (Chinn 2007b; Tsai 2007)

In contrast, for Feed2 gas, the stream still contained significant heavy components and was sent to the turbo expander and then fractionation columns to simultaneously remove the heavy components from the LNG and recover the valuable hydrocarbon products. Detailed flowsheets in HYSYS of the amine process for both feeds are attached in Appendix B.

2.2. Ryan-Holmes (RH) Process

The dehydrated Feed1 stream from the dehydration process was subsequently sent to a typical 3-column RH process, presented in Figure 2-6. Feed2 gas required additional fractionation columns to recover the differentiated hydrocarbon components such as propane, butane, and condensate commercial products (Figure 2-7).

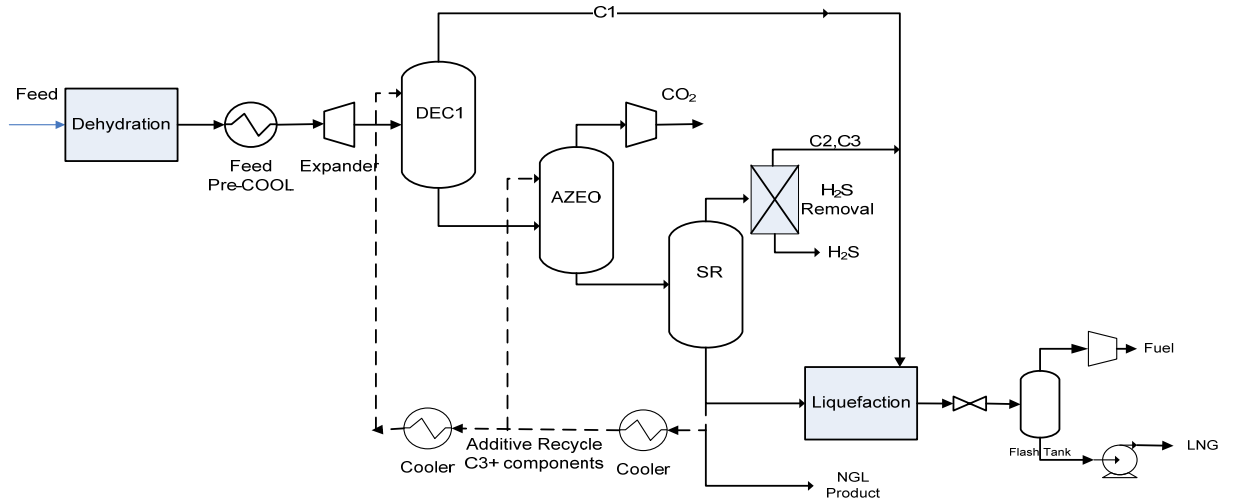


Figure 2-6. A 3-column Ryan-Holmes process.

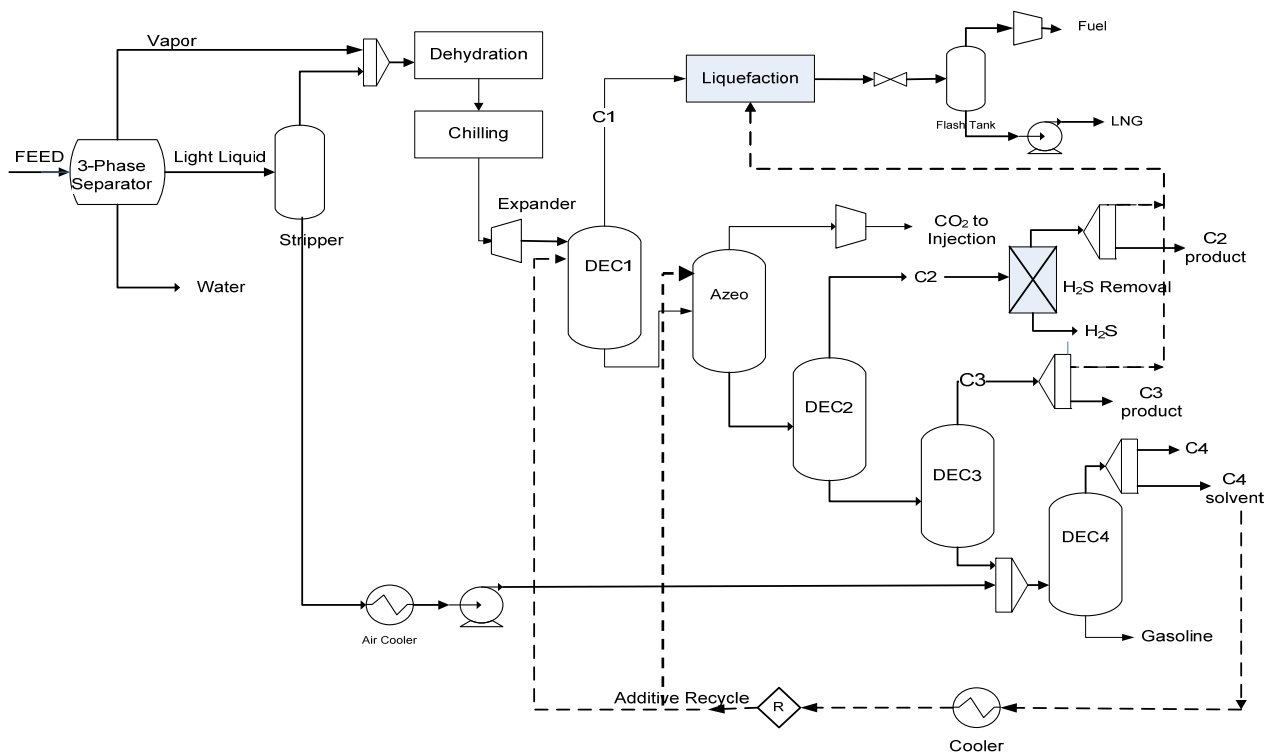


Figure 2-7. Ryan-Holmes process flowsheet for Feed2 gas.

It was noticeable that the two feed streams required different flowsheets to generate the products. The decision to select which flowsheet to use was subject to the plant objective. Initially, feed1 was examined to generate differentiated hydrocarbons besides LNG and CO₂. However, it was impossible because the hydrocarbon components needed to be blended with the C1 component to produce LNG with the

required heating value. As a result, the flowsheet for Feed1 process is simpler than for Feed2. As shown in Figure 2-6 and Figure 2-7, the products from the RH Feed1 process were the LNG, CO₂, and a broad fraction NGL stream while the RH Feed2 process generated the LNG, C₂, C₃, C₄, and C₅₊ products. The composition of the condensate stream in the RH1 process was different from the condensate product in the amine1 process. For both feeds, the stream from the dehydration process was first cooled prior to sending it to the demethanizer column (DEC1). The stream was cooled by heat exchange with the DEC1 column side reboilers. Following that, further cooling was done by using propane refrigerant and expanding the high pressure stream from about 8,500 kPa down to 4,000 kPa in a turbo-expander and generating a cold stream at a temperature of approximately -68°C. The expansion work was recovered for the fuel compressors. Alternative methods to achieve a high hydrocarbon recovery for the differentiated product simulation such as the gas subcooled process (GSP) or the residue recycle (RR) process (GPSA 2004) were not considered in this study. In DEC1, the major methane component in the feed stream was separated. The key specifications of the DEC1 column were to obtain high purity methane for LNG production and a small methane loss in the bottom product.

The separation of methane and CO₂ key components in DEC1 requires the addition of the light hydrocarbon solvent to avoid CO₂ freezing because it is impossible to separate methane-CO₂ mixture without passing the CO₂ solid region as shown in Figure 2-8.

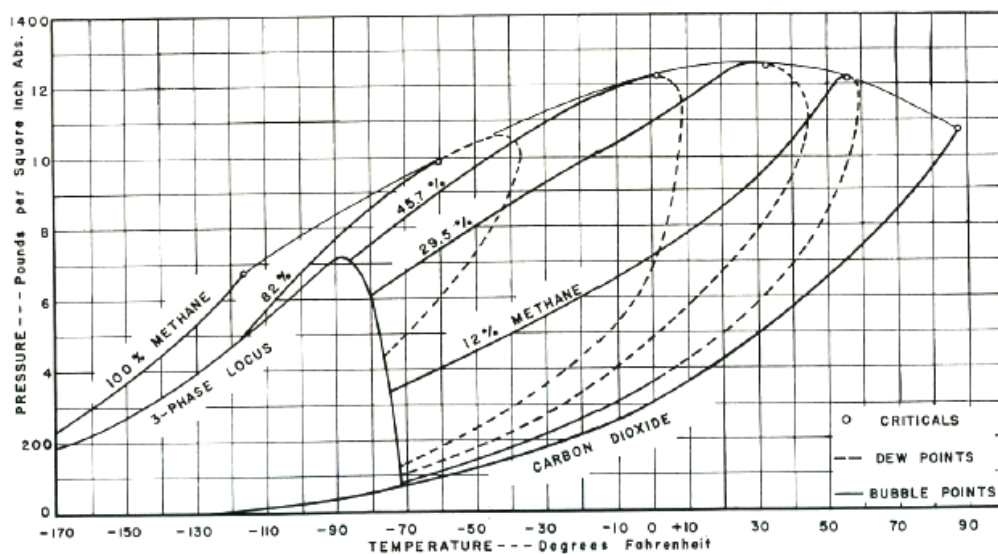


Figure 2-8. Pressure-temperature diagram for CO₂-methane system (Katz et al. 1959).

The RH process demonstrates another benefit that overcomes this problem. The RH process utilizes the Natural Gas Liquid (NGL) based solvent that is derived from the natural gas itself. This solvent was added near or at the top of the column to avoid the CO₂ solid formation in the low temperatures region at the upper section of the DEC1. The amount of solvent required is dependent on the feed composition, column pressure, minimum temperature approach to the CO₂ freezing point, and also on the solvent composition. In all of the simulations, a 5.5°C (10°F) margin to the CO₂ freezing temperatures in the stream and in all of the trays in the DEC1 was maintained. This column operates at cryogenic temperatures and recovers the high purity methane vapour in the overhead. A refrigerated condenser is required to provide reflux for the column.

The second column installed in the series of RH processes is the azeo column or the CO₂ recovery column. This column aimed to obtain a high purity CO₂ in the overhead product for geological injection. The problem encountered in the azeo column is the formation of an azeotrope between CO₂ and C₂ (ethane). CO₂ and C₂ form a binary azeotrope at approximately 67%-mole CO₂ and 33%-mole C₂ and this azeotrope does not change much with operating pressure. This problem was solved by using the same NGL solvent used in DEC1 as an azeotrope breaker (Holmes et al. 1982). The solvent amount required in the azeo column is governed by the feed composition, product purity required, and solvent composition and temperature. However, unlike the application of solvent in DEC1, the solvent in the azeo column was added several trays below the top tray to reduce carried over solvent in the CO₂ product. The amount of solvent used was related to the reflux ratio and the sizing of the azeo column and subsequent columns, and therefore, was optimized to achieve the minimum operational and capital costs.

The bottom stream from the azeo column was made up of the C₂+ components from the feed stream plus the solvent fed to the azeo column. This stream was sent to the subsequent fractionation columns to separate the hydrocarbon components into the commercial hydrocarbon products; however, only one fractionation column was necessary for Feed1, which was the solvent recovery (SR) column. The SR column generated the NGL solvent at the bottom stream and the remaining hydrocarbons were separated in the overhead stream and mixed with the methane from the DEC1

column. The solvent generated from the bottom of SR column was suitable for Feed1 process because it contained mainly the C4 and C5 components. Further discussion on the solvent composition is presented in chapter 4. The overhead stream from the SR column contained C2 and C3 components with a small amount of H₂S impurity.

The H₂S has to be removed to meet the LNG specification and an additional H₂S removal facility is required. The amount of H₂S flow rate was 61 kg/h in the RH process for Feed1. Several H₂S removal methods were assessed. Puraspec (Zinc Oxide) solid adsorbent removal unit was found incapable of handling the associated H₂S amount. An amine removal unit is another approach typically added in the RH process to separate the H₂S (Holmes et al. 1982; Ryan and Schaffert 1984; Schaffert and Ryan 1985; Schendel 1983). However, the additional H₂S removal facility selected in this study was the molecular sieve because it was suitable to handle large or small liquid ethane stream (GPSA 2004), and the sizing and economic calculation method applied for this molecular sieve was similar to the molecular sieve used in the water dehydration process. A portion of the CO₂ product stream was used to regenerate the molecular sieve bed (GPSA 2004; Kidnay and Parrish 2006; Schweitzer 1997).

The adsorption process is a common method for sweetening NGL streams and is able to remove the sulphur component down to low level when water is not present. The molecular sieve bed diameter was calculated based on a liquid upflow velocity of 1.5 m/s (Kidnay and Parrish 2006). The bed height was estimated from the H₂S adsorption isotherm at various temperatures with 13X molecular sieve and the regeneration calculation was performed using an identical approach as in the regeneration of the molecular sieve in the dehydration process (GPSA 2004; Schweitzer 1997). The capital cost for the H₂S removal facility was trivial compared to the total equipment cost ($\pm 0.20\%$).

The specifications in the fractionation columns for Feed2 process were either set following the commercial specification or optimized economically. The result is presented in Table 3-9. Summary of column specifications (%-mole) for RH process. Table 3-9. The solvent used for RH1 and RH2 was generated from different column. In RH1, the solvent was generated from the bottom of the solvent recovery

(SR) column while in RH2; it was generated in the overhead of DEC4. It was because these generated solvent streams contained mainly the C4 component which was found to be the most cost effective solvent from the study presented in chapter 4. Therefore, the solvent composition for Feed2 was implicitly fixed by the column specification used to generate a commercial C4 product in the DEC4; however, the solvent composition for Feed1 case was more flexible.

From the discussion of the RH process above, it is clear that various design variables such as the number of distillation stages, feed inlet location, solvent inlet location, solvent temperature, solvent composition, column pressure, and some column specifications were not defined and therefore optimization procedures were required to obtain the most economical process flowsheet. A detailed flowsheet of the RH process setup in HYSYS for both feeds is attached in Appendix C.

2.3. Hybrid Membrane Ryan-Holmes (HRH) Process

The main difference between the RH and the HRH process flowsheet was the addition of membrane modules in the overhead of the azeo column. The membrane offers alternative way to move the CO₂-ethane separation past the azeotrope. Therefore, the HRH process was investigated to specifically observe the prospect of membrane modules to replace the additive solvent in the azeo column. It was identified that after the methane was separated in the demethanizer column and propane plus components were separated from the CO₂-ethane in the azeo column, the vapour from the azeo is essentially binary CO₂/ethane and was amenable for membrane separation. The HRH process setup for Feed1 and Feed2 are displayed in Figure 2-9 and Figure 2-10.

It is important to note that the main advantage of membrane utilization was the removal of solvent in the azeo column which significantly reduced the capital cost of the azeo and the subsequent columns due to the lower flow rate.

cellulose triacetate membrane was provided by Chevron. Membranes function by selectively allowing the more permeable components through the membrane while retaining the remaining components. The more permeable components are concentrated in the permeate stream and the remaining components in the retentate stream. The driving force in the membrane gas separation process is the components' partial pressure difference between the feed side and the permeate side. The permeation of gases through a non-porous membrane follows the mechanism described by Fick's law:

$$J_i = \frac{P_i}{l} (p_i^F - p_i^P)$$

Notations:

- J_i = Flux of component i through membrane
- P_i = Permeability coefficient for component i
- l = Membrane thickness
- p_i^F = partial pressure of gas i in feed
- p_i^P = partial pressure of gas i in permeate stream

Fick's law illustrates two parts related to the flux of components through the membrane:

1. P_i/l is a property of the membrane and characterizes the selectivity of the membrane to the components and hence the separation performance.
2. $(p_i^F - p_i^P)$ corresponds to the operation condition in which separation is performed. A high partial pressure difference results in a higher flux through the membrane.

The composite membrane structure which consists of a dense non-porous layer supported by the porous membrane structure is typically used for CO₂ removal membranes. This structure provides the high selective permeation properties through the dense non-porous layer and improves the mechanical strength of the membrane for high pressure operation with the porous structure. The hollow fiber type membrane was used and the feed was located on the shell side. The hollow fiber membrane gives a higher packing density (greater membrane area per volume) and thus smaller plant than the other type of membrane configuration (flat sheet or spiral wound). The shell side feed inlet is typical for high pressure gas separation application because the pressure drop is lower than the bore side inlet. Furthermore, the fibers are much stronger under compression than expansion. The flow patterns can be arranged in counter-current, co-current, or cross flow. In this simulation, counter-current flow pattern was selected to maximize the efficiency of the

separation. The components' permeability depends on the interaction between the gas molecules and the polymer membrane. In this study, the components' permeabilities were assumed constant and the permeability values were supplied by Chevron.

The hollow fiber type membrane consists of thousands of fibers packaged in bundles and is manufactured in a standard sized pipe. The commercial membrane module sizes range from 10 to 30 cm in diameter and 1 to 6 m in length. The Cynara membrane size was referenced to estimate the number of modules required in this project. The design flow of the Cynara hollow fiber-CO₂ selective removal membrane for each module/case was 6 MMSCFD (0.17 STD_m³/d) and every 6 cases of membranes arranged as one cluster (Chinn 2007a). The permeability constants of the components in this study and the properties of the membrane module are shown in the Table 2-3 (Baker 1991; Echt 2002; Ho and Sirkar 1992; Kohl and Nielsen 1997).

Table 2-3. Component permeability constants and membrane properties used in HRH simulation.

Membrane	Cellulose Triacetate
Temperature (°C)	-6.7
CO ₂ (GPU)*	41.2
H ₂ S (GPU)	41.2
N ₂ (GPU)	1.03
Methane (GPU)	1.14
Ethane (GPU)	1.07
Propane (GPU)	0.40
i-Butane (GPU)	0.17
n-Butane (GPU)	0.41
i-Pentane (GPU)	0.41
nC5+ (GPU)	0.41
*1 GPU = 10 ⁻⁶ cm ³ (STP)/(cm ² .s.cmHg)	
Flow direction	Counter-current
Feed location	Shell-side
Bundle count	40
Fiber count	300,000
Fiber active length (m)	0.8128
Fiber pot length (m)	0.1016
Fiber outer diameter (mm)	0.3
Fiber inner diameter (mm)	0.15

For some applications, membrane separations have advantages relative to other technologies (Dortmundt and Doshi 1999): lower capital and operating costs, deferred capital investment, operational simplicity, high reliability, good weight and space efficiency, adaptability and flexibility in handling variations of CO₂ in the feed, environmentally friendly, and ideal for remote locations. On the other hand, some limitations of membranes in CO₂ separation applications are: incapability to achieve high recovery CO₂ without significant hydrocarbon loss, not suitable for high flow rate gas because the increase in flow rate is directly proportional to membrane area, and not suitable for applications in which both the feed and product pressure are low, e.g. below 2412 kPag (Spillman 1989).

The number of membrane modules in the HYSYS simulation was determined to obtain a similar result with the RH process in terms of the purity and the recovery of CO₂ for injection. The CO₂ purity target in this project was defined at 99% to minimize the amount of C1 and C2+ components from the feed and solvent to be lost in the CO₂ product stream. Table 2-4 shows the initial simulation with only a single stage membrane. It is shown that with 16 membrane modules, the CO₂ recovery is higher than 98%; however, the CO₂ purity is less than 99%. Therefore, the number of membrane modules was reduced to obtain a lower CO₂ recovery with higher purity level. It was found that with the establishment of 13 membrane modules, the recovery level reached below 98%; but the CO₂ purity was still below the 99% requirement.

Table 2-4. Separation performance with one single stage membrane – HRH1.

Number of membrane module	Permeate pressure (kPa)	CO ₂ purity	CO ₂ recovery
16	344.6	96.48%	99.13%
15	344.6	96.81%	98.79%
14	344.6	97.15%	98.31%
13	344.6	97.48%	97.59%
12	344.6	97.80%	96.48%

Therefore, a two-stage membrane system was required to achieve a higher than 99%-mole CO₂ purity and 98% CO₂ recovery rate. A methane purge stream from the overhead of the ethane recovery column was installed to avoid methane build up in

the system. This methane purge was sent to the fuel system. The two-stage membrane system is presented in Figure 2-11.

The feed from the azeo column overhead was first heated to achieve a temperature of 25°C at the inlet of the first stage membrane (Membrane-1). This heat was supplied by a cross-exchange with the hot compressed stream going into the second stage membrane (Membrane-2).

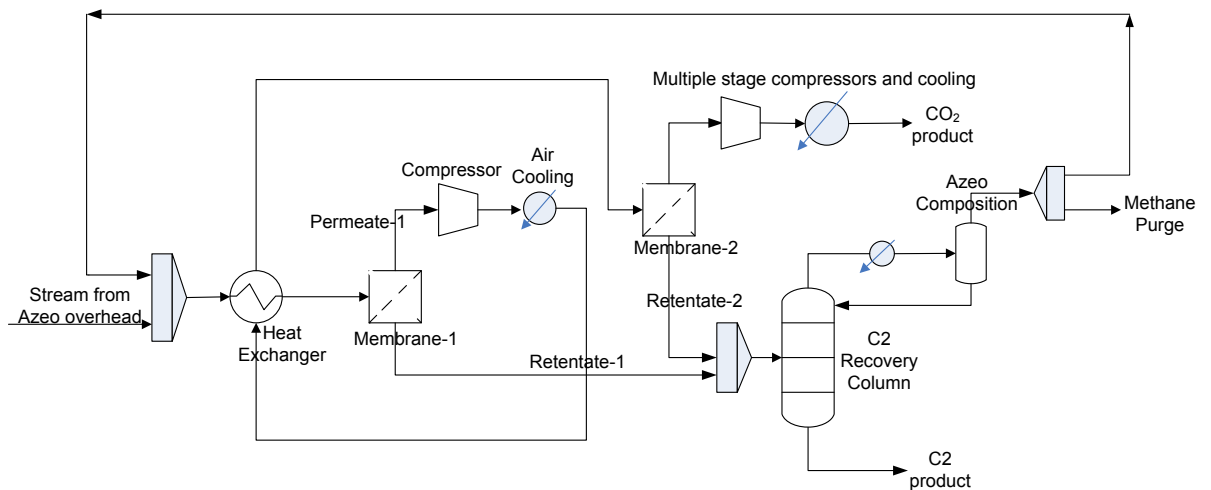


Figure 2-11. Two-stage membrane system in the HRH process.

For Feed1, membrane-1 consists of 18 modules with a total membrane area of 165,500 m² and membrane-2 consists of 10 modules with a total membrane area of 92,000 m². For Feed2 gas, membrane-1 and membrane-2 consists of 16 and 8 modules, respectively with a total membrane area of 147,100 m² and 73,540 m², respectively. Membrane-1 was placed for a rough split on the feed gas by utilizing large membrane area and low permeate pressure (345 kPa) to allow more gas to flow through the membrane and hence achieve a high recovery of CO₂. Membrane-2 performed a more strict separation on the stream from permeate-1 by utilizing less membrane area and higher pressure on the permeate side (760 kPa) to recover a high purity CO₂. An air cooler was required to cool the compressed permeate-1 stream before sending it to membrane-2. In addition, a C2 recovery column was installed to recover ethane from retentate-1 and retentate-2 streams. The result of the 2-stage membrane simulation with >98% CO₂ recovery is displayed in Table 2-5.

The design variables to be specified for the membrane system include: the number of membrane modules for each membrane stage, permeate pressures, and design specifications for the C2 recovery column. The variations of the number of membrane modules and permeate pressures in each stage of the membrane system were manipulated until an equivalent CO₂ recovery and CO₂ purity to the RH process were achieved. The other design variables were optimized in terms of economic impact.

Table 2-5. Two-stage membrane-RH simulation result.

	Feed1		Feed2	
	CO ₂ product	C2 product	CO ₂ product	C2 product
Temperature (°C)	25.14	11.14	25	8.93
Pressure (kPa)	758.4	3,447	758.4	3,723
CO ₂ - %mole	99.02	0.0040	98.90	0.0005
C1 - %mole	0.014	0	0.02	0
C2 - %mole	0.940	90.35	1.060	99.83
C3 - %mole	0.001	7.31	0.0002	0.17
H ₂ S – ppm	150	8	225	35
Molar flow (kgmole/h)	8,817	1,730	6,884	2,965
Volume flow (m ³ /h)	473	148	369	251

The result from the membrane area study was used to determine how many membrane modules were required for this process. A comparison with Cynara membrane size (6 MMSCFD/case) from the Chevron internal report was carried out. The number of modules required for membrane-1 and membrane-2 in this simulation with feed flows of 2.541x10⁵ STD_m³/h (215.5 MMSCFD) and 2.170e5 STD_m³/h (183.9 MMSCFD) respectively is displayed in Table 2-6. However, these results have not been verified by any membrane vendors and no commercial application reference can be found to evaluate them.

Table 2-6. Estimation of number of membrane modules for HRH Feed1 process.

	Chevron Reference	Membrane-1	Membrane-2
Feed Flow, MMSCFD		215.5	183.9
Design/case	6 MMSCFD/case	36 cases	31 cases
Clusters	6 clusters/36 cases	6 clusters	6 clusters

A reference study was made on a commercial membrane plant in Calgary, Canada to have a picture of the membrane system size. Typical commercial membrane modules with a size of 4-in. diameter by 40-in. long designed as interconnected banks were installed to handle 20 MMSCFD of gas consisting of 20%-mole CO₂ in a Calgary membrane plant. The membrane skid size is 9 ft (2.7 m) wide, 9 ft (2.7 m) high, and 12 ft (3.7 m) long (Coady and Davis 1982). Since membrane area increases proportionally to the flow rate, it can be estimated that the footprint dimension for membrane-1 and membrane-2 are 11 and 10 times larger than the Calgary membrane size. Using a similar comparison, the membrane system for the HRH Feed2 process occupied a space of 12 and 8 times larger for membrane-1 and membrane-2, respectively. A detailed flowsheets of the HRH process in HYSYS for both feeds are attached in Appendix D.

2.4. Utilities and Heat Integration System

The utilities operated in this plant are the air cooling, the propane, ethylene, and methane refrigeration, and the hot oil system.

2.4.1. Air Cooling

Air cooling is used to condense the propane refrigerant, cool down the recycled solvent, decrease the temperature of the bottom stream of the azeo and SR columns, and cool the CO₂ product throughout the recompression stages. The condensing target temperature using the air cooling was 44°C (111.2°F) based on a design air temperature of 26°C. It was observed that the highest air cooling duty requirement was for condensing the propane refrigerant. The demand for air cooling duty in the CO₂ recompression stages was not significant.

2.4.2. Refrigeration System

A cascade refrigeration using three refrigerants was used for the LNG liquefaction process for all the cases. The cascade refrigeration system was also utilized in the condenser of the distillation columns and solvent coolers. Each of the refrigerants operated at different temperature levels to meet the various condensing or cooling

temperatures. However, identical refrigerant temperatures were operated in the different process alternatives. Exceptions were applied to the refrigerant temperatures that were dictated by the condensing temperature in the distillation columns and also at the last step of the liquefaction system where the final cooling temperature was adjusted to meet the fuel demand for the plant. The temperature approach in the heat exchangers was economically optimized; however, a 1.11°C (2°F) minimum temperature approach was selected for operability issues. The entire compression requirement for the refrigeration system was driven by gas turbines.

For all of the processes, it was observed that the highest energy demand in the refrigeration system was for condensing the ethylene and methane refrigerants. It consumed more than 50% of the total cooling duty requirement. The second major consumption for refrigeration duties is to completely liquefy the LNG stream. Additionally for the RH Feed1 process, the DEC1 and azeo condenser duties were identified as the third biggest energy consumption which accounted for 7% and 5% of the total refrigeration duty, respectively. A similar trend was observed for the Feed2 gas, however, the percentages were lower due to the smaller CO₂ fraction to be removed. In the HRH process, the azeo condenser duty requirement was reduced significantly, down to 1% of the total refrigeration duty.

2.4.3. Hot Oil

A hot oil system was selected to supply heat to the reboilers of the azeo column, the SR columns, the fractionation columns, and also to the regeneration gas in the dehydration system. The heat generated from the fuel turbine exhaust was used to heat the hot oil to 200°C. The turbine exhaust gas conditions were at 537°C and 138 kPa. The hot oil flow rate was computed to get a temperature of 150°C in the hot oil stream returned from the units requiring heat input.

2.4.4. Heat Integration System

Several heat integrations between the streams in the flow sheet was made. Firstly, feed pre-cooling was supplied by the side reboilers in the DEC1 column. Secondly, the heat supplied to the two side-reboilers in the azeo column was provided by sub-

cooling the propane refrigerant and lastly, the heat supply in the DEC1 reboiler was utilized from a heat exchange with the propane refrigerant sub-cooling. In the HRH process, the C2 recovery column reboiler duty was also supplied by propane refrigerant sub-cooling. In the amine process, the heat for the feed pre-heater prior to sending the stream to the amine process was supplied from propane sub-cooling. The propane refrigerant temperature was lower down to a sub-cooled condition in these processes in order to provide reduced compression horsepower. This is a key part of the power optimization in a RH process. A study of fuel gas cross exchange prior to compressing the fuel has also been studied however, the result showed that this heat integration was not effective due to the insignificant temperature drop in the LNG stream.

3. SIMULATION AND OPTIMIZATION OF PROCESS ALTERNATIVES

3.1. Simulation Setup and Constraints

Three process alternatives were assessed for each of the two feeds. Hence, a total of six flowsheets were developed with the main process, refrigeration system, and embedded energy and economic calculations. The process synthesis started with the separation processes and the LNG liquefaction system setup. Then the refrigeration system was built to meet the cooling requirement in the separation and liquefaction processes. Once the complete flowsheet was developed, the energy and economic calculations were added in the HYSYS spreadsheets.

The separation process setup was established with respect to the product specifications and constraints imposed. The product specifications are listed in Table 3-1 and the simulation constraints implemented in the optimization processes were a 5.5°C (10°F) approach to the CO₂ freezing temperature and a minimum temperature approach of 1.11°C (2°F) in the heat exchangers. The liquefaction system cooled the process streams gradually and produced the LNG at approximately -160°C.

A cascade refrigeration system with a three closed refrigerants scheme was utilized for all of the six flowsheets. Identical cooling temperatures were used in the refrigeration system, except where the temperature levels were dictated by the economically optimized condensing temperatures in the overhead of the distillation columns and also at the last stage of the liquefaction part to provide fuel for the plant. The temperature levels of the refrigeration system were economically optimized in the RH process and the other alternative processes utilized the identical temperature levels, except for the above mentioned exclusions. The optimization of the refrigerant temperature levels and minimum approach temperature in the heat exchangers are discussed further in section 3.4.

The energy calculations incorporated in the fuel requirement calculation were for the compression horsepower, pump and air cooling fan power, heat supply in the

reboilers, and also the regeneration duty in the dehydration and the amine system. The efficiency of the compressor driver was calculated based on the GE (General Electric) frame 7 gas turbine heat rate of 13,850 kJ/kW-h (9,795 Btu/shp-hr) and the efficiency of the fuel in the fired heater to supply the total heat duty of the hot oil system was defined at 80% (Brooks 2006; Petchers 2003). The heat recaptured from the turbine exhaust was accounted for as a source of energy to supply heat to the hot oil system; however, the amount of heat from fuel combustion was also included. The calculation of the equivalent fuel demand required the net heating value of the fuel gas supplied. Detailed calculations are presented in appendix E.

Table 3-1. Product Specification Requirement.

Product	Required Specification
LNG	Purity Specification (%-mole): CO ₂ < 100 ppm C1 > 88 % C2 < 6 % C3 < 3.5 % i-C4 < 2 % n-C4 < 2 % i-C5 < 0.1 % N ₂ < 1 % H ₂ S < 3.2 ppm Heating Value Specification: 39.2 – 40.3 MJ/Sm ³ (1050-1080 Btu/scf)
CO ₂ product	> 99%-mole CO ₂ > 98% CO ₂ recovery
C2 product	Common High Purity Ethane (%-mole): C1 and lighter < 2.5 % C2 90 % C3 6.0 % i-C4+ 2.0 % CO ₂ < 10 ppmw H ₂ S < 10 ppmw
C3 product	Commercial Propane: Vapor pressure at 37.8°C, < 1434 kPag C4+ < 2.5%-vol
C4 product	Commercial Butane: Vapor pressure at 37.8°C, < 483 kPag C5+ < 2.0%-vol
Condensates product	RVP = 69 kPa

3.1.1. Capital Cost Estimation

The economic estimation was carried out by the standard chemical engineering formulas and the equations were adopted primarily from the chemical process equipment book by Walas (Walas 1990); (Gerrard 2000). Although this evaluation of the total capital and operational costs is not accurate enough for commercial decisions, the method provides a reasonable estimate of the differences between the process alternatives.

Estimates were made of the investment and operational costs. The total investment cost is estimated from the purchased equipment cost which is assumed to be 15% of the total investment cost. The purchased equipment cost typically represents 15-40% of the total capital investment (Peters, Timmerhaus, and West 2003). The estimation of the total purchased equipment costs will be discussed first. Basically; all of the main equipment established in the process flowsheets was included in the capital cost estimation. This included equipment for the dehydration system, distillation columns with reflux pumps, condensers, reflux drums, and reboilers, all of the heat exchangers, air coolers, economizers for the refrigeration system and fuel flash tank, compressors, expanders, pumps and spare pumps, and the solvent and LNG tanks.

The solvent tank sizes were calculated with an assumed storage capacity of 0.675 to the stream volumetric flow rate based on the internal reference data for the amine solvent. This storage capacity permitted a solvent residence time of 20 minutes with 50% liquid volume level in the tank. The LNG tank sizes were also calculated using the assumed storage capacity of 0.675 to the stream volumetric flow rate in all of the alternatives. The valves and piping system were calculated as a function of the total purchased cost of the equipments utilizing a factor of 0.12 (Garrett 1989). Furthermore, the capital cost calculation also included the cost of the gas turbines and the generator set to drive the gas turbines. The number of the gas turbines was estimated based on the GE frame 7 gas turbine output rate of 85.4 MW and the cost for the generator driver was calculated using an average value of \$400/kW for simple cycle gas turbine (Boyce 2006; Brooks 2006). Five gas turbines were required in all cases.

In the HRH process, the cost of membrane replacement in every 5 years (Grainger and Hagg 2008) has also been taken into account in the capital cost calculation. Although not every piece of equipment was included in the capital estimate (such as the refrigerant make up tank and the air-cooler axial fans), the differential economics between projects should still accurately reflect the relative process costs since this type of equipment will be similar across all of the applications. Furthermore, the total investment cost for all of the process alternatives was slightly less than the total investment cost figure announced in the media at around US\$ 8 billion (Bell 2007; Bruns 2005; Marriott 2006), therefore the additional costs for the missed items might have been accounted for in the difference between the total investment cost calculated in this study with the figure reported in the media.

An initial solvent supply from the solvent tank is necessary and the amount should be adequate to fill the distillation columns in the start-up procedure of the RH/HRH processes. It is imperative to initially feed the distillation columns with the solvent in order that as soon as the feed gas is introduced into the process, the operability problem due to CO₂ solid formation in DEC1 is avoided and the separation of CO₂-ethane azeotrope in the azeo column is achieved. The solvent can be recycled back to the solvent tank during the start-up process. The solvent tank capital cost was included in the capital cost estimation; however, the initial hydrocarbon solvent purchase cost was excluded because it was assumed that after the process achieved the desired steady state operation, the solvent demand was sufficient from the feed stream, and thus the initial solvent could be traded. A surge tank is also necessary to anticipate the off spec product during the start up process. It is important to introduce the feed gas gradually so that the products generated from the distillation process meet the product requirement; therefore, a surge tank should be available for collection of the off-spec product prior to recycling it to the feed stream. The capital cost for the surge tank was also excluded because it was assumed to be necessary in all of the process alternatives. The complete equipment list incorporated in the capital cost estimation is presented in Appendix F.

3.1.2. Operational Cost Estimation

Secondly, the operational costs of a plant consist of (Garrett 1989):

1. Variable costs: raw materials, solvents, fuel, utilities, labour charges, transportation, distribution, and research development.

2. Fixed costs: depreciation, taxes, licensing fees, patents and royalties, and interest.

In the present work, only the natural gas feed cost was included in the annual operational cost calculation. The hydrocarbon solvent required for the RH and HRH processes was generated from the natural gas feed itself; however the initial purchase of the MDEA solvent was calculated in the capital investment. Furthermore, normal losses of the MDEA solvent in the amine process were considered utilizing the make up stream in the simulation. The fuel requirement to drive the gas turbine was supplied from a fraction of the LNG generated and thus the annual cost for fuel consumption was subtly considered. Also, a supply availability of the fuel to start up the plant was considered in all of the process alternatives.

In terms of the utilities, the refrigerant and hot oil purchase was included in the capital investment calculation but the make up stock was not considered because it was assumed to be the same in all of the process alternatives. For the air cooling system, the bare tube area requirement was incorporated in the capital cost calculation and the fan horsepower was included in the fuel demand estimation. The air cooling calculation procedure was taken from Ludwig (Ludwig 2001). The labour and maintenance costs as well as the transportation, distribution, and research development charges were not included as it was assumed to be comparable between the process alternatives.

For this assessment, plant was estimated to operate for 20 years. Depreciation of the capital cost was computed linearly in the first 10 years of operation and no salvage value was considered at the end of the project. An income tax of 40% was charged to the revenue after the depreciation. A chart listing all of the variables included in the economic evaluation is presented in Table 3-2.

In order to identify the best option in treating Feed1 and Feed2, comparisons between the process alternatives should be done at the optimized conditions. In this study, a conventional economic feasibility measure was used as the optimization objective. However, the required product specifications and the safe operability constraints were also consistently applied in the optimization processes. In the

following sections, a concise identification as Amine1, RH1, and HRH1 was applied for each of the process alternatives treating Feed1, and Amine2, RH2, and HRH2 for Feed2.

3.2. Optimization Objective

The optimization objective is the goal of the optimization processes and in this research, the objective was a quantifiable economic measure identified as IRR (Internal Rate of Return). The IRR was calculated using the DCF (Discounted Cash Flow) method which discounted all of the investment and cash flow acquired during the project life to the present value. The procedure for calculating DCF is shown in Table 3-2. The investment and cash flows tabulated in each year of the project life were discounted to present values by an assumed interest rate (IRR).

Using the DCF method, the interest rate was manipulated until the accumulation of the discounted cash flow values plus the total capital investment was equal to zero (at row O). The calculated interest rate is the Internal Rate of Return (IRR) for the project. The more attractive process alternative should provide a higher IRR value. Therefore, optimization processes were performed in all of the process alternatives to obtain a maximum DECF or IRR subject to the constraints given in the project. A simple yet complete description on the DCF or IRR profitability analysis has been presented for further study (Garrett 1989).

Another approach to analyse the profitability of a project is the present worth or present value (PV) method. This method calculated the discounted value of the cash flow from a project using a specified interest rate – usually the minimum acceptable return on an investment. The interest rate is used to calculate the present values of all the investments and cash flows made during the project life. Thus, the actual dollar returns are shown and the project with the greatest present worth in the one selected (Garrett 1989). In this study, the PV method will be discussed in brief to show the dollars saving that is achievable with different process alternatives, however, the IRR value will be mainly used to evaluate the process alternatives.

Table 3-2. Detailed economic presentation of the project.

		Years									
		0	1	2	3	...	10	11	...	20	
A	Capital Investment	A									
B	UTILITIES Initial Buying	B=B1+B2+B3+B4+B5+B6									
	1. Propane	B1									
	2. Ethylene	B2									
	3. Methane	B3									
	4. Hot Oil	B4									
	5. Amine (for Amine only)	B5									
	6. Fuel	B6									
C	Feed Stock Price, \$/MMBtu	0.5									
D	Production Days	337.3									
E	Production Rate		0.8	0.9	1	1	1	1	1	1	
F	Feedstock Cost		F = Feed flow rate x C x D x E								
G	SALES		G = G1+G2+G3+G4+G5								
	1. LNG		G1	G1	G1	
	2. C2 product		G2	G2	G2	
	3. C3 product		G3	G3	G3	
	4. C4 product		G4	G4	G4	
	5. C5 product		G5	G5	G5	
H	Depreciation		A/10 for the 1 st 10 years					0	0	0	0
I	Salvage Value									0	
J	Taxable Income		G-H	
K	Income Tax, %		40								
L	Cash Flow, \$		L = G - (40% x J)								
M	IRR (Internal Rate of Return)	M = %IRR									
N	Discounted Cash Flow, \$	(A+B) x M	L x M	L x M	
O	Cumulative DCF	Sum of row N = 0									

As shown in Table 3-2, the calculation of IRR considered the energy consumption as well as the total operational and capital costs of the major equipment. The energy consumption was evaluated in terms of the equivalent fuel demand and this fuel was generated from the LNG plant itself. It should be noted that the same volume of feed gas was used for all of the alternatives, which is either converted to product or consumed as fuel. Increasing fuel consumption reduced the LNG production thus cutting the plant revenue. The operational costs were computed annually in the lines

for feedstock cost (F), sales (G), depreciation (H), and cash flow (L) and the capital cost was incorporated in the capital investment (row A and B). Some assumptions were made in the DCF calculations: initial investment was made at time zero, all future cash flows were assumed to be received at one time at the end of each year and compounded continuously, and the interests were not withdrawn, but added to the principal. Furthermore, no inflation was considered in the economic calculation. Calculation spreadsheet, including the product pricing information, is presented in Appendix G.

In order to obtain a maximum IRR, the design variables were adjusted. These included the number of equilibrium stages, feed inlet location, solvent inlet location, solvent temperature, solvent composition, and column pressure, some of the column specifications (such as the methane specification at the bottom of the DEC1, the overhead specification of the azeo column, and the overhead and bottom specifications of the SR column), refrigerant temperature level, and the minimum approach temperature. Besides design variables, there were obviously changes in dependant variables including the heat exchanger UA values, reflux ratio, condenser and reboiler duties, column diameter, etc. These design variables and the calculated parameters determined the final IRR value.

In general, there are three optimization methods, i.e.: analytical, graphical or tabular, and incremental (Jelen and Peters 1970). This study utilized the graphical or tabular and the incremental methods. The analytical method was not applicable since a global optimization of the entire flowsheet is required and it was impractical to formulate the optimization objective in terms of all the design variables. The graphical or tabular and incremental optimization procedures are simple and straightforward. However, the design variables in this study were numerous. Therefore, the optimization procedure was quite elaborate with each design variable optimized incrementally around its steady state value while other process variables were fixed. The result was presented in a graphical form and the optimum decision on the design variables was made. With regard to the interacting design variables, a repeat optimization procedure was conducted to confirm the optimized result in the first attempt, for example the optimization of solvent temperature and solvent amount in the azeo column (Figure 3-16). A tabular form of optimization result was

also useful to observe the interacting design variables, for example the number of ideal stages and the feed inlet location (Table 3-3). It is shown that there was an increasing trend of optimization objective (IRR) towards the optimum result. The optimum result is 70 ideal stages and feed inlet location at stage 38 from the top.

Table 3-3. Optimization of number of ideal stages (N) and feed inlet location (Nf) in the azeo column – RH1 process

DCF	Nf = 30	Nf = 32	Nf = 34	Nf = 36	Nf = 38	Nf = 40	Nf = 42	Nf = 44
N = 60	10.101%	10.099%	10.103%	10.086%				
N = 65	10.093%	10.122%	10.131%	10.132%	10.099%			
N = 70	10.104%	10.125%	10.130%	10.134%	10.136%	10.132%		
N = 75				10.129%	10.132%	10.133%	10.133%	10.127%

3.3. Sensitivity Analysis of Process Variables

Sensitivity analysis is a method to investigate how an output variable is changed with varying input variables. The objectives are to obtain an indication of which variables are the most significant to improve the output variable and to study the effect of the varying assumptions used in the calculation. The results are generally plotted as percent change in the input variable versus the percent change in the output result (Baasel 1990; Saltelli et al. 2004).

To begin a sensitivity analysis study, the measured output variable was first identified. In this study, the output variable examined was the IRR and the varying input variables were all of the design parameters. The design variables examined were: column pressure, number of ideal stage and feed inlet location for all cases. In the RH/HRH process, the solvent amount, solvent temperature, solvent inlet stage, and the solvent composition were also investigated.

The simplest approach to sensitivity analysis is to present the IRR values as a function of the changing design variables. Typically several input variables are perturbed from the base case condition and the change in the output variable is observed and compared. However, it was not possible to perform such analysis in this study because of the variety difference in the measurement unit. For example, a 25% increase in the solvent temperature raised the temperature from a value of -89°C to -71°C which was still within the feasible operation range. However, an equal

percent increase of the DEC1 column pressure for the RH1 process changed the input variable from 4,067 kPa to 5,083 kPa. This upper pressure value was far beyond the methane critical temperature at 4,600 kPa (Reid, Prausnitz, and Poling 1987). Therefore, the initial proposal to rank the input variables according to the magnitude of its effect on IRR was invalid. Also, it was observed that the IRR sensitivity might increase significantly at a certain range of input variable, but only change slightly at another particular range. Thus, this result did not represent the overall sensitivity of that particular input variable on the IRR. One of the examples was observed in the RH1 process. When the DEC1 column pressure was raised from 3,800 kPa to 3,930 kPa, the IRR only changed slightly from 10.06% to 10.08%. However, when the column pressure was decreased down to 3,620 kPa, the IRR dropped to 9.68%. This was because at lower pressure, the fuel demand was higher and thus the turbine power limit was reached. Therefore, an additional gas turbine was added to the process and this decreased the IRR as much as 0.38%. Nevertheless, the sensitivity of the design variables on IRR will be presented to examine the trend and restrictions in optimizing the design variables.

It was important to note that when one of the design variables was changed, all other design variables were kept at the base case value, except when the optimization constraints were violated. Also, all of the required constraints and product specifications were examined and kept within the acceptable threshold. The key parameters to be monitored in all of the simulation procedures were the product requirement, the CO₂ product purity and recovery, the minimum CO₂ freezing approach temperature of 5.5°C in the feed stream of the DEC1 and at all trays in the DEC1 column. An additional calculated output that was examined was the difference between the available and the required equivalent fuel, the value was always greater than ± 0.5 MMSCFD. Also, the side reboilers' of DEC1 and azeo columns minimum temperature approach was maintained at a value of approximately 2.78°C.

The optimization and the sensitivity analysis of the amine process will be discussed first since it was quite straightforward due to the smaller number of design variables and less flexibility in terms of meeting the product requirements. However, for the RH and HRH processes, the column specifications were initially determined in order to meet all of the separation requirements. Then, the optimization of the other design

variables, i.e.: the column pressure and solvent properties were carried out with the product requirement strictly monitored. The optimization on the refrigerant temperature levels and minimum approach temperature were performed lastly after the main process and liquefaction system were established.

In the optimization process for the distillation column variables, the constraints specified were the product requirement in the overhead and bottom products of the distillation column. After the column operating conditions (number of ideal stages, feed inlet location, solvent inlet location, and pressure) were set, the column still had two degrees of freedom. Therefore, two specifications were required to solve the column. The specifications used in the distillation column for each cases is presented in Table 3-5, Table 3-9, Table 3-12.

3.3.1. Optimization and Sensitivity Analysis of the Amine Process

The optimization procedure for the amine1 process was relatively straightforward. The optimization was only conducted on the liquefaction portion of the process. The acid gas removal process was not optimized but it was evaluated against internal reference data (Chan 2008). There were only two variable processes to be optimized in the amine1 process, i.e.: the expander pressure outlet to the scrub column and the number of stages in the scrub column (Figure 2-4). The scrub column was equipped with a reboiler and no condenser was utilized in the overhead. This column was installed to remove some of the heavier hydrocarbon components to avoid freeze-out in the LNG cycle and to match the LNG heating value in the other process alternatives. The scrub column only used the reboiler at the bottom of the column. Therefore, only one degree of freedom was required to generate a solution for the column. The C3 spec in the bottom product was selected to control the heating value in the LNG product. Therefore, this parameter was a dependent variable because the value must be adjusted to keep the LNG Btu value constant at approximately 39.5 MJ/Sm³.

The optimization of the expander outlet pressure entailed a balance between the reboiler duty in the scrub column and the expander horsepower recovery. With lower expander outlet pressure, the inlet feed temperature was colder and thus the reboiler

duty was higher; however, more expander horsepower was generated. The optimized expander outlet pressure was 2758 kPa. The overhead pressure of the scrub column was set at 2654 kPa to allow for a 104 kPa pressure drop from the expander outlet to the overhead outlet stream. The variation of the ideal number of stages used in the scrub column affected the heating value of the LNG product. A smaller number of stages with a fixed C3 bottom spec allowed more C3 and heavier components to be discharged in the overhead; therefore the C3 spec for the bottom stream should be increased to maintain an equivalent LNG heating value in all simulation cases. The effect of the number of stages on the IRR was not significant, but 8 ideal stages was found to be optimum as shown in Table 3-4.

Table 3-4. Effect of the number of ideal stage in the scrub column on IRR.

Number of stage	4	6	8	10	15
C3 Spec @ Bottom	0.068	0.035	0.022	0.01	0.002
%IRR	11.27	11.26	11.28	11.27	11.27

In contrast, the amine2 process optimization was more complex because the richer feed gas justifies a more elaborate fractionation train. It involved four fractionation columns subsequent to the dehydration process to generate the purified C1 for LNG production, C2, C3, C4, and condensate products simultaneously. However, the specifications determined in these columns were easy to establish. The column specifications utilized were set according to the following commercial requirements presented in Table 3-1. For example, the specifications used in the DEC1 were 0.01%-mole C1 at the bottom and 4.5%-mole C2 at the overhead. The specification in the bottom of the DEC1 column was set to allow C2 product, generated in the next column, with C1 and lighter fraction less than 2.5%-mole and CO₂ less than 10 ppmw. In addition, the specification in the overhead of the DEC1 assured that the produced LNG contained less than 6%-mole ethane. A summary of the column specifications used in the amine process is presented in Table 3-5.

Table 3-5. Summary of column specifications (%-mole) for amine process.

	Feed1	Feed2
DEC1	-	OH: 4.5% C2 B: 0.01% C1
DEC2	-	OH: 5.5% C3 B: 2% C2
DEC3	-	OH: 1.2% iC4 B: 2% C3
Condensate Stabilizer	B: 9%-mole C3	OH: 1.3% iC5 B: RVP = 68.95 kPa

Prior to sending the stream to the DEC1, the stream from the dehydration process was sent to an expander. The optimized expander outlet pressure in the amine2 process was found to be 3792 kPa. The optimization of the expander outlet pressure in the amine2 process was more complicated than in the amine1 process because it involved some additional factors, i.e.: reflux ratio in the DEC1, condensing temperature in the DEC1 overhead, heating value of the LNG product, and the horsepower recovery of the expander. With the competing effects of these variables on IRR, it was found that the effect of the expander outlet pressure on the IRR was negligible in the range of 2400 kPa to 3800 kPa as shown in Figure 3-1. However, the IRR dropped significantly at 4150 kPa due to the requirement to obtain the reboiler heat duty from the hot oil system as the temperature was elevated at higher pressure. The higher expander outlet pressure affected the IRR so strongly because it required the heat supply to the reboiler of DEC1 column from the hot oil system which was met by sub-cooling the propane refrigerant at lower expander pressure outlet.

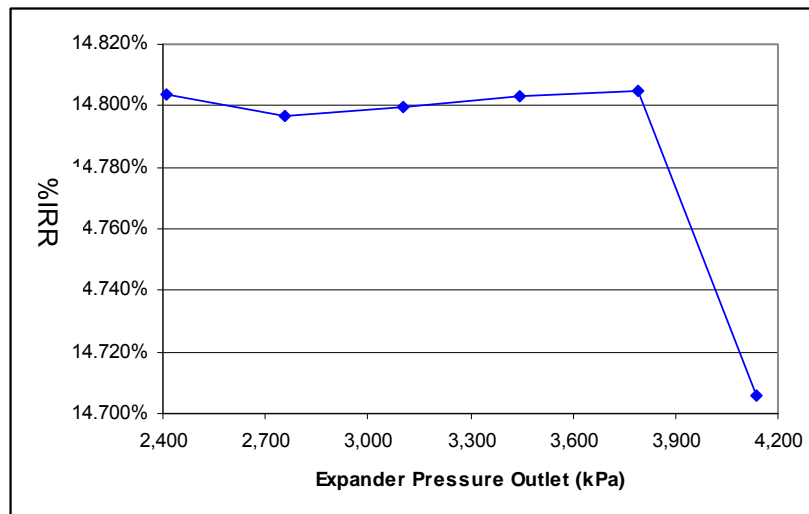


Figure 3-1. Expander outlet pressure effect on IRR for amine2 process.

The other design variable in addition to the expander outlet pressure that was economically optimized was the DEC2 column pressure. The operating parameters affected by varying the DEC2 column pressure in order to meet the overhead and bottom product specs were the DEC2 reflux ratio and the condensing temperature. At higher pressure, an increase in reflux ratio was needed and the condensing temperature level was warmer. To meet product specs, these opposite effects generated an optimum DEC2 column pressure at 2068 kPa. DEC3 and DEC4 column pressures were not optimized because they were adjusted to allow air cooling condensing temperature in the overhead.

Table 3-6 shows the effect of varying the number of ideal stages (N) and the feed inlet location (Nf) on the IRR in the amine2 process. It is shown that the IRR change was trivial in the range observed.

Table 3-6. Effect of number of ideal stage and feed inlet location on IRR - amine2 process.

DEC1 N/Nf	3	4	5	6	8	10
10	11.27%		11.16%			
16		11.29%	11.29%		11.29%	11.27%
20			11.28%	11.28%		
25						

DEC2 N/Nf	12	13	15	18	21
20		11.55%		11.49%	
25			11.56%		
30	11.56%		11.56%	11.56%	11.55%
35					11.56%
40				11.55%	

DEC3 N/Nf	5	7	9	13	15	16
15		11.56%				
20	11.56%		11.56%		11.55%	
30				11.56%		
37						11.56%

DEC4 N/Nf	4	6	12	18	24	30
15			11.56%			
25	11.57%	11.57%	11.57%	11.56%		
35		11.56%	11.57%	11.57%	11.56%	
45			11.56%			11.56%

3.3.2. Optimization and Sensitivity Analysis of the RH Process.

This section describes the optimization and sensitivity analysis of the RH process design variables for both Feed1 and Feed2. The differences and similarities applied to both feed conditions are also presented.

After the initial feed stream is dehydrated, it was sent to the RH fractionation process. Prior to entering the DEC1 column for a low temperature separation, the stream was cooled gradually by heat exchange with the DEC1 side reboilers and propane refrigerant. Furthermore, an expander is used to drop the temperature down

to -66.40°C . A separator should be installed prior to the expander to catch any liquid trace and to anticipate any liquid existence in the stream. However, this separator was not included in the economic calculation because the additional cost for installing the separator was comparable to all of the process alternatives. The outlet stream of the expander was directly sent to DEC1.

The RH1 process required 3 fractionation columns to generate the LNG feed stream, CO_2 product, and solvent recycle streams simultaneously. Two specifications were needed in each of the distillation column to solve the columns. In the DEC1, a 60 ppm CO_2 limit in the overhead product was specified. This specification was used to ensure that the CO_2 level in the LNG produced was kept below 100 ppm-mole after mixing with the hydrocarbon streams generated from the SR column to meet the required heating value. A 0.08%-mole methane specification for the bottom product was added to complete the degrees of freedom in the DEC1. This value was found by using the IRR optimization process.

The C1 specification at the DEC1 bottom product had a small effect on the IRR; however, higher C1 fractions would generate a CO_2 product with less than 99%-mole purity. It was realized that the 99% CO_2 purity can be achieved either with a relaxed C1 spec in DEC1 but tighter C2 impurity spec in the azeo column or lower C1 specification with higher C2 spec in the azeo column. The simulation results show that the optimized value was obtained at 0.08% C1 as shown in Table 3-7.

It is also important to monitor the maximum amount of methane and lighter constituents exiting in the CO_2 gas to be less than 4% to maintain miscibility of the injecting gas in the reservoir well below the reservoir fracture limit (Friedman, Wissbaum, and Anderson 2004; Ryan and Schaffert 1984; Schaffert and Ryan 1985).

Table 3-7. Optimization of C1 specification for DEC1 bottom product – RH1.

C1 spec at DEC1 Bottom	1.00E-03	1.00E-03	8.00E-04	6.00E-04	2.00E-04
C2 spec at Azeo OH	6.50E-03	6.00E-03	6.50E-03	6.70E-03	7.20E-03
%IRR	10.980%	10.962%	10.983%	10.981%	10.946%
DEC1 Reflux	1.1650	1.1649	1.1650	1.1651	1.1657
Azeo Reflux	1.435	1.571	1.437	1.403	1.330
CO2 product					
Mole fraction C1	1.85E-03	1.85E-03	1.48E-03	1.11E-03	3.70E-04
Mole fraction C2	6.50E-03	6.00E-03	6.50E-03	6.70E-03	7.20E-03
Mole fraction C3	1.81E-03	1.70E-02	1.81E-03	1.85E-03	1.92E-03
Mole fraction iC4	1.02E-04	7.44E-05	1.02E-04	1.11E-04	1.34E-04
Mole fraction nC4	1.73E-06	1.19E-06	1.72E-06	1.90E-06	2.39E-06
Mole fraction iC5	1.99E-10	1.36E-10	1.98E-10	2.19E-10	2.76E-10
Mole fraction CO2	9.90E-01	0.9904	0.9901	0.9902	0.9904
Mole fraction N2	1.63E-12	1.63E-12	1.32E-12	1.05E-12	4.58E-13
Interest 10%, NPV	4.816E+08	4.734E+08	4.831E+08	4.817E+08	4.653E+08

A different flowsheet setup was established for Feed2 gas as it required six columns to generate the LNG, CO₂, and the differentiated hydrocarbon products (ethane, propane, butane, and condensates) simultaneously. The six columns included a stripper, a demethanizer (DEC1), an azeo column, a deethanizer (DEC2), a depropanizer (DEC3), and a condensate stabilizer. A stripper was installed upfront in the Feed2 process flowsheet to prevent the heavy components from entering the low temperature conditions in the DEC1. The separated heavy components were then mixed with the bottom stream of the DEC3 to recover the valuable commercial butane and condensate products. The specification used to solve the stripper column was the C3 fraction in the bottom stream. The C3 fraction was fixed at the same value with the C3 spec at the bottom of DEC3 column.

The design variables required to specify the stripper were the feed inlet temperature, column pressure, and the number of ideal stages. Figure 3-2 presents the front section of the flowsheets in treating the Feed2 gas with a stripper. Prior to entering the stripper, the stream from the 3-phase separator was heat exchanged with the overhead outlet of the stripper. The overhead of the stripper was at the air cooling temperature and its temperature was reduced, to match the overhead stream temperature from the 3-phase separator which was at 7°C, before going into the dehydration process.

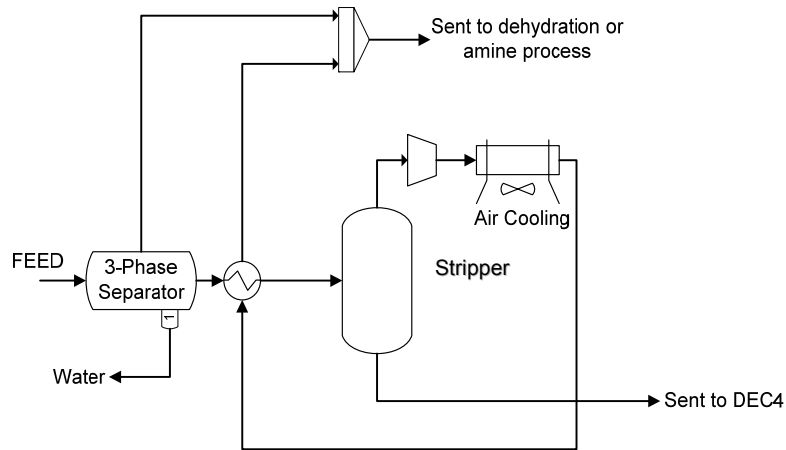


Figure 3-2. Stripper column setup for Feed2 gas.

The optimization process showed that a higher inlet temperature going into the stripper required less reboiler duty, however, the heat exchanger UA increased due to the smaller minimum approach.

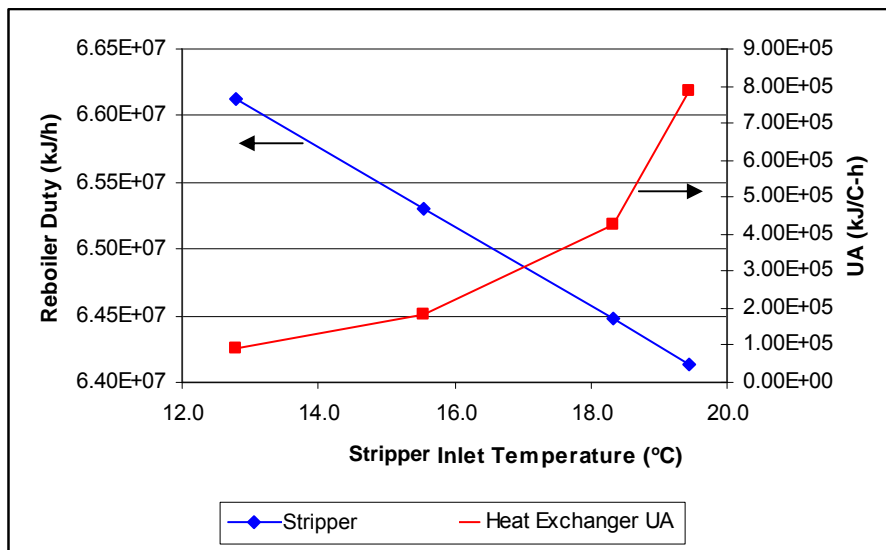


Figure 3-3. Optimization of the stripper inlet temperature.

The changing of the column pressure affected the reboiler duty and the compression power for the overhead stream and the pumping energy demand for the bottom stream of the stripper column. Lower column pressure required less reboiler duty, however, the compression and pumping horsepower increased. The optimum number of ideal stages in the stripper struck a balance between the reboil ratio and the increased capital cost.

Figure 3-4 and Figure 3-5 present the optimization of the column pressure and the number of ideal stages of the stripper column, respectively. A stripper at the upfront location of the flowsheets was also established in the HRH2 and amine2 processes. However, the specifications used to solve the column were different. The bottom specification in the stripper column was set at the same value with the bottom specification of the DEC3 column. This was because these two bottom streams were mixed and sent as the feed to DEC4.

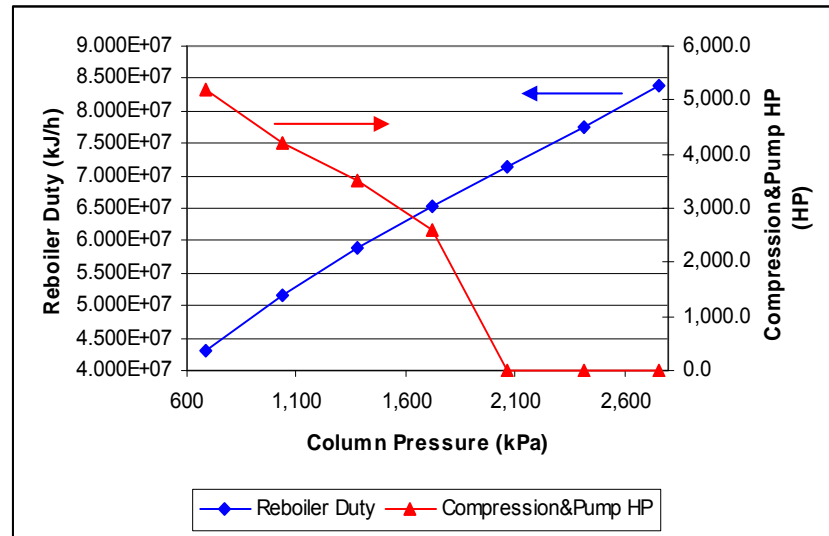


Figure 3-4. Optimization of the stripper column pressure.

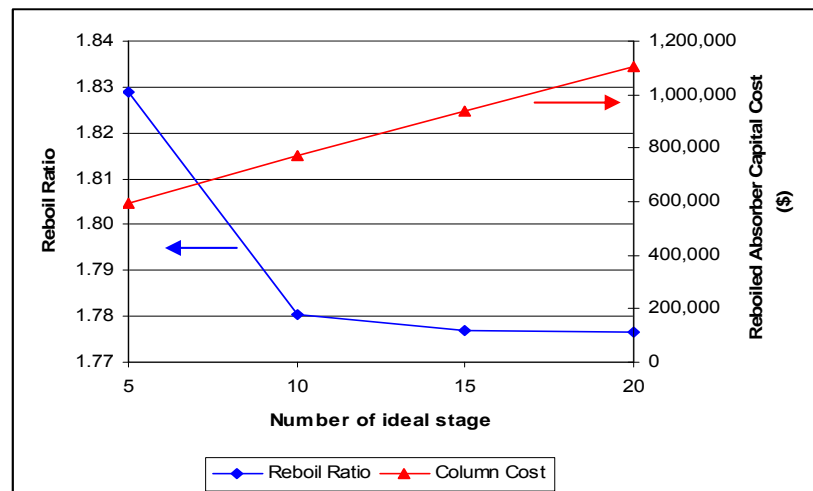


Figure 3-5. Optimization of the number of ideal stages in the stripper.

The stream from the overhead of the stripper column was subsequently sent to the dehydration system in the RH and HRH processes while in the amine process, the stream was sent to the acid gas removal process. However, the bottom stream of the

stripper was mixed with the bottom product of DEC3 and sent to the DEC4 in all cases.

After dehydration, the stream then entered the fractionation processes, starting with the DEC1. The CO₂ specification in the overhead of DEC1 for Feed2 was set at 85 ppm. This value was higher than the spec in the Feed1 process because the overhead stream generated was mixed with high purity ethane and propane products (CO₂ impurity of 5 ppm-mole). In contrast, the C2 and C3 product from the overhead of the SR column in RH1 process contained 350 ppm-mole CO₂. However, the C1 fraction in the bottom stream was kept at a value of 0.08%-mole.

The bottom stream from the DEC1 was subsequently sent to the azeo column where the separation of CO₂ from the remaining hydrocarbon was performed in an extractive distillation process. A 40 ppm-mole CO₂ fraction in the bottom product of the azeo column was specified for Feed1 while a CO₂ spec of 0.8 ppm was used for Feed2. A tighter CO₂ spec for Feed2 was necessary to ensure that the CO₂ impurity limit in the C2 product, separated in the subsequent column, was below the maximum threshold (<10 ppmw). The result shows that it was achievable with a reflux ratio of 1.59 and sensible reboiler and condenser duties in the azeo column of RH2 process. In the overhead stream, a higher than 99%-mole CO₂ purity was required as a product; however, the overhead specification used was the C2 impurity instead of the CO₂ purity to observe the separation effectiveness of the CO₂-ethane azeotrope with variable solvent composition. When the solvent amount was added, for example, the C2 fraction in the CO₂ product overhead might be the same, but the CO₂ purity decreased due to the increased solvent amount carried over in the CO₂ product. The same result observed when the solvent inlet stage was higher in the column. Consequently, the generated CO₂ might have purity less than 99% when the optimization of the design variables such as the solvent amount and the solvent inlet stage was performed. Thus, a frequent check on the CO₂ purity was required. A C2 fraction of 0.65%-mole and 0.30%-mole in the overhead was used for Feed1 and Feed2, respectively. Figure 3-6 presents the optimization of the C2 specification at the azeo column overhead in the RH1 process. A higher C2 fraction in the overhead CO₂ product was definitely easier to obtain and thus lower reflux ratio and solvent

amount were required. However, a decrease in CO₂ purity was observed. Figure 3-6 shows that the 99% CO₂ purity was achieved with the 0.65% C2 specification.

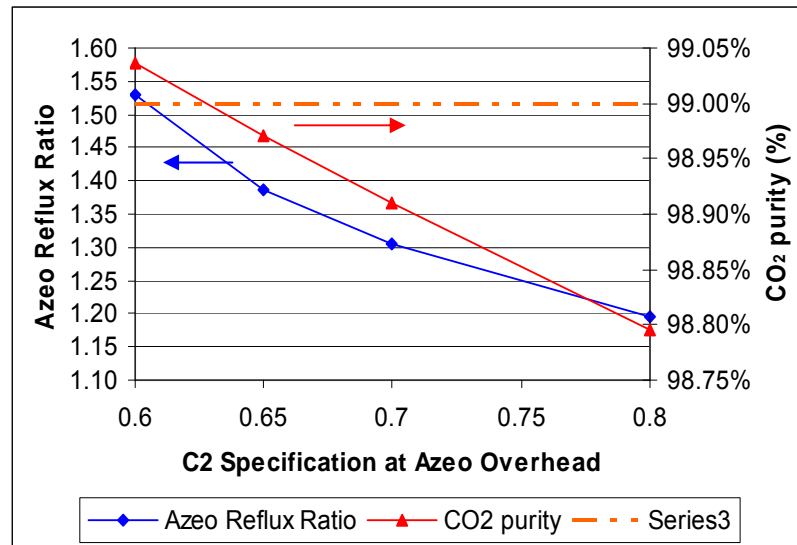


Figure 3-6. Optimization of C2 specification at the azeo column overhead of RH1.

The next column in the RH1 process was the SR column. The main objective of the SR column was to generate the recycle solvent used in the DEC1 and azeo columns. It is important to control the bottom specification of the SR column to maintain the extractive distillation performance during upset conditions because it dictates the composition of the solvent (Grassi 1992). Therefore, the C4 spec in the overhead and C3 spec at the bottom were used in the SR column to control the solvent composition.

Table 3-8 shows the optimization result of these two specifications in the SR column. It was observed that the optimized C4 spec in the overhead stream involved a trade-off between the reduced operational costs due to the lower reflux ratios at higher C4 spec with the decreased sellable condensate product. However, the sensitivity of the C4 spec in the SR column overhead on the IRR was trivial in the range observed. In contrast, the C3 spec was more sensitive to the IRR because this value directly determined the solvent composition and hence affected the separation in DEC1 and azeo columns, especially the CO₂ product purity. From this table, the optimum specification for the SR column is 0.5% C3 at the bottom and 0.5% C4 at the overhead to meet the CO₂ purity requirement and maximize IRR.

Table 3-8. Effect of C3 and C4 specs in SR column on IRR – RH1 process.

C3 Spec in SR column bottom	C4 Spec in SR column overhead			CO ₂ product purity
	0.25%-C4	0.5%-C4	1%-C4	
0.5%-C3	8.631%	8.634%	8.633%	± 99.0%
1%-C3	8.668%	8.675%	8.670%	± 98.9%
5%-C3	8.742%	8.742%	8.734%	± 98.6%
10%-C3	8.771%	8.771%	8.766%	± 98.2%

In the RH2 process, a series of columns is used downstream of the azeo column to produce NGL products and the solvent. This was because the bottom stream of the azeo column still contained significant amounts of heavy hydrocarbons (C3+ components, up to C10) to be recovered. The DEC2, DEC3, and DEC4 were required to generate the commercial hydrocarbon products. The specifications used were set to meet the product requirement described in Table 3-1 with minimum energy requirement. For example, the C3 spec in the overhead of the DEC2 was set at 6% following the high purity ethane product requirement, while for the bottom product, a 0.22% C2 spec was set to generate a C3 product having a vapor pressure of less than 1330 kPag at 37.8°C. A summary of the specifications used in the RH process is presented in Table 3-9.

Table 3-9. Summary of column specifications (%-mole) for RH process.

	Feed1	Feed2
DEC1	Overhead (OH): 60 ppm CO ₂ Bottom (B): 0.08% C1	OH: 85 ppm CO ₂ B: 0.08% C1
Azeo	OH: 0.65% C2 B: 40 ppm CO ₂	OH: 0.3% C2 B: 0.8 ppm CO ₂
SR	OH: 0.5% C4 B: 2% C3	-
DEC2	-	OH: 6% C3 B: 0.22% C2
DEC3	-	OH: 1.5% C4 B: 6% C3
DEC4	-	OH: 1% iC5 B: RVP = 68.95 kPa

3.3.3. Optimization and Sensitivity Analysis of the HRH Process

This section explains in detail the HRH process optimization and the sensitivity analysis for both Feed1 and Feed2. The HRH process differs from conventional RH in that no solvent stream is sent to the azeo column and therefore the azeo column

overhead is a CO₂-ethane azeotrop (Figure 2-9 and Figure 2-10). In addition, the removal of solvent from the azeo column came with an additional cost for a C2 recovery column for Feed1 process and a membrane system for both Feed1 and Feed2.

In the HRH process, similar to the standard RH, the methane was removed in the DEC1. The specifications used to optimize DEC1 were the same as the RH process. The bottom stream from the DEC1 contained mainly the CO₂ and was sent to the azeo column. The specifications in the azeo column for the HRH1 process were 40 ppm CO₂ in the bottom stream and 1.2% C3 in the overhead product. The CO₂ specification was the same as in the RH process and the C3 requirement in the overhead stream was obtained from the economic optimization. A higher C3 fraction in the overhead required a lower reflux; however, C3 loss in the CO₂ product increased and thus reduced the condensate sales revenue. However, the CO₂ product purity appeared to be constant, regardless of the increasing C3 fraction sent to the overhead, as a result of the membrane separation. It was also observed that when a higher fraction of C3 was specified for the azeo column overhead, the compositional fraction of C5 in the solvent increased gradually and this prompted a higher solvent demand for the DEC1 to avoid CO₂ freezing. The optimization result is presented in Table 3-10 and Figure 3-7.

Table 3-10. Effect of C3 fraction in the azeo overhead on solvent composition and C3 Loss – HRH1 Process.

C3 Spec in Azeo OH (%)	0.05	0.1	0.2	0.4	0.8	1.2	1.3	1.4
Solvent Composition								
mole fraction C3	0.0100	0.0100	0.0100	0.0100	0.0100	0.0100	0.0100	0.0100
mole fraction iC4	0.3272	0.3274	0.3266	0.3258	0.3270	0.2279	0.1737	0.1305
mole fraction nC4	0.3517	0.3516	0.3520	0.3525	0.3516	0.4027	0.3305	0.2055
mole fraction iC5	0.3110	0.3110	0.3114	0.3117	0.3114	0.3594	0.4857	0.6540
%C3 loss	0.008%	0.016%	0.032%	0.065%	0.131%	0.197%	0.214%	0.234%

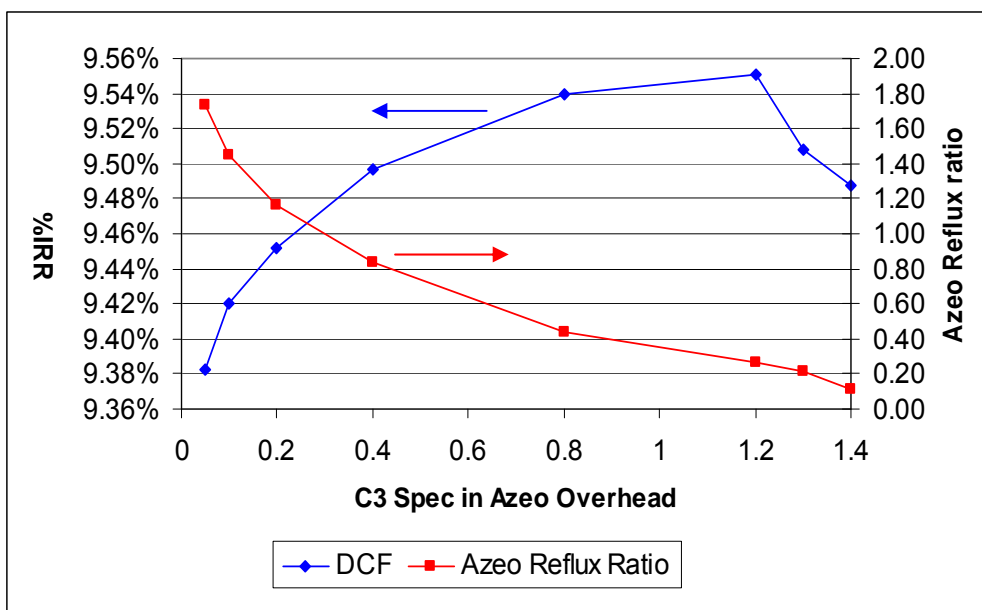


Figure 3-7. Sensitivity of C3 spec in azeo overhead on IRR for HRH1 process.

Different specifications were used in the azeo column of the HRH2 process. C2 and C3 specifications were utilized since the C2 amount in the C3 product, generated in the subsequent column, was constrained. The C2 fraction at the bottom was set at 1% to obtain the C3 product with a vapor pressure of less than 1434 kPag at 37.8°C. The C3 fraction in the overhead was economically optimized with a maximum IRR obtained at 0.05 mole % C3. The variation of the C3 fraction involved trade offs between the decreased reflux ratio and column diameter as well as the decreased revenue from the C3 product sales. However, the sensitivity of this specification on the IRR was not significant as shown in Table 3-11.

Table 3-11. Optimization of C3 fraction in the overhead of azeo column – HRH2 process.

C3 Fraction (%-mole)	0.025	0.05	0.1	0.2	0.4	0.8
IRR	14.31%	14.39%	14.32%	14.24%	14.24%	14.22%

The overhead stream from the azeo column was CO₂-ethane azeotrope and this stream was sent to the membrane system. Membrane area and permeate pressure variations were studied to achieve comparable purity and recovery conditions with the RH process. The pressure drop in the high pressure side was assumed to be 34.5 kPa. This pressure drop is actually nominal and does not exceed 172 kPa (Coady and

Davis 1982; Russell and Coady 1982). The discussion on the membrane system setup is presented in section 2.3.

The retentate from the membrane system was sent to the C2 recovery column. The retentate streams from the membrane stage 1 and stage 2 still contained approximately 85% of C2 in total. The products generated from this column were a CO₂-ethane azeotrope in the overhead and a high purity ethane at the bottom. A CO₂ fraction of 40 ppm and 8 ppm at the bottom stream were determined for HRH1 and HRH2, respectively. A less stringent spec for the HRH1 was adequate because this bottom product was mixed with the LNG stream to increase the LNG heating value while in the HRH2 process, the bottom product was sold as a high purity ethane. The second specification used for the C2 recovery column was the condenser temperature. The purpose was to control the condensing temperature level. The overhead temperature selection affected the azeotrope composition in the overhead. Higher overhead temperature related to higher C2 fraction in the overhead, lower reflux ratio, and warmer refrigerant temperature. In the optimization process, the minimum approach of the overhead stream temperature to the refrigerant temperature in the C2 recovery column condenser was kept constant at 2.8°C. The optimized temperature specifications were -16.7°C and -12.2°C for Feed1 and Feed2, respectively.

The last column required in the HRH1 process was the solvent recovery (SR) column. Again C3 and C4 specifications utilized in the SR column were optimized to obtain a maximum IRR. The results were 1 mole % C3 and 1 mole % C4 in the bottom and overhead, respectively. Similar to the optimization of the C4 spec in the SR overhead of RH1 case, the result was generated from an optimized trade off between the lower reflux ratio in the SR column and the decreased production of sellable condensates. A higher C3 fraction in the bottom stream required a lower reflux ratio in the SR column; however the offsets were higher reflux ratios in the DEC1 and azeo columns.

The HRH2 process had two additional fractionation columns which were the DEC3 and DEC4 columns. These columns generated C3, C4, and condensate commercial products. The specifications used in these columns were set to the maximum

permissible value, typical for commercial production, presented in Table 3-1. A summary of the specifications used in the HRH process are presented in Table 3-12.

Table 3-12. Summary of column specifications (%-mole) for HRH process.

	Feed1	Feed2
DEC1	Overhead (OH): 60 ppm CO ₂ Bottom (B): 0.08% C1	OH: 85 ppm CO ₂ B: 0.08% C1
Azeo	OH: 1.2% C3 B: 40 ppm CO ₂	OH: 0.05% C3 B: 1% C2
C2 Recovery Column	OH: Temperature -16.7°C B: 40 ppm CO ₂	OH: Temperature -12.2°C B: 8 ppm CO ₂
SR	OH: 1% C4 B: 1% C3	-
DEC3	-	OH: 1% C4 B: 6% C3
DEC4	-	OH: 1% iC5 B: RVP = 68.95 kPa

3.3.4. Column Pressure and Solvent Properties.

After the specifications in the columns were set, the other design variables were then optimized in terms of economics. The design variables examined were column pressure, number of ideal stages, feed and solvent location, solvent temperature, and solvent amount. The change in the dependent operating parameters, which affected the IRR value, is discussed below.

1. Column pressure.

After the separation specifications in the distillation processes were decided, the column pressure was then determined. The selection of column pressure is usually controlled to allow the use of air cooling or water cooling in the overhead condenser. However, when the separation of the key components is accomplished in the low temperature region, the use of refrigerant is inevitable. The bottom pressure was generally estimated at 69 kPa higher than the condenser pressure. (Seider, Seader, and Lewin 2004). Therefore, a pressure drop of 69 kPa was fixed in all of the distillation columns.

As the column pressure in the DEC1 varied, there were conflicting variables that contributed opposite effects to the IRR. A higher column pressure required higher reflux ratio due to the lower relative volatility between the key components. However, a lower solvent demand was required to maintain the ΔT approach to the CO₂ freezing temperature above 5.5°C (Figure 3-8 and Figure 3-9). This in turn affected the capital cost due to the smaller columns required in the subsequent processes. In addition, higher pressure also allowed warmer condensing temperature in the DEC1 condenser, and thus reducing the refrigeration fuel consumption.

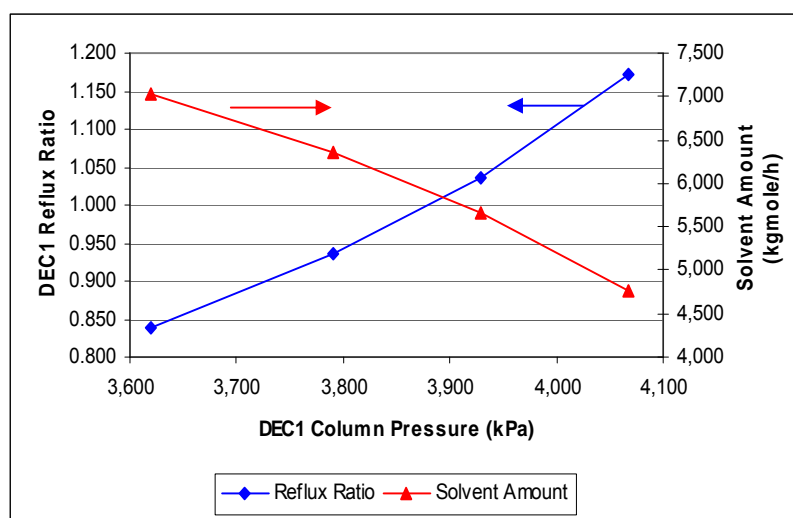


Figure 3-8. Effect of DEC1 column pressure on reflux ratio and solvent demand (ΔT Freeze \pm 5.5°C) – RH1 Process.

It was observed that for Feed1, the highest possible pressure at 4068 kPa was the optimum point. This was the maximum feasible pressure for DEC1 as the methane critical pressure (4596 kPa) was approached at higher pressure. On the other hand, the increased reflux ratio was dominant over the other factors at higher pressure for Feed2. The optimized DEC1 column pressure for Feed2 was 3620 kPa.

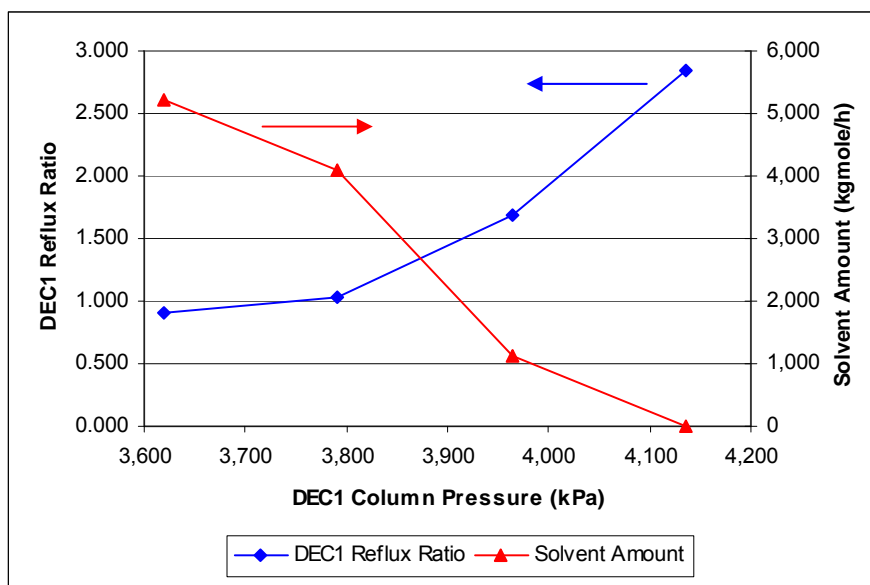


Figure 3-9. Effect of DEC1 column pressure on reflux ratio and solvent demand (ΔT Freeze $\pm 5.5^\circ\text{C}$) – HRH2 Process.

It was also discovered that no solvent was required for Feed2 gas when the DEC1 was operated at 4137 kPa. This result confirmed the conclusion that the rich feed mixtures are more capable of handling high CO_2 feed than the lean mixtures (Fernandez et al. 1991). The DEC1 column setup for both feeds was similar; however, it was observed that the solvent composition entering the DEC1 was quite different. The solvent in Feed2 contained more C3 and C4 components than the solvent in Feed1 case. A further study on the solvent composition is presented in Chapter 4.

The column pressure optimization for other columns showed a similar trade off. The optimum column pressure was obtained at a balance between the advantages of lower reflux ratio and column diameter against the cooler condensing temperature as pressure was decreased. It was also important to note that the minimum temperature approach in the condenser was maintained at a constant value during the optimization process and therefore the effect of varying pressure on the refrigerant duties was included.

Figure 3-10 shows the optimization of the azeo column pressure in the HRH2 process. In the HRH process, a lower column pressure in the azeo column also reduced the CO₂ recovery due to the lower driving force in the membrane process.

The SR column pressure in the HRH1, and the DEC3 and DEC4 column pressures in the amine2, RH2, and HRH2 processes were set to have air cooling condensers in the column overhead. Table 3-13 shows the column pressure of the distillation columns.

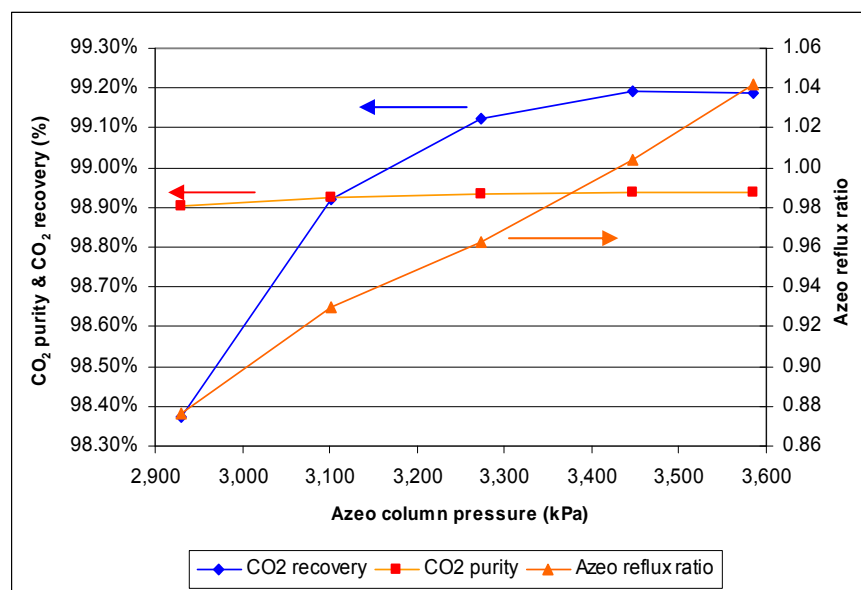


Figure 3-10. Optimization of azeo column pressure - HRH2 process.

Table 3-13. Summary of column pressure.

Column Pressure (kPa)	Amine1	RH1	HRH1	Amine2	RH2	HRH2
DEC1	-	4068	4068	3689	3620	3792
Azeo	-	2758	3378	-	2275	3275
SR	-	1551	2916	-	-	-
C2 Recovery Column	-	-	2620	-	-	2758
DEC2	-	-	-	2068	1689	-
DEC3	-	-	-	1600	1655	1675
DEC4	-	-	-	593	565	579

2. Number of ideal stages (N) and feed inlet location (Nf)

The optimization result of the number of the ideal stages and the feed inlet location demonstrated that these factors had small effects on the IRR value. The optimum N hit the balance between the reflux ratio and column capital cost. The optimum Nf was related to the near optimum reflux ratio. The example of the optimization procedure of the number of ideal stages and feed inlet location is presented in Table 3-6. The results for all cases are summarized in Table 3-14

Table 3-14. Number of ideal stages and feed inlet location.

N/Nf	Amine1	RH1	HRH1	Amine2	RH2	HRH2
DEC1	-	45/26	45/21	16/5	55/22	55/22
Azeo	-	70/38	70/49	-	85/38	75/33
SR	-	35/16	35/12	-	-	-
C2 Recovery Column	-	-	40/7	-	-	70/4
DEC2	-	-	-	30/18	25/10	-
DEC3	-	-	-	20/9	30/16	35/20
DEC4	-	-	-	25/6	12/8	10/3

3. Solvent inlet location

In this section, the solvent inlet location for the RH and HRH processes will be discussed. Solvent was required in the DEC1 and azeo columns for the RH process and only in the DEC1 column for the HRH process. In the DEC1, the optimized solvent inlet stage was near the top of the column as a lower solvent inlet stage required a higher reflux ratio. However, caution should be exercised especially when the solvent temperature was warmer than the temperatures in the upper column because it increased the temperature in the DEC1 overhead stream. A higher overhead stream temperature needed more cooling duty requirement in the liquefaction process. The alteration of the solvent inlet position changes the reflux ratio, the overhead temperature, the ΔT freeze approach to CO₂ freezing temperature, and also the LNG Btu value generated. The optimized solvent inlet location for the DEC1 was found at stage 1 from the top for RH1, HRH1, and HRH2; however the optimized solvent location for RH2 was at the condenser. In RH2 process, when the solvent inlet location was at the condenser, the generated LNG Btu value was relatively higher than when the Ns was at lower stages. Thus, the C3 stream added to

produce the LNG was reduced and consequently generated more C3 product.

Figure 3-11 shows that the variation of the solvent inlet stage in the azeo column of the RH2 process. The solvent inlet location affects the azeo reflux ratio and the solvent impurity level in the overhead. A lower solvent inlet location required a higher reflux ratio; however, the solvent loss in the CO₂ product was decreased and offset the disadvantage of the increased reflux ratio. The resultant solvent inlet stage was dictated by the maximum solvent limit in the CO₂ product rather than the economics because the economics were virtually steady as shown in Figure 3-12.

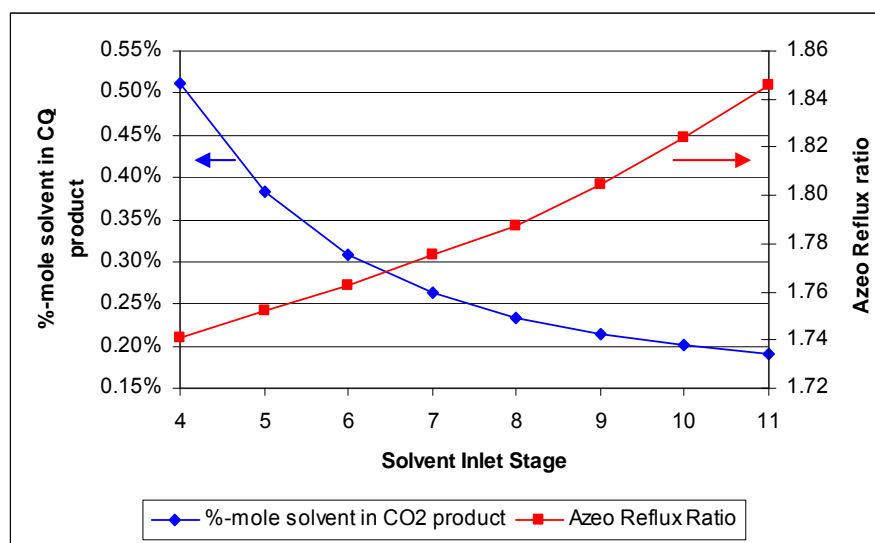


Figure 3-11. Effect of solvent inlet stage for RH2 process.

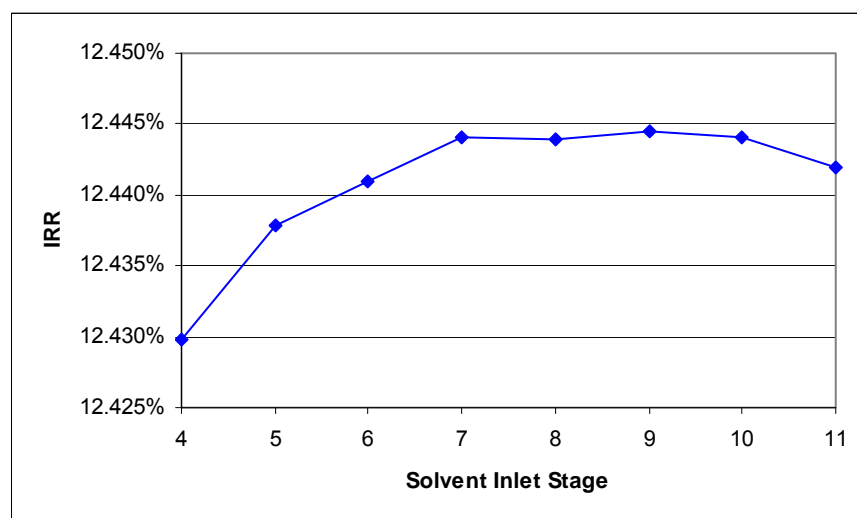


Figure 3-12. Effect of solvent inlet stage on IRR for RH2 process.

4. Solvent temperature

The selection of solvent temperature to be used in the DEC1 mainly related to the trade off between the reflux ratio and the additional refrigeration duty and heat exchanger capital cost for solvent cooling. With a lower solvent temperature, the reflux ratio and condenser duty required were reduced, but the additional refrigeration duty and heat exchanger area for solvent cooling were increased. However, these effects on the total energy demand and economic cost were marginal and therefore, the sensitivity on IRR was also insignificant (Figure 3-13). The effect of this factor on the ΔT to CO₂ freezing temperature in DEC1 was negligible.

A similar result for the solvent temperature in the azeo column was observed. It was the balance between the reflux ratio and the additional refrigeration and capital costs that determined the optimum solvent temperature. Figure 3-14 shows the optimization of solvent temperature in the azeo column for the RH2 process.

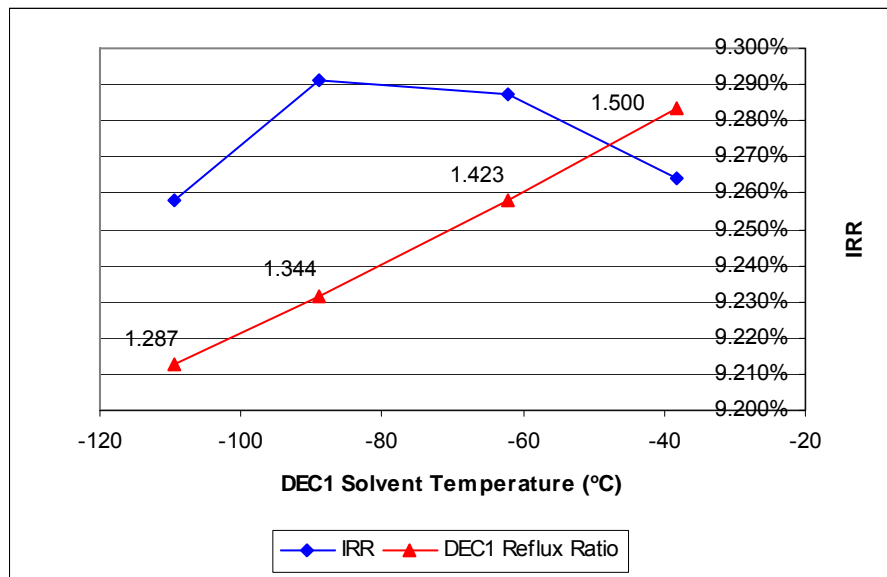


Figure 3-13. Effect of DEC1 solvent temperature on IRR and DEC1 reflux ratio - HRH1.

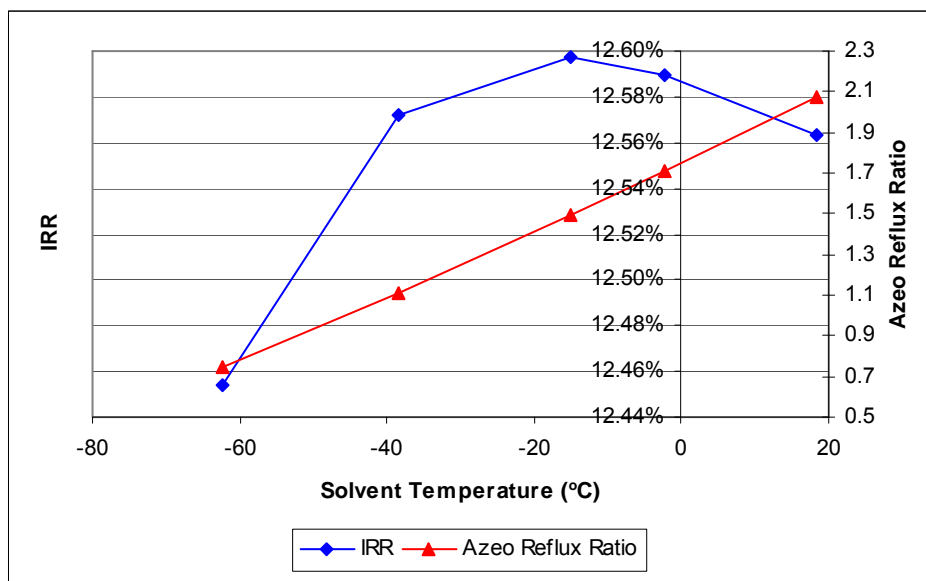


Figure 3-14. Effect of azeo solvent temperature on IRR and azeo reflux ratio - RH2 process.

5. Solvent pressure

Solvent pressure was supplied at the required delivery pressure to the DEC1 and azeo columns.

6. Solvent amount

The required solvent amount in the DEC1 and azeo columns was dependent on different constraints. In the DEC1, the solvent amount was constrained by the minimum 5.5°C approach to the CO₂ freezing temperature. In the azeo column, a minimum solvent amount was necessary to break the CO₂-ethane azeotrope. Consequently, the solvent quantity optimization in the DEC1 column was dictated by the minimum approach temperature constraint whereas the solvent rate in the azeo column was adjusted above its minimum to achieve the maximum economic value. Furthermore, an increase in solvent amount for the DEC1 was a solution anytime a variation in design variable decreased the ΔT freeze to CO₂ freezing point below 5.5°C (10°F). In contrast, the addition of solvent quantity to the azeo column reduced the CO₂ purity when all the other design variables were kept at the initial condition (Figure 3-15).

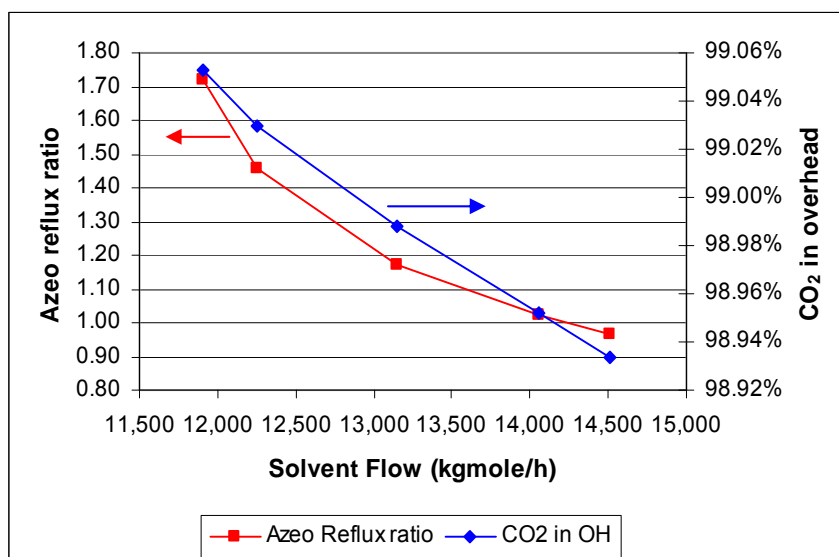


Figure 3-15. Effect of solvent flow on reflux ratio and CO₂ purity in the overhead of the azeo column.

The solvent demand in the DEC1 is dictated by the minimum approach to the CO₂ freezing temperature with variation of the feed composition, column pressure, and solvent composition. A lower solvent amount is required in the DEC1 when the feed composition contains lower fractions of CO₂. On the other hand, the optimum solvent demand in the azeo column is not only dependent on the feed composition, column pressure, and solvent composition but also directly related to the reflux ratio applied in the column. With fixed column specifications, as the solvent rate increased, the reflux ratio decreased. However, the increased solvent rate required bigger column diameters for the azeo and subsequent fractionation columns.

It was also observed that the interaction between the design variables affected the IRR. Figure 3-16 shows the solvent amount variations at temperatures of -11°C and 18°C in the azeo column. It is shown that in general, a lower solvent temperature gave higher IRR. However, it is also observed that a higher IRR was obtained with a lower solvent quantity at -11°C than at 18°C. Also, the change in IRR is more sensitive with variation in solvent amount than in the solvent temperature although with a solvent flow in the range of 13000 to 14000 kgmole/h, the IRR sensitivity is trivial.

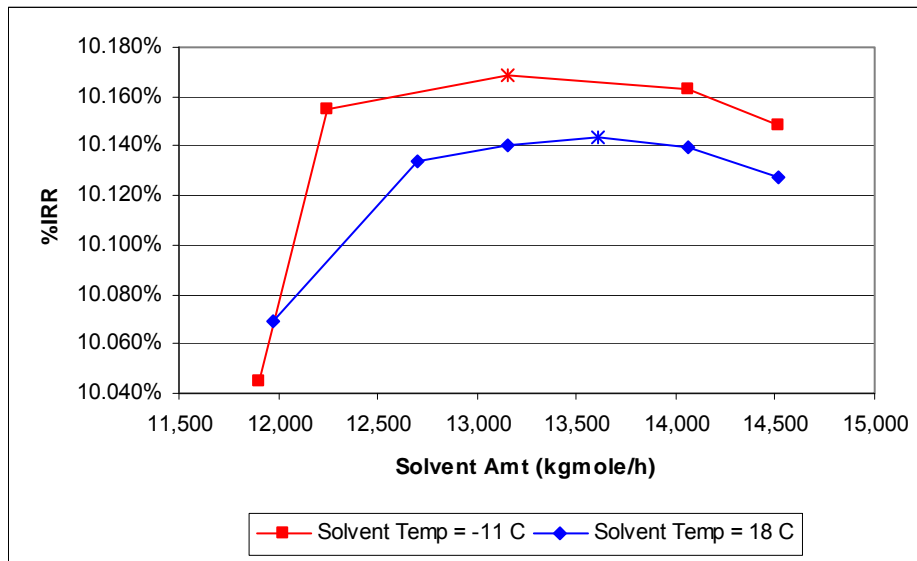


Figure 3-16. Interaction between solvent temperature and solvent amount in the azeo column improved IRR.

3.4. Effect of Minimum Approach Temperature

The closed cascade refrigeration system used propane, ethylene, and methane in a decreasing temperature scheme respectively as shown in Table 3-15 below:

Table 3-15. Cooling temperature range in the cascade refrigeration cycle.

Condensing Agent	Condensing Temperature Range
Propane	11 to -39 °C
Ethylene	-66 to -96 °C
Methane	-102 to -141 °C

The schematic diagram of the cascade refrigeration system is shown in Figure 3-17 respectively.

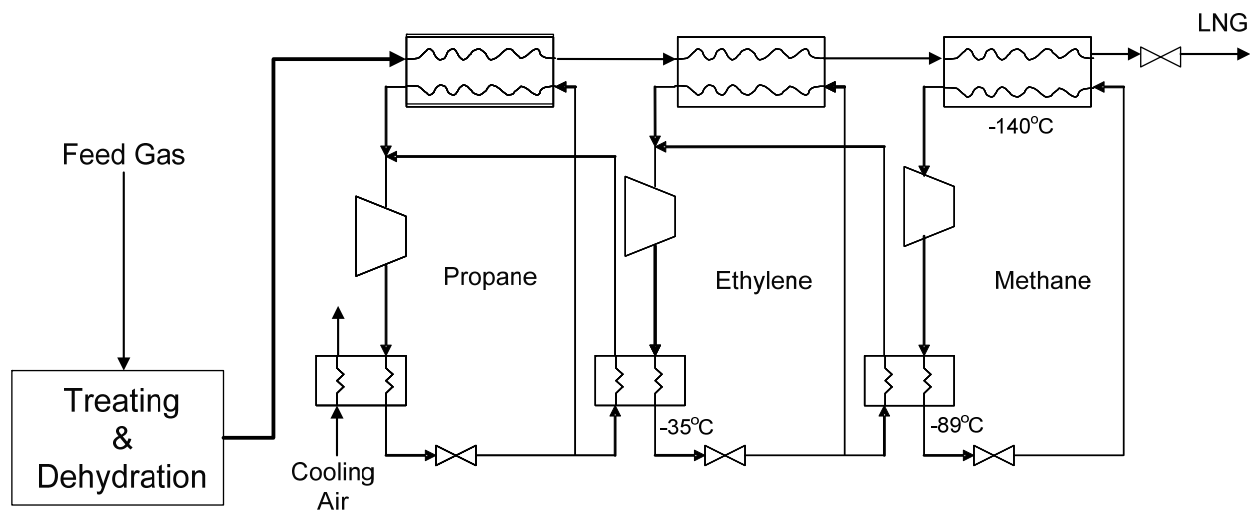


Figure 3-17. Schematic diagram of the cascade refrigeration system.

In this study, there were mainly two design variables in setting up the refrigeration system, i.e.: the refrigeration temperature level and the minimum approach temperature in the heat exchanger at each temperature level. When the refrigeration temperature level was fixed at a certain value, the minimum approach was varied and the process temperature was calculated from the difference. On the other hand, when the minimum approach temperature was examined, the refrigerant temperature was altered to observe the optimum minimum approach temperature. The example of the minimum approach temperature optimization procedure for propane refrigerant stage-1 is presented in Table 3-16.

Table 3-16. Example of the minimum approach temperature optimization for the propane refrigerant stage1 – RH1 process.

Refrigerant Temp (oC)	-42	-42	-42	-42	-42
Minimum Approach (oC)	3.3	4.4	6.7	8.9	11.1
Stream Temp (oC)	-38	-37	-35	-33	-31
IRR	10.673%	10.727%	10.745%	10.682%	10.556%

Other factors contributing to the optimal cycle configuration such as the distribution of refrigeration demand, the number of refrigeration levels, relative weights of

operating and capital costs (Barnes and King 1974) were not included. The refrigeration temperature level was set to be the same between the alternative processes to have an accurate energy comparison. However, when the refrigerants were used in the overhead condensers where the process temperatures were set by optimizing the operational column pressures and also at the last stage of the liquefaction where the temperature was adjusted to match the fuel requirement, only the minimum temperature approach was optimized.

The minimum approach temperature in the heat exchangers for the same refrigeration stage was kept the same. Table 3-16 shows various refrigeration loads for each refrigerant and Figure 3-18 shows the schematic diagram of the propane refrigeration cycle in the RH1 process. The study of minimum approach temperature effect on IRR was conducted with two methods:

1. When the refrigerant temperature level was dictated by the condensing temperature in the distillation columns, only the minimum approach temperature optimization was conducted. For example at the 2nd stage of the propane refrigerant (Figure 3-18) and at the 2nd stage of the ethylene refrigerant. The 2nd stage of propane refrigerant temperature was determined by the azeo and SR condensing temperature and the 2nd stage of ethylene refrigerant was controlled by the DEC1 condensing temperature.
2. For the other temperature stages, the refrigerant temperature level and the minimum approach temperature were optimized. It should be noted that these optimizations were conducted for the RH process only. The other process alternatives utilized the same temperature level and minimum approach temperature.
3. For the 2nd stage of methane refrigerant, the temperature level was set 1.1°C lower than the process temperature. The process temperature was set to meet the fuel requirement of the plant in each case. The process temperature was higher to generate more fuel. A higher process temperature produced more vapour phase to the fuel system when this stream was expanded to a near atmospheric pressure.

Table 3-17. Refrigeration utilization in process flowsheet.

	Refrigeration function	Feed1			Feed2		
		Amine	RH	HRH	Amine	RH	HRH
Propane Refrigerant							
1 st stage	1. Solvent Cooling		X	X		X	X
	2. Ethylene Condensing	X	X	X	X	X	X
	3. LNG liquefaction	X			X	X	X
2 nd stage	1. Azeo Condenser			X			X
	2. Solvent Cooling						X
	3. LNG liquefaction						X
3 rd stage	1. Solvent Cooling		X	X		X	X
	2. Ethylene Condensing	X	X	X	X	X	X
	3. LNG liquefaction	X		X	X	X	X
	4. Azeo Condenser		X			X	
	5. SR/DEC2 Condenser		X		X	X	
	6. C2 Recovery Cond			X			X
4 th stage	1. Solvent Cooling		X	X		X	X
	2. Ethylene Condensing	X	X	X	X	X	X
	3. LNG liquefaction		X	X	X	X	X
	4. DEC1 Feed		X	X		X	X
Ethylene Refrigerant							
1 st stage	1. Solvent Cooling		X	X		X	X
	2. LNG liquefaction	X	X	X	X	X	X
2 nd stage	1. DEC1 Condenser		X	X	X		
3 rd stage	1. Solvent Cooling		X	X		X	X
	2. LNG liquefaction	X	X	X		X	X
	3. Methane Condensing	X	X	X	X	X	X
	4. DEC1 Condenser					X	X
Methane Refrigerant							
1 st stage	1. LNG liquefaction	X	X	X	X	X	X
2 nd stage	1. LNG liquefaction	X	X	X	X	X	X

Finding the best minimum temperature approach involves a trade-off between the fuel requirement and the heat exchanger area capital cost. Therefore, it is strongly

influenced by the fuel calculation and the heat exchanger capital cost estimation. In principal, having a tight minimum approach temperature in heat exchangers allows for a higher heat recovery between the related hot and refrigerant streams and thus associates with less utility and lower fuel demand, however, the heat exchanger area requirement is higher. The heat exchanger capital cost was evaluated as a function of heat exchanger area, type, and material of construction. The heat exchanger capital cost formula was adopted from Chevron internal reference data as shown in Figure 3-19 and Figure 3-20. These two figures were the basis for all of the heat exchanger cost calculation. The heat exchanger cost was calculated on the basis of the heat exchanger area, type of heat exchanger (BEM or NKN/kettle type), and material (CS, SS, and A516).

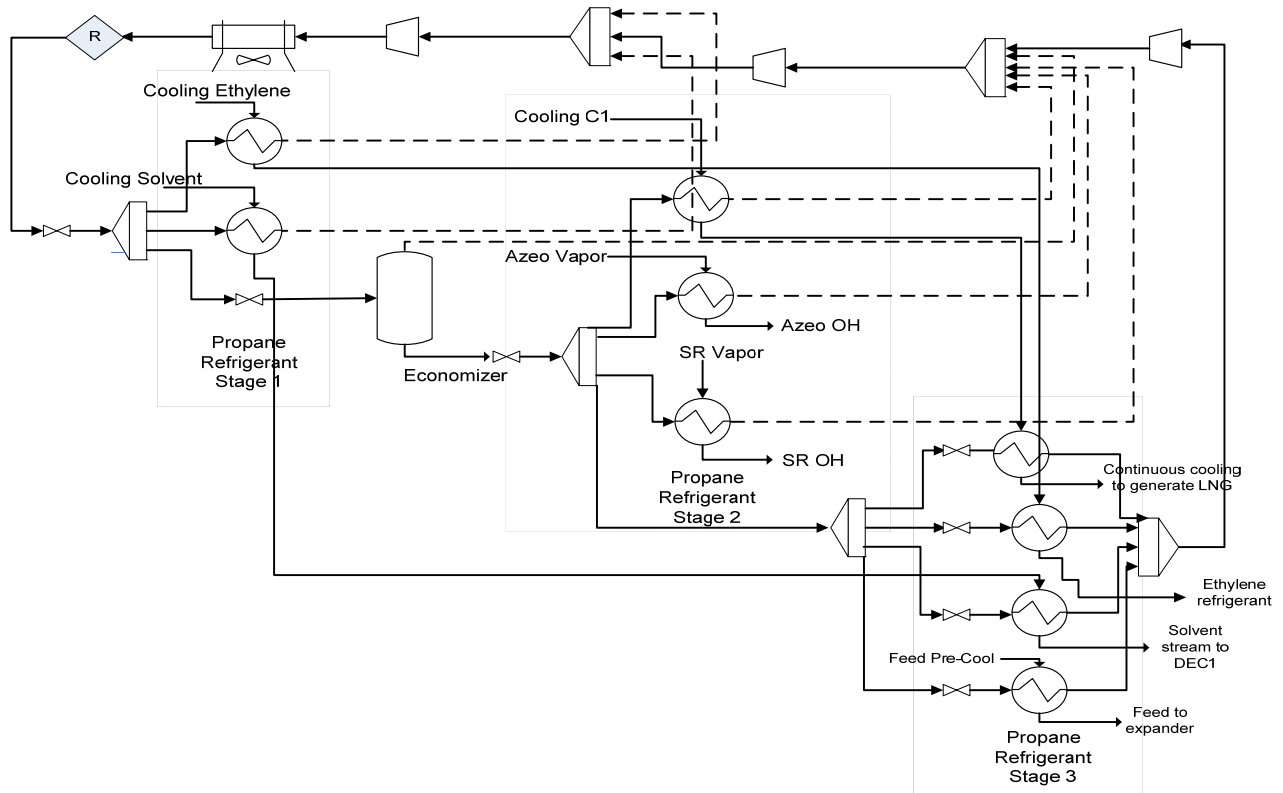


Figure 3-18. Schematic diagram of the propane refrigeration cycle – RH1 process.

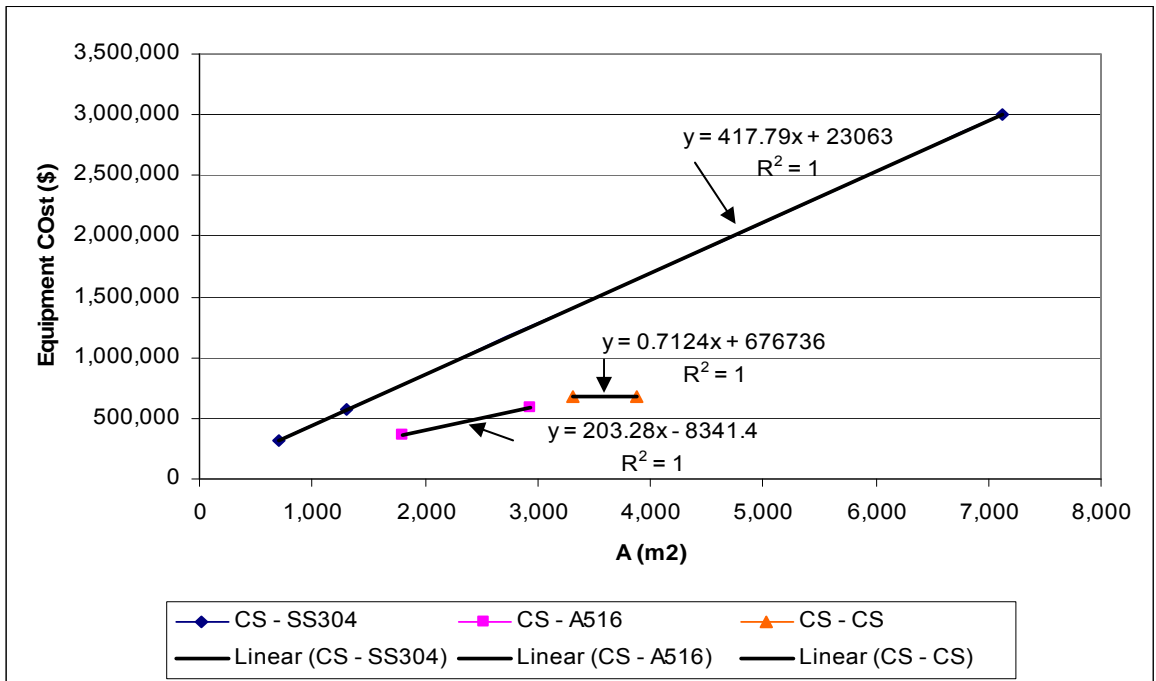


Figure 3-19. Cost estimation of the BEM type heat exchanger.

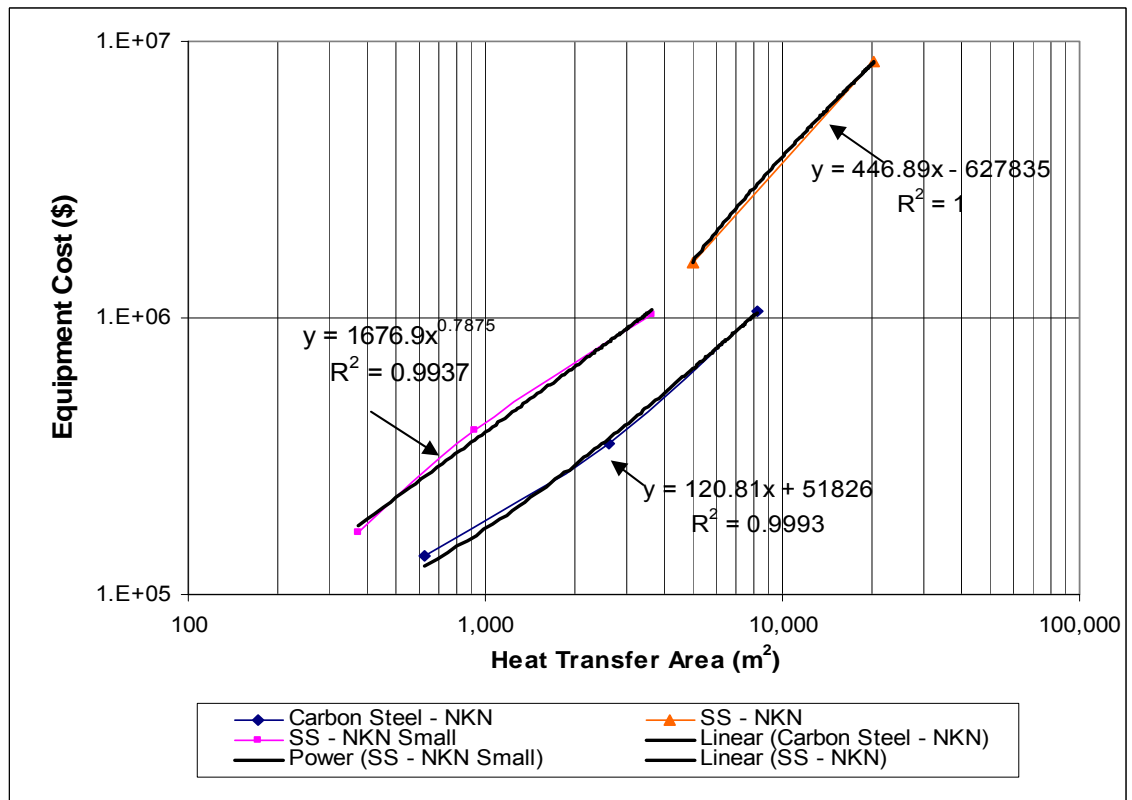


Figure 3-20. Cost estimation of the NKN type heat exchanger.

Figure 3-21 presents an optimization example of the refrigerant temperature level and minimum approach temperature of the 1st stage of propane refrigerant. It was observed that both variables have a noticeable effect on IRR. Similar optimization simulations were conducted for the 1st stage of ethylene and methane refrigerants.

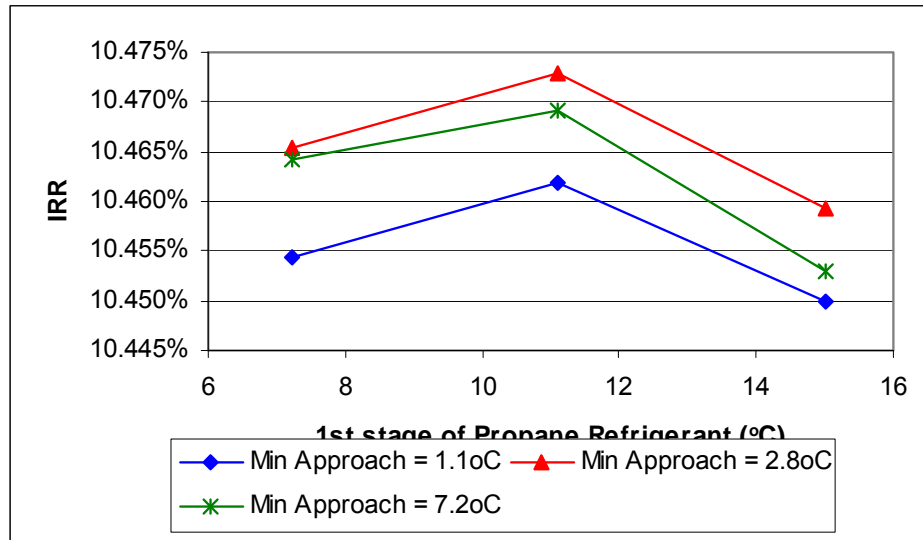


Figure 3-21. Optimization of refrigeration temperature level and minimum temperature approach of the 1st stage of propane refrigerant.

At the 2nd and 3rd stage of propane refrigerant (Figure 3-18), the stream temperature was defined from the optimization of the azeo and SR or DEC2 column pressure. Therefore, only the minimum approach temperature was optimized to fix the refrigerant temperature. In the RH1 process, the azeo and SR condenser temperatures were set at the same value was to have a same compressor stage in the refrigeration system and thus a same refrigerant temperature level was used to condense these streams. The result for the RH1 process is presented in Figure 3-22.

The last (4th) stage of propane refrigerant was used to cool the solvent going into the DEC1, final step of ethylene condensing, liquefy LNG, and cool the DEC1 feed. Initially, the process stream temperatures were fixed. Then the refrigeration temperature level was manipulated to achieve variable minimum approach in the heat exchanger. However, for the propane refrigerant at -39°C, this was the minimum possible temperature due to the acceptable compressor intake which was slightly above the atmospheric pressure. Therefore, to study the variable temperature approach, the process temperature was manipulated. The heat exchanger area was not

observed in this study. The results showed that caution should be exercised in optimizing the operating stream temperatures because with higher DEC1 feed temperature, although the heat exchanger area was decreased, higher solvent demand and fuel consumption were necessary in the DEC1 column to keep the ΔT freeze margin above 5.5°C . The optimized minimum approach temperature was 6.7°C as shown in Figure 3-23. It was also observed that the IRR change in optimizing the 4th stage of propane was higher than in the other stages of refrigeration due to the considerable cooling duty demand for condensing the ethylene.

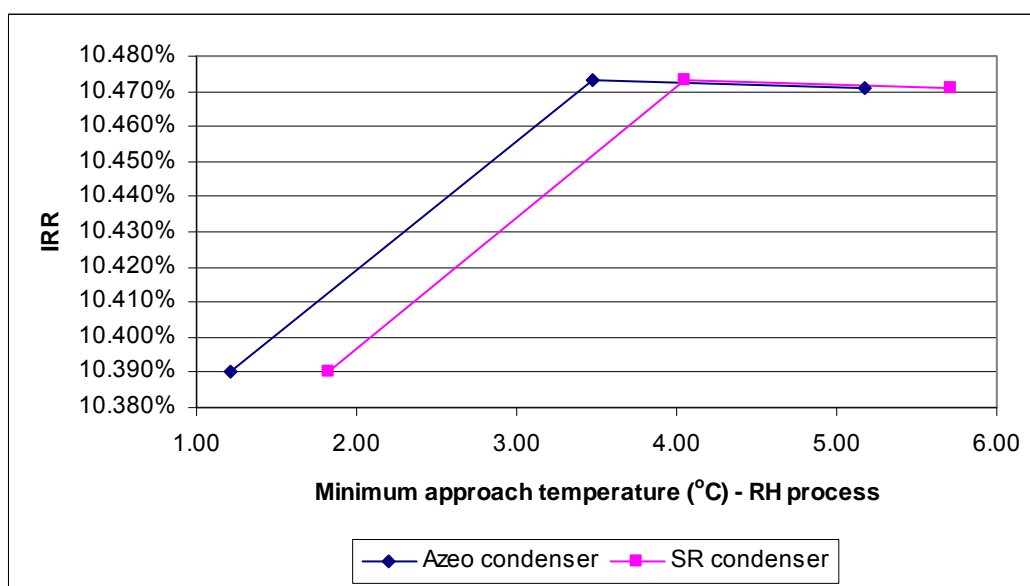


Figure 3-22. Minimum approach temperature effect on IRR in the azeo and SR condensers.

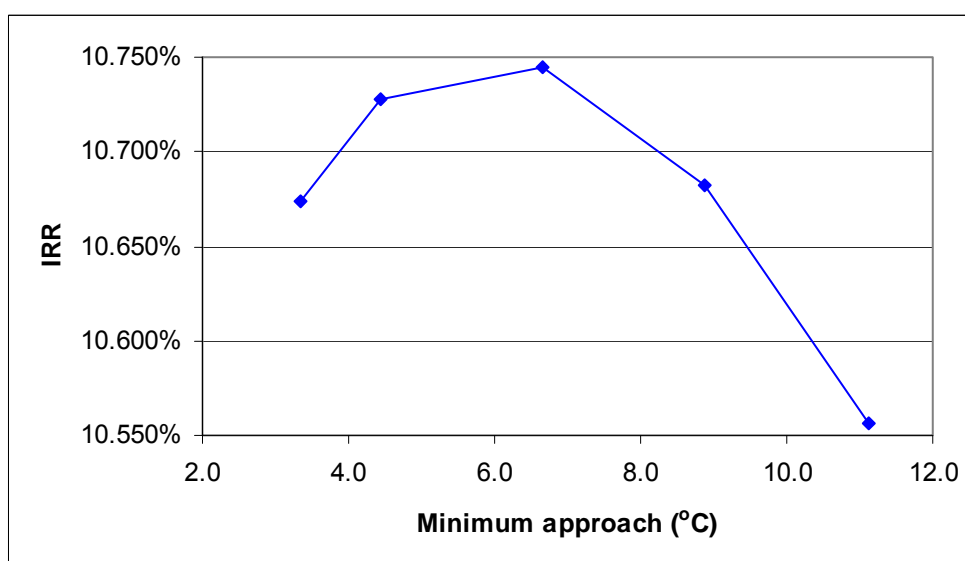


Figure 3-23. Minimum approach temperature effect on IRR – 4th stage propane refrigerant – RH1 process.

Similar evaluations were conducted for the other refrigeration levels and in other process alternatives. The optimization result is presented in Table 3-18.

Table 3-18. Refrigerant temperature level and minimum approach optimization result.

(°C)	Feed1						Feed2					
	Amine		RH		HRH		Amine		RH		HRH	
	Temp	Min.Appr	Temp	Min.Appr	Temp	Min.Appr	Temp	Min.Appr	Temp	Min.Appr	Temp	Min.Appr
Propane												
1st stage	11.1	2.8	11.1	2.8	11.1	2.8	7.2	2.8	7.2	2.8	7.2	2.8
2nd stage					-6.7	2.8					-13.9	6.1
3rd stage	-12.2	3.9	-12.2	3.9	-19.4	2.8	-12.2	8.3	-19.4	4.4	-15.6	2.8
4th stage	-39.4	6.7	-39.4	6.7	-39.4	6.7	-39.4	6.1	-39.4	6.1	-39.4	6.1
Ethylene												
1st stage	-65.6	3.3	-65.6	3.3	-65.6	3.3	-65.6	3.3	-65.6	3.3	-65.6	3.3
2nd stage	-94.4	5.6	-94.4	5.6	-94.4	5.6	-80.6	2.8				
3rd stage							-96.1	5.6	-96.1	5.6	-95.0	5.6
Methane												
1st stage	-105	1.1	-105	1.1	-105	1.1	-102	1.1	-102	1.1	-102	1.1
2nd stage	-140	1.1	-141	1.1	-141	1.1	-137	1.1	-138	1.1	-139	1.1

3.5. Heuristics for Optimization

The optimization of the design variables generally involves opposite effects of several operating variables on the IRR. The number of the affected variables and the magnitude of change on these parameters determine whether there is any significant effect on the IRR.

Analysis on the rigorous simulation and optimization processes revealed the heuristics to optimizing design variables in a process flowsheet, particularly the RH and HRH processes, as follow:

1. First, define the separation specification and constraints required for the process. Separation specification includes the product purity requirement, commercial product specification, LNG heating value, and impurity level in the generated products. The operational and safety issue such as the minimum temperature approach to the CO₂ freezing temperature and also the minimum temperature approach in the heat exchangers are considered as the constraints for the process. This is the first principal step since all of the specifications used for the separation processes is based on the given product requirements and constraints. The importance of this first heuristic was highlighted in the process of obtaining

the optimum C2 specification at the azeo column overhead in the RH1 process. Increasing C2 fraction in the overhead of the azeo column gave higher IRR, but when the minimum 99% CO₂ purity limit was reached, a higher IRR was not considered.

2. After the separation requirements and constraints have been identified, the design variables are next to being decided. Investigation on the various design variables in the RH and HRH processes emphasized the following issues:
 - a. The selection of DEC1 column pressure should be the first to be estimated because it is related to the reflux ratio and the solvent demand. Since the condensing temperature in the DEC1 was at the cryogenic temperature, the reflux ratio strongly influenced the fuel consumption and the capital cost in terms of the number of turbines required to generate the power. The solvent demand was dependent on the CO₂ fraction in the feed, the specified approach to the CO₂ freezing temperature, and the solvent composition. It also affected the size of the DEC1 and subsequent fractionation columns.
 - b. Similar to the DEC1 column, the selection of the azeo column pressure is related to the reflux ratio, solvent amount, overhead condensing temperature, and column diameter of the azeo and subsequent columns. The optimization of these variables determines the optimum azeo column pressure. However, in the HRH process, even though a higher IRR might be achieved with lower azeo column pressure, the minimum CO₂ recovery limit should be considered.
 - c. The selection of column pressures in the other fractionation columns also related to the reflux ratio, column diameter, and the overhead condensing temperature which affects the fuel consumption and capital cost; however, the effects are marginal.
 - d. The selection of the solvent temperature to be used in the DEC1 and azeo columns is optimized between the demand for higher refrigeration duty and heat exchanger UA with the lower reflux ratio as the solvent temperature is colder.
 - e. The solvent composition for the DEC1 and azeo columns was determined by the column specifications used at the bottom of SR column for Feed1 process and at the overhead of DEC4 column for Feed2 process (Figure 2-6 and Figure 2-7). The solvent specification used in the Feed2 process was

easier to identify since it was similar to the commercial C4 product specification. However, for the Feed1 process, the composition was more flexible since the remaining of the unused recycled solvent was sold as a mixed NGL product. Further study on the solvent composition is presented in section 4.2.

3. It was observed that the shape of IRR trend generated from the optimization processes was quite variable. The movement could be a smooth unimodal trend, a steep increase or decrease, a constant gradient, or a fluctuating trend. Figure 3-24 shows the smooth unimodal trend in optimizing the solvent temperature for the DEC1 column, Figure 3-25 presents the steep increase in the optimization of the DEC1 column pressure in the RH1 process, Figure 3-26 shows the steady increasing trend in optimizing the DEC1 column pressure in HRH1 process, and Figure 3-27 presents the fluctuating IRR values in optimizing the overhead specification of the SR column in the RH1 process. These are typical behaviours in the optimization process especially when they involve a large number of variables and constraints (Jelen and Peters 1970). Therefore, there are different decisions to make related to the sensitivity of the process variables on IRR.

4.

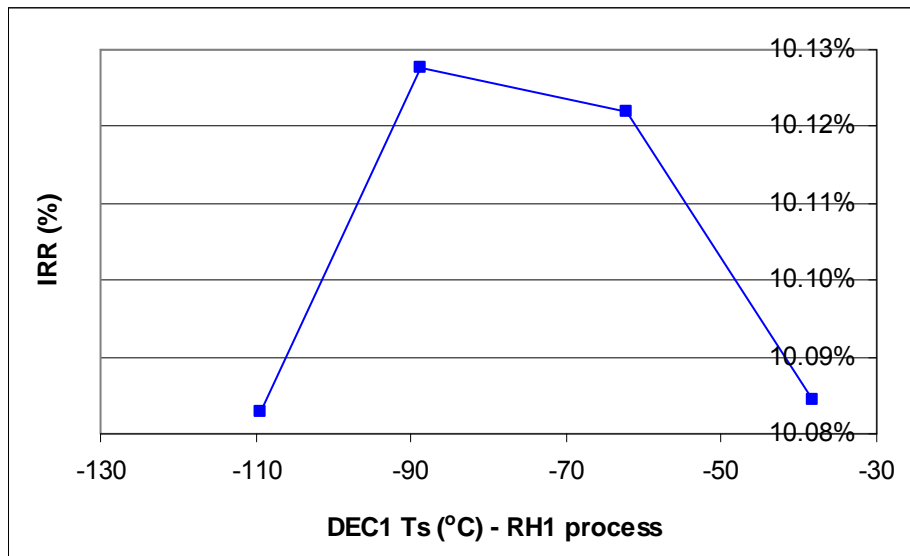


Figure 3-24. Sensitivity of DEC1 solvent temperature on IRR – RH1 process.

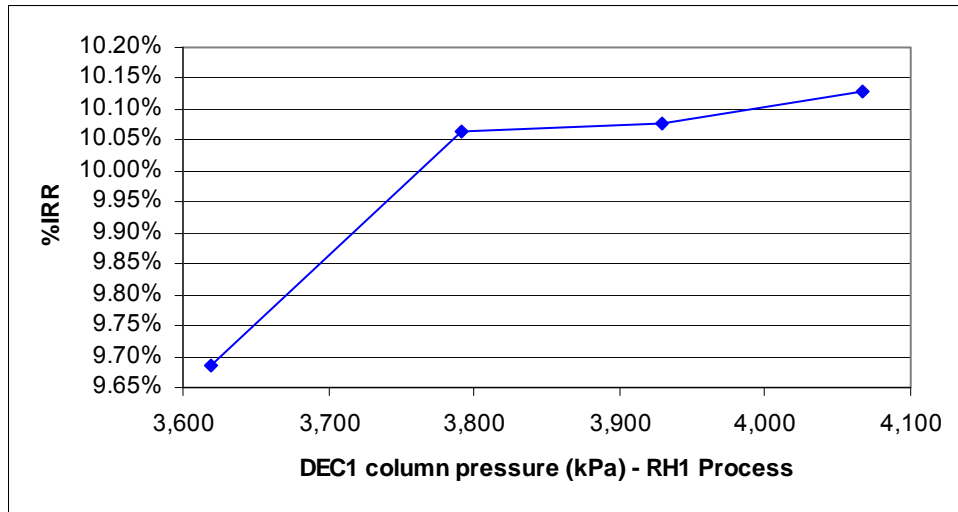


Figure 3-25. Sensitivity of DEC1 column pressure on IRR – RH1 process.

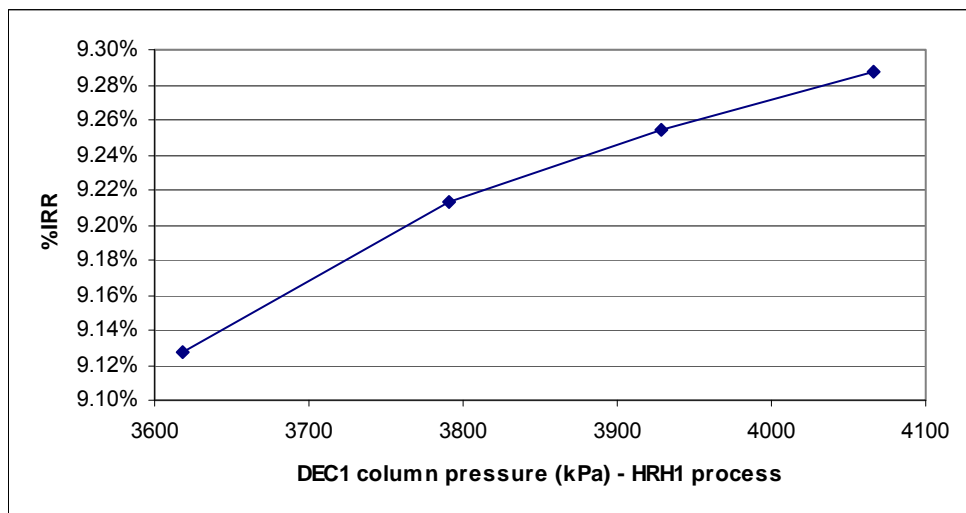


Figure 3-26. Sensitivity of DEC1 column pressure on IRR - HRH1 process.

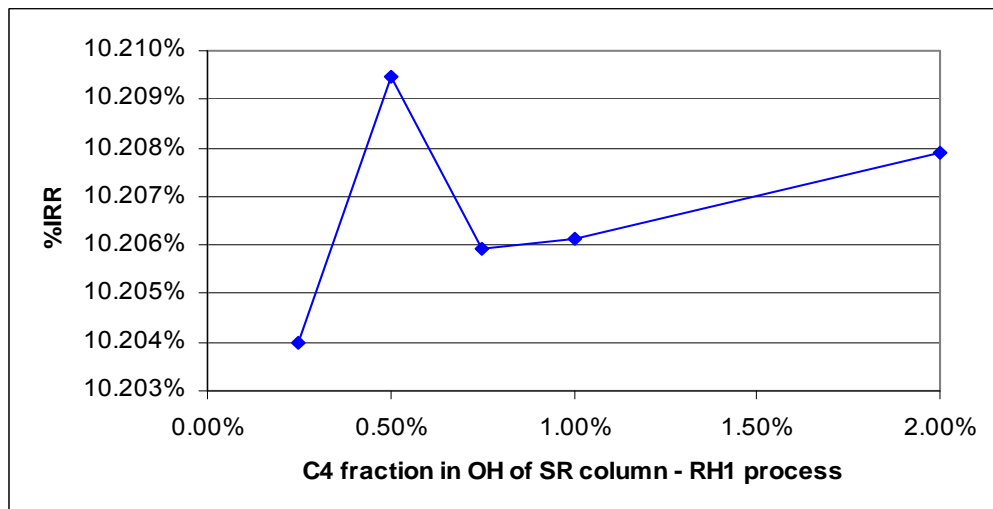


Figure 3-27. Sensitivity of C4 fraction in the overhead of SR column on IRR.

When the IRR shows a smooth unimodal trend in the range observed, the maximum IRR point is the optimum condition. If a steep increase or decrease is observed in the IRR with alteration in design variables, the cause of the sharp change should be observed. When a continuous decrease or increase in the IRR is obtained, the specification limit defined in step 1 will be the restraint of the optimization process. With the fluctuating trend, an analysis on the whole process should be performed to find the cause of the oscillating results; however, when the change in the fluctuating IRR was minor, the value of the design variable within the observed range should be selected.

3.6. Conclusions

The optimization and sensitivity analysis show that it is not possible to formulate general optimum design variables for all feed conditions in the RH and HRH processes. However, the effects on various operating variables were observed and thus the optimization process needs to consider all of these contributing variables to arrive at the optimized conditions.

The results show that the selection of DEC1 and azeo column pressures strongly affects the operational and capital costs due to the reflux ratio operating at the cryogenic temperature and the solvent quantity required for the separation processes. In the other subsequent fractionation columns, the air cooling condensing temperature is allowed to be used. Variation of the number of ideal stage and feed inlet location has a trivial effect on the IRR.

The IRR is more improved with solvent inlet location higher in the DEC1 and azeo columns; however, the solvent impurity fraction in the CO₂ product is increased. The optimum solvent temperature strikes a balance between lower reflux ratio and additional cooling duty and heat exchanger UA with the colder solvent temperature. The amount of solvent required in the DEC1 depends on the CO₂ fraction in the feed, the minimum approach to CO₂ freezing temperature constraint, column pressure, and the solvent composition. In contrast, for the azeo column, the optimum solvent

demand is also related to the reflux ratio and capital costs of the azeo and subsequent fractionation columns.

The sensitivity of the refrigeration temperature level and minimum approach temperature on the IRR was strongly related to the fuel demand and cost estimation of the heat exchangers. It was shown that for the low temperature methane refrigerant, the optimum minimum temperature approach was the lowest operability approach of 1.1°C. Different minimum approach temperature values for the other refrigeration levels were obtained dependent on the fuel consumption and the heat exchanger economic calculation. The effect of the refrigerant temperature level and minimum approach temperature on the IRR was also related to the cooling duty involved in the particular refrigeration stage. The variation in refrigeration temperature level and minimum approach temperature of refrigerant which is related to a high energy demand in the process (such as DEC1 and azeo condensers) significantly influenced the IRR value.

5. EXTRACTIVE DISTILLATION and SOLVENT COMPOSITION

4.1. Extractive Distillation

This section highlights the separation of the CO₂-ethane azeotrope in an extractive distillation process with an emphasis on analysing the column performance with varying solvent amount and solvent composition. These two variables were examined due to their significant impacts on the plant economics.

Extractive distillation is a widely acceptable technique when ordinary distillation is impractical for the separation of azeotropic mixtures or close-boiling key components. In an extractive distillation process, a higher boiling solvent is added to enhance the relative volatility between the key components and improve the separation. The solvent selection and the amount of solvent are the important aspects of an extractive distillation process. The selection of solvent strongly influences the extractive distillation performance and determines which key component will be the overhead product in the process. An outline for solvent screening and selection has been presented (Seader, Siirola, and Barnicki 1997). The fundamental concept for extractive distillation process is based on the relative volatility equation:

$$\alpha_{i/j} = \frac{y_i/x_i}{y_j/x_j} = \left(\frac{P_i^{sat}}{P_j^{sat}} \right) \left(\frac{\gamma_i}{\gamma_j} \right)$$

Notations:

$\alpha_{L/H}$	= Relative volatility
y	= vapor phase
x	= liquid phase
i	= light key component
j	= heavy key component
P^{sat}	= saturated liquid pressure
γ	= activity coefficient in liquid phase

The relative volatility of an azeotropic mixture is equal to 1. When a solvent is added to the azeotropic mixture, the solvent has molecular interactions with the key components and thus alters the liquid activity coefficients. The solvent and the key component that have similar liquid phase behaviour tend to show less molecular interactions and exhibit an ideal or near ideal liquid solution. On the other hand, with dissimilar key components, the activity coefficient increases. In the separation of

CO₂-ethane azeotrope with a hydrocarbon solvent, the CO₂ is generated as the distillate because the ratio of $P_1^{\text{sat}}/P_j^{\text{sat}}$ is greater than 1 and the relative volatility is increased due to the higher activity coefficient of CO₂ with the hydrocarbon solvent. It is possible to generate CO₂ as the bottom product; however, the solvent selected should alter the ratio of the activity coefficient such that the $\alpha_{L/H}$ is less than unity in the presence of solvent.

The solvent amount has a significant impact on the extractive distillation process because it is directly related to the process economics. There is a minimum solvent amount below which the separation is impossible (Seader, Siirola, and Barnicki 1997). An approximate minimum solvent amount (minimum solvent to feed ratio) can be calculated by plotting the $\alpha_{L/H}=1$ line on the ternary diagram or observing the disappearance of azeotrope in the corner of a pseudo-binary diagram (Laroche et al. 1991). Typically, a higher than minimum solvent amount is required for an economically feasible process. Higher solvent to feed ratio reduces the number of equilibrium stage and reflux ratio; however, it leads to higher column diameters for the extractive and solvent recovery columns as well as an increase in the utility cost due to a higher reboiler temperature (Seader, Siirola, and Barnicki 1997).

The reflux ratio also plays an important role in the extractive distillation column. A minimum reflux ratio is required to make the separation feasible; however, in contrast to the ordinary distillation process, an excess reflux in an extractive distillation process dilutes the solvent concentration in the upper section of the column and delivers an overhead product with lower purity for a given number of stages (Seader, Siirola, and Barnicki 1997). Figure 5-1 shows the effect of the excess reflux ratio on the composition in the overhead product stream.

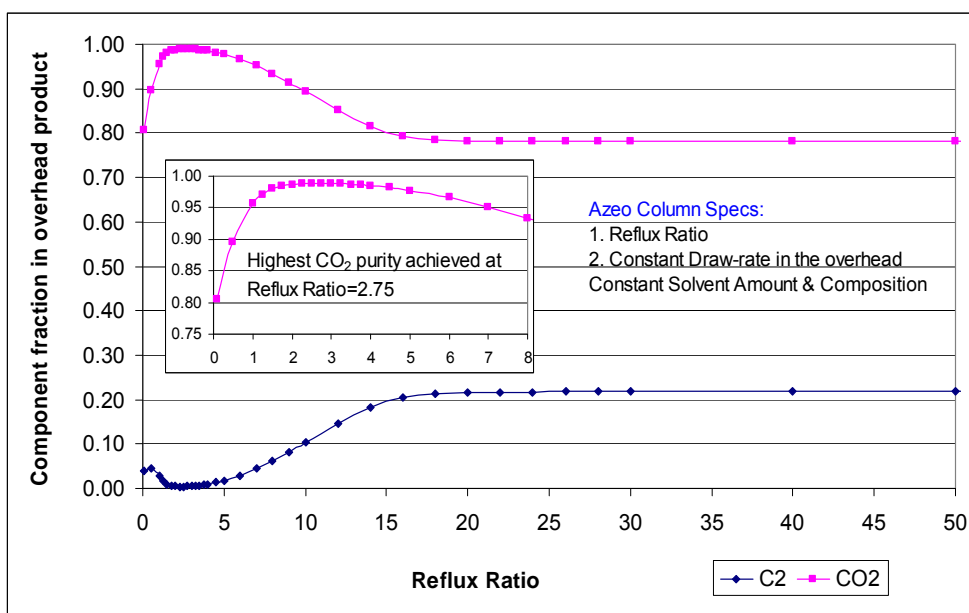


Figure 5-1. Effect of an excessive reflux ratio in an extractive distillation process.

Initially, a study focusing on the extractive and solvent recovery (SR) column as shown in Figure 5-2 was conducted and a ternary system of CO₂, C₂, and C₅ was examined. An equimolar CO₂-C₂ feed at 3860 kPa and 22.3°C, a typical DEC1 bottom stream condition, was examined. This study was performed with a fixed feed condition and a number of theoretical stages of 50 and 25 for the extractive and the SR columns, respectively. The objective was to understand the solvent demand with varying feed and solvent inlet stages of the extractive column. The separation requirements for the azeo column were 95% CO₂ purity in the overhead and 40 ppm-mole (33 ppmw) of CO₂ at the bottom product. In the solvent recovery column, a 99.9%-mole purity of C₂ in the overhead and C₅ in the bottom streams were specified.

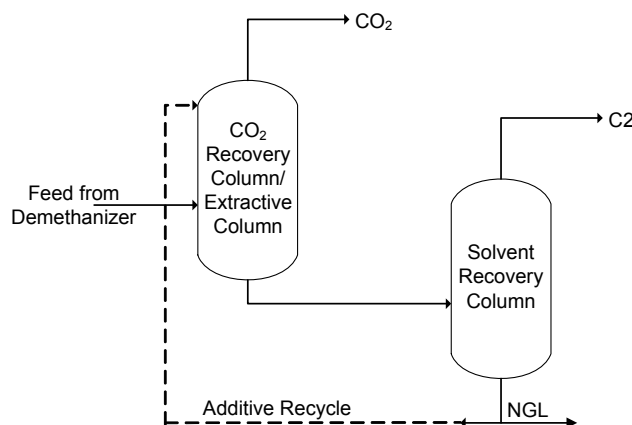


Figure 5-2. Schematic diagram of an extractive distillation column and a solvent recovery column.

The minimum solvent amount was first investigated in achieving the specified purity. Figure 5-3 presents the relation between minimum solvent amount (in terms of molar ratio of solvent to feed), reflux ratio, and the CO₂ purity in the overhead. The feed inlet location at stage 29 and solvent inlet at stage 3 from the top were used in the simulation to treat an equimolar CO₂-ethane azeotrope with a pure nC5 solvent. The reflux ratio and CO₂ impurity of 40 ppm-mole (33 ppmw) at the bottom were used to solve the azeo column.

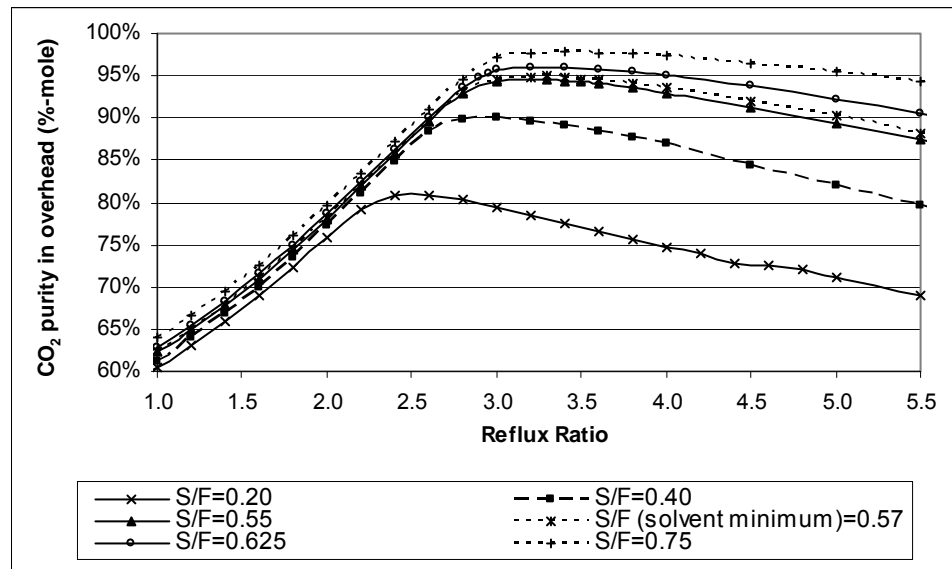


Figure 5-3. Minimum solvent amount and reflux ratio effects on CO₂ purity in the overhead.

For fixed feed and solvent inlet stages, Figure 5-3 shows that below a minimum solvent amount (solvent to feed rate ratio, $S/F_{\min}=0.57$), the desired purity of 95% CO₂ in the overhead was not achievable regardless of the reflux ratio applied. When the minimum solvent amount was used, the required CO₂ purity was achieved at a reflux ratio of about 3.3. As the reflux ratio was increased above this value, the CO₂ purity declined. This trend was also observed for all other solvent amounts. This peculiar behaviour is typical for extractive distillation processes as excessive reflux ratio effectively dilutes the solvent thus worsening the separation (Laroche et al. 1991; Seader, Siirola, and Barnicki 1997). When the S/F ratio was greater than the minimum, S/F_{\min} , the optimum reflux ratio decreased moderately. These two variables, i.e. the solvent quantity and the reflux ratio, both have a direct consequence on the energy requirement and capital cost. Therefore, to decide the most economical solvent amount, an analysis on the energy requirements for the

process was first conducted.

The optimum solvent amount in terms of the total energy demand for the process depicted in Figure 5-2 was examined. The result is presented in Figure 5-4 and it was calculated that the molar ratio of the optimum solvent to the minimum solvent quantity was 1.053.

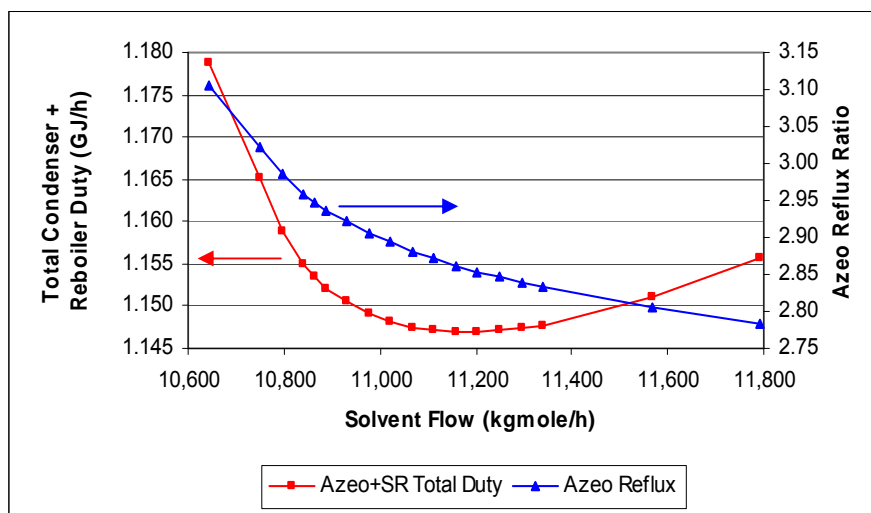


Figure 5-4. Optimum azeo solvent amount in terms of energy demand.

Following the above study on the extractive and solvent recovery columns, a global optimization on the solvent amount in the RH1 and RH2 process flowsheet was performed. A comparative study in terms of the energy demand and overall optimization (which took into account both energy and capital costs) was conducted to find out whether a similar ratio of optimum to minimum solvent amount was obtained. The comparison could be used to evaluate if a simple energy optimization was adequate to represent the overall economic optimization. A ratio of 1.105 between the optimum to minimum solvent amount was calculated for the RH1 with an azeo feed composition of 52% CO₂ - 11% C₂ and 1.046 for the RH2 with a feed composition of 39% CO₂ - 18% C₂. These values are in the proximity of the result optimized in terms of the energy demand only. Therefore, the optimization in terms of the energy requirement can be used to predict the optimum solvent amount for the azeo column. The solvent amount optimization for the azeo column of RH1 is presented in Figure 5-5.

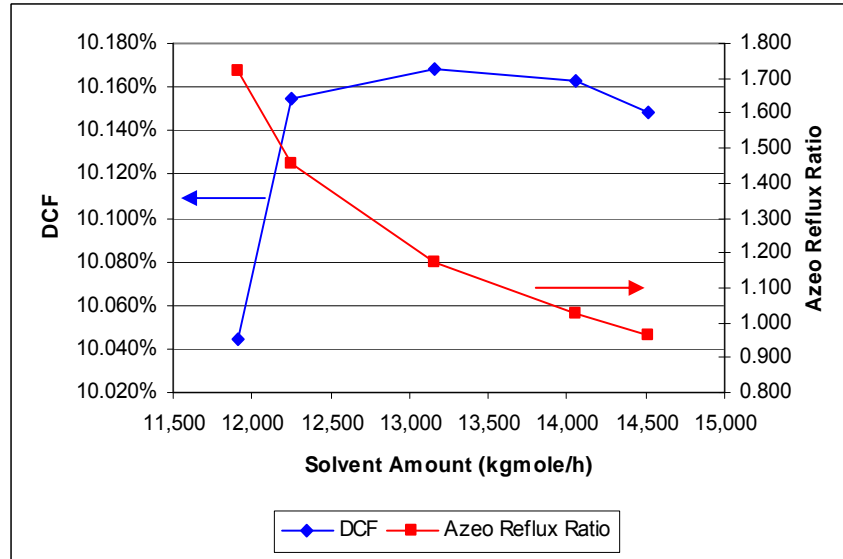


Figure 5-5. Optimum azeo solvent amount in terms of total capital and energy costs – RH1 process.

The location of the feed inlet stage strongly affects the required amount of solvent and the reflux ratio. Figure 5-6 shows the minimum solvent amount and the related optimum reflux ratio as a function of the feed inlet stage for the ternary system observed. For a column with 50 total theoretical stages, the lowest minimum solvent demand was observed when the feed inlet was at stage 29. When the feed inlet stage was moved, the reflux ratio was also altered to maintain the compositional product specifications. As a result of the altered reflux ratio, the solvent amount, which is governed by the vapour liquid equilibrium at the solvent inlet stage, was also changed.

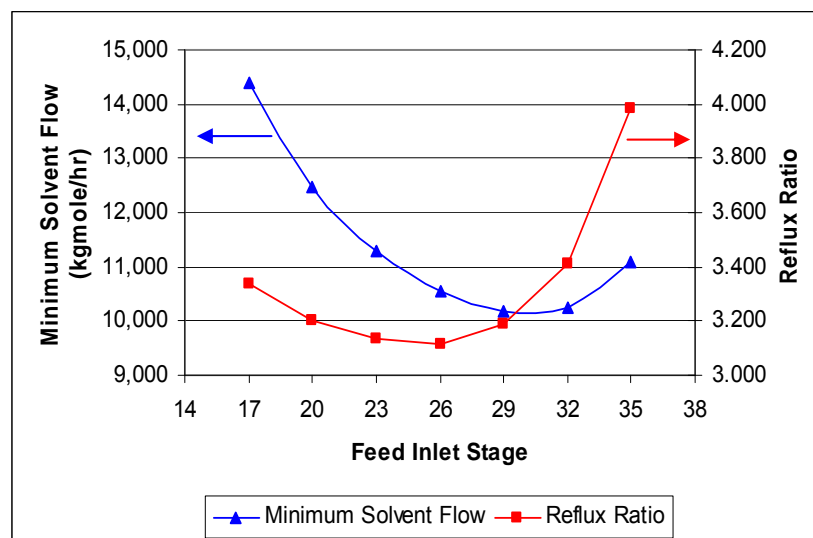


Figure 5-6. Reflux ratio and minimum solvent amount as a function of feed inlet stage.

However, at the solvent inlet stage, it was observed that the C2, CO₂, and nC5 vapour fractions were 0.021, 0.971, and 0.008, respectively, and the C2 liquid fraction was 0.019. The CO₂ and nC5 liquid fractions had different values for different minimum solvent amounts. For a minimum energy requirement, Figure 4-6 also indicates that there is an optimum feed inlet stage for both the solvent amount and the reflux ratio.

The solvent inlet stage effect on the azeo column performance for the ternary system was also observed. As shown in Figure 5-7, the solvent inlet stage has a direct impact on the reflux ratio and the solvent impurity in the overhead product. As the solvent inlet stage was lowered, simulation showed that a higher reflux ratio was required. This was due to a decrease in the nC5 solvent in the liquid phase above the solvent inlet stage. Although moving the solvent inlet stage upwards decreased the reflux ratio, it also increased the amount of nC5 solvent going to the overhead. Therefore, the solvent stage should be optimally determined not only to decrease the reflux ratio but also to prevent excessive amounts of solvent going to the overhead.

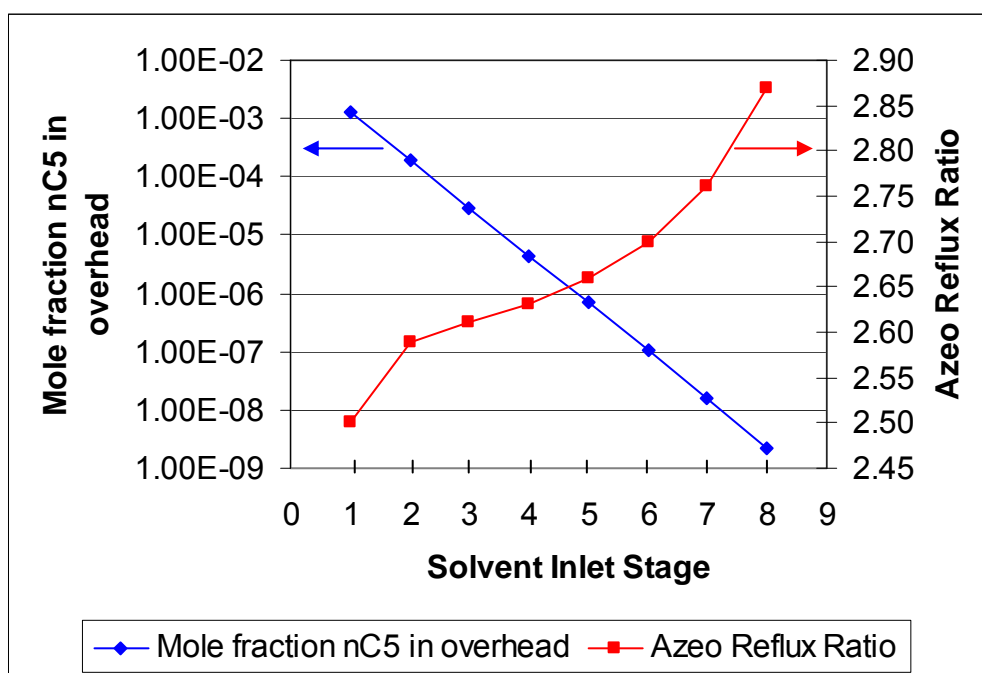


Figure 5-7. Effect of solvent inlet stage.

Figure 5-8 shows the typical composition profile of an extractive distillation column for the CO₂-C2-nC5 ternary system. The liquid profile in the rectifying and stripping sections start at the distillate (pure CO₂) end and bottom (C2-C5) side, respectively.

The vapour profile moves along the CO₂-C2 side (low solvent content). It was observed that, at the minimum solvent amount, the composition profile of the nC5 in the liquid phase was practically constant along the column; however, with excess solvent, the nC5 liquid fraction varied considerably from the top to the bottom of the column. Thus, the nC5 liquid profile can be used to indicate if the column is operating with an efficient amount of solvent. Furthermore, as more solvent was employed, the nC5 fraction in the vapour phase was higher and thus more solvent was lost in the overhead product.

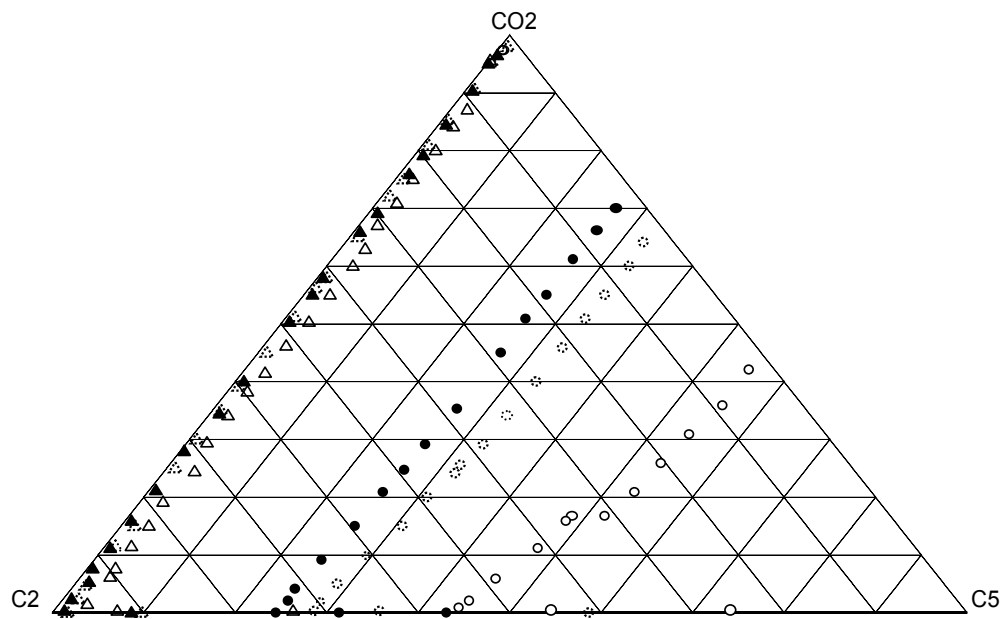


Figure 5-8. Composition profiles as a function of solvent amount (●=liquid profile; ▲= vapor profile with minimum solvent 10,636 kgmole/h; ⊙=liquid profile; ⊔=vapor profile with solvent 12,475 kgmole/h; ○=liquid profile; △=vapor profile with excess solvent 24,950 kgmole/h).

All of the simulations performed displayed similar composition profiles to those shown in Figure 5-8. The rectifying section started at the pure CO₂ end and the stripping section started at the bottom (C2-C5) side, depending on the mass balance. The extractive section acted as a bridge connecting the rectifying section to the stripping section by passing through the triangular space. The extractive section could be near the nC5 node when a high solvent flow and low reflux were utilized; however, it could be located near the CO₂-C2 side when minimum solvent amount or a high reflux was applied.

4.2. Solvent Composition

It was observed that the evaluation of the extractive distillation performance with regard to solvent composition is a relatively complex process because it was associated with the performance of the solvent recovery column where the solvent composition was specified and also with the performance in the extractive column.

Figure 5-9 and Figure 5-10 show that a lower C3 fraction in the solvent is preferred due to the lower reflux ratio and higher CO₂ product purity.

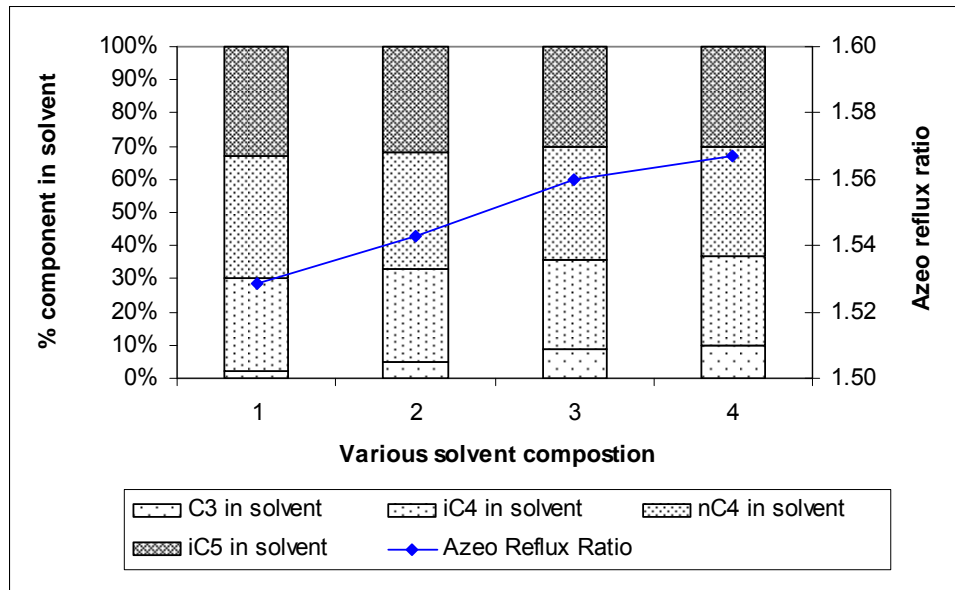


Figure 5-9. Effect of C3 fraction in solvent on azeo reflux ratio.

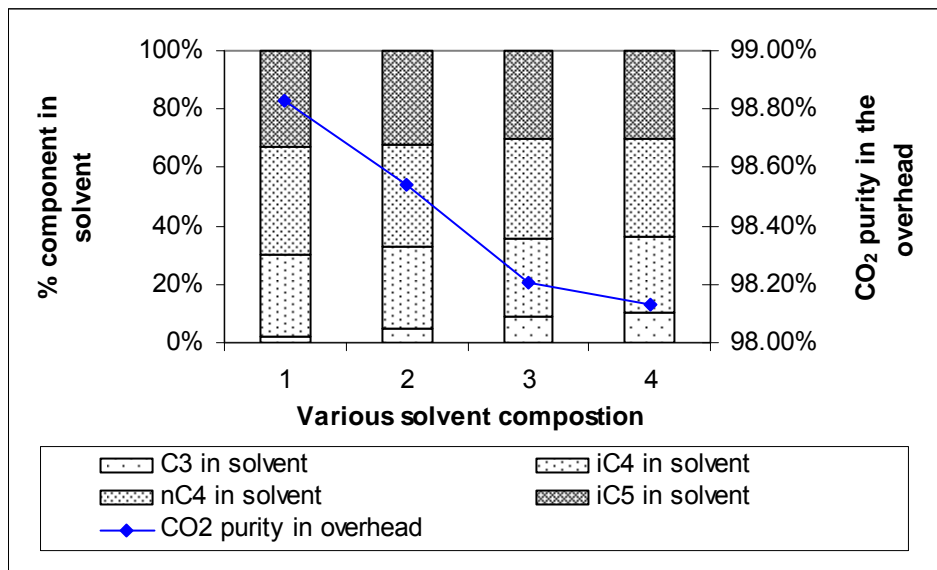


Figure 5-10. Effect of C3 fraction in solvent on CO₂ purity in the overhead.

Further complication was identified when the solvent composition was examined with regard to the separation in the DEC1. Figure 5-11 shows the ΔT to CO_2 freezing point as a function of solvent composition. It is clear that a solvent with a higher fraction of the lighter components could increase the ΔT margin to the CO_2 freezing point. As the light components in the solvent increases, the vapour phase rising in the extraction section contains more of these components and increases the temperature of the tray as well as the CO_2 freezing point.

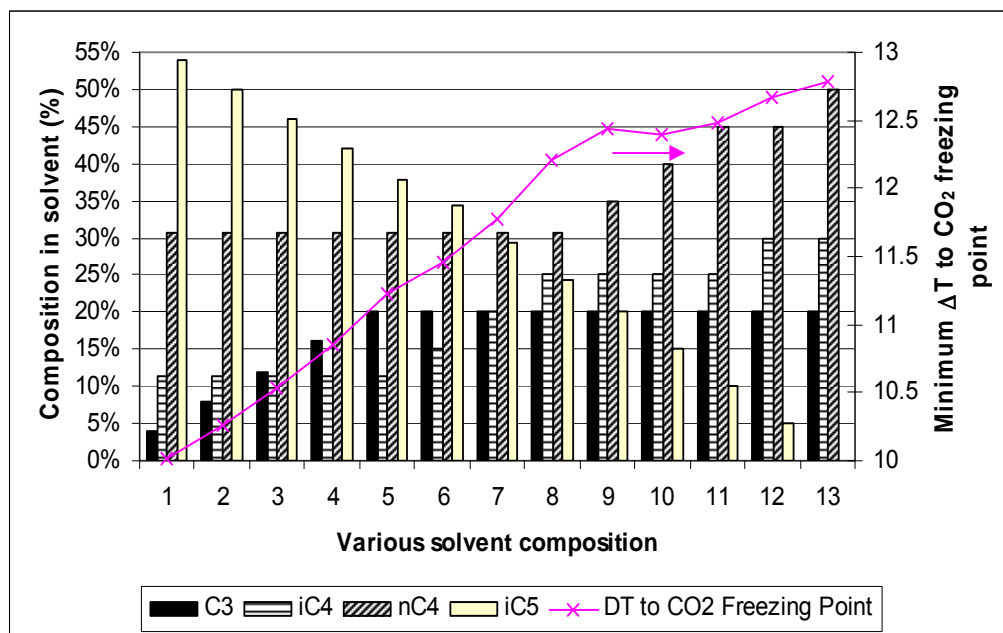


Figure 5-11. Effect of solvent composition on minimum ΔT to CO_2 freezing point in DEC1.

However, it was observed that in the DEC1, the decreased ΔT to CO_2 freezing point with variation of solvent composition could be resolved with higher solvent flows. This was not the case for the azeo column because higher solvent amounts might decrease the CO_2 purity below 99%-mole with other design variables being constant. Therefore the selection of solvent composition should be carefully examined because it is vital to the separation performances. Another example of solvent composition complexity was that a higher solvent inlet stage in the azeo column needed a lower reflux ratio resulting in increased impurity levels in the CO_2 product. However, when the solvent composition was altered with a lower C3 fraction, the solvent inlet location could be adjusted to a higher inlet stage to seize the opportunity of lower reflux ratio while maintaining the required CO_2 purity.

The effect of solvent composition on the CO₂-ethane separation was first analysed by investigating the separation efficiency of the azeotropic components using the single component solvent. A CO₂ pseudo-binary diagram on a solvent free basis (Figure 5-12) was utilized to quantitatively examine the minimum fraction of each single hydrocarbon component to eliminate the azeotropic point ($y=x$). The minimum fraction of each single component to break the CO₂-ethane azeotrope is shown in Figure 5-13.

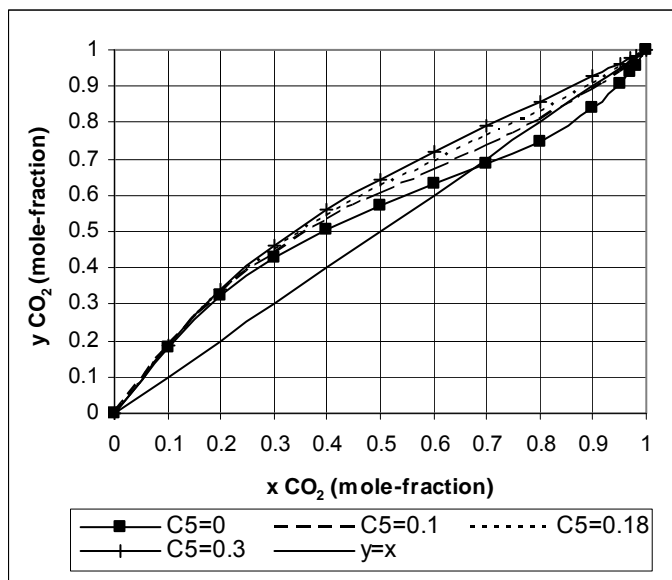


Figure 5-12. Phase equilibrium of CO₂-ethane mixture as a function of nC5 additive.

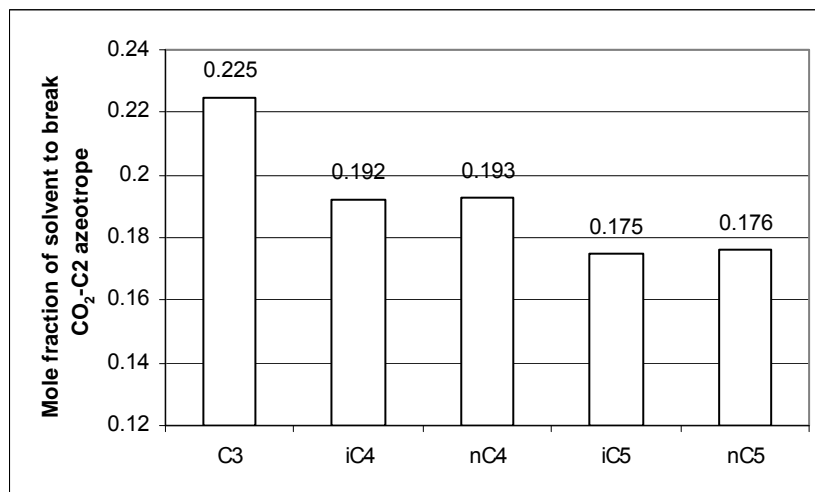


Figure 5-13. Mole fraction of the solvent required to break CO₂-ethane azeotrope.

It is clear from Figure 5-13 that the solvent demand is lower with a heavier hydrocarbon as the solvent. Table 5-1 shows energy requirements as a function of solvent type and amount (reported as the ratio of solvent amount to minimum

solvent). From Table 5-1, it is evident that the ratios of the optimum solvent to the minimum solvent amounts are similar for all of the hydrocarbon solvents; however, the energy demand is highest with C3 solvent due to the higher reflux ratio requirements in the both extractive and the solvent recovery columns.

Table 5-1. Ratio of optimum solvent to the minimum solvent for single component solvents.

Solvent	Ratio of optimum solvent to minimum solvent	Energy Requirement (kJ/h)
C3	1.052	1.394E+09
iC4	1.064	1.077E+09
nC4	1.063	1.055E+09
iC5	1.054	1.130E+09
nC5	1.053	1.147E+09

Following the single-component solvent study, the column performance in a fixed column configuration (fixed number of stages, feed inlet stage, and solvent inlet stage) was observed with varying solvent composition. The effect of several solvent compositions on the minimum solvent amount, reflux ratio, and the total energy requirement is presented in Figure 5-14 to Figure 5-16.

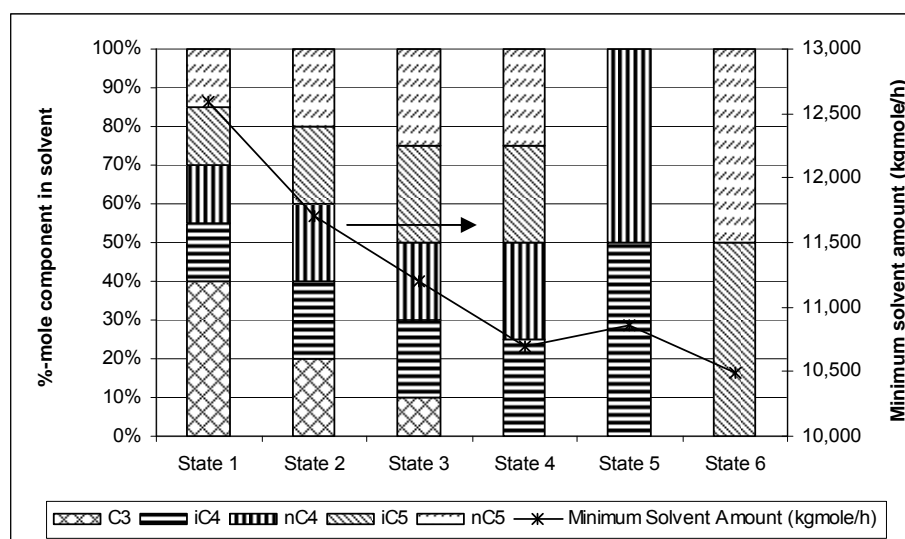


Figure 5-14. Minimum solvent amount required for different solvent compositions.

For the minimum amount of solvent, the results in Figure 5-14 are similar to those in Figure 5-13 with solvent demand being higher for lower hydrocarbons. The lowest solvent demand was found with the C5 mixture solvent. The increased requirement of solvent for lower hydrocarbons poses further problems due to their higher relative

volatility, which increases their composition in the overhead product. Therefore, in order to ensure the required product purity, a significantly higher reflux ratio is needed with C3 as the solvent as shown in Figure 5-15. These observations lead to the conclusion that C3 is not a desirable solvent for CO₂-ethane separation.

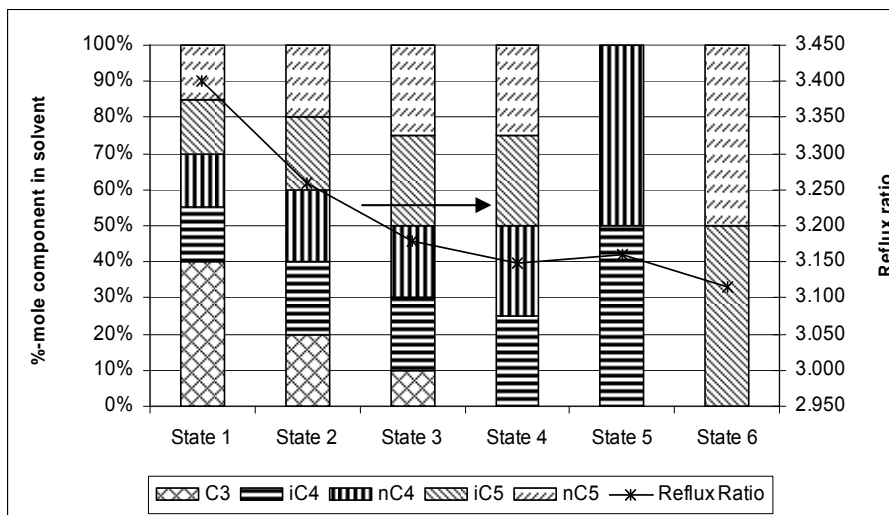


Figure 5-15. Effect of the solvent composition on the reflux ratio.

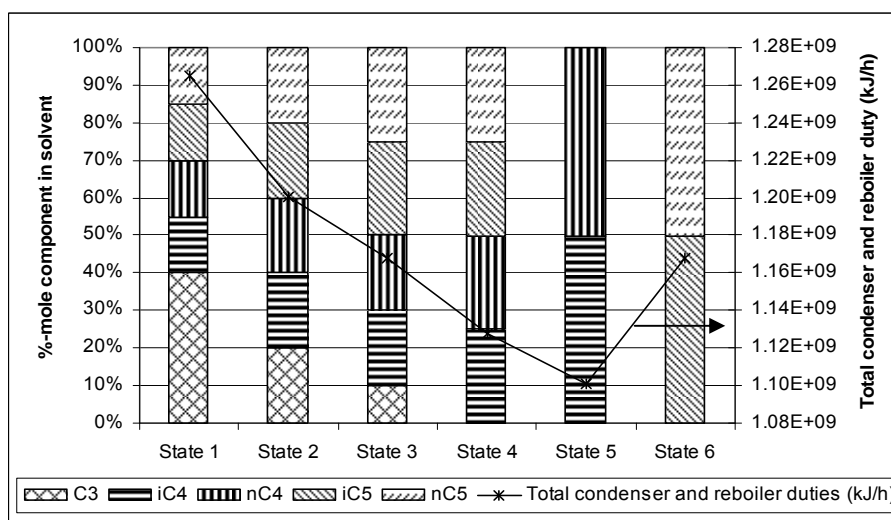


Figure 5-16. Total energy requirement as a function the solvent composition.

Figure 5-16 shows the effect of solvent composition on the total energy requirement in both the extractive and solvent recovery columns. It was observed that the lowest energy demand was found with the C4 solvent. The higher energy demand with the C5 solvent could be attributed to corresponding higher reboiler duties in the columns. Of the existing options, the C4 composite solvent was the best option in terms of the energy demand.

It is also important to observe the loss of valuable hydrocarbon in the CO₂ overhead product. Table 5-2 shows that with a specified CO₂ level in the overhead, the solvent loss is lower when heavier hydrocarbon solvents are used. A “state” in these figures refers to a solvent mixture with compositions similar to Figure 5-16.

Table 5-2. CO₂ recovery column overhead product

	State 1	State 2	State 3	State 4	State 5	State 6
%-mole C2	0.030	0.038	0.043	0.049	0.048	0.050
%-mole Total Solvent	0.020	0.012	0.007	0.001	0.002	0.00004
%-mole CO ₂	0.95	0.95	0.95	0.95	0.95	0.95

4.3. Conclusions

The extractive distillation column configuration with minimum solvent amount does not directly indicate the optimum setup in terms of the overall energy and economic optimization. The minimum solvent amount indicates the quantity required to achieve the product specifications, whereas the optimum solvent amount is associated with the optimized economic rate. The ratio of the optimum to the minimum solvent in this study was in the range of 1.05 - 1.10.

Design of an optimum extractive distillation is a complex procedure because of the interactive effects between the design variables subject to the CO₂ purity specified. The required solvent amount changes dependent on the feed inlet stage, solvent inlet stage, and solvent composition. On the other hand, the solvent amount as well as the reflux ratio dictates the overall economic calculation.

The optimum feed inlet stage is associated with the maximum economic rate. The best solvent inlet stage is generally near the top of the column, but may not be the top tray as it will result in an increase loss of solvent in the overhead CO₂ product.

The preferred solvent composition for the separation in DEC1 and azeo columns is slightly different. Solvent with lighter hydrocarbon is more advantageous to prevent CO₂ freezing in the DEC1 while heavier hydrocarbon solvent is desirable for the azeo column due to the lower reflux ratio and solvent loss in the CO₂ product. The

best solvent composition is therefore optimized in terms of economics to obtain the best result for the whole process.

5. ANALYSIS of BASE CASE SCENARIOS

A summary of the overall simulation results and also the energy and economic comparison in all of the process alternatives is presented in this chapter. The product generation from the optimized simulation is presented in Table 5-1.

Table 5-1. Product generation from optimized simulation.

Process Alternatives	Req. Spec	Amine1	RH1	HRH1	Amine2	RH2	HRH2
LNG Product							
%-mole C1	> 88	93.12	93.25	93.37	93.25	93.23	93.78
%-mole C2	< 6	4.66	4.52	4.31	5.48	5.62	4.42
%-mole C3	< 3.5	1.26	1.24	1.28	1.14	0.91	1.66
%-mole iC4	< 2	0.15	0.12	0.17	0.014	0.08	0.025
%-mole nC4	< 2	0.12	0.11	0.12	0.002	0.04	0.0033
%-mole iC5+	< 0.1	0.046	0.0984	0.098	0	0.0004	0
mole fraction CO ₂ (ppm)	< 100 ppm	88	90	77	69	98	97
mole fraction H ₂ S (ppm)	< 3.2 ppm	0	0	0	0	0	1
%-mole N ₂	< 1	0.64	0.63	0.64	0.103	0.1	0.11
Btu value (MJ/Sm ³)	39.2 - 40.3	39.40	39.38	39.38	39.58	39.57	39.49
CO₂ product							
%-mole CO ₂	>= 99	99.5	99	99.0	99.4	99.0	98.9
%-mole C1	< 4	0.058	0.15	0.01	0.088	0.2	0.02
%-mole C2		0.0058	0.65	0.94	0.014	0.3	1.06
%-mole C3+		0.0017	0.19	0.01	0.005	0.5	0.0002
%-mole H ₂ S		0.0213	0	0.02	0.0264	0	0.022
%-mole H ₂ O		0.403	0	0	0.426	0	0
CO ₂ Recovery (%)	> 98	89.75%	99.96%	99.39%	93.62%	99.94%	98.33%
C2 product							
%-mole C1	< 2.5				0.027	0	0
%-mole C2	90				94.5	93.96	99.83
%-mole C3	6				5.5	6	0.17
%-mole iC4+	2				0	0.03	0
mass fraction CO ₂	< 10 ppmw				6	8	8
mass fraction H ₂ S	< 10 ppmw				3	0	0
C3 product							
Vapor Pressure @ 37.8°C (kPag)	< 1,434				1,290	1,328	1,367
%-vol iC4+	< 2.5				1.6	1.5	1.2
C4 product							
Vapor Pressure @ 37.8°C (kPag)	< 483				401	375	390
%-vol iC5+	2				1.8	1.6	1.7
Condensate product							
RVP (kPa)	69				69	69	69
%-mole C2		0.1	0	0	0	0	0
%-mole C3		9	2	1	0	0.005	5 ppm
%-mole iC4		18.57	29.26	18.77	1.33	2.47	1.77
%-mole nC4		28.97	36.25	42.24	10.92	9.29	10.29
%-mole iC5+		43.36	32.48	37.99	87.74	88.22	87.95

5.1. Energy Comparison and Economic Evaluation.

Table 5-2 presents a comparison between the total energy consumption and economic evaluation for different process alternatives. Table 5-2 shows that in terms of the economic objective (IRR), the amine process is the best alternative for treating Feed1 and the RH process is the best for Feed2. In terms of the capital cost, the lowest capital investment for Feed1 was observed for the amine process while for Feed2 it was the RH process. In terms of the energy requirement, the HRH process was observed to have the lowest overall fuel requirement for both Feed1 and Feed2 which indicated that the membrane application was assertive in generating a fuel efficient process. The highest LNG production was found with the HRH process as it required the least amount of fuel.

A detailed analysis on the capital cost and energy demand was also conducted to evaluate the key factors that made up the overall economic assessment in each of the process alternatives. For Feed1, the highest total equipment cost was for the HRH1 process while for Feed2 it was for the amine2 process. The membrane system accounted for 12.3% and 10.8% of the total equipment cost for the Feed1 and Feed2 cases respectively. The additional membrane costs were somewhat offset by lower capital costs with smaller column diameters for the azeo and the subsequent columns. The amine2 equipment cost was slightly higher than the RH2 process due to the 10% bigger installed equipment cost for the amine system and the fractionation columns. Figure 5-1 shows the installed capital cost comparison of the amine system, fractionation columns, and the membrane system.

The total energy requirement for the processes is represented by the total equivalent fuel. The total equivalent fuel was the sum of the fuel quantity for the overall compression and pump horsepower (HP), heat flow for reboilers, and duties for the dehydration and amine processes. The fuel was supplied by the plant itself and thus the LNG production was altered with the fuel demand of the plant.

Table 5-2. Comparison of the energy consumption and economic evaluation.

Process Alternatives	Amine1	RH1	HRH1	Amine2	RH2	HRH2
IRR (%)	11.44%	11.17%	10.12%	15.98%	17.08%	16.46%
CAPITAL COST						
Total Equipment Cost (\$)	6.668E+08	6.797E+08	7.597E+08	7.767E+08	7.075E+08	7.358E+08
Turbine+Generator Set (\$)	3.368E+08	3.502E+08	3.588E+08	3.542E+08	3.442E+08	3.586E+08
Total Capital Cost (\$)	6.690E+09	6.866E+09	7.457E+09	7.540E+09	7.011E+09	7.296E+09
ENERGY REQUIREMENT						
Fuel Consumption						
Compression HP	146.9	163.2	163.1	141.3	136.3	142.2
Heating Duty	34.1	22.4	12.0	31.3	37.3	16.8
Pumps	5.1	1.5	0.3	3.8	0.97	0.4
Dehydration	3.5	0.5	0.5	3.8	0.4	0.4
Membrane Process	-	-	9.6	-	-	6.3
Off Gas Supply	0.299	0	0.038	0.2	0	0.2
Total Fuel (MMSCFD)	189.2	187.7	185.5	180.1	174.9	165.9
Number of turbines	5	5	5	5	5	5
Compression HP						
Refrigeration system	4.044E+05	4.860E+05	4.670E+05	4.595E+05	4.643E+05	4.569E+05
CO ₂ compression	5.015E+04	1.620E+04	3.623E+04	4.477E+04	1.500E+04	2.878E+04
Fuel compression	2.376E+04	2.356E+04	2.327E+04	2.261E+04	2.199E+04	2.085E+04
Air Cooler Fan HP	1.841E+04	1.497E+04	1.290E+04	1.807E+04	2.008E+04	1.228E+04
Membrane recompression	0	0	2.957E+04	0	0	2.366E+04
Expander (HP Recovery)	1.992E+04	1.160E+04	1.160E+04	1.627E+04	1.195E+04	1.128E+04
Total Compressor HP	4.768E+05	5.291E+05	5.574E+05	5.316E+05	5.123E+05	5.341E+05
Cooling Duties (kJ/h)						
Condensers (kJ/h)	-	4.653E+08	2.653E+08	3.171E+08	3.992E+08	3.081E+08
Solvent (kJ/h)	-	1.866E+08	8.744E+07	-	1.910E+08	8.036E+07
Liquefaction (kJ/h)	6.284E+08	3.527E+08	3.584E+08	4.036E+08	3.772E+08	3.619E+08
Refrigeration (kJ/h)	1.574E+09	1.172E+09	1.177E+09	1.757E+09	1.555E+09	1.548E+09
Feed Pre-Cooling (kJ/h)	-	7.567E+07	9.255E+07	-	7.655E+07	9.548E+07
Total Cooling Duties (kJ/h)	2.203E+09	2.252E+09	1.980E+09	2.477E+09	2.599E+09	2.394E+09
Initial Utilities (\$)	1.518E+07	1.427E+07	8.586E+06	1.261E+07	1.724E+07	8.083E+06
Total UA (kJ/°C.h)	3.234E+08	3.835E+08	3.202E+08	3.444E+08	4.568E+08	3.329E+08
Air Cooling Duty						
AC Duty - Propane condensing	1.646E+09	1.932E+09	1.827E+09	1.849E+09	1.855E+09	1.807E+09
AC Duty - CO ₂ compression	2.398E+08	1.038E+08	1.810E+08	2.067E+08	8.824E+07	1.424E+08
AC Duty - Amine System	8.023E+08	0	0	6.533E+08	0	0
AC Duty - Fract. Process	0	5.036E+08	3.113E+08	1.341E+08	1.046E+09	4.055E+08
AC Duty - Membrane System	0	0	7.440E+07	0	0	5.126E+07
Total Air Cooling Duties (kJ/h)	2.688E+09	2.539E+09	2.394E+09	2.843E+09	2.989E+09	2.406E+09
Products						
LNG (kg/h)	710,961	714,485	715,740	691,735	699,291	703,498
CO ₂ (m ³ /h)	421.4	475.4	472.8	346.5	374.5	369.2
C ₂ (m ³ /h)	-	-	-	87.6	79.6	100
C ₃ (m ³ /h)	-	-	-	55.7	62.9	42.3
C ₄ (m ³ /h)	-	-	-	39.0	34.1	38.83
Condensate (m ³ /h)	14.33	12.63	10.39	187.7	187.2	187.5
Constraints						
DT Freeze (°C)	-	5.73	5.6	-	5.69	5.77

In all of the processes, the majority of the energy requirement was for compressor HP followed by the heating duty requirement. In the HRH process, the heat flow is reduced significantly compared to the RH process as a result of a decrease in the recycle solvent flow, however, the membrane process required additional HP for recompression of the permeate stream going into the second stage of membrane and the recompression of the CO₂ product from a low permeate pressure to the injection pressure. Nevertheless, it was observed that the reduction in the heating duty was more than membrane process HP.

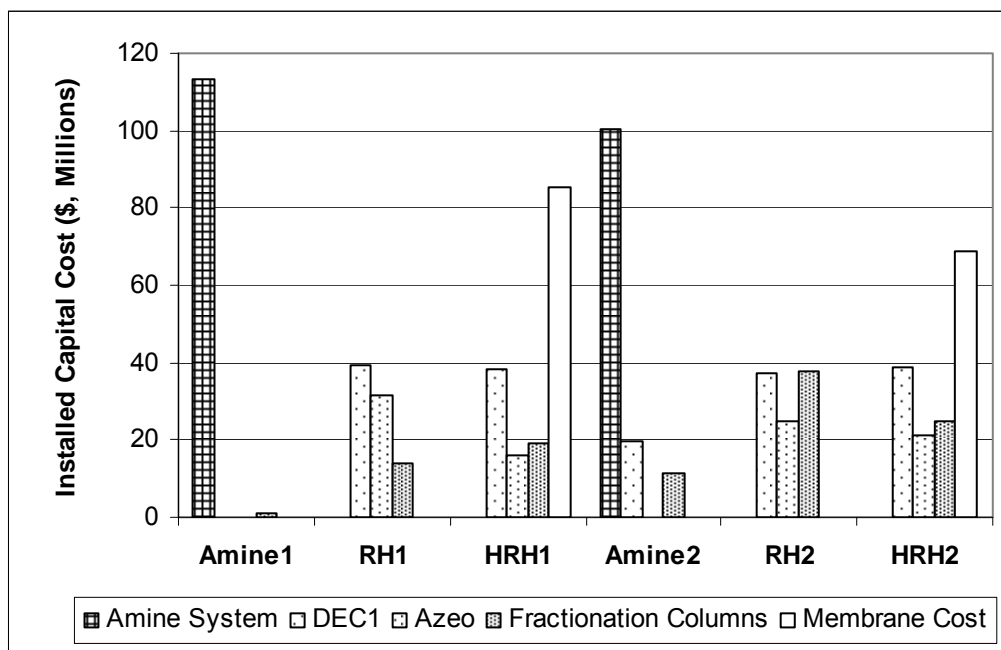


Figure 5-1. Comparison of installed equipment costs.

In Feed1 case, the total fuel requirement for the amine process was slightly higher than the RH process. The amine process consumes more energy for the heating duty, pump HP for solvent circulation, and the dehydration process; however the compression HP is lower due to the excessive refrigeration system demand in the RH process. In the Feed2 case, the compressor HP is comparable between the alternatives because of the similar condensing duty in the fractionation columns and the LNG liquefaction requirement.

The total compressor HP represents the majority of the fuel consumption therefore a further analysis on the HP consumption was examined to indicate which primary process contributed to the energy demand. Table 5-2 shows the distribution of the

total compressor HP in the process. It is shown that for all of the process alternatives, the refrigeration system accounts for more than 83% of the total compressor HP. This is obvious since the process involves LNG liquefaction and fractionation at cryogenic temperatures. The details of the refrigeration system were analysed further with an itemization of the cooling duty requirements. The demand for CO₂ compression HP was highest with the amine process since the high purity CO₂ was generated from a low pressure stripper column, and it was lowest for the RH process with CO₂ product being at a higher pressure. The fuel compression HP corresponded to the equivalent fuel demand. The air cooler fan HP was related to the air cooling duty requirement. The membrane recompression HP accounts for 5% and 4% of the total compressor HP for Feed1 and Feed2, respectively. The majority of the membrane recompression HP was for recompressing the permeate stream from membrane stage 1 going into membrane stage 2.

The refrigeration system provided the condensing duty in the fractionation column overhead (condensers), solvent cooling, LNG liquefaction, cooling and condensing of the recycled refrigerants (refrigeration), and feed pre-cooling prior to DEC1 feeding. For the amine system, the solvent cooling was performed using the air cooler and thus no refrigeration for solvent was required. Figure 5-2 shows the allocation of the cooling duties in each alternative processes.

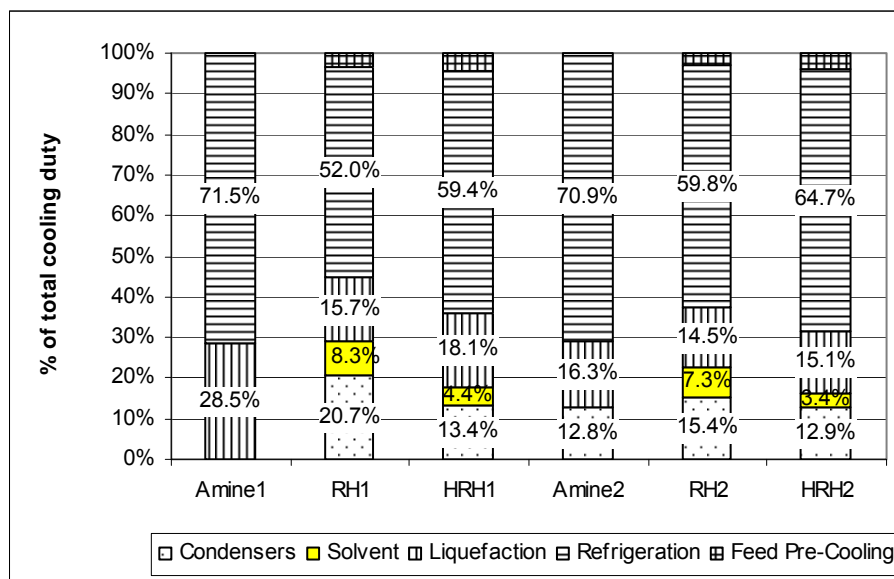


Figure 5-2. Cooling duties distribution in each process alternatives.

For all of the processes, it was observed that the majority of the cooling duty was for the refrigeration cycle, i.e. condensing the ethylene and methane refrigerants. It accounts for more than 59% in all of the alternatives. The second biggest cooling duty expense for the RH1 process was the condensers duty followed by the liquefaction duty; however a reverse trend was observed for the HRH1 process. A higher condensing duty fraction for the RH1 process highlights the significant demand for DEC1 and azeo column condenser duties. This implied that lower reflux ratios of these columns, warmer condensing temperature, or more relaxed column specifications could provide a considerable energy reduction. The application of membrane in place of the additive in the azeo column reduced the condenser duty by as much as 40% and the solvent cooling duty by as much as 53%. The notable decrease in condenser duty for the HRH1 application was due to the higher relative volatility with CO₂ and C3 key components used in the azeo column. The CO₂-ethane azeotrope was allowed to exit in the overhead and thus a lower reflux ratio was generated. The amine system liquefaction duty was approximately doubled compared to the RH and HRH processes in the Feed1 case. This was evidence in support of the RH and HRH processes due to the inherent synergies between the low temperature separation processes with the liquefaction cycle.

With regard to the Feed2 case, the condenser duties were slightly more comparable between the process alternatives than in the Feed1 case. This was due to the fractionation columns for all of the alternatives to generate differentiated hydrocarbon products. However, a higher condensing duty for the RH2 process was observed due to the difference in the column specifications. The RH2 process utilized the C2 and CO₂ specifications at the overhead and bottom products while the HRH2 utilized the C2 and C3 as the key components for the separation to allow CO₂-C2 azeotrope in the overhead stream. Furthermore, a higher relative volatility was observed for C2/C3 separation than for the CO₂/C2. The solvent cooling duty was only about 50% due to the removal of the additive from the azeo column. The liquefaction duty was comparable as a result of the synergy between the liquefaction processes with the hydrocarbon fractionation processes at low temperature conditions.

Table 5-3 shows the 5 main allocations of the refrigeration duties. The biggest refrigeration duty was needed for condensing the ethylene in all of the alternatives. It accounts for approximately 40-60% of the total refrigeration duty. The main utilization of ethylene refrigerant was for the DEC1 condenser and methane refrigerant condensing. The second biggest refrigeration duty for Feed1 was for the liquefaction process because the C3 and C4 products were mixed back with the methane stream to generate the LNG with specified Btu value. In Feed2 case, only a certain fraction of the C2 and C3 products were blended back with the methane stream from DEC1 to generate LNG. Therefore, the liquefaction demand for Feed2 was reduced.

Table 5-3. The majority of the refrigeration distribution.

Amine1		RH1		HRH1	
Ethylene condensing	46.9%	Ethylene condensing	50.2%	Ethylene condensing	57.2%
Liquefaction	28.5%	Liquefaction	9.6%	Liquefaction	10.8%
Methane condensing	24.6%	DEC1 condenser	9.0%	DEC1 condenser	10.2%
		Azeo condenser	6.4%	Liquefaction - Fuel	6.1%
		SR condenser	5.3%	Feed pre-cooling	4.7%

Amine2		RH2		HRH2	
Ethylene condensing	50.0%	Ethylene condensing	41.43%	Ethylene condensing	45.2%
Methane condensing	21.0%	Methane condensing	18.41%	Methane condensing	19.5%
Liquefaction	11.40%	Liquefaction	9.23%	Liquefaction	9.0%
DEC1 condenser	11.37%	DEC1 condenser	5.71%	DEC1 condenser	7.4%
Liquefaction - Fuel	4.7%	Azeo condenser	5.20%	Liquefaction - Fuel	5.1%

It was shown that the DEC1 condenser duty contributed to a significant portion of the total refrigeration demand when methane fractionation in the DEC1 was involved. DEC1 condensing duty was listed in all of the process alternatives, except for amine1 process where the DEC1 distillation column was not required. In the RH process, the azeo condenser duty also needed a significant refrigeration duty; however, with the application of membrane this demand was significantly reduced. The result showed that the membrane application decreased the azeo condenser duty demand as much as 80% and 50% for Feed1 and Feed2, respectively.

Based on the analysis on the energy consumption and overall economic costs, it was shown that the optimization of the DEC1 operating parameters in the RH and HRH processes was the most important factor as it affects the energy demand significantly due to the considerable condensing requirement and low temperature conditions. The

design parameters of the azeo column were also crucial although it was shown that the effect on the total energy consumption and capital cost were less profound than DEC1 design variables.

The initial utilities included purchasing of the propane, ethylene, and methane refrigerants, hot oil, amine solvent, and also the fuel. The initial utilities for the refrigerants were comparable; however, the hot oil initial utility was relatively different for different process alternatives. It is clear from Table 5-2 that the HRH processes required the lowest initial utilities due to the lower reboiler duties in the process. The higher initial utility for the amine process was due to the regeneration duty in the stripper column while for the RH, it was related to the solvent consumption in the DEC1 and azeo columns.

One of the obvious weakness of the RH process compared to amine process was with the large heat exchanger UA requirement. The RH process required a 19% larger heat exchanger UA in Feed1 case which would result in a higher capital expense. A 33% extra heat exchanger UA for Feed2 case was also observed. The main UA requirement for the RH process was for the condensers in the fractionation column, particularly for the DEC1 and azeo columns. The application of membranes in the HRH process offered a 17% and 27% reduction in the exchanger UA requirement for Feed1 and Feed2, respectively.

Table 5-2 shows that the air cooling requirements for both feeds were comparable; however the lowest values were obtained with the HRH process. It is evident that the air cooling requirement for the condensing of propane refrigerant is relatively similar. The highest air cooling demand for CO₂ recompression stages was for the amine process due to the low pressure CO₂ product generated from the stripper column and thus several recompression stages and intercoolers were required. On the other hand, the RH process which generated CO₂ at a higher pressure required the least air cooling duty. The amine process also needed a significant amount of air cooler in the overhead of the stripper column and for cooling the recycled amine solvent. The demand for air cooling duty in the acid removal process accounted for 30% and 23% of the total requirement for Feed1 and Feed2 respectively. It was also observed that a substantial air cooling was required for the RH process, particularly

for cooling the bottom stream from the azeo and SR column. Thus, a decreased air cooling demand was achieved in the HRH process due to the lower circulation rates of process streams.

The comparison of feed flow rate into the distillation columns between the RH and HRH processes is shown in Figure 5-3. The flow rate was reduced to about 50% in the azeo column and 25% in the SR column with the application of a membrane in the HRH process. Consequently, a significant reduction in air cooling demand and capital cost was achieved.

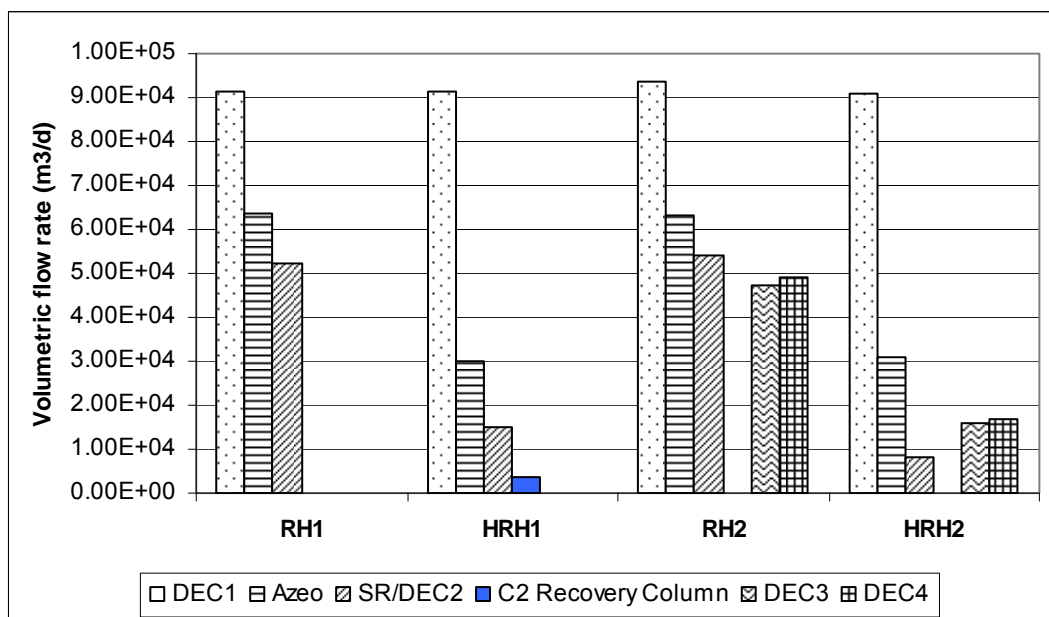


Figure 5-3. Feed flow rate reduction with membrane utilization in HRH process.

Table 5-2 also shows that the HRH process generates the highest LNG production. The RH process delivered a lower LNG product due to the higher fuel demand in the plant whereas the amine process lost some of the methane product in the off-gas stream. In terms of CO₂ recovery, the RH process was more advantageous since the HRH process lost some of the CO₂ in the purge stream and the amine process lost the CO₂ in the off gas stream.

The evaluation of the process alternatives was also performed in terms of the Present Value (PV) method. The PV method utilizes the desired interest rate to calculate the present values of the initial investment and cash flows of the investment project.

Thus, it shows the actual difference in dollars with a particular interest rate. The PV comparison of the process alternatives with 10% interest rate is shown in Table 5-4. The application with a lower interest rate would generate a higher difference in the present values of the process alternatives. However, the PV method shows the same result as the IRR method, that is the amine process is more economical for Feed1 and the RH process is more advantageous for Feed2.

Table 5-4. Comparison of PV values.

PV method (10%)	Amine	RH	HRH
Feed1	\$ 686,754,718	\$ 568,184,547	\$ 60,782,317
Feed2	\$ 3,530,629,723	\$ 3,970,079,834	\$ 3,715,376,753

5.2 Comparison between process alternatives

From the design point of view, it was observed that the amine process setup was more straightforward because both CO₂ and H₂S were removed upfront and thus the stream was left with the remaining hydrocarbon. In Feed1 case, the condensate product was sent directly as a sellable product whereas in Feed2 case, the specification for the fractionation columns was adjusted simply by following the commercial specification without considerable concerns about the acid gas level in the generated products. However, for the RH and the HRH processes, the recycled solvent stream generated from the solvent recovery column affected the separation in DEC1 and azeo columns. In Feed1 case, the column specification utilized in SR column determined the solvent composition and thus affected the LNG Btu value, C5+ fraction in the LNG and the minimum temperature approach in DEC1. Consequently, some options were available to generate the required separation. For example, higher C4 in the SR overhead increased the LNG Btu value and reduced the condensate product, however the solvent contained less C4 and this caused a higher solvent demand to keep the minimum approach temperature above 5.5°C in DEC1. On the other hand, a lower C4 fraction caused an opposite outcomes. This illustration described the complexity of the design aspect in the RH/HRH process; however, the IRR economic measure was used in this study to decide the most optimum condition.

Furthermore, the RH/HRH processes required an additional H₂S removal facility to separate the H₂S in the C2 product stream. This will impose an additional capital and

operating costs. In contrast, the amine process typically removes the CO₂ and H₂S simultaneously upfront in the contactor using the amine solvent.

The results from HRH process for both feed conditions showed that the HRH is less economical than the RH process. The primary reason was due to the additional membrane system cost. It was observed that the capital cost reduction of the azeo and subsequent columns due to the removal of the additive stream did not compensate the membrane cost. Furthermore, an additional C2 recovery column was needed to recapture the C2 product for Feed1 case and thus a bigger difference in total equipment cost was generated. However, it was revealed that the HRH process fuel consumption was the lowest in both conditions due to the lower heating duty and pump horsepower. With higher CO₂ fraction in the feed, this benefit might be more apparent as the reduced solvent demand and flow rate significantly affects the energy and capital costs. Furthermore, with higher CO₂ fraction in the feed, a second stage membrane might be removed thus reducing the capital cost and the recompression horsepower.

5.3. Analysis of Process Alternatives with Various CO₂ Range

This section observed the economic evaluation of the RH and HRH process in treating higher CO₂ content feeds. Figure 5-4 shows the increasing solvent demand in the DEC1 with higher CO₂ fraction in the feed using a stand alone DEC1 column. Feed1 was used in this study. The increased CO₂ was compensated with a reduced C1 content. It is shown that initially the solvent demand increases slightly and then is approximately constant before having a steep increase at higher CO₂ concentration. This behaviour was related to the properties of the stream itself. As the CO₂ fraction increased, the inlet temperature going into the DEC1 was set warmer to avoid the liquid existence in the expander inlet stream and there was no CO₂ freeze out issue observed with the use of solvent in the DEC1 column. The amount of solvent was altered to meet the lowest minimum approach to CO₂ freezing point of 5.5°C in all of the trays.

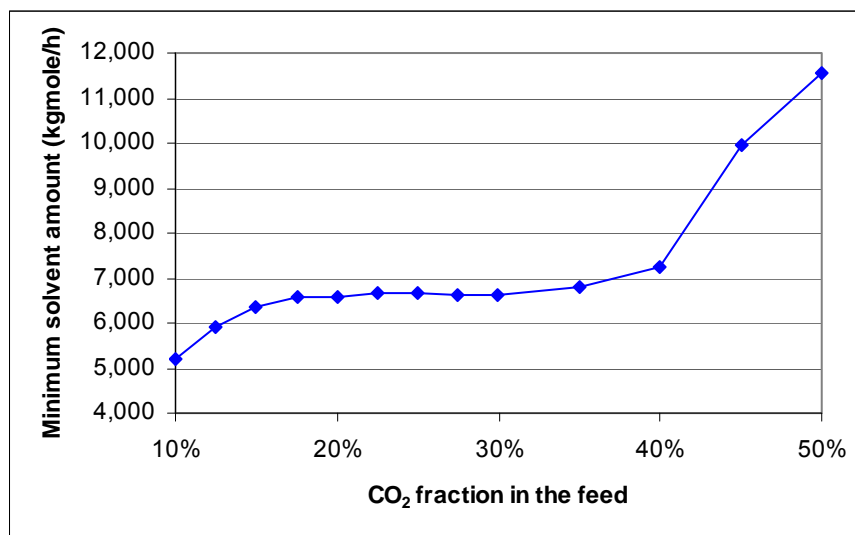


Figure 5-4. Solvent demand in DEC1 as a function of CO₂ variation in the feed.

The lowest CO₂ minimum approach temperature was observed at varying tray location as the CO₂ content in the feed was altered. The location at which this minimum was observed related to the equilibrium temperature at each tray and the CO₂ freezing temperature which was a function of the CO₂ concentration at the corresponding tray.

A sensitivity study on the solvent requirement in the extractive distillation process was also performed with varying CO₂ content in the feed since the solvent amount is one of the most important factors in process economics. This study was conducted in a single extractive distillation column utilizing a pure nC₅ solvent. Figure 5-5 shows the solvent and reflux ratio demands for various CO₂ feeds for an extractive distillation column with 50 theoretical stages. The product specifications were 95% CO₂ purity in the overhead and 40 ppm mole in the bottom product. At low reflux ratios, the solvent amount decreased with the CO₂ fraction in the feed, while an opposite behaviour was observed for higher reflux ratios. This particular behaviour explains that the solvent quantity is a function of the amount of ethane in the column. At lower reflux ratios, a higher CO₂ content in the feed means less C₂ and therefore, a lower solvent quantity is required. At higher reflux ratios, although the C₂ fraction in the feed decreases with CO₂ fraction, the liquid flow in the column still contains higher amount of C₂ because of the increased reflux flow and thus needing a higher solvent amount.

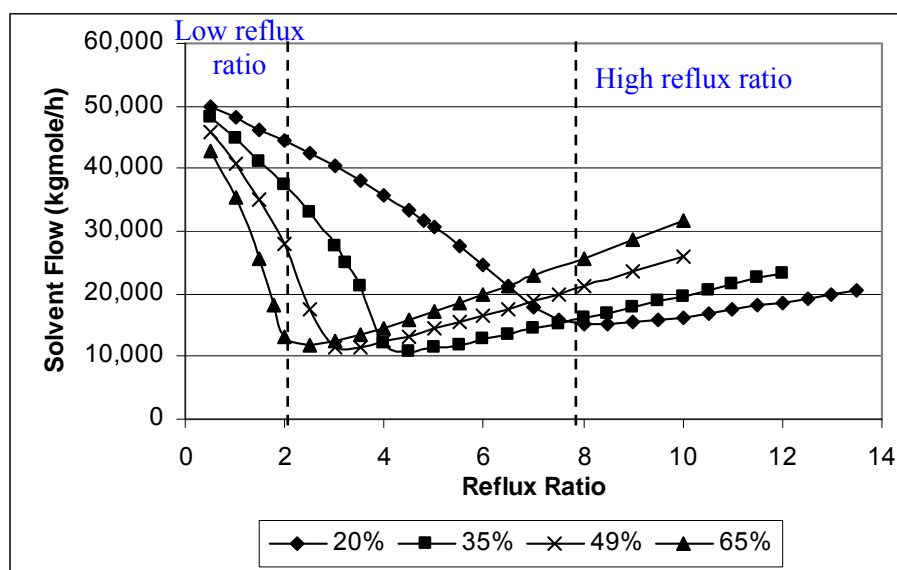


Figure 5-5. Reflux ratio and minimum solvent amount with variation of CO₂ content in the feed.

In terms of operability and economics, a low reflux ratio operation is generally preferred. Therefore, Figure 5-5 suggested that as the CO₂ content in the feed increases, the solvent demand in the azeo column is lower; however, the generated hydrocarbon product decreases for the same amount of feed.

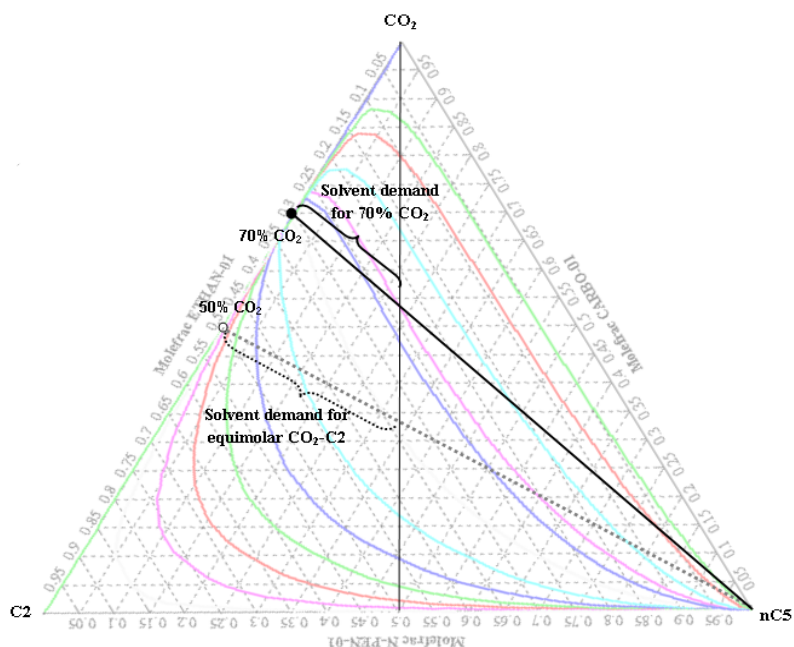


Figure 5-6. Lever-arm rule for calculating solvent demand in a residue curve.

This result confirmed the lever arm rule method in a residue curve for calculating the solvent demand (Figure 5-6). It is shown that a higher CO₂ fraction in the CO₂-

ethane azeotrope mixture requires less solvent amount to obtain a high purity CO₂. However, this treatment was not applicable in the analysis of the global flowsheet which involved a recycle stream and mixed solvent composition.

In the analysis with varying the CO₂ content in the global flowsheets, the increased CO₂ content in the feed was compensated by a decrease in methane fraction. Figure 5-7 shows the minimum solvent demand for DEC1 as a function of CO₂ fraction in the feed. CO₂ fraction in Feed1 was varied in the range of 7%, 15%, and 30% while Feed2 with richer hydrocarbon was varied with CO₂ content of 5%, 11%, and 20%. It is apparent that in both cases the solvent demand in the DEC1 increases with the CO₂ fraction in the feed; however, the rise is not linear.

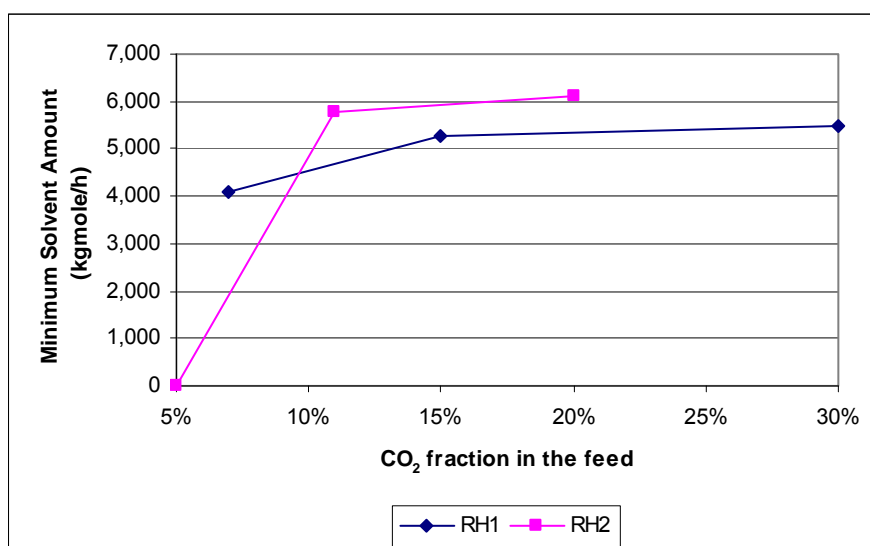


Figure 5-7. Minimum solvent amount in DEC1 as a function of CO₂ fraction in the feed.

A study to observe the effect of CO₂ content in the feed to the solvent amount demand in the azeo column was also observed. The amount of CO₂ fed into the azeo column increased with the CO₂ fraction in the feed; however, the ethane content was fixed at a certain molar flow rate. The flow rate to the azeo column was also increased with higher CO₂ fraction in the feed as this stream came from the bottom of the DEC1. The solvent amount was calculated based on a ratio of 1.105 to the minimum solvent demand. Figure 5-8 shows a linear trend in solvent amount with increasing CO₂ feed. This graph shows that the solvent demand is directly related to the CO₂ fraction in the feed.

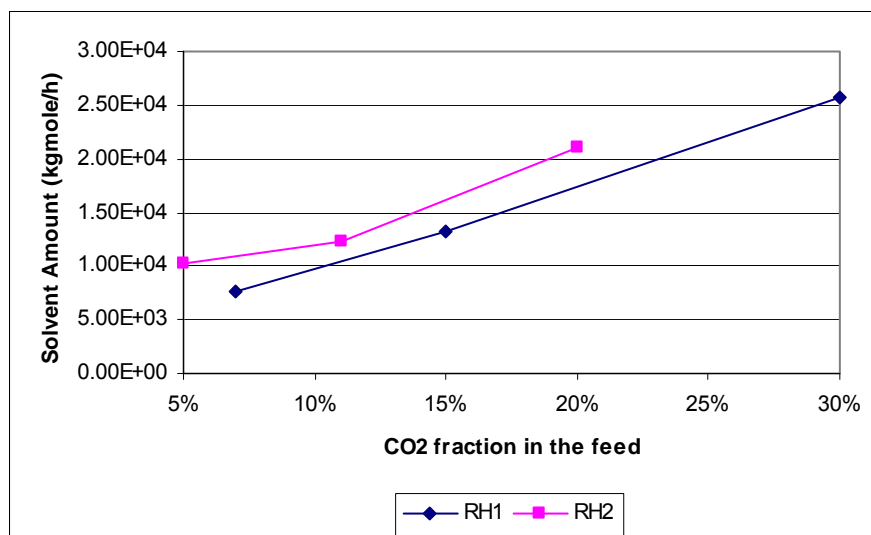


Figure 5-8. Solvent amount in azeo column as a function of CO₂ fraction in the feed.

Figure 5-9 shows that the economic rate decreases with CO₂ fraction in the feed for all of the alternative processes as the solvent demand increases and thus the energy and capital costs escalate. It is also shown that the CO₂ variation in the feed did not alter the DCF trend of the process alternatives, the amine was the best option for Feed1 and RH process was superior for Feed2.

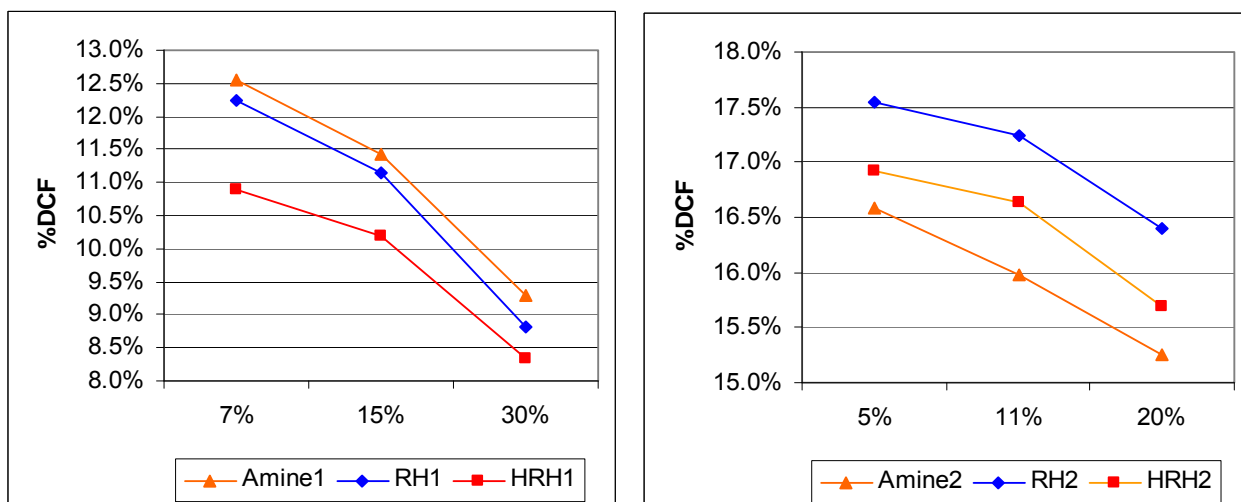


Figure 5-9. %DCF as a function of CO₂ fraction in the feed.

Figure 5-10 and Figure 5-11 show that solvent flow rate increases with the concentration of CO₂ in the feed for both the RH and amine processes. It is shown that the solvent demand increases in a linear pattern for the amine process and the

azeo column of RH process; however, the rise of solvent demand in the DEC1 is slightly invariant at higher CO₂ fraction.

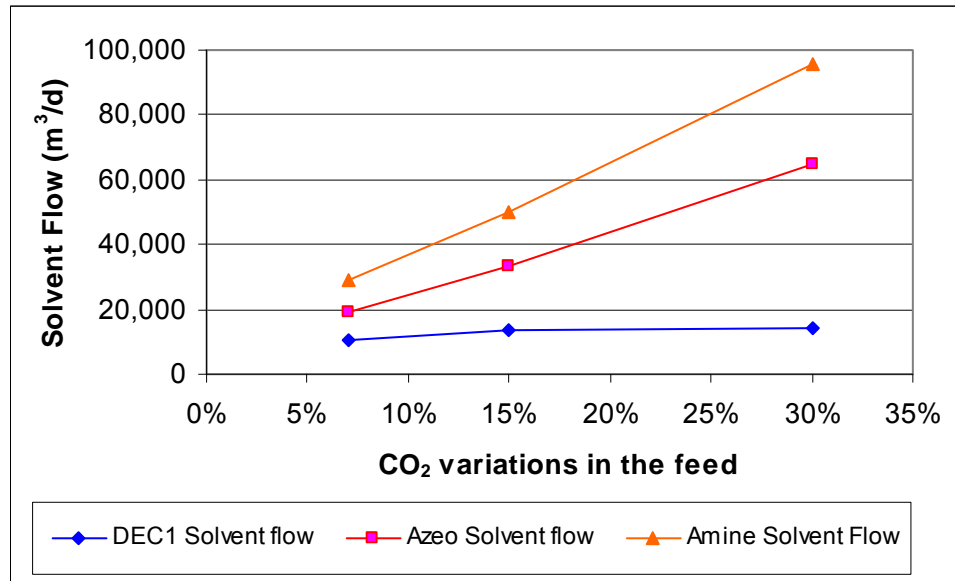


Figure 5-10. Solvent flow as a function of CO₂ variations in Feed1.

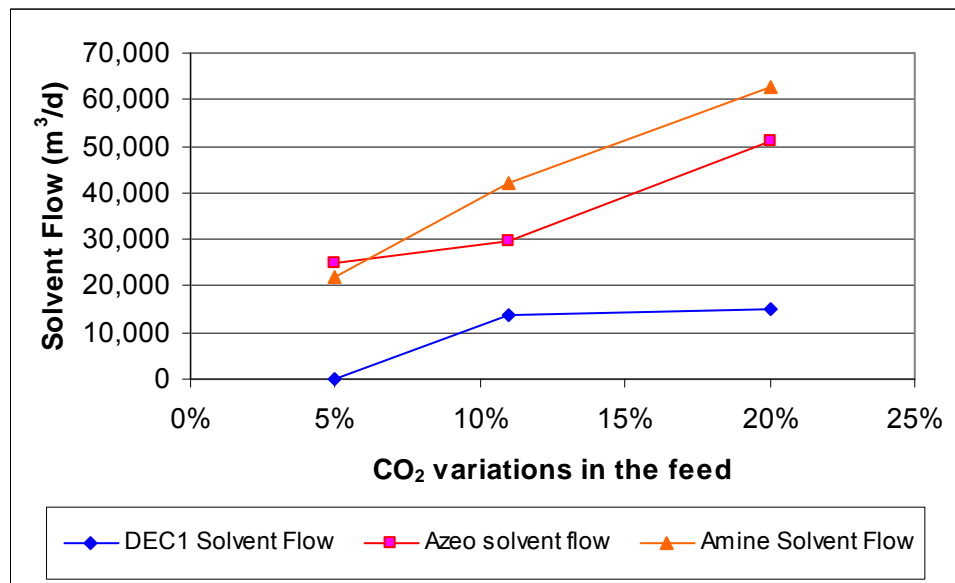


Figure 5-11. Solvent flow as a function of CO₂ variations in Feed2.

5.4. Conclusions

Three different alternatives for producing LNG and high purity CO₂ for geological injection, and where possible differentiated hydrocarbon products, were studied. Table 5-5 summarises the strengths and weaknesses of each process alternatives.

Table 5-5. Summary of comparative benefits and drawbacks of process alternatives.

	Amine	RH	HRH
(+)	Beneficial for lean feed gas and fractionation columns were not necessary	<ul style="list-style-type: none"> • Favourable when feed stream contained significant level of valuable hydrocarbon products. The separation units were operating at a similar low temperature conditions and thus a direct feed to the liquefaction system was facilitated. • Lower CO₂ recompression HP for CO₂ geological sequestration. 	<ul style="list-style-type: none"> • Decreased solvent circulation rate in the azeo column. • Lowest fuel consumption. • Highest LNG production. • Lowest air cooling demand. • Lowest initial hot oil utility.
(-)	<ul style="list-style-type: none"> • Higher heating duty for acid gas removal. • Highest CO₂ recompression HP • Highest liquefaction duty because the sweet gas enters the liquefaction system at air cooling temperature • No synergies between the separation units and the liquefaction system • Higher dehydration system cost • Lowest LNG production because of methane loss in the off gas. 	<ul style="list-style-type: none"> • Substantial heat exchanger UA. • Significant condensing duties in DEC1 and azeo condensers. • Additional cost for H₂S removal facility to purify the C2 product. 	<ul style="list-style-type: none"> • Less economical in treating Feed1 and Feed2. • Higher capital cost than the RH process because of the additional membrane system and a C2 recovery column for Feed1 case. • High purity CO₂ demand was difficult to obtain and thus a double stage membrane and higher recompression and capital costs were required. • Additional cost for H₂S removal facility to purify the C2 product.

One of the main differences between the process alternatives was the energy required for CO₂ recompression to generate high pressure CO₂ for geological injection. This is a significant contributor to the overall cost, when the CO₂ fraction in the feed is high.

However, it was observed that the percentage of power required for CO₂ recompression was trivial compared to the energy required for the compressors for the refrigeration duty.

The DCF decreased with the CO₂ fraction in the feed for all of the alternatives in the CO₂ range observed. The solvent demand in the amine process and azeo column increased sharply with the CO₂ fraction in the feed, however, the DEC1 solvent demand remained nearly constant.

6. CONCLUSIONS AND RECOMMENDATIONS

6.1. Guidelines for securing the Ryan-Holmes process and the hybrid membrane Ryan-Holmes process

Detailed analysis on the process alternatives for treating both feeds highlighted the strengths and weaknesses of each process for LNG production and facilitated guidelines for selecting the RH and HRH over the amine process. The summary of this study is presented below:

1. The suitable candidate for the RH process should have the following properties:
 - a. A high CO₂ content feed with a significant amount of hydrocarbon heavier than CH₄. This compositional feed requires fractionation columns to generate the differentiated hydrocarbon products. The RH process facilitates a synergy between the separation units and the liquefaction units which is unfeasible in the amine process. In addition, it was observed that in terms of CO₂ acid gas removal and simultaneous hydrocarbon generation, a series of distillation column was more economical than using a comprehensive amine unit plus the fractionation columns. It also offers the possibility to circumvent the need for NGL solvent to prevent CO₂ solidification in the DEC1. In addition, the valuable hydrocarbon products also provide significant revenue to the plant.
 - b. High pressure natural gas feed. The high pressure feed allows for expansion work to gain low temperature stream for direct feeding to DEC1. Horsepower recovery can be utilized by other unit operations.
 - c. H₂S is not present in the feed. Additional H₂S removal facility is required for the RH/HRH process to separate the H₂S component concentrated in the C2 product.
 - d. When a gas treating facility already exists, the design variables in the DEC1 column can be relaxed with a lower purity specification in the overhead stream of DEC1 to generate methane with less stringent CO₂ spec and warmer condensing temperature to reduce the energy and economic requirement of the plant.
2. The HRH process was not suitable for treating either of the feeds because of two main reasons. Firstly, the high flow rate imposed the need for a large membrane

area to achieve the required recovery level; however, the purity level had to be still compromised. Secondly, the high CO₂ purity requirement also entailed a second stage membrane to increase the CO₂ product purity. The installation of the second stage membrane led to additional energy demand and capital cost. Furthermore, the HRH process also required an additional upfront H₂S removal facility to prevent the H₂S split in the CO₂ and C₂ products. Membrane application would be more suitable for a low feed rate and a reduced CO₂ purity requirement application.

6.2. Conclusions

A simulation based approach was performed to analyse three different LNG process alternatives for treating two different feed conditions. The result showed the choice of process alternatives strongly depended on the feed conditions, largely the composition. A detailed analysis of the process alternatives is therefore valuable in terms of deciding the most optimum process. The conclusions from this research may be summarised as follows:

1. With respect to the three alternative processes, the simulation results showed that the optimum selection depends on the natural gas feed composition. The most economical process for Feed1 was the amine process and for Feed2 was the RH process. In terms of the fuel consumption, the HRH process was the most fuel efficient process and generated the highest LNG production. Although the HRH process offered lower energy consumption for both feed conditions and reduced solvent circulation rate in the process, it was the most uneconomical in terms of the capital cost due to the membrane system installation. The process with the least capital cost for Feed1 was the amine process and for Feed2 was the RH process.
2. The application of the RH process for LNG production from a high CO₂ natural gas feed has proven to be an effective alternative when the feed contains high levels of hydrocarbon heavier than CH₄. When a considerable amount of hydrocarbons are available, the fractionation columns are required to produce differentiated products and thus the RH offers a better solution as shown in the Feed2 case.

3. The suitable candidate for the RH process would be the high CO₂ natural gas feed with considerable amount of hydrocarbon fractions which enables the CO₂ removal and the differentiated product generations through fractionation processes. The feed should also be at a high pressure condition to allow for expansion work to lower the stream temperature for a direct feeding to DEC1. Furthermore, it is preferable if H₂S is not present in the feed gas or at least in a small amount to allow the use of a solid adsorbent bed for H₂S removal. For both feed conditions and for the CO₂ range evaluated in this work, it was shown that the RH process was superior compared to the HRH process.
4. The HRH process was less economical than the both amine and RH processes for treating either of the feeds. It was demonstrated that the high flow rate application and the high purity CO₂ requirements resulted in a high capital cost for the HRH process. Larger membrane area was required to accommodate the high flow rate stream from the azeo overhead. However, when the high membrane area was applied, the purity value was compromised and thus a second stage membrane was required to improve the purity level.
5. The analysis of various CO₂ ranges in the feed for LNG production shows that the preference of the process alternative was not affected with the variation of CO₂ in the feed. RH process was superior to the HRH and amine processes when the feed contained significant amount of valuable hydrocarbons; however, when a lean feed gas was treated, the amine process proved to be a better option than the RH/HRH processes.
6. The key parameters in designing the RH/HRH process were the design variables of the DEC1 and azeo columns since the performance of these columns related significantly to the cooling duty requirement. In particular, the selection of the column pressure, solvent amount, and solvent composition used in the DEC1 and azeo columns was of significant importance. The effect of the minimum approach temperature on the IRR was only significant when the duty required at a particular refrigeration stage was considerable compared to the total cooling duty and involved a low temperature condition such as the DEC1 condensing duty.

7. The design of the extractive distillation column for the separation of CO₂-ethane azeotrope is a complex process since it involves the interactive effects of the design variables. The key parameter related to the economics of the plant is the solvent amount. The solvent amount is a function of feed composition, feed inlet stage, solvent inlet stage, and solvent composition. It is also related to the reflux ratio of the column. The result also shows that the optimum feed inlet stage corresponds to the maximum economic rate. The optimum solvent inlet stage in terms of the economics was near the top of the column due to the reduced reflux ratio; however, the solvent impurity limit dictates the final solvent inlet location. A study on various CO₂ ranges in the feed showed that the solvent demand in the extractive column is related to the CO₂ and C2 flow rate in the column. As the CO₂ fraction in the feed increases, the solvent demand also rises. However, the solvent amount is also related to the C2 amount in the column when the reflux ratio applied is above the optimum value.

8. The required composition of hydrocarbon fractions in the solvent was slightly different for the DEC1 and azeo columns. A solvent with higher C3 fraction was preferred in the DEC1 since it provided a higher ΔT approach to the CO₂ freezing point; however, a higher reflux ratio in the azeo column and C3 loss in the CO₂ product were observed.

6.3. Recommendations for future work

During this work, several ideas have arisen for further examination to improve the certainty of the result:

1. Some of the equipment purchase costs were computed based on the general plant design and economic textbooks and have not been validated with any industrial data. Also, the sensitivity of the numerous parameters used in the capital cost calculation has not been addressed yet. Since these two factors directly related to the economic comparison of the process alternatives, the purchase cost validation and sensitivity analysis of the costing parameters would improve the research confidence.

2. A validation with real plant data would be valuable to analyse the simulation result of the single distillation column and the relation between the multiple distillation columns with the recycle streams. In particular, the validation of the extractive distillation column would confirm the conclusion generated from this study.
3. This study was conducted using a cascaded refrigeration system. Using a mixed refrigerant may provide further opportunities for process integration. Therefore, it is highly recommended to conduct this study using a mixed refrigerant cycle.
4. The economic analysis in this study does not include the cost of emissions. It is believed that some sort of an emission trading scheme (ETS) is likely to come into force in the coming years. Inclusion of any ETS cost may significantly affect the choice process alternatives. It is therefore, highly recommended to include the ETS component in the economic analysis in a future study.
5. Investigation on the alternative methods to increase the hydrocarbon recovery in the differentiated product simulation such as the Gas Subcooled Process (GSP) or the Residue Recycle (RR) process would be valuable to improve the economics of the process (GPSA 2004).
6. Further study on the operability and controllability issues of the distillation processes in the RH and HRH processes in comparison with the mature amine process is an important area for further research.

REFERENCES

- Arnold, K., and M. Stewart. 1999. *Surface production operations*. 2nd ed. Vol. 2. Houston: Gulf Publishing Co.
- Baasel, W. D. 1990. *Preliminary Chemical Engineering Plant Design*. 2nd ed. New York: Van Nostrand Reinhold.
- Baker, R. W. 1991. *Membrane separation systems: recent developments and future directions*. Park Ridge, USA: Noyes Data Corporation.
- Barnes, F. J., and C. J. King. 1974. Synthesis of Cascade Refrigeration and Liquefaction System. *Ind. Eng Chem. Process Des. Dev.* 13 (4): 421-433.
- Bell, S. 2007. Chevron's Gorgon LNG Clears State Environment Hurdle, edited by D. J. Newswires.
- Bhide, B. D., A. Voskericyan, and S. A. Stern. 1998. Hybrid processes for the removal of acid gases from natural gas. *Journal of Membrane Science* 140: 27-49.
- Blizzard, G., D. Parro, and K. Hornback. 2005. Mallet gas processing facility uses membranes to efficiently separate CO₂. *Oil & Gas Journal* 103 (14): 48-53.
- Boyce, M. P. 2006. *Gas Turbine Engineering Handbook*. 3rd ed: Elsevier.
- Brooks, F. J. 2006. *GE Gas Turbine Performance Characteristics*, November 2007).
- Bruns, A. 2005. Chevron, Shell and ExxonMobil Move Ahead Down Under, edited by T. S. Selection.
- Bullin, J. A., J. C. Polasek, and S. T. Donnelly. 1990. *69th GPA Annual Convention, The use of MDEA and Mixtures of Amines for Bulk CO₂ Removal*. Tulsa, Oklahoma: Gas Processors Association(accessed
- Carmody, P. 2006. *CO₂ Produced Gas Treating and Reinjection*. HESS.
- Chan, K. I. 2008. Gorgon Amine Process Simulation PFD. 28-September-2008. Chevron ETC, Houston.
- Chinn, D. 2007a. Commercial membrane specification, Perth.
- Chinn, D. 2007b. Question (RVP and HHV). 22-August-2007. Chevron ETC, Richmond, CA.
- Coady, A. B., and J. A. Davis. 1982. CO₂ Recovery by Gas Permeation. *Chemical Engineering Progress* October: 44-49.

- Cook, P. J., and M. S. Losin. 1995. Membrane provides cost-effective natural gas processing. *Hydrocarbon Processing* April: 79-84.
- Denton, R. D., and D. D. Rule. 1985. Two combined cryogenic processes cut sour natural-gas processing cost. *Oil & Gas Journal* Aug 19: 120-124.
- Dortmundt, D., and K. Doshi. 1999. Recent Development in CO₂ Removal Membrane Technology.
- Echt, W. 2002. Hybrid Systems: Combining Technologies Leads to More Efficient Gas Conditioning. In *Laurance Reid Gas Conditioning Conference*. UOP.
- Fernandez, L., J. A. Bandoni, A. M. Eliceche, and E. A. Brignole. 1991. Optimization of ethane extraction plants from natural gas containing carbon dioxide. *Gas Separation & Purification* 5 (December): 229-234.
- Fleming, K. B., M. L. Spears, and J. A. Bullin. 1988. *63rd Annual SPE Technical Conference, Design Alternatives for Sweetening LPG's and Liquid Hydrocarbons with Amines*. Houston, TX.: Society of Petroleum Engineers(accessed
- Friedman, B. M., R. J. Wissbaum, and S. P. Anderson. 2004. Various recovery processes supply CO₂ for EOR projects. *Oil & Gas Journal*: 37-43.
- Garrett, D. E. 1989. *Chemical Engineering Economics*. New York: Van Nostrand Reinhold.
- Gerrard, A. M. 2000. *Guide to Capital Cost Estimating*. 4th ed. Rugby, Warwickshire: McGraw-Hill.
- GPSA. 2004. *Engineering Data Book*. Edited by F. Version. 12th ed. Vol. Volume I&II, *Gas Processors Suppliers Association*. Tulsa, Oklahoma: Gas Processors Suppliers Association.
- Grainger, D., and M. B. Hagg. 2008. Techno-economic evaluation of PVAm CO₂-selective membrane in an IGCC power plant with CO₂ capture. *Fuel* 87: 14-24.
- Grassi, V. G. 1992. Process Design and Control of Extractive Distillation. In *Practical Distillation Control*, ed. W. L. Luyben, 533. New York: Van Nostrand Reinhold.
- Ho, W. S. W., and K. Sirkar. 1992. *Membrane Handbook*. New York: Van Nostrand Reinhold.
- Holmes, A. S., J. M. Ryan, B. C. Price, and R. E. Styring. 1982. Process improves acid gas separation. *Hydrocarbon Processing* May: 131-136.
- Inc., C. E. C. 2006. Engineered Systems, Ryan Holmes Process Introduction. Chart Energy & Chemicals Inc.

- Jelen, F. C., and M. S. Peters. 1970. *Cost and Optimization Engineering*. USA: McGraw-Hill, Inc.
- Jou, F., A. E. Mather, and F. D. Otto. 1982. Solubility of H₂S and CO₂ in Aqueous Methyl-diethanolamine Solutions. *Ind. Eng. Chem. Process Des. Dev.* 21: 539-544.
- Katz, D. L., D. Cornell, R. Kobayashi, F. H. Poettmann, J. A. Vary, J. R. Elenbaas, and C. F. Weinaug. 1959. *Handbook of Natural Gas Engineering*. York, Pennsylvania: McGraw-Hill Book Company, Inc.
- Kidnay, A. J., and W. Parrish. 2006. *Fundamentals of natural gas processing*. USA: Taylor and Francis Group, LLC.
- Kohl, A., and R. Nielsen. 1997. *Gas Purification*. 5th ed. Houston, Texas: Gulf Publishing Company.
- Laroche, L., N. Bekiaris, H. W. Andersen, and M. Morari. 1991. Homogeneous Azeotropic Distillation: Comparing Entrainers. *The Canadian Journal of Chemical Engineering* 69 (December): 1302-1319.
- Lastari, F., and K. Maeda. 2008. Validation of CO₂-ethane vapor liquid equilibrium in HYSYS using several Equations of States. Research Collaboration. Himeji and Perth. University of Hyogo and Curtin University of Technology.
- Ludwig, E. E. 2001. *Applied Process Design for Chemical and Petrochemical Plants*. 3rd ed. Vol. 3. Louisiana: Gulf Professional Publishing.
- Lunsford, K. M., and J. A. Bullin. 1996. *AIChE Spring National Meeting, Optimization of Amine Sweetening Unit*. New York: AIChE (accessed
- MacKenzie, D. H., F. C. Prambil, C. A. Daniels, and J. A. Bullin. 1987. Design & Operation of a Selective Sweetening Plant Using MDEA. *Energy Progress*: 31-36.
- Marriott, P. 2006. Turtle Power Threatens Chevron's Gorgon Gas Project, edited by R. N. Service.
- McKee, R. L., M. K. Changela, and G. J. Reading. 1991. CO₂ removal: membrane plus amine. *Hydrocarbon Processing* April: 63-65.
- Nordstad, K. H., T. K. Kristiansen, and D. Dortmund. 2003. Hybrid separation of CO₂ from ethane using membranes. <http://www.tkk.fi/Units/ChemEng/efce/2003/presentations/nordstad.pdf>.
- Petchers, N. 2003. *Combustion Gas Turbines* 15 November 2007).
- Peters, M. S., K. D. Timmerhaus, and R. E. West. 2003. *Plant design and economics for chemical engineers*. 5th ed. New York: McGraw-Hill.

- Polasek, J. C., G. A. Iglesias-Silva, and J. A. Bullin. 1992. *71st GPA Annual Convention, Using Mixed Amine Solutions for Gas Sweetening*. Tulsa, Oklahoma: Gas Processor Association (accessed
- Price, B. C., and F. L. Gregg. 1983. CO₂/EOR: from source to resource. *Oil & Gas Journal*: 116-122.
- Reid, R. C., J. M. Prausnitz, and B. E. Poling. 1987. *The properties of gases & liquids*. 4th ed. Mexico: McGraw-Hill.
- Russell, F. G., and A. B. Coady. 1982. Gas-permeation process economically recovers CO₂ from heavily concentrated streams. *Oil & Gas Journal*: 126-134.
- Ryan, J. M., and J. V. O'Brien. 1986. Distillation technology increases propane recovery in carbon-dioxide floods. *Oil & Gas Journal*: 62-67.
- Ryan, J. M., and F. W. Schaffert. 1984. CO₂ Recovery by the Ryan/Holmes Process. *Chemical Engineering Progress* October: 53-56.
- Saltelli, A., S. Tarantola, F. Campolongo, and M. Ratto. 2004. *Sensitivity Analysis in practice: A guide to assessing scientific models* West Sussex, England: John Wiley & Sons, Ltd.
- Schaffert, F. W., and J. M. Ryan. 1985. Ryan/Holmes technology lands EOR projects. *Oil & Gas Journal*: 133-136.
- Schendel, R. L. 1982. EOR + CO₂ = A gas-processing challenge. *Oil & Gas Journal*: 158-166.
- Schendel, R. L. 1983. Process can efficiently treat gases associated with CO₂ miscible flood. *Oil & Gas Journal*: 82-86.
- Schendel, R. L. 1984. Using Membranes for the Separation of Acid Gases and Hydrocarbons. *Chemical Engineering Progress* May: 39-43.
- Schendel, R. L., and F. T. Selleck. 1981. Process of Separating Acid Gases from Hydrocarbons. USA 4,374,657, filed June 3, and issued
- Schendel, R. L., and J. Seymour. 1985. Take care in picking membranes to combine with other processes for CO₂ removal. *Oil & Gas Journal*: 84-86.
- Schweitzer, P. A. 1997. *Handbook of separation techniques for chemical engineers*. 3rd ed. New York: McGraw-Hill.
- Seader, J. D., J. J. Siirola, and S. D. Barnicki. 1997. Distillation. In *Perry's Chemical Engineers' Handbook*, ed. R. H. Perry and D. W. Green, 13-75. McGraw-Hill.

- Seider, W. D., J. D. Seader, and D. R. Lewin. 2004. *Product&Process Design Principles: synthesis, analysis, and evaluation*. 2nd ed. USA: John Wiley and Sons, Inc.
- Spears, M. L., K. M. Hagan, J. A. Bullin, and C. J. Michalik. 1996. *75th GPA Annual Convention, Converting the DEA/MDEA Mix Ups Sweetening Capacity*. Tulsa, Oklahoma: Gas Processor Association(accessed
- Spillman, R. W. 1989. Economics of Gas Separation Membranes. *Chemical Engineering Progress* January: 41-62.
- Stacey, J. 2005. Western Australia Oil and Gas Review, edited by D. o. I. a. Resources.
- Tsai, N. C. 2007. Product Specification. 8-August-2007. Chevron ETC, Houston.
- Walas, S. M. 1990. *Chemical Process Equipment - Selection and Design*. Edited by H. Brenner. Newton: Butterworth-Heinemann.
- Wood, N. V., J. V. O'Brien, and F. W. Schaffert. 1986. Seminole CO₂-flood gas plant has successful early operations. *Oil & Gas Journal*: 50-54.
- Younger, A. 2004. *Natural Gas Processing Principles and Technology - Part II*. Calgary, Alberta: University of Calgary.

Every reasonable effort has been made to acknowledge the owners of copyright material. I would be pleased to hear from any copyright owner who has been omitted or incorrectly acknowledged.

Appendix A. Dehydration System Calculation

Adopted from GPSA Electronic Databook (GPSA 2004)

This is the example calculation for Feed1 gas for RH1/HRH1 process.

Dehydration Stage

1. Determine the diameter of the dehydration column which depends on the superficial velocity to prevent channelling (too low superficial flow) and high pressure drop (too high pressure drop).

Data:

Design column pressure = 1367 psig = 9423 kPag.

Gas flow rate = 6907 ACFM = 11735 ACT_m³/h.

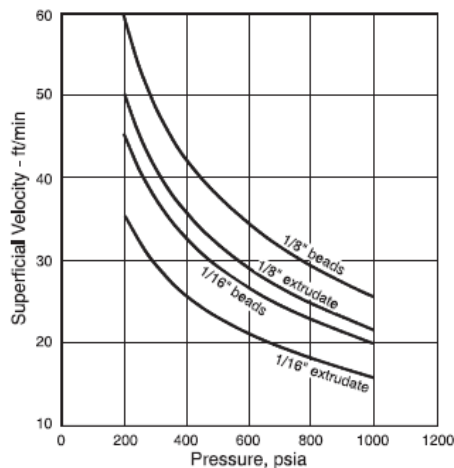


Figure A-1. Allowable Velocity for Mol-Sieve Dehydrator (GPSA 2004)

From Figure A-1, using 1/16" beads, the maximum superficial velocity allowed is approximately: 17.5 ft/min.

- a. Calculating the superficial area:

$$A = \text{Gas flow rate} / \text{Superficial velocity} = 6907 / 17.5 = 394.7$$

$$A = \pi \cdot D^2 / 4 \rightarrow D = 22.4 \text{ ft.}$$

- b. Using 3 columns:

$$\text{Diameter for each column} = 7.47 \text{ ft} \sim 7.5 \text{ ft.}$$

Therefore the adjusted velocity:

$$V_{\text{adjusted}} = V_{\text{max}} \left(\frac{D_{\text{min}}}{D_{\text{selected}}} \right)^2 = 17.36 \text{ ft} / \text{min}$$

2. Amount of water to be removed during cycle
 - a. Define the adsorption cycle time = 24 hrs (trial and error to achieve the desirable result and considerable comparison with the amine process).

- b. Calculate the water removed for each hour in each molecular-sieve:
 Data: Amount of water in the feed stream = 558.47 lb/hr = 253 kg/h.
 Amount of water removed for each hour in each molecular-sieve =

$$\left(\frac{558.47 \text{ lb/hr} \times 24 \text{ hrs}}{3 \text{ columns}} \right) = 4,468 \text{ lb} = 2,026 \text{ kg}$$

- c. Calculate amount of desiccants/sieves required to remove the water.

$$S = \frac{W_r}{(0.13) * (C_{ss}) * (C_T)} = \frac{4,468 \text{ lb}}{0.13 * 0.90 * 1.00} = 38,186 \text{ lb}$$

C_{SS} (correction factor for percent relative saturation) and C_T (Mol sieve capacity correction for temperature) values are given from Figure A.2 below:

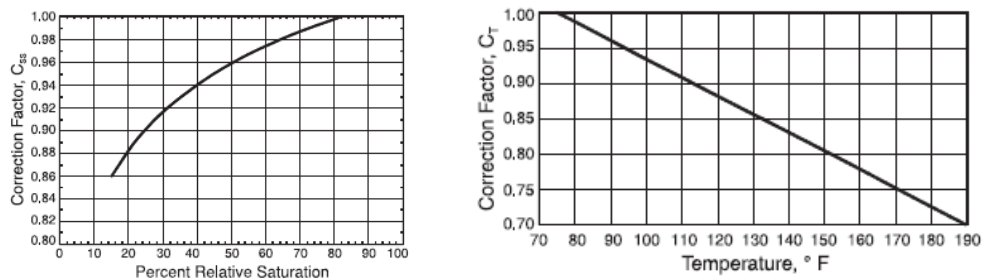


Figure A-2. Mol-Sieve Capacity Correction Factor for Percent Relative Saturation and Temperature (GPSA 2004)

3. Length of sieve in saturation zone (~ equilibrium zone between the desiccant and wet inlet gas).

Data: Sieve density of 1/16" beads = 40-44 lb/ft³.

$$L_s = \frac{S_s * 4}{(\pi D^2)(\text{bulk density})} = \frac{38,186 * 4}{(\pi(7.5)^2) * 42} = 20.57 \text{ ft bed height}$$

4. LMTZ = Length of Mass Transfer Zone (middle zone), where the water content in the gas is reduced to < 1 ppm.

$$L_{MTZ} = \left(\frac{V_{adjusted}}{35} \right)^{0.3} \times Z \quad \text{where } Z = 0.85 \text{ for } 1/16'' \text{ sieve}$$

$$L_{MTZ} = 0.6888 \text{ ft} = 0.21 \text{ m.}$$

5. Minimum total bed height: $L = L_s + L_{MTZ} = 20.57 + 0.69 = 21.26 \text{ ft.}$

6. Total sieve = $(L/L_s) * S = (21.26/20.57) * 38,186 = 39,465$ lb.

For 6 columns of molecular sieve = $39,465 * 6 = 236,790$ lb = 107,383 kg.

7. Check the $L/D = 21.26/7.5 = 2.84$

8. Check the total pressure drop:

$$\left(\frac{\Delta P}{L}\right)_{adjusted} = (0.33 \text{ psi} / \text{ft}) \left(\frac{V_{adjusted}}{V_{max}}\right)^2 \rightarrow \left(\frac{\Delta P}{L}\right) = 0.325 \text{ psi} / \text{ft} \rightarrow \Delta P = 6.91 \text{ psi}$$

The ΔP range is between 5-8 psi.

9. The total cylindrical tower height = $21.26 + 3 \text{ ft} = 24.26 \text{ ft} = 7.4 \text{ m}$ ($L/D = 3.23$).

Additional 3 ft provides space for inlet distributor and bed support and hold-down balls under and on top of the sieve bed.

Regeneration Stage

The regeneration step entails several steps: desorption of water from the desiccants, bed heating stage, and bed cooling stage. The temperature curve of the regeneration step can be seen in Figure A-3 below:

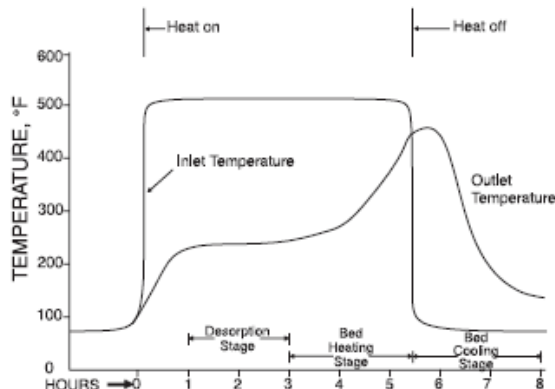


Figure A-3. Inlet and Outlet Temperature during Typical Solid Desiccant Bed Regeneration Period (GPSA 2004)

Regeneration calculation (regenerating 3 columns):

1. Calculate the size (weight) of the mol-sieve

a. Column thickness

$$t(\text{inches}) = \frac{12D_{bed}P_{design}}{(2 \times 19,400) - 1.2P_{design}} = 3.66 \text{ inches}$$

Note: Maximum tensile strength of 19,400 at 600°F.

b. Weight of steel

$$\text{Weight}(lb) = 155(t + 0.125) * (L_{TOTAL} + 4)D_{bed} = 131,421 lb$$

2. Calculate heat required for regeneration (3 columns)

a. Heat to desorb water

$$Q_w = 1800 \text{ Btu/lb} * (\text{lbs of water on bed})$$

$$= 1800 * 4,468 \text{ lb} * 3 \text{ columns} = 2.413 \text{e}7 \text{ Btu.}$$

b. Duty to heat up the desiccant

$$Q_{si} = (\text{lb of sieve}) * (0.24 \text{ Btu/lb.}^\circ\text{F}) * (T_{rg} - T_i) = 1.279 \text{e}7 \text{ Btu.}$$

Note: T_{rg} = Regeneration temperature at 550°F (from graph).

T_i = Temperature initial of bed (approximately 100°F)

c. Duty to heat the steel:

$$Q_{st} = (\text{lb of steel}) * (0.12 \text{ Btu/lb.}^\circ\text{F}) * (T_{rg} - T_i) = 2.129 \text{e}7 \text{ Btu.}$$

d. Heat loss: $Q_{hl} = (Q_w + Q_{si} + Q_{st}) * 0.1 = 5.820 \text{e}6 \text{ Btu.}$

e. $Q \text{ total} = (2.5) * (Q_w + Q_{si} + Q_{st} + Q_{hl}) = 1.601 \text{e}8 \text{ Btu.}$

3. Calculate the flow rate of regeneration gas

$$m_{regeneration} = \frac{Q_{total}}{Cp(T_{hot} - T_b) * (\text{heating - time})}$$

Enthalpy values for Regeneration Gas with molecular weight = 21.41 are shown in Table A-1 below:

Table A-1. Enthalpy Values of Regeneration Gas (MW=21.41), (Figure 24-14 from (GPSA 2004))

Enthalpy (Btu/lb)	1000 psia	1500 psia	1256 psia
T = 65.32°F	165	140	152.2
T = 550°F	490	485	487.4

Cp value was calculated by interpolation of enthalpy values at regeneration operating condition:

$$Cp = \frac{H_{hot} - H_i}{T_{hot} - T_i} = \frac{487.4 - 152.2}{550 - 65.32} = 0.6917 \text{ Btu} / \text{lb.}^\circ\text{F}$$

Note:

Assume the heating time = 60% of the total regeneration period = (60% * 24 hours).

$$m_{regeneration} = \frac{1.601 \text{e}8 \text{ Btu}}{0.6917 * (550 - 65.32)^\circ\text{F} * (0.6 * 24) \text{ hr}} = 33,156 \text{ lb} / \text{hr}$$

4. Check the value of $\Delta P/L$ in the Regeneration column.

a. Density of regeneration gas:

$$\rho = \frac{PMW}{RT} = \frac{(1367 + 14.7) * 21.41}{10.73 * (550 + 460)} = 2.729 \text{ lb} / \text{ft}^3$$

b. Calculate superficial velocity of regeneration gas per column:

$$q = \frac{m_{\text{regeneration}}}{\rho} = \frac{\left(33,156 \frac{\text{lb}}{\text{hr}} / 1\right)}{2.729 \frac{\text{lb}}{\text{ft}^3} * 60} = 202 \text{ ft}^3 / \text{min} \rightarrow V = \frac{4q}{\pi D^2} = 4.58 \text{ ft} / \text{min}$$

c. Equation to calculate the pressure drop in the column:

For 1/16" beads, B = 0.152 and C = 0.000136

$$\frac{\Delta P}{L} = B\mu V + C\rho V^2 = 0.018 \text{ psi} / \text{ft}.$$

The minimum value of $\Delta P/L$ is 0.01 psi/ft to prevent channelling.

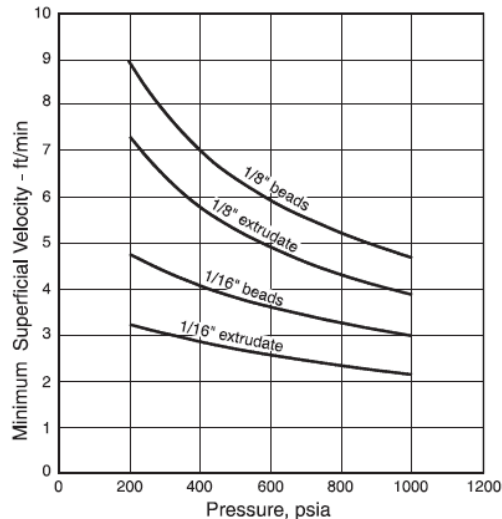


Figure A-4 Minimum Regeneration Velocity for Mol-Sieve Dehydrator (GPSA 2004)

5. Energy Requirement for Dehydration process:

$$\begin{aligned} \text{Energy (Btu/hr)} &= Q_{\text{total}} / (\text{Heating Hour}) = Q_{\text{total}} / (0.6 * 24 \text{ hours}) \\ &= 1.601e8 / (0.6 * 24) = 1.112e7 \text{ Btu/hr.} \end{aligned}$$

The same calculation was performed for the amine process and the result is summarized in Table 2-1.

Appendix B-1. Amine1 process

Appendix B-2. Amine2 process

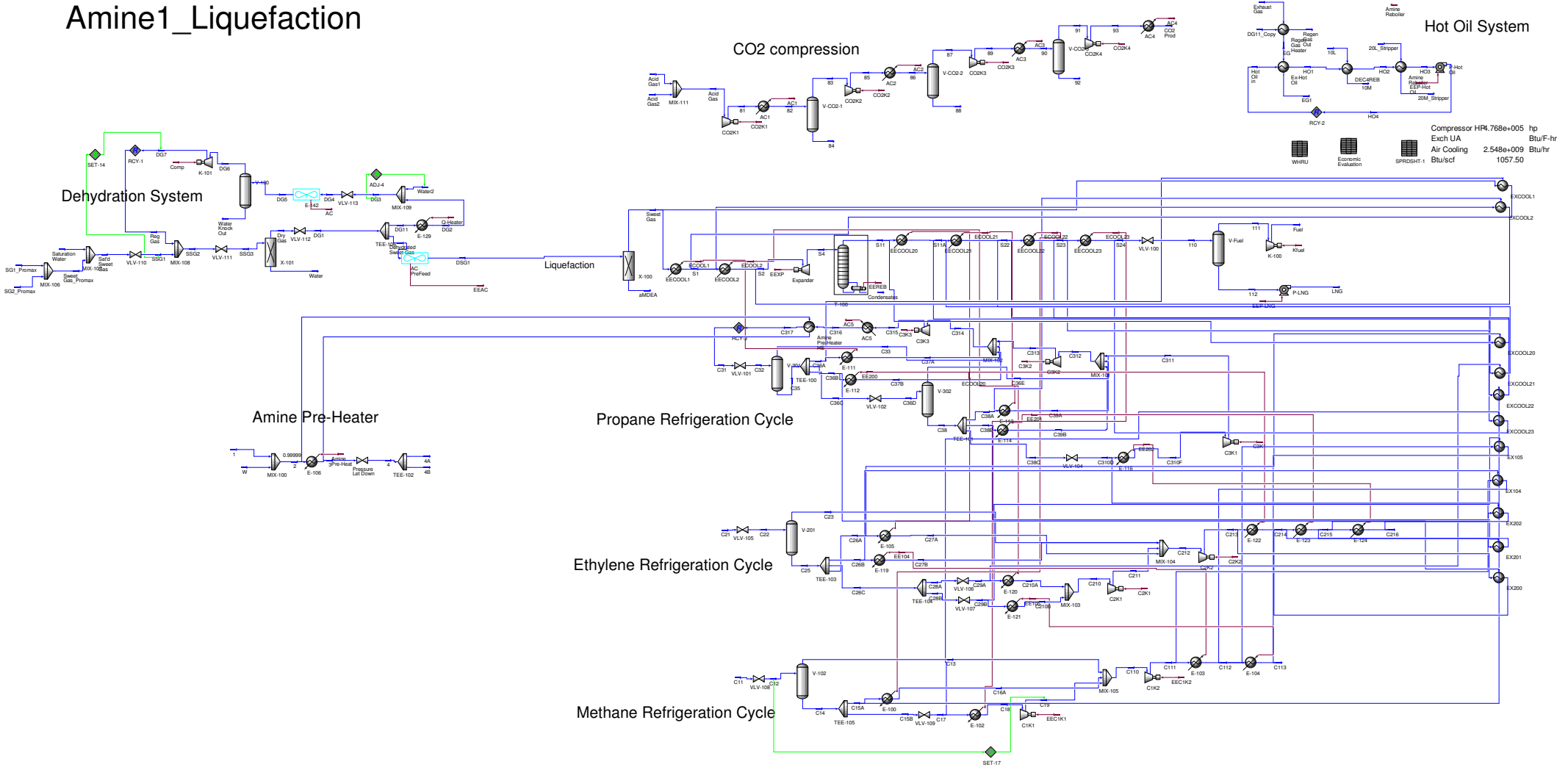
Appendix C-1. RH1 process

Appendix C-2. RH2 process

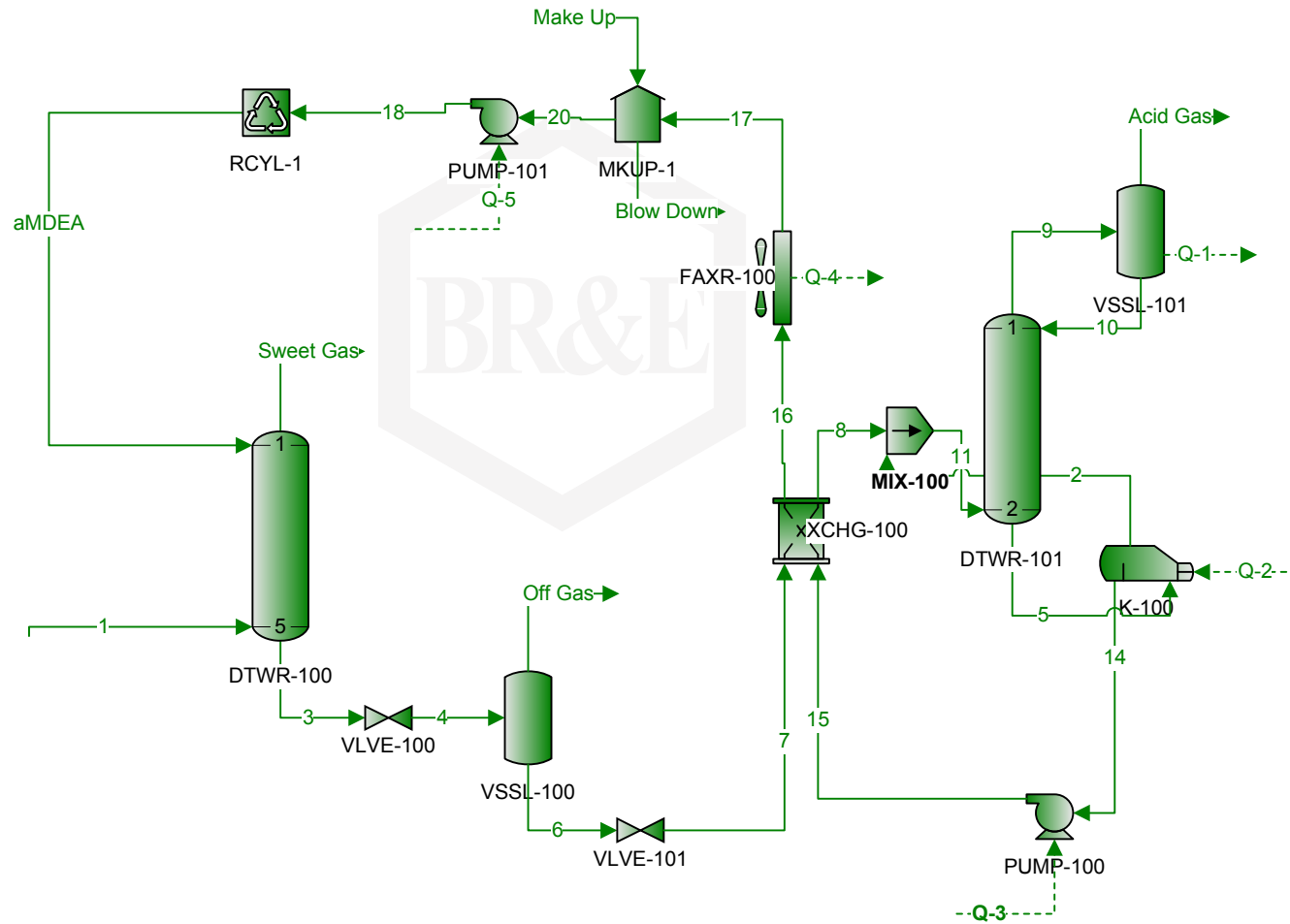
Appendix D-1. HRH1 process

Appendix D-2. HRH2 process

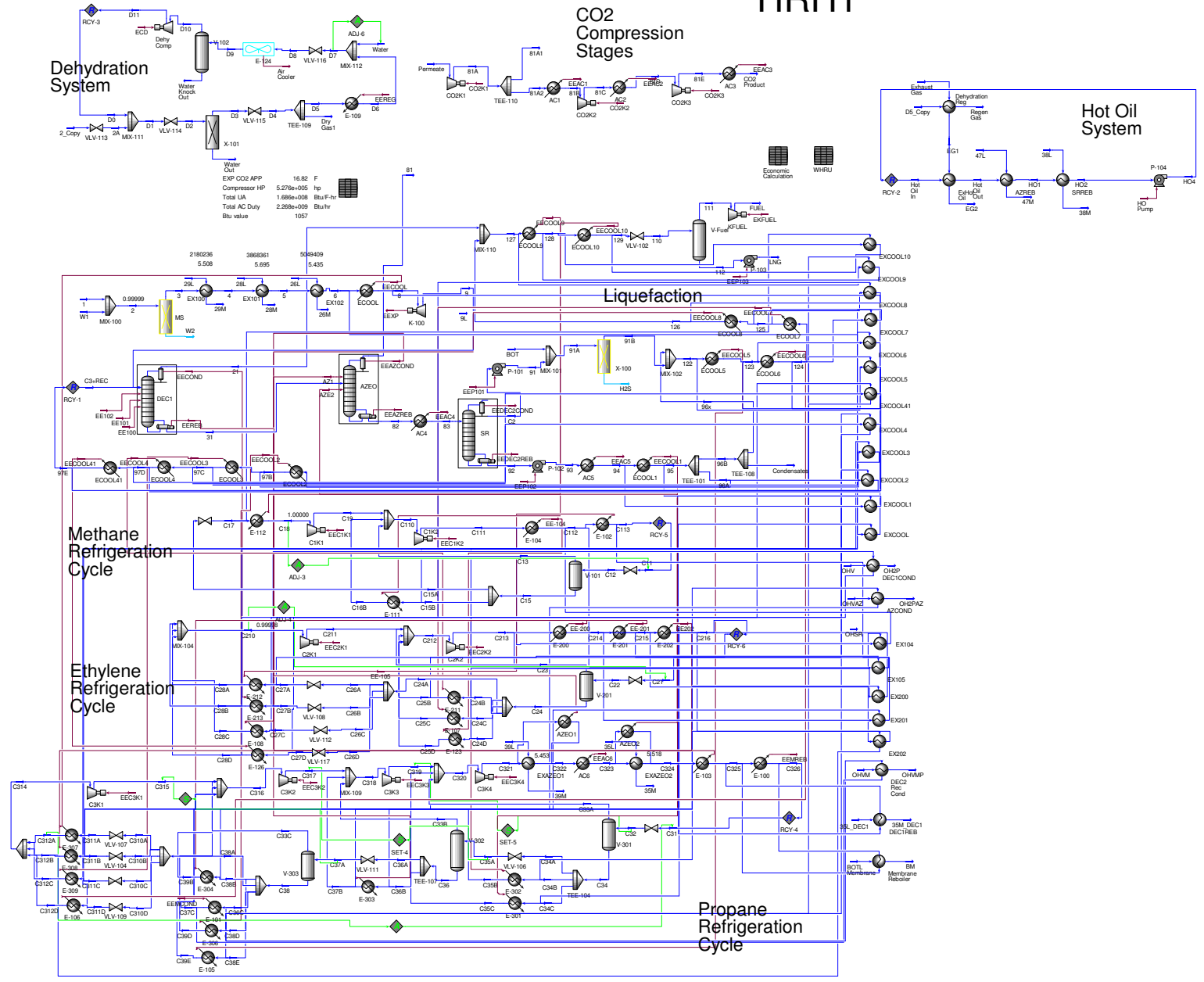
Amine1_Liquefaction



Amine2_Acid Gas Removal Unit (AGRU)



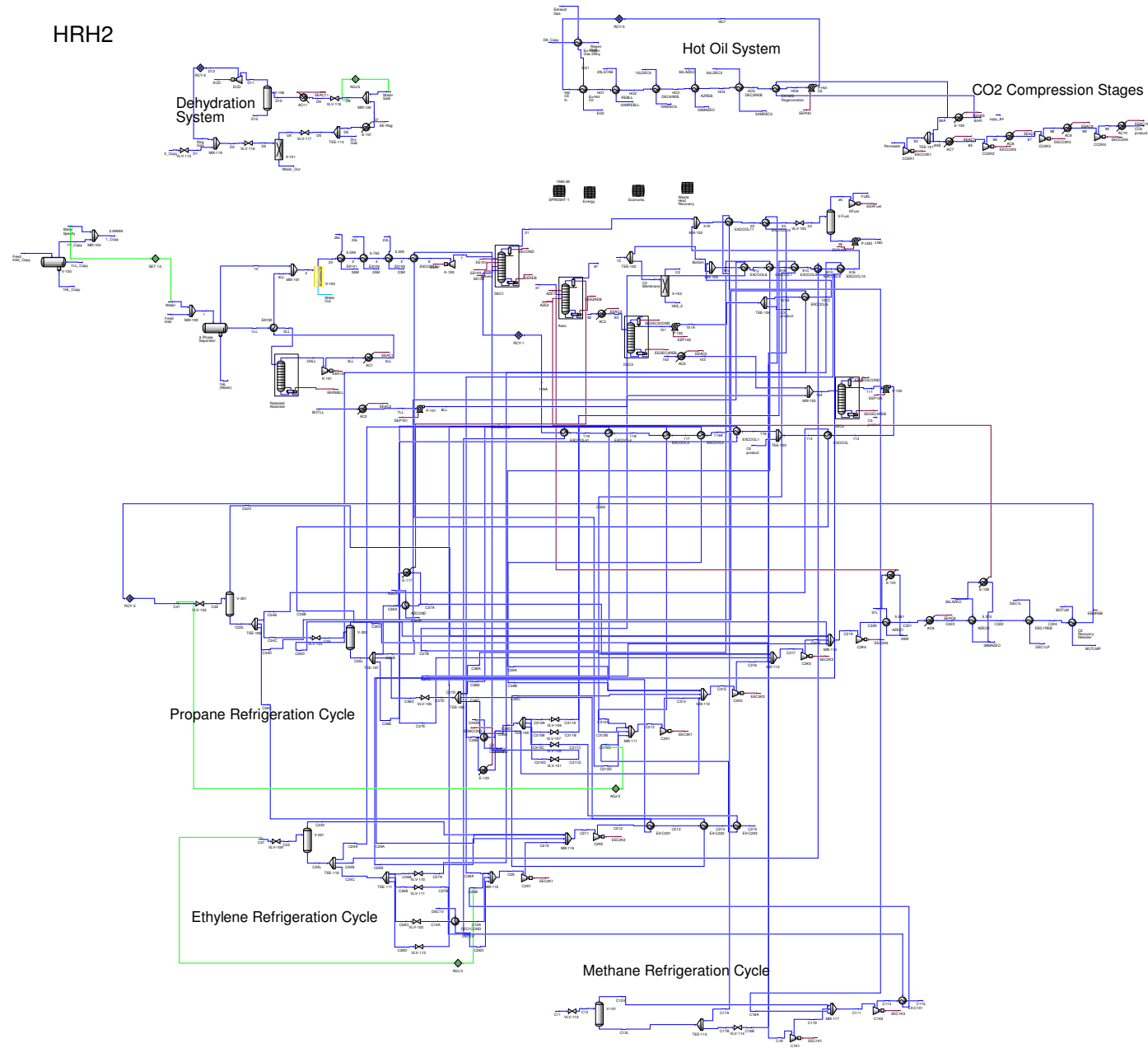
HRH1



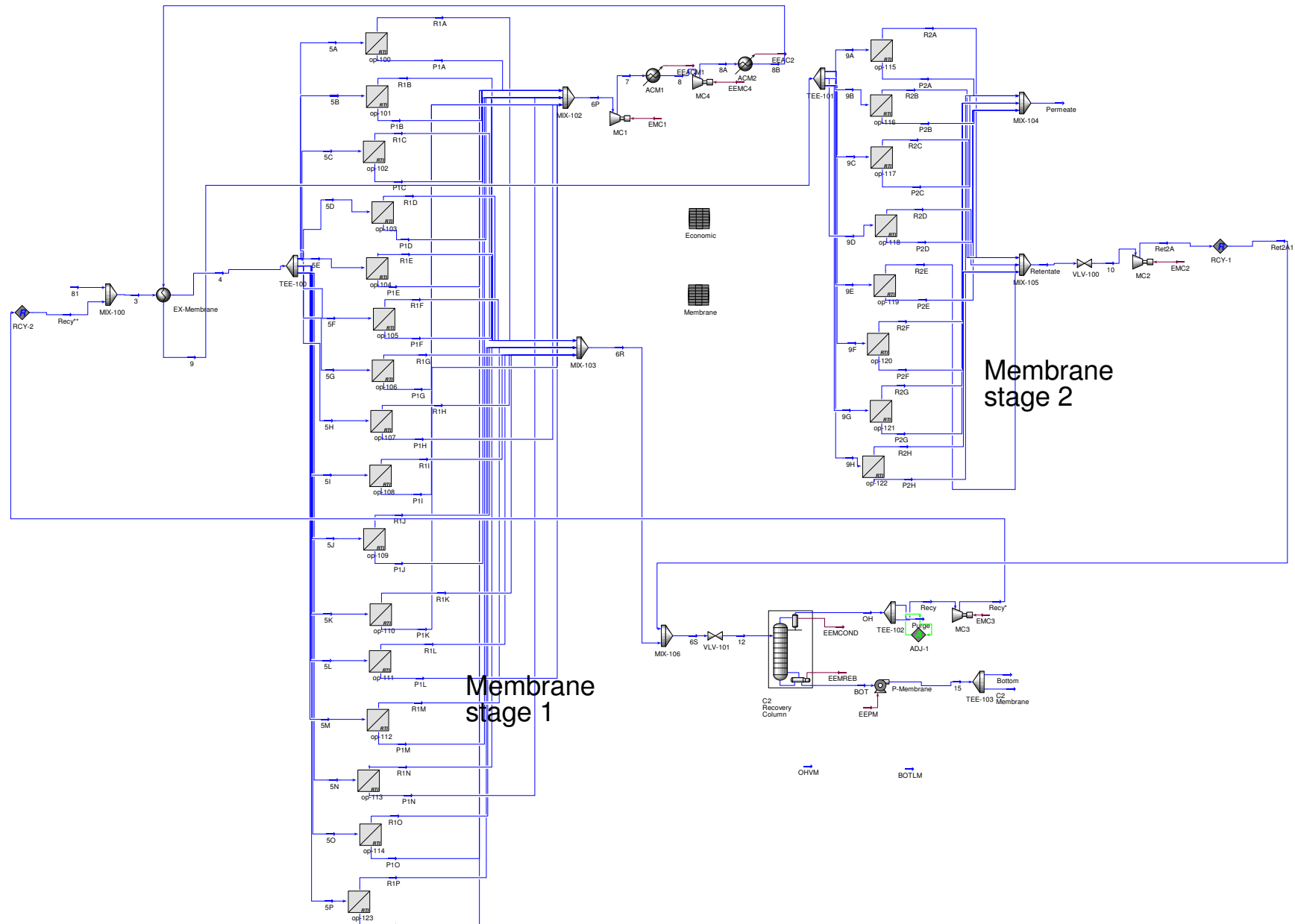
EXP CO2 APP
Compressor HP 16.82 F
5.278e+005 hp
Total LIA 1.686e+008 Btu-F-hr
Total AC Duty 2.288e+009 Btu-hr
Blu value 1057

Economic Calculation
WHRU

HRH2




HRH2_Membrane




Summary of flowsheet design

	Amine1	RH1	HRH1	Amine2	RH2	HRH2
DEC1						
Pressure (atm)		40.15	40.15	36.4	35.72	37.43
N (Number of ideal stage)		45	45	16	55	55
Nf (Feed inlet stage)		26	21	5	22	22
Ns (Solvent inlet stage)		1	1	-	Condenser	1
Condenser Duty (kJ/h)		2.017E+08	2.016E+08	2.818E+08	1.484E+08	1.763E+08
Reboiler Duty (kJ/h)		1.407E+08	1.143E+08	3.446E+07	1.267E+08	1.334E+08
Azeo						
Pressure (atm)		27.22	33.34		22.46	32.32
N/Nf/Ns		70/38/13	70/49		85/38/9	75/33
Condenser Duty (kJ/h)		1.437E+08	2.935E+07		1.351E+08	6.564E+07
Reboiler Duty (kJ/h)		2.852E+08	1.290E+08		1.364E+08	1.396E+08
SR						
Pressure (atm)		15.31	28.78			
N/Nf		35/16	35/12			
Condenser Duty (kJ/h)		1.199E+08	8.242E+07			
Reboiler Duty (kJ/h)		3.150E+08	1.929E+08			
DEC2						
Pressure (atm)			25.86	20.41	16.67	27.22
N/Nf			40/7	30/18	25/10	70/4
Condenser Duty (kJ/h)			3.435E+07	3.535E+07	1.158E+08	6.621E+07
Reboiler Duty (kJ/h)			1.948E+07	2.829E+07	2.607E+08	3.660E+07
DEC3						
Pressure (atm)				15.79	16.33	16.54
N/Nf				20/9	30/16	35/20
Condenser Duty (kJ/h)				4.111E+07	1.190E+08	8.263E+07
Reboiler Duty (kJ/h)				5.082E+07	2.813E+08	1.320E+08
DEC4						
Pressure (atm)				5.85	5.58	5.72
N/Nf				25/6	12/8	10/3
Condenser Duty (kJ/h)				1.507E+07	3.875E+08	1.217E+08
Reboiler Duty (kJ/h)				4.538E+07	4.182E+08	1.519E+08
Condensate Stabilizer						
Pressure (atm)	26.2					
N	8					
Reboiler Duty (kJ/h)	9.464E+06					
Reboiled Absorber						
Pressure (atm)				17	17	17
N				10	10	10
Reboiler Duty (kJ/h)				6.800E+07	6.007E+07	6.008E+07
Amine Absorber						
Pressure (atm)	68.05			68.05		
Amine Stripper						
Pressure (atm)	2.1			2.1		
Condenser Duty (kJ/h)	1.976E+08			1.630E+08		
Reboiler Duty (kJ/h)	4.469E+08			3.732E+08		
Membrane module						
1st stage-number of module			18			16
2nd stage-number of module			10			8
Membrane area1 (m ²)			165,474			147,088
Membrane area2 (m ²)			91,930			73,544
Permeate1 pressure (atm)			3.4			3.4
Permeate2 pressure (atm)			7.5			7.5

A sample of material and energy stream information generated by Aspen HYSYS simulation for the RH1 process is given below.

1	 CURTIN UNIV OF TECH Calgary, Alberta CANADA		Case Name:	D:\1FONNY'S DOCUMENTS\OPTIMIZED FLOWSHEET\CO2 80S PPM		
2			Unit Set:	SI		
3			Date/Time:	Sat Dec 05 20:37:17 2009		
4						
5						
6	Material Stream: 1			Fluid Package:	Basis-1	
7				Property Package:	Peng-Robinson	
8						
9	CONDITIONS					
10						
11		Overall	Vapour Phase			
12	Vapour / Phase Fraction	1.0000	1.0000			
13	Temperature: (C)	7.000 *	7.000			
14	Pressure: (kPa)	8800 *	8800			
15	Molar Flow (kgmole/h)	5.977e+004 *	5.977e+004			
16	Mass Flow (kg/h)	1.280e+006	1.280e+006			
17	Std Ideal Liq Vol Flow (m3/h)	3258	3258			
18	Molar Enthalpy (kJ/kgmole)	-1.233e+005	-1.233e+005			
19	Molar Entropy (kJ/kgmole-C)	141.9	141.9			
20	Heat Flow (kJ/h)	-7.372e+009	-7.372e+009			
21	Liq Vol Flow @Std Cond (m3/h)	---	---			
22	PROPERTIES					
23						
24		Overall	Vapour Phase			
25	Molecular Weight	21.42	21.42			
26	Molar Density (kgmole/m3)	5.093	5.093			
27	Mass Density (kg/m3)	109.1	109.1			
28	Act. Volume Flow (m3/h)	1.173e+004	1.173e+004			
29	Mass Enthalpy (kJ/kg)	-5759	-5759			
30	Mass Entropy (kJ/kg-C)	6.625	6.625			
31	Heat Capacity (kJ/kgmole-C)	57.31	57.31			
32	Mass Heat Capacity (kJ/kg-C)	2.676	2.676			
33	Lower Heating Value (kJ/kgmole)	7.007e+005	7.007e+005			
34	Mass Lower Heating Value (kJ/kg)	3.272e+004	3.272e+004			
35	Phase Fraction [Vol. Basis]	---	1.000			
36	Phase Fraction [Mass Basis]	4.941e-324	1.000			
37	Partial Pressure of CO2 (kPa)	1294	---			
38	Cost Based on Flow (Cost/s)	0.0000	0.0000			
39	Act. Gas Flow (ACT_m3/h)	1.173e+004	1.173e+004			
40	Avg. Liq. Density (kgmole/m3)	18.35	18.35			
41	Specific Heat (kJ/kgmole-C)	57.31	57.31			
42	Std. Gas Flow (STD_m3/h)	1.413e+006	1.413e+006			
43	Std. Ideal Liq. Mass Density (kg/m3)	392.9	392.9			
44	Act. Liq. Flow (m3/s)	---	---			
45	Z Factor	0.7418	0.7418			
46	Watson K	15.52	15.52			
47	User Property	---	---			
48	Cp/(Cp - R)	1.170	1.170			
49	Cp/Cv	1.915	1.915			
50	Heat of Vap. (kJ/kgmole)	---	---			
51	Kinematic Viscosity (cSt)	0.1356	0.1356			
52	Liq. Mass Density (Std. Cond) (kg/m3)	---	---			
53	Liq. Vol. Flow (Std. Cond) (m3/h)	---	---			
54	Liquid Fraction	0.0000	0.0000			
55	Molar Volume (m3/kgmole)	0.1963	0.1963			
56	Mass Heat of Vap. (kJ/kg)	---	---			
57	Phase Fraction [Molar Basis]	1.0000	1.0000			
58	Surface Tension (dyne/cm)	---	---			
59	Thermal Conductivity (W/m-K)	3.844e-002	3.844e-002			
60	Viscosity (cP)	1.479e-002	1.479e-002			
61	Cv (Semi-Ideal) (kJ/kgmole-C)	48.99	48.99			
62	Mass Cv (Semi-Ideal) (kJ/kg-C)	2.288	2.288			
63	Cv (kJ/kgmole-C)	29.93	29.93			
64	Mass Cv (kJ/kg-C)	1.398	1.398			
65	Cv (Ent. Method) (kJ/kgmole-C)	29.93	29.93			
66	Mass Cv (Ent. Method) (kJ/kg-C)	1.398	1.398			
67	Cp/Cv (Ent. Method)	1.915	1.915			
68	Reid VP at 37.8 C (kPa)	---	---			
69	Hyprotech Ltd.		Aspen HYSYS Version 2004.2 (13.3.0.6612)		Page 1 of 19	

1	 CURTIN UNIV OF TECH Calgary, Alberta CANADA	Case Name:	D:\1FONNY'S DOCUMENTS\OPTIMIZED FLOWSHEET\CO2 80S PPM
2		Unit Set:	SI
3		Date/Time:	Sat Dec 05 20:37:17 2009
4			
5			

Material Stream: 1 (continued)

Fluid Package: Basis-1

Property Package: Peng-Robinson

PROPERTIES

9						
10		Overall	Vapour Phase			
11						
12	True VP at 37.8 C (kPa)	---	---			
13	Liq. Vol. Flow - Sum(Std. Cond) (m3/h)	0.0000	0.0000			

COMPOSITION

Overall Phase

Vapour Fraction 1.0000

18	COMPONENTS	MOLAR FLOW (kgmole/h)	MOLE FRACTION	MASS FLOW (kg/h)	MASS FRACTION	LIQUID VOLUME FLOW (m3/h)	LIQUID VOLUME FRACTION
20	Methane	46468.6137 *	0.7775 *	745491.3261 *	0.5824 *	2490.0008 *	0.7644 *
21	Ethane	1930.4646 *	0.0323 *	58048.8783 *	0.0454 *	163.2040 *	0.0501 *
22	Propane	531.9237 *	0.0089 *	23456.2386 *	0.0183 *	46.2942 *	0.0142 *
23	i-Butane	89.6501 *	0.0015 *	5210.8201 *	0.0041 *	9.2725 *	0.0028 *
24	n-Butane	89.6501 *	0.0015 *	5210.8201 *	0.0041 *	8.9345 *	0.0027 *
25	i-Pentane	77.6967 *	0.0013 *	5605.8959 *	0.0044 *	8.9918 *	0.0028 *
26	n-Pentane	0.0000 *	0.0000 *	0.0000 *	0.0000 *	0.0000 *	0.0000 *
27	n-Hexane	0.0000 *	0.0000 *	0.0000 *	0.0000 *	0.0000 *	0.0000 *
28	CO2	8785.7057 *	0.1470 *	386656.2804 *	0.3021 *	468.4840 *	0.1438 *
29	Nitrogen	1793.0012 *	0.0300 *	50227.3427 *	0.0392 *	62.2879 *	0.0191 *
30	H2O	0.0000 *	0.0000 *	0.0000 *	0.0000 *	0.0000 *	0.0000 *
31	H2S	1.7930 *	0.0000 *	61.0983 *	0.0000 *	0.0775 *	0.0000 *
32	Oxygen	0.0000 *	0.0000 *	0.0000 *	0.0000 *	0.0000 *	0.0000 *
33	SO2	0.0000 *	0.0000 *	0.0000 *	0.0000 *	0.0000 *	0.0000 *
34	Ethylene	0.0000 *	0.0000 *	0.0000 *	0.0000 *	0.0000 *	0.0000 *
35	DTRM-G	0.0000 *	0.0000 *	0.0000 *	0.0000 *	0.0000 *	0.0000 *
36	Total	59768.4987	1.0000	1.279968700e+06	1.0000	3257.5472	1.0000

Vapour Phase

Phase Fraction 1.000

39	COMPONENTS	MOLAR FLOW (kgmole/h)	MOLE FRACTION	MASS FLOW (kg/h)	MASS FRACTION	LIQUID VOLUME FLOW (m3/h)	LIQUID VOLUME FRACTION
41	Methane	46468.6137	0.7775	745491.3261	0.5824	2490.0008	0.7644
42	Ethane	1930.4646	0.0323	58048.8783	0.0454	163.2040	0.0501
43	Propane	531.9237	0.0089	23456.2386	0.0183	46.2942	0.0142
44	i-Butane	89.6501	0.0015	5210.8201	0.0041	9.2725	0.0028
45	n-Butane	89.6501	0.0015	5210.8201	0.0041	8.9345	0.0027
46	i-Pentane	77.6967	0.0013	5605.8959	0.0044	8.9918	0.0028
47	n-Pentane	0.0000	0.0000	0.0000	0.0000	0.0000	0.0000
48	n-Hexane	0.0000	0.0000	0.0000	0.0000	0.0000	0.0000
49	CO2	8785.7057	0.1470	386656.2804	0.3021	468.4840	0.1438
50	Nitrogen	1793.0012	0.0300	50227.3427	0.0392	62.2879	0.0191
51	H2O	0.0000	0.0000	0.0000	0.0000	0.0000	0.0000
52	H2S	1.7930	0.0000	61.0983	0.0000	0.0775	0.0000
53	Oxygen	0.0000	0.0000	0.0000	0.0000	0.0000	0.0000
54	SO2	0.0000	0.0000	0.0000	0.0000	0.0000	0.0000
55	Ethylene	0.0000	0.0000	0.0000	0.0000	0.0000	0.0000
56	DTRM-G	0.0000	0.0000	0.0000	0.0000	0.0000	0.0000
57	Total	59768.4987	1.0000	1.279968700e+06	1.0000	3257.5472	1.0000


Material Stream: 9

Fluid Package: Basis-1

Property Package: Peng-Robinson

CONDITIONS

63		Overall	Vapour Phase	Liquid Phase		
64	Vapour / Phase Fraction	0.8297	0.8297	0.1703		
65	Temperature: (C)	-64.34	-64.34	-64.34		
66	Pressure: (kPa)	4137 *	4137	4137		
67	Molar Flow (kgmole/h)	5.977e+004	4.959e+004	1.018e+004		
68	Mass Flow (kg/h)	1.280e+006	9.853e+005	2.947e+005		

1	 CURTIN UNIV OF TECH Calgary, Alberta CANADA	Case Name:	D:\1FONNY'S DOCUMENTS\OPTIMIZED FLOWSHEET\CO2 80S PPM
2		Unit Set:	SI
3		Date/Time:	Sat Dec 05 20:37:17 2009
4			
5			

Material Stream: 9 (continued)

Fluid Package: Basis-1


Property Package: Peng-Robinson

CONDITIONS

		Overall	Vapour Phase	Liquid Phase	
12	Std Ideal Liq Vol Flow (m3/h)	3258	2663	595.0	
13	Molar Enthalpy (kJ/kgmole)	-1.268e+005	-1.120e+005	-1.987e+005	
14	Molar Entropy (kJ/kgmole-C)	131.5	136.7	105.9	
15	Heat Flow (kJ/h)	-7.576e+009	-5.554e+009	-2.023e+009	
16	Liq Vol Flow @Std Cond (m3/h)	---	---	---	

PROPERTIES

		Overall	Vapour Phase	Liquid Phase	
20	Molecular Weight	21.42	19.87	28.95	
21	Molar Density (kgmole/m3)	4.294	3.700	19.72	
22	Mass Density (kg/m3)	91.97	73.52	571.0	
23	Act. Volume Flow (m3/h)	1.392e+004	1.340e+004	516.1	
24	Mass Enthalpy (kJ/kg)	-5919	-5636	-6863	
25	Mass Entropy (kJ/kg-C)	6.139	6.881	3.659	
26	Heat Capacity (kJ/kgmole-C)	68.95	65.64	85.09	
27	Mass Heat Capacity (kJ/kg-C)	3.220	3.304	2.939	
28	Lower Heating Value (kJ/kgmole)	7.007e+005	7.063e+005	6.730e+005	
29	Mass Lower Heating Value (kJ/kg)	3.272e+004	3.555e+004	2.325e+004	
30	Phase Fraction [Vol. Basis]	0.8174	0.8174	0.1826	
31	Phase Fraction [Mass Basis]	0.7698	0.7698	0.2302	
32	Partial Pressure of CO2 (kPa)	445.6	---	---	
33	Cost Based on Flow (Cost/s)	0.0000	0.0000	0.0000	
34	Act. Gas Flow (ACT_m3/h)	---	1.340e+004	---	
35	Avg. Liq. Density (kgmole/m3)	18.35	18.62	17.11	
36	Specific Heat (kJ/kgmole-C)	68.95	65.64	85.09	
37	Std. Gas Flow (STD_m3/h)	1.413e+006	1.173e+006	2.407e+005	
38	Std. Ideal Liq. Mass Density (kg/m3)	392.9	370.0	495.3	
39	Act. Liq. Flow (m3/s)	0.1434	---	0.1434	
40	Z Factor	---	0.6440	0.1208	
41	Watson K	15.52	16.23	13.15	
42	User Property	---	---	---	
43	Cp/(Cp - R)	1.137	1.145	1.108	
44	Cp/Cv	1.917	2.447	1.108	
45	Heat of Vap. (kJ/kgmole)	6848	---	---	
46	Kinematic Viscosity (cSt)	---	0.1422	0.1500	
47	Liq. Mass Density (Std. Cond) (kg/m3)	---	---	---	
48	Liq. Vol. Flow (Std. Cond) (m3/h)	---	---	---	
49	Liquid Fraction	0.1703	0.0000	1.000	
50	Molar Volume (m3/kgmole)	0.2329	0.2703	5.071e-002	
51	Mass Heat of Vap. (kJ/kg)	319.8	---	---	
52	Phase Fraction [Molar Basis]	0.8297	0.8297	0.1703	
53	Surface Tension (dyne/cm)	10.37	---	10.37	
54	Thermal Conductivity (W/m-K)	---	2.695e-002	0.1041	
55	Viscosity (cP)	---	1.045e-002	8.566e-002	
56	Cv (Semi-Ideal) (kJ/kgmole-C)	60.64	57.33	76.77	
57	Mass Cv (Semi-Ideal) (kJ/kg-C)	2.832	2.885	2.652	
58	Cv (kJ/kgmole-C)	35.97	26.83	76.77	
59	Mass Cv (kJ/kg-C)	1.680	1.350	2.652	
60	Cv (Ent. Method) (kJ/kgmole-C)	---	26.60	---	
61	Mass Cv (Ent. Method) (kJ/kg-C)	---	1.339	---	
62	Cp/Cv (Ent. Method)	---	2.468	---	
63	Reid VP at 37.8 C (kPa)	---	---	---	
64	True VP at 37.8 C (kPa)	---	---	---	
65	Liq. Vol. Flow - Sum(Std. Cond) (m3/h)	0.0000	0.0000	0.0000	

1	 CURTIN UNIV OF TECH Calgary, Alberta CANADA	Case Name: D:\1FONNY'S DOCUMENTS\OPTIMIZED FLOWSHEET\CO2 80S PPM
2		Unit Set: SI
3		Date/Time: Sat Dec 05 20:37:17 2009
4		
5		

Material Stream: 9 (continued)

Fluid Package: Basis-1

Property Package: Peng-Robinson

COMPOSITION

Overall Phase

Vapour Fraction 0.8297

13	COMPONENTS	MOLAR FLOW (kgmole/h)	MOLE FRACTION	MASS FLOW (kg/h)	MASS FRACTION	LIQUID VOLUME FLOW (m3/h)	LIQUID VOLUME FRACTION
15	Methane	46468.6137	0.7775	745491.3261	0.5824	2490.0008	0.7644
16	Ethane	1930.4646	0.0323	58048.8783	0.0454	163.2040	0.0501
17	Propane	531.9237	0.0089	23456.2386	0.0183	46.2942	0.0142
18	i-Butane	89.6501	0.0015	5210.8201	0.0041	9.2725	0.0028
19	n-Butane	89.6501	0.0015	5210.8201	0.0041	8.9345	0.0027
20	i-Pentane	77.6967	0.0013	5605.8959	0.0044	8.9918	0.0028
21	n-Pentane	0.0000	0.0000	0.0000	0.0000	0.0000	0.0000
22	n-Hexane	0.0000	0.0000	0.0000	0.0000	0.0000	0.0000
23	CO2	8785.7057	0.1470	386656.2804	0.3021	468.4840	0.1438
24	Nitrogen	1793.0012	0.0300	50227.3427	0.0392	62.2879	0.0191
25	H2O	0.0000	0.0000	0.0000	0.0000	0.0000	0.0000
26	H2S	1.7930	0.0000	61.0983	0.0000	0.0775	0.0000
27	Oxygen	0.0000	0.0000	0.0000	0.0000	0.0000	0.0000
28	SO2	0.0000	0.0000	0.0000	0.0000	0.0000	0.0000
29	Ethylene	0.0000	0.0000	0.0000	0.0000	0.0000	0.0000
30	DTRM-G	0.0000	0.0000	0.0000	0.0000	0.0000	0.0000
31	Total	59768.4987	1.0000	1.279968700e+06	1.0000	3257.5472	1.0000

Vapour Phase


Phase Fraction 0.8297

34	COMPONENTS	MOLAR FLOW (kgmole/h)	MOLE FRACTION	MASS FLOW (kg/h)	MASS FRACTION	LIQUID VOLUME FLOW (m3/h)	LIQUID VOLUME FRACTION
36	Methane	41297.6556	0.8328	662534.1628	0.6724	2212.9172	0.8311
37	Ethane	1083.8669	0.0219	32591.7710	0.0331	91.6315	0.0344
38	Propane	133.7549	0.0027	5898.1881	0.0060	11.6409	0.0044
39	i-Butane	10.2309	0.0002	594.6596	0.0006	1.0582	0.0004
40	n-Butane	7.1303	0.0001	414.4422	0.0004	0.7106	0.0003
41	i-Pentane	2.5236	0.0001	182.0796	0.0002	0.2921	0.0001
42	n-Pentane	0.0000	0.0000	0.0000	0.0000	0.0000	0.0000
43	n-Hexane	0.0000	0.0000	0.0000	0.0000	0.0000	0.0000
44	CO2	5341.1426	0.1077	235062.0858	0.2386	284.8081	0.1070
45	Nitrogen	1712.4919	0.0345	47972.0351	0.0487	59.4910	0.0223
46	H2O	0.0000	0.0000	0.0000	0.0000	0.0000	0.0000
47	H2S	0.8831	0.0000	30.0909	0.0000	0.0382	0.0000
48	Oxygen	0.0000	0.0000	0.0000	0.0000	0.0000	0.0000
49	SO2	0.0000	0.0000	0.0000	0.0000	0.0000	0.0000
50	Ethylene	0.0000	0.0000	0.0000	0.0000	0.0000	0.0000
51	DTRM-G	0.0000	0.0000	0.0000	0.0000	0.0000	0.0000
52	Total	49589.6797	1.0000	985279.5151	1.0000	2662.5878	1.0000

Liquid Phase

Phase Fraction 0.1703

55	COMPONENTS	MOLAR FLOW (kgmole/h)	MOLE FRACTION	MASS FLOW (kg/h)	MASS FRACTION	LIQUID VOLUME FLOW (m3/h)	LIQUID VOLUME FRACTION
57	Methane	5170.9580	0.5080	82957.1633	0.2815	277.0836	0.4657
58	Ethane	846.5977	0.0832	25457.1073	0.0864	71.5725	0.1203
59	Propane	398.1688	0.0391	17558.0505	0.0596	34.6533	0.0582
60	i-Butane	79.4192	0.0078	4616.1604	0.0157	8.2143	0.0138
61	n-Butane	82.5197	0.0081	4796.3778	0.0163	8.2239	0.0138
62	i-Pentane	75.1731	0.0074	5423.8163	0.0184	8.6998	0.0146
63	n-Pentane	0.0000	0.0000	0.0000	0.0000	0.0000	0.0000
64	n-Hexane	0.0000	0.0000	0.0000	0.0000	0.0000	0.0000
65	CO2	3444.5632	0.3384	151594.1947	0.5144	183.6760	0.3087
66	Nitrogen	80.5093	0.0079	2255.3076	0.0077	2.7969	0.0047
67	H2O	0.0000	0.0000	0.0000	0.0000	0.0000	0.0000
68	H2S	0.9099	0.0001	31.0074	0.0001	0.0393	0.0001

1	 CURTIN UNIV OF TECH Calgary, Alberta CANADA	Case Name:	D:\1FONNY'S DOCUMENTS\OPTIMIZED FLOWSHEET\CO2 80S PPM
2		Unit Set:	SI
3		Date/Time:	Sat Dec 05 20:37:17 2009
4			

5	Material Stream: 9 (continued)	Fluid Package:	Basis-1
6		Property Package:	Peng-Robinson
7			

COMPOSITION

8	Liquid Phase (continued)						Phase Fraction	0.1703
9								
10								
11								
12								
13	COMPONENTS	MOLAR FLOW (kgmole/h)	MOLE FRACTION	MASS FLOW (kg/h)	MASS FRACTION	LIQUID VOLUME FLOW (m3/h)	LIQUID VOLUME FRACTION	
14								
15	Oxygen	0.0000	0.0000	0.0000	0.0000	0.0000	0.0000	
16	SO2	0.0000	0.0000	0.0000	0.0000	0.0000	0.0000	
17	Ethylene	0.0000	0.0000	0.0000	0.0000	0.0000	0.0000	
18	DTRM-G	0.0000	0.0000	0.0000	0.0000	0.0000	0.0000	
19	Total	10178.8190	1.0000	294689.1853	1.0000	594.9594	1.0000	


20	Material Stream: 21	Fluid Package:	Basis-1
21		Property Package:	Peng-Robinson
22			

CONDITIONS

23							
24							
25		Overall	Vapour Phase				
26	Vapour / Phase Fraction	1.0000	1.0000				
27	Temperature: (C)	-88.44	-88.44				
28	Pressure: (kPa)	4068	4068				
29	Molar Flow (kgmole/h)	4.826e+004	4.826e+004				
30	Mass Flow (kg/h)	7.960e+005	7.960e+005				
31	Std Ideal Liq Vol Flow (m3/h)	2552	2552				
32	Molar Enthalpy (kJ/kgmole)	-7.849e+004	-7.849e+004				
33	Molar Entropy (kJ/kgmole-C)	126.5	126.5				
34	Heat Flow (kJ/h)	-3.788e+009	-3.788e+009				
35	Liq Vol Flow @Std Cond (m3/h)	---	---				

PROPERTIES

36							
37							
38		Overall	Vapour Phase				
39	Molecular Weight	16.49	16.49				
40	Molar Density (kgmole/m3)	5.570	5.570				
41	Mass Density (kg/m3)	91.87	91.87				
42	Act. Volume Flow (m3/h)	8664	8664				
43	Mass Enthalpy (kJ/kg)	-4758	-4758				
44	Mass Entropy (kJ/kg-C)	7.671	7.671				
45	Heat Capacity (kJ/kgmole-C)	172.2	172.2				
46	Mass Heat Capacity (kJ/kg-C)	10.44	10.44				
47	Lower Heating Value (kJ/kgmole)	7.731e+005	7.731e+005				
48	Mass Lower Heating Value (kJ/kg)	4.687e+004	4.687e+004				
49	Phase Fraction [Vol. Basis]	---	1.000				
50	Phase Fraction [Mass Basis]	4.941e-324	1.000				
51	Partial Pressure of CO2 (kPa)	0.2441	---				
52	Cost Based on Flow (Cost/s)	0.0000	0.0000				
53	Act. Gas Flow (ACT_m3/h)	8664	8664				
54	Avg. Liq. Density (kgmole/m3)	18.91	18.91				
55	Specific Heat (kJ/kgmole-C)	172.2	172.2				
56	Std. Gas Flow (STD_m3/h)	1.141e+006	1.141e+006				
57	Std. Ideal Liq. Mass Density (kg/m3)	311.9	311.9				
58	Act. Liq. Flow (m3/s)	---	---				
59	Z Factor	0.4756	0.4756				
60	Watson K	18.68	18.68				
61	User Property	---	---				
62	Cp/(Cp - R)	1.051	1.051				
63	Cp/Cv	6.492	6.492				
64	Heat of Vap. (kJ/kgmole)	2675	---				
65	Kinematic Viscosity (cSt)	0.1129	0.1129				
66	Liq. Mass Density (Std. Cond) (kg/m3)	---	---				
67	Liq. Vol. Flow (Std. Cond) (m3/h)	---	---				
68	Liquid Fraction	0.0000	0.0000				

1	 CURTIN UNIV OF TECH Calgary, Alberta CANADA	Case Name:	D:\1FONNY'S DOCUMENTS\OPTIMIZED FLOWSHEET\CO2 80S PPM
2		Unit Set:	SI
3		Date/Time:	Sat Dec 05 20:37:17 2009
4			
5			

Material Stream: 21 (continued)

Fluid Package: Basis-1

Property Package: Peng-Robinson

PROPERTIES

	Overall	Vapour Phase		
12 Molar Volume (m ³ /kgmole)	0.1795	0.1795		
13 Mass Heat of Vap. (kJ/kg)	162.2	---		
14 Phase Fraction [Molar Basis]	1.0000	1.0000		
15 Surface Tension (dyne/cm)	---	---		
16 Thermal Conductivity (W/m-K)	3.079e-002	3.079e-002		
17 Viscosity (cP)	1.037e-002	1.037e-002		
18 Cv (Semi-Ideal) (kJ/kgmole-C)	163.9	163.9		
19 Mass Cv (Semi-Ideal) (kJ/kg-C)	9.935	9.935		
20 Cv (kJ/kgmole-C)	26.52	26.52		
21 Mass Cv (kJ/kg-C)	1.608	1.608		
22 Cv (Ent. Method) (kJ/kgmole-C)	26.42	26.42		
23 Mass Cv (Ent. Method) (kJ/kg-C)	1.602	1.602		
24 Cp/Cv (Ent. Method)	6.517	6.517		
25 Reid VP at 37.8 C (kPa)	---	---		
26 True VP at 37.8 C (kPa)	---	---		
27 Liq. Vol. Flow - Sum(Std. Cond) (m ³ /h)	0.0000	0.0000		

COMPOSITION

Overall Phase


Vapour Fraction 1.0000

COMPONENTS	MOLAR FLOW (kgmole/h)	MOLE FRACTION	MASS FLOW (kg/h)	MASS FRACTION	LIQUID VOLUME FLOW (m ³ /h)	LIQUID VOLUME FRACTION
34 Methane	46455.1938	0.9627	745276.0318	0.9363	2489.2817	0.9753
35 Ethane	0.0001	0.0000	0.0031	0.0000	0.0000	0.0000
36 Propane	0.9504	0.0000	41.9117	0.0001	0.0827	0.0000
37 i-Butane	2.8205	0.0001	163.9373	0.0002	0.2917	0.0001
38 n-Butane	1.9247	0.0000	111.8701	0.0001	0.1918	0.0001
39 i-Pentane	0.3647	0.0000	26.3165	0.0000	0.0422	0.0000
40 n-Pentane	0.0000	0.0000	0.0000	0.0000	0.0000	0.0000
41 n-Hexane	0.0000	0.0000	0.0000	0.0000	0.0000	0.0000
42 CO2	2.8954	0.0001	127.4264	0.0002	0.1544	0.0001
43 Nitrogen	1793.0012	0.0372	50227.3427	0.0631	62.2879	0.0244
44 H2O	0.0000	0.0000	0.0000	0.0000	0.0000	0.0000
45 H2S	0.0000	0.0000	0.0000	0.0000	0.0000	0.0000
46 Oxygen	0.0000	0.0000	0.0000	0.0000	0.0000	0.0000
47 SO2	0.0000	0.0000	0.0000	0.0000	0.0000	0.0000
48 Ethylene	0.0000	0.0000	0.0000	0.0000	0.0000	0.0000
49 DTRM-G	0.0000	0.0000	0.0000	0.0000	0.0000	0.0000
50 Total	48257.1508	1.0000	795974.8396	1.0000	2552.3324	1.0000

Vapour Phase

Phase Fraction 1.000

COMPONENTS	MOLAR FLOW (kgmole/h)	MOLE FRACTION	MASS FLOW (kg/h)	MASS FRACTION	LIQUID VOLUME FLOW (m ³ /h)	LIQUID VOLUME FRACTION
53 Methane	46455.1938	0.9627	745276.0318	0.9363	2489.2817	0.9753
54 Ethane	0.0001	0.0000	0.0031	0.0000	0.0000	0.0000
55 Propane	0.9504	0.0000	41.9117	0.0001	0.0827	0.0000
56 i-Butane	2.8205	0.0001	163.9373	0.0002	0.2917	0.0001
57 n-Butane	1.9247	0.0000	111.8701	0.0001	0.1918	0.0001
58 i-Pentane	0.3647	0.0000	26.3165	0.0000	0.0422	0.0000
59 n-Pentane	0.0000	0.0000	0.0000	0.0000	0.0000	0.0000
60 n-Hexane	0.0000	0.0000	0.0000	0.0000	0.0000	0.0000
61 CO2	2.8954	0.0001	127.4264	0.0002	0.1544	0.0001
62 Nitrogen	1793.0012	0.0372	50227.3427	0.0631	62.2879	0.0244
63 H2O	0.0000	0.0000	0.0000	0.0000	0.0000	0.0000
64 H2S	0.0000	0.0000	0.0000	0.0000	0.0000	0.0000
65 Oxygen	0.0000	0.0000	0.0000	0.0000	0.0000	0.0000
66 SO2	0.0000	0.0000	0.0000	0.0000	0.0000	0.0000

1	 CURTIN UNIV OF TECH Calgary, Alberta CANADA	Case Name:	D:\1FONNY'S DOCUMENTS\OPTIMIZED FLOWSHEET\CO2 80S PPM
2		Unit Set:	SI
3		Date/Time:	Sat Dec 05 20:37:17 2009
4			
5			

Material Stream: 21 (continued)

Fluid Package: Basis-1
Property Package: Peng-Robinson

COMPOSITION

Vapour Phase (continued)

Phase Fraction 1.000

13	COMPONENTS	MOLAR FLOW (kgmole/h)	MOLE FRACTION	MASS FLOW (kg/h)	MASS FRACTION	LIQUID VOLUME FLOW (m3/h)	LIQUID VOLUME FRACTION
15	Ethylene	0.0000	0.0000	0.0000	0.0000	0.0000	0.0000
16	DTRM-G	0.0000	0.0000	0.0000	0.0000	0.0000	0.0000
17	Total	48257.1508	1.0000	795974.8396	1.0000	2552.3324	1.0000

Material Stream: 31


Fluid Package: Basis-1
Property Package: Peng-Robinson

CONDITIONS

23		Overall	Vapour Phase	Liquid Phase	
24	Vapour / Phase Fraction	0.0000	0.0000	1.0000	
25	Temperature: (C)	23.60	23.60	23.60	
26	Pressure: (kPa)	4137	4137	4137	
27	Molar Flow (kgmole/h)	1.677e+004	5.475e-002	1.677e+004	
28	Mass Flow (kg/h)	8.123e+005	2.366	8.123e+005	
29	Std Ideal Liq Vol Flow (m3/h)	1262	3.313e-003	1262	
30	Molar Enthalpy (kJ/kgmole)	-2.780e+005	-3.391e+005	-2.780e+005	
31	Molar Entropy (kJ/kgmole-C)	105.4	142.0	105.4	
32	Heat Flow (kJ/h)	-4.663e+009	-1.856e+004	-4.663e+009	
33	Liq Vol Flow @Std Cond (m3/h)	1172 *	3.194e-003	1169	

PROPERTIES

36		Overall	Vapour Phase	Liquid Phase	
37	Molecular Weight	48.43	43.21	48.43	
38	Molar Density (kgmole/m3)	13.93	2.480	13.93	
39	Mass Density (kg/m3)	674.6	107.2	674.6	
40	Act. Volume Flow (m3/h)	1204	2.207e-002	1204	
41	Mass Enthalpy (kJ/kg)	-5741	-7846	-5741	
42	Mass Entropy (kJ/kg-C)	2.177	3.285	2.177	
43	Heat Capacity (kJ/kgmole-C)	127.8	74.96	127.8	
44	Mass Heat Capacity (kJ/kg-C)	2.638	1.735	2.638	
45	Lower Heating Value (kJ/kgmole)	1.164e+006	3.642e+005	1.164e+006	
46	Mass Lower Heating Value (kJ/kg)	2.404e+004	8429	2.404e+004	
47	Phase Fraction [Vol. Basis]	2.626e-006	2.626e-006	1.000	
48	Phase Fraction [Mass Basis]	2.912e-006	2.912e-006	1.000	
49	Partial Pressure of CO2 (kPa)	3327	---	---	
50	Cost Based on Flow (Cost/s)	0.0000	0.0000	0.0000	
51	Act. Gas Flow (ACT_m3/h)	---	2.207e-002	---	
52	Avg. Liq. Density (kgmole/m3)	13.30	16.53	13.30	
53	Specific Heat (kJ/kgmole-C)	127.8	74.96	127.8	
54	Std. Gas Flow (STD_m3/h)	3.966e+005	1.294	3.966e+005	
55	Std. Ideal Liq. Mass Density (kg/m3)	643.9	714.2	643.9	
56	Act. Liq. Flow (m3/s)	0.3345	---	0.3345	
57	Z Factor	---	0.6760	0.1204	
58	Watson K	11.49	9.929	11.49	
59	User Property	---	---	---	
60	Cp/(Cp - R)	1.070	1.125	1.070	
61	Cp/Cv	1.668	1.983	1.669	
62	Heat of Vap. (kJ/kgmole)	1.495e+004	---	---	
63	Kinematic Viscosity (cSt)	---	0.1448	0.1811	
64	Liq. Mass Density (Std. Cond) (kg/m3)	694.6	740.8	694.6	
65	Liq. Vol. Flow (Std. Cond) (m3/h)	1172	3.194e-003	1169	
66	Liquid Fraction	1.000	0.0000	1.000	
67	Molar Volume (m3/kgmole)	7.179e-002	0.4032	7.179e-002	
68	Mass Heat of Vap. (kJ/kg)	308.7	---	---	

1		CURTIN UNIV OF TECH Calgary, Alberta CANADA	Case Name:	D:\1FONNY'S DOCUMENTS\OPTIMIZED FLOWSHEET\CO2 80S PPM
2			Unit Set:	SI
3			Date/Time:	Sat Dec 05 20:37:17 2009
4				
5				

Material Stream: 31 (continued)

Fluid Package: Basis-1

Property Package: Peng-Robinson

PROPERTIES

	Overall	Vapour Phase	Liquid Phase	
12 Phase Fraction [Molar Basis]	0.0000	0.0000	1.0000	
13 Surface Tension (dyne/cm)	5.306	---	5.306	
14 Thermal Conductivity (W/m-K)	7.184e-002	2.303e-002	7.184e-002	
15 Viscosity (cP)	0.1222	1.552e-002	0.1222	
16 Cv (Semi-Ideal) (kJ/kgmole-C)	119.5	66.65	119.5	
17 Mass Cv (Semi-Ideal) (kJ/kg-C)	2.467	1.542	2.467	
18 Cv (kJ/kgmole-C)	76.62	37.80	76.58	
19 Mass Cv (kJ/kg-C)	1.582	0.8748	1.581	
20 Cv (Ent. Method) (kJ/kgmole-C)	---	36.86	---	
21 Mass Cv (Ent. Method) (kJ/kg-C)	---	0.8529	---	
22 Cp/Cv (Ent. Method)	---	2.034	---	
23 Reid VP at 37.8 C (kPa)	3903	---	3903	
24 True VP at 37.8 C (kPa)	5167	---	5167	
25 Liq. Vol. Flow - Sum(Std. Cond) (m3/h)	1169	3.194e-003	1169	

COMPOSITION

Overall Phase


Vapour Fraction 0.0000

COMPONENTS	MOLAR FLOW (kgmole/h)	MOLE FRACTION	MASS FLOW (kg/h)	MASS FRACTION	LIQUID VOLUME FLOW (m3/h)	LIQUID VOLUME FRACTION
32 Methane	13.4199	0.0008	215.2942	0.0003	0.7191	0.0006
33 Ethane	1930.4656	0.1151	58048.9090	0.0715	163.2041	0.1294
34 Propane	636.2053	0.0379	28054.7433	0.0345	55.3700	0.0439
35 i-Butane	1626.4227	0.0970	94534.1962	0.1164	168.2205	0.1333
36 n-Butane	1995.4664	0.1190	115984.4884	0.1428	198.8682	0.1576
37 i-Pentane	1786.4902	0.1065	128897.0532	0.1587	206.7507	0.1639
38 n-Pentane	0.0000	0.0000	0.0000	0.0000	0.0000	0.0000
39 n-Hexane	0.0000	0.0000	0.0000	0.0000	0.0000	0.0000
40 CO2	8782.8103	0.5236	386528.8541	0.4758	468.3296	0.3712
41 Nitrogen	0.0000	0.0000	0.0000	0.0000	0.0000	0.0000
42 H2O	0.0000	0.0000	0.0000	0.0000	0.0000	0.0000
43 H2S	1.7930	0.0001	61.0985	0.0001	0.0775	0.0001
44 Oxygen	0.0000	0.0000	0.0000	0.0000	0.0000	0.0000
45 SO2	0.0000	0.0000	0.0000	0.0000	0.0000	0.0000
46 Ethylene	0.0000	0.0000	0.0000	0.0000	0.0000	0.0000
47 DTRM-G	0.0000	0.0000	0.0000	0.0000	0.0000	0.0000
48 Total	16773.0734	1.0000	812324.6370	1.0000	1261.5396	1.0000

Vapour Phase

Phase Fraction 3.264e-006

COMPONENTS	MOLAR FLOW (kgmole/h)	MOLE FRACTION	MASS FLOW (kg/h)	MASS FRACTION	LIQUID VOLUME FLOW (m3/h)	LIQUID VOLUME FRACTION
53 Methane	0.0001	0.0026	0.0023	0.0010	0.0000	0.0023
54 Ethane	0.0066	0.1198	0.1973	0.0834	0.0006	0.1674
55 Propane	0.0009	0.0169	0.0407	0.0172	0.0001	0.0243
56 i-Butane	0.0013	0.0232	0.0738	0.0312	0.0001	0.0396
57 n-Butane	0.0012	0.0224	0.0714	0.0302	0.0001	0.0369
58 i-Pentane	0.0006	0.0108	0.0426	0.0180	0.0001	0.0206
59 n-Pentane	0.0000	0.0000	0.0000	0.0000	0.0000	0.0000
60 n-Hexane	0.0000	0.0000	0.0000	0.0000	0.0000	0.0000
61 CO2	0.0440	0.8042	1.9376	0.8190	0.0023	0.7087
62 Nitrogen	0.0000	0.0000	0.0000	0.0000	0.0000	0.0000
63 H2O	0.0000	0.0000	0.0000	0.0000	0.0000	0.0000
64 H2S	0.0000	0.0001	0.0002	0.0001	0.0000	0.0001
65 Oxygen	0.0000	0.0000	0.0000	0.0000	0.0000	0.0000
66 SO2	0.0000	0.0000	0.0000	0.0000	0.0000	0.0000
67 Ethylene	0.0000	0.0000	0.0000	0.0000	0.0000	0.0000
68 DTRM-G	0.0000	0.0000	0.0000	0.0000	0.0000	0.0000

1	 CURTIN UNIV OF TECH Calgary, Alberta CANADA	Case Name:	D:\1FONNY'S DOCUMENTS\OPTIMIZED FLOWSHEET\CO2 80S PPM
2		Unit Set:	SI
3		Date/Time:	Sat Dec 05 20:37:17 2009
4			
5			

Material Stream: 31 (continued)

Fluid Package: Basis-1
Property Package: Peng-Robinson

COMPOSITION

Vapour Phase (continued)

Phase Fraction 3.264e-006

13	Total	0.0547	1.0000	2.3659	1.0000	0.0033	1.0000
----	-------	--------	--------	--------	--------	--------	--------

Liquid Phase

Phase Fraction 1.000

16	COMPONENTS	MOLAR FLOW (kgmole/h)	MOLE FRACTION	MASS FLOW (kg/h)	MASS FRACTION	LIQUID VOLUME FLOW (m3/h)	LIQUID VOLUME FRACTION
18	Methane	13.4198	0.0008	215.2919	0.0003	0.7191	0.0006
19	Ethane	1930.4591	0.1151	58048.7117	0.0715	163.2035	0.1294
20	Propane	636.2043	0.0379	28054.7026	0.0345	55.3699	0.0439
21	i-Butane	1626.4215	0.0970	94534.1224	0.1164	168.2204	0.1333
22	n-Butane	1995.4651	0.1190	115984.4170	0.1428	198.8680	0.1576
23	i-Pentane	1786.4896	0.1065	128897.0106	0.1587	206.7506	0.1639
24	n-Pentane	0.0000	0.0000	0.0000	0.0000	0.0000	0.0000
25	n-Hexane	0.0000	0.0000	0.0000	0.0000	0.0000	0.0000
26	CO2	8782.7663	0.5236	386526.9165	0.4758	468.3273	0.3712
27	Nitrogen	0.0000	0.0000	0.0000	0.0000	0.0000	0.0000
28	H2O	0.0000	0.0000	0.0000	0.0000	0.0000	0.0000
29	H2S	1.7930	0.0001	61.0983	0.0001	0.0775	0.0001
30	Oxygen	0.0000	0.0000	0.0000	0.0000	0.0000	0.0000
31	SO2	0.0000	0.0000	0.0000	0.0000	0.0000	0.0000
32	Ethylene	0.0000	0.0000	0.0000	0.0000	0.0000	0.0000
33	DTRM-G	0.0000	0.0000	0.0000	0.0000	0.0000	0.0000
34	Total	16773.0186	1.0000	812322.2711	1.0000	1261.5363	1.0000

Material Stream: 81


Fluid Package: Basis-1
Property Package: Peng-Robinson

CONDITIONS

40		Overall	Vapour Phase
41	Vapour / Phase Fraction	1.0000	1.0000
42	Temperature: (C)	-8.223	-8.223
43	Pressure: (kPa)	2758	2758
44	Molar Flow (kgmole/h)	8870	8870
45	Mass Flow (kg/h)	3.892e+005	3.892e+005
46	Std Ideal Liq Vol Flow (m3/h)	475.4	475.4
47	Molar Enthalpy (kJ/kgmole)	-3.937e+005	-3.937e+005
48	Molar Entropy (kJ/kgmole-C)	136.6	136.6
49	Heat Flow (kJ/h)	-3.493e+009	-3.493e+009
50	Liq Vol Flow @Std Cond (m3/h)	477.9 *	475.2

PROPERTIES

53		Overall	Vapour Phase
54	Molecular Weight	43.88	43.88
55	Molar Density (kgmole/m3)	1.694	1.694
56	Mass Density (kg/m3)	74.32	74.32
57	Act. Volume Flow (m3/h)	5237	5237
58	Mass Enthalpy (kJ/kg)	-8973	-8973
59	Mass Entropy (kJ/kg-C)	3.113	3.113
60	Heat Capacity (kJ/kgmole-C)	56.01	56.01
61	Mass Heat Capacity (kJ/kg-C)	1.277	1.277
62	Lower Heating Value (kJ/kgmole)	1.453e+004	1.453e+004
63	Mass Lower Heating Value (kJ/kg)	331.0	331.0
64	Phase Fraction [Vol. Basis]	---	1.000
65	Phase Fraction [Mass Basis]	4.941e-324	1.000
66	Partial Pressure of CO2 (kPa)	2730	---
67	Cost Based on Flow (Cost/s)	0.0000	0.0000
68	Act. Gas Flow (ACT m3/h)	5237	5237

1		CURTIN UNIV OF TECH Calgary, Alberta CANADA	Case Name:	D:\1FONNY'S DOCUMENTS\OPTIMIZED FLOWSHEET\CO2 80S PPM
2			Unit Set:	SI
3			Date/Time:	Sat Dec 05 20:37:17 2009
4				
5				

Material Stream: 81 (continued)

Fluid Package: Basis-1

Property Package: Peng-Robinson

PROPERTIES


	Overall	Vapour Phase		
12	Avg. Liq. Density (kgmole/m3)	18.66	18.66	
13	Specific Heat (kJ/kgmole-C)	56.01	56.01	
14	Std. Gas Flow (STD_m3/h)	2.097e+005	2.097e+005	
15	Std. Ideal Liq. Mass Density (kg/m3)	818.7	818.7	
16	Act. Liq. Flow (m3/s)	---	---	
17	Z Factor	0.7392	0.7392	
18	Watson K	8.591	8.591	
19	User Property	---	---	
20	Cp/(Cp - R)	1.174	1.174	
21	Cp/Cv	1.840	1.840	
22	Heat of Vap. (kJ/kgmole)	1.143e+004	---	
23	Kinematic Viscosity (cSt)	0.1908	0.1908	
24	Liq. Mass Density (Std. Cond) (kg/m3)	819.1	819.1	
25	Liq. Vol. Flow (Std. Cond) (m3/h)	477.9	475.2	
26	Liquid Fraction	0.0000	0.0000	
27	Molar Volume (m3/kgmole)	0.5904	0.5904	
28	Mass Heat of Vap. (kJ/kg)	260.5	---	
29	Phase Fraction [Molar Basis]	1.0000	1.0000	
30	Surface Tension (dyne/cm)	---	---	
31	Thermal Conductivity (W/m-K)	1.794e-002	1.794e-002	
32	Viscosity (cP)	1.418e-002	1.418e-002	
33	Cv (Semi-Ideal) (kJ/kgmole-C)	47.70	47.70	
34	Mass Cv (Semi-Ideal) (kJ/kg-C)	1.087	1.087	
35	Cv (kJ/kgmole-C)	30.44	30.44	
36	Mass Cv (kJ/kg-C)	0.6936	0.6936	
37	Cv (Ent. Method) (kJ/kgmole-C)	31.55	31.55	
38	Mass Cv (Ent. Method) (kJ/kg-C)	0.7191	0.7191	
39	Cp/Cv (Ent. Method)	1.775	1.775	
40	Reid VP at 37.8 C (kPa)	---	---	
41	True VP at 37.8 C (kPa)	---	---	
42	Liq. Vol. Flow - Sum(Std. Cond) (m3/h)	475.2	475.2	

COMPOSITION

Overall Phase

Vapour Fraction 1.0000

COMPONENTS	MOLAR FLOW (kgmole/h)	MOLE FRACTION	MASS FLOW (kg/h)	MASS FRACTION	LIQUID VOLUME FLOW (m3/h)	LIQUID VOLUME FRACTION	
49	Methane	13.4199	0.0015	215.2942	0.0006	0.7191	0.0015
50	Ethane	57.6561	0.0065	1733.7138	0.0045	4.8743	0.0103
51	Propane	16.2223	0.0018	715.3554	0.0018	1.4119	0.0030
52	i-Butane	0.9398	0.0001	54.6225	0.0001	0.0972	0.0002
53	n-Butane	0.0160	0.0000	0.9318	0.0000	0.0016	0.0000
54	i-Pentane	0.0000	0.0000	0.0001	0.0000	0.0000	0.0000
55	n-Pentane	0.0000	0.0000	0.0000	0.0000	0.0000	0.0000
56	n-Hexane	0.0000	0.0000	0.0000	0.0000	0.0000	0.0000
57	CO2	8781.9680	0.9901	386491.7848	0.9930	468.2847	0.9851
58	Nitrogen	0.0000	0.0000	0.0000	0.0000	0.0000	0.0000
59	H2O	0.0000	0.0000	0.0000	0.0000	0.0000	0.0000
60	H2S	0.0001	0.0000	0.0051	0.0000	0.0000	0.0000
61	Oxygen	0.0000	0.0000	0.0000	0.0000	0.0000	0.0000
62	SO2	0.0000	0.0000	0.0000	0.0000	0.0000	0.0000
63	Ethylene	0.0000	0.0000	0.0000	0.0000	0.0000	0.0000
64	DTRM-G	0.0000	0.0000	0.0000	0.0000	0.0000	0.0000
65	Total	8870.2223	1.0000	389211.7077	1.0000	475.3888	1.0000

1	 CURTIN UNIV OF TECH Calgary, Alberta CANADA	Case Name:	D:\1FONNY'S DOCUMENTS\OPTIMIZED FLOWSHEET\CO2 80S PPM
2		Unit Set:	SI
3		Date/Time:	Sat Dec 05 20:37:17 2009
4			
5			

Material Stream: 81 (continued)

Fluid Package: Basis-1

Property Package: Peng-Robinson

COMPOSITION

Vapour Phase

Phase Fraction 1.000

13	COMPONENTS	MOLAR FLOW (kgmole/h)	MOLE FRACTION	MASS FLOW (kg/h)	MASS FRACTION	LIQUID VOLUME FLOW (m3/h)	LIQUID VOLUME FRACTION
15	Methane	13.4199	0.0015	215.2942	0.0006	0.7191	0.0015
16	Ethane	57.6561	0.0065	1733.7138	0.0045	4.8743	0.0103
17	Propane	16.2223	0.0018	715.3554	0.0018	1.4119	0.0030
18	i-Butane	0.9398	0.0001	54.6225	0.0001	0.0972	0.0002
19	n-Butane	0.0160	0.0000	0.9318	0.0000	0.0016	0.0000
20	i-Pentane	0.0000	0.0000	0.0001	0.0000	0.0000	0.0000
21	n-Pentane	0.0000	0.0000	0.0000	0.0000	0.0000	0.0000
22	n-Hexane	0.0000	0.0000	0.0000	0.0000	0.0000	0.0000
23	CO2	8781.9680	0.9901	386491.7848	0.9930	468.2847	0.9851
24	Nitrogen	0.0000	0.0000	0.0000	0.0000	0.0000	0.0000
25	H2O	0.0000	0.0000	0.0000	0.0000	0.0000	0.0000
26	H2S	0.0001	0.0000	0.0051	0.0000	0.0000	0.0000
27	Oxygen	0.0000	0.0000	0.0000	0.0000	0.0000	0.0000
28	SO2	0.0000	0.0000	0.0000	0.0000	0.0000	0.0000
29	Ethylene	0.0000	0.0000	0.0000	0.0000	0.0000	0.0000
30	DTRM-G	0.0000	0.0000	0.0000	0.0000	0.0000	0.0000
31	Total	8870.2223	1.0000	389211.7077	1.0000	475.3888	1.0000

Material Stream: 82

Fluid Package: Basis-1


Property Package: Peng-Robinson

CONDITIONS

37		Overall	Liquid Phase		
38	Vapour / Phase Fraction	0.0000	1.0000		
39	Temperature: (C)	120.9	120.9		
40	Pressure: (kPa)	2827	2827		
41	Molar Flow (kgmole/h)	2.106e+004	2.106e+004		
42	Mass Flow (kg/h)	1.244e+006	1.244e+006		
43	Std Ideal Liq Vol Flow (m3/h)	2177	2177		
44	Molar Enthalpy (kJ/kgmole)	-1.365e+005	-1.365e+005		
45	Molar Entropy (kJ/kgmole-C)	122.0	122.0		
46	Heat Flow (kJ/h)	-2.873e+009	-2.873e+009		
47	Liq Vol Flow @Std Cond (m3/h)	2140 *	2137		

PROPERTIES

49		Overall	Liquid Phase		
51	Molecular Weight	59.08	59.08		
52	Molar Density (kgmole/m3)	6.967	6.967		
53	Mass Density (kg/m3)	411.6	411.6		
54	Act. Volume Flow (m3/h)	3022	3022		
55	Mass Enthalpy (kJ/kg)	-2310	-2310		
56	Mass Entropy (kJ/kg-C)	2.065	2.065		
57	Heat Capacity (kJ/kgmole-C)	238.1	238.1		
58	Mass Heat Capacity (kJ/kg-C)	4.031	4.031		
59	Lower Heating Value (kJ/kgmole)	2.697e+006	2.697e+006		
60	Mass Lower Heating Value (kJ/kg)	4.565e+004	4.565e+004		
61	Phase Fraction [Vol. Basis]	---	1.000		
62	Phase Fraction [Mass Basis]	2.122e-314	1.000		
63	Partial Pressure of CO2 (kPa)	0.0000	---		
64	Cost Based on Flow (Cost/s)	0.0000	0.0000		
65	Act. Gas Flow (ACT_m3/h)	---	---		
66	Avg. Liq. Density (kgmole/m3)	9.673	9.673		
67	Specific Heat (kJ/kgmole-C)	238.1	238.1		
68	Std. Gas Flow (STD_m3/h)	4.979e+005	4.979e+005		

1		CURTIN UNIV OF TECH Calgary, Alberta CANADA	Case Name:	D:\1FONNY'S DOCUMENTS\OPTIMIZED FLOWSHEET\CO2 80S PPM
2			Unit Set:	SI
3			Date/Time:	Sat Dec 05 20:37:17 2009
4				
5				

Material Stream: 82 (continued)

Fluid Package: Basis-1

Property Package: Peng-Robinson

PROPERTIES

		Overall	Liquid Phase		
12	Std. Ideal Liq. Mass Density (kg/m3)	571.4	571.4		
13	Act. Liq. Flow (m3/s)	0.8396	0.8396		
14	Z Factor	0.1238	0.1238		
15	Watson K	13.71	13.71		
16	User Property	---	---		
17	Cp/(Cp - R)	1.036	1.036		
18	Cp/Cv	1.036	1.036		
19	Heat of Vap. (kJ/kgmole)	1.243e+004	---		
20	Kinematic Viscosity (cSt)	0.1646	0.1646		
21	Liq. Mass Density (Std. Cond) (kg/m3)	582.0	582.0		
22	Liq. Vol. Flow (Std. Cond) (m3/h)	2140	2137		
23	Liquid Fraction	1.000	1.000		
24	Molar Volume (m3/kgmole)	0.1435	0.1435		
25	Mass Heat of Vap. (kJ/kg)	210.5	---		
26	Phase Fraction [Molar Basis]	0.0000	1.0000		
27	Surface Tension (dyne/cm)	2.258	2.258		
28	Thermal Conductivity (W/m-K)	5.311e-002	5.311e-002		
29	Viscosity (cP)	6.774e-002	6.774e-002		
30	Cv (Semi-Ideal) (kJ/kgmole-C)	229.8	229.8		
31	Mass Cv (Semi-Ideal) (kJ/kg-C)	3.890	3.890		
32	Cv (kJ/kgmole-C)	229.8	229.8		
33	Mass Cv (kJ/kg-C)	3.890	3.890		
34	Cv (Ent. Method) (kJ/kgmole-C)	203.0	---		
35	Mass Cv (Ent. Method) (kJ/kg-C)	3.437	---		
36	Cp/Cv (Ent. Method)	1.173	---		
37	Reid VP at 37.8 C (kPa)	565.5	565.5		
38	True VP at 37.8 C (kPa)	684.1	684.1		
39	Liq. Vol. Flow - Sum(Std. Cond) (m3/h)	2137	2137		

COMPOSITION

Overall Phase


Vapour Fraction 0.0000

COMPONENTS	MOLAR FLOW (kgmole/h)	MOLE FRACTION	MASS FLOW (kg/h)	MASS FRACTION	LIQUID VOLUME FLOW (m3/h)	LIQUID VOLUME FRACTION
46	Methane	0.0000	0.0000	0.0000	0.0000	0.0000
47	Ethane	1872.8123	0.0889	56315.2799	0.0453	158.3300
48	Propane	883.0738	0.0419	38940.9072	0.0313	76.8553
49	i-Butane	5472.6751	0.2599	318093.7711	0.2557	566.0374
50	n-Butane	6765.4337	0.3213	393234.0705	0.3161	674.2431
51	i-Pentane	6060.5347	0.2878	437273.6435	0.3515	701.3862
52	n-Pentane	0.0000	0.0000	0.0000	0.0000	0.0000
53	n-Hexane	0.0000	0.0000	0.0000	0.0000	0.0000
54	CO2	0.8423	0.0000	37.0692	0.0000	0.0449
55	Nitrogen	0.0000	0.0000	0.0000	0.0000	0.0000
56	H2O	0.0000	0.0000	0.0000	0.0000	0.0000
57	H2S	1.7929	0.0001	61.0938	0.0000	0.0775
58	Oxygen	0.0000	0.0000	0.0000	0.0000	0.0000
59	SO2	0.0000	0.0000	0.0000	0.0000	0.0000
60	Ethylene	0.0000	0.0000	0.0000	0.0000	0.0000
61	DTRM-G	0.0000	0.0000	0.0000	0.0000	0.0000
62	Total	21057.1648	1.0000	1.243955835e+06	1.0000	2176.9744

Liquid Phase

Phase Fraction 1.000

COMPONENTS	MOLAR FLOW (kgmole/h)	MOLE FRACTION	MASS FLOW (kg/h)	MASS FRACTION	LIQUID VOLUME FLOW (m3/h)	LIQUID VOLUME FRACTION
67	Methane	0.0000	0.0000	0.0000	0.0000	0.0000
68	Ethane	1872.8123	0.0889	56315.2799	0.0453	158.3300

1	 CURTIN UNIV OF TECH Calgary, Alberta CANADA	Case Name:	D:\1FONNY'S DOCUMENTS\OPTIMIZED FLOWSHEET\CO2 80S PPM
2		Unit Set:	SI
3		Date/Time:	Sat Dec 05 20:37:17 2009
4			
5			


6	Material Stream: 82 (continued)	Fluid Package:	Basis-1
7		Property Package:	Peng-Robinson

COMPOSITION								
Liquid Phase (continued)								
							Phase Fraction	1.000
COMPONENTS	MOLAR FLOW (kgmole/h)	MOLE FRACTION	MASS FLOW (kg/h)	MASS FRACTION	LIQUID VOLUME FLOW (m3/h)	LIQUID VOLUME FRACTION		
15	Propane	883.0738	0.0419	38940.9072	0.0313	76.8553	0.0353	
16	i-Butane	5472.6751	0.2599	318093.7711	0.2557	566.0374	0.2600	
17	n-Butane	6765.4337	0.3213	393234.0705	0.3161	674.2431	0.3097	
18	i-Pentane	6060.5347	0.2878	437273.6435	0.3515	701.3862	0.3222	
19	n-Pentane	0.0000	0.0000	0.0000	0.0000	0.0000	0.0000	
20	n-Hexane	0.0000	0.0000	0.0000	0.0000	0.0000	0.0000	
21	CO2	0.8423	0.0000	37.0692	0.0000	0.0449	0.0000	
22	Nitrogen	0.0000	0.0000	0.0000	0.0000	0.0000	0.0000	
23	H2O	0.0000	0.0000	0.0000	0.0000	0.0000	0.0000	
24	H2S	1.7929	0.0001	61.0938	0.0000	0.0775	0.0000	
25	Oxygen	0.0000	0.0000	0.0000	0.0000	0.0000	0.0000	
26	SO2	0.0000	0.0000	0.0000	0.0000	0.0000	0.0000	
27	Ethylene	0.0000	0.0000	0.0000	0.0000	0.0000	0.0000	
28	DTRM-G	0.0000	0.0000	0.0000	0.0000	0.0000	0.0000	
29	Total	21057.1648	1.0000	1.243955835e+06	1.0000	2176.9744	1.0000	

30	Material Stream: C3+REC	Fluid Package:	Basis-1
31		Property Package:	Peng-Robinson

CONDITIONS			
	Overall	Liquid Phase	
35			
36	Vapour / Phase Fraction	0.0000	1.0000
37	Temperature: (C)	-88.89 *	-88.89
38	Pressure: (kPa)	4137 *	4137
39	Molar Flow (kgmole/h)	5262 *	5262
40	Mass Flow (kg/h)	3.283e+005	3.283e+005
41	Std Ideal Liq Vol Flow (m3/h)	556.3	556.3
42	Molar Enthalpy (kJ/kgmole)	-1.733e+005	-1.733e+005
43	Molar Entropy (kJ/kgmole-C)	7.140	7.140
44	Heat Flow (kJ/h)	-9.118e+008	-9.118e+008
45	Liq Vol Flow @Std Cond (m3/h)	554.1 *	553.5

PROPERTIES			
	Overall	Liquid Phase	
46			
47			
48			
49	Molecular Weight	62.40	62.40
50	Molar Density (kgmole/m3)	11.23	11.23
51	Mass Density (kg/m3)	700.9	700.9
52	Act. Volume Flow (m3/h)	468.4	468.4
53	Mass Enthalpy (kJ/kg)	-2777	-2777
54	Mass Entropy (kJ/kg-C)	0.1144	0.1144
55	Heat Capacity (kJ/kgmole-C)	102.4	102.4
56	Mass Heat Capacity (kJ/kg-C)	1.641	1.641
57	Lower Heating Value (kJ/kgmole)	2.842e+006	2.842e+006
58	Mass Lower Heating Value (kJ/kg)	4.555e+004	4.555e+004
59	Phase Fraction [Vol. Basis]	---	1.000
60	Phase Fraction [Mass Basis]	2.122e-314	1.000
61	Partial Pressure of CO2 (kPa)	0.0000	---
62	Cost Based on Flow (Cost/s)	0.0000	0.0000
63	Act. Gas Flow (ACT_m3/h)	---	---
64	Avg. Liq. Density (kgmole/m3)	9.458	9.458
65	Specific Heat (kJ/kgmole-C)	102.4	102.4
66	Std. Gas Flow (STD_m3/h)	1.244e+005	1.244e+005
67	Std. Ideal Liq. Mass Density (kg/m3)	590.2	590.2
68	Act. Liq. Flow (m3/s)	0.1301	0.1301

1		CURTIN UNIV OF TECH Calgary, Alberta CANADA	Case Name:	D:\1FONNY'S DOCUMENTS\OPTIMIZED FLOWSHEET\CO2 80S PPM
2			Unit Set:	SI
3			Date/Time:	Sat Dec 05 20:37:17 2009
4				
5			Fluid Package:	Basis-1
6			Property Package:	Peng-Robinson

Material Stream: C3+REC (continued)

PROPERTIES

	Overall	Liquid Phase		
12	Z Factor	0.2404	0.2404	
13	Watson K	13.43	13.43	
14	User Property	---	---	
15	Cp/(Cp - R)	1.088	1.088	
16	Cp/Cv	1.268	1.268	
17	Heat of Vap. (kJ/kgmole)	---	---	
18	Kinematic Viscosity (cSt)	1.131	1.131	
19	Liq. Mass Density (Std. Cond) (kg/m3)	593.2	593.2	
20	Liq. Vol. Flow (Std. Cond) (m3/h)	554.1	553.5	
21	Liquid Fraction	1.000	1.000	
22	Molar Volume (m3/kgmole)	8.903e-002	8.903e-002	
23	Mass Heat of Vap. (kJ/kg)	---	---	
24	Phase Fraction [Molar Basis]	0.0000	1.0000	
25	Surface Tension (dyne/cm)	25.62	25.62	
26	Thermal Conductivity (W/m-K)	0.1291	0.1291	
27	Viscosity (cP)	0.7930	0.7930	
28	Cv (Semi-Ideal) (kJ/kgmole-C)	94.09	94.09	
29	Mass Cv (Semi-Ideal) (kJ/kg-C)	1.508	1.508	
30	Cv (kJ/kgmole-C)	80.76	80.76	
31	Mass Cv (kJ/kg-C)	1.294	1.294	
32	Cv (Ent. Method) (kJ/kgmole-C)	---	---	
33	Mass Cv (Ent. Method) (kJ/kg-C)	---	---	
34	Cp/Cv (Ent. Method)	---	---	
35	Reid VP at 37.8 C (kPa)	334.8	334.8	
36	True VP at 37.8 C (kPa)	340.1	340.1	
37	Liq. Vol. Flow - Sum(Std. Cond) (m3/h)	553.5	553.5	


COMPOSITION

Overall Phase							Vapour Fraction	0.0000
COMPONENTS	MOLAR FLOW (kgmole/h)	MOLE FRACTION	MASS FLOW (kg/h)	MASS FRACTION	LIQUID VOLUME FLOW (m3/h)	LIQUID VOLUME FRACTION		
44	Methane	0.0000 *	0.0000 *	0.0000 *	0.0000 *	0.0000 *	0.0000 *	
45	Ethane	0.0011 *	0.0000 *	0.0338 *	0.0000 *	0.0001 *	0.0000 *	
46	Propane	105.2320 *	0.0200 *	4640.4164 *	0.0141 *	9.1585 *	0.0165 *	
47	i-Butane	1539.5932 *	0.2926 *	89487.3135 *	0.2726 *	159.2397 *	0.2862 *	
48	n-Butane	1907.7410 *	0.3626 *	110885.5384 *	0.3377 *	190.1254 *	0.3418 *	
49	i-Pentane	1709.1582 *	0.3248 *	123317.4738 *	0.3756 *	197.8010 *	0.3555 *	
50	n-Pentane	0.0000 *	0.0000 *	0.0000 *	0.0000 *	0.0000 *	0.0000 *	
51	n-Hexane	0.0000 *	0.0000 *	0.0000 *	0.0000 *	0.0000 *	0.0000 *	
52	CO2	0.0000 *	0.0000 *	0.0000 *	0.0000 *	0.0000 *	0.0000 *	
53	Nitrogen	0.0000 *	0.0000 *	0.0000 *	0.0000 *	0.0000 *	0.0000 *	
54	H2O	0.0000 *	0.0000 *	0.0000 *	0.0000 *	0.0000 *	0.0000 *	
55	H2S	0.0000 *	0.0000 *	0.0002 *	0.0000 *	0.0000 *	0.0000 *	
56	Oxygen	0.0000 *	0.0000 *	0.0000 *	0.0000 *	0.0000 *	0.0000 *	
57	SO2	0.0000 *	0.0000 *	0.0000 *	0.0000 *	0.0000 *	0.0000 *	
58	Ethylene	0.0000 *	0.0000 *	0.0000 *	0.0000 *	0.0000 *	0.0000 *	
59	DTRM-G	0.0000 *	0.0000 *	0.0000 *	0.0000 *	0.0000 *	0.0000 *	
60	Total	5261.7255	1.0000	328330.7762	1.0000	556.3248	1.0000	

Liquid Phase

Phase Fraction 1.000

COMPONENTS	MOLAR FLOW (kgmole/h)	MOLE FRACTION	MASS FLOW (kg/h)	MASS FRACTION	LIQUID VOLUME FLOW (m3/h)	LIQUID VOLUME FRACTION
65	Methane	0.0000	0.0000	0.0000	0.0000	0.0000
66	Ethane	0.0011	0.0000	0.0338	0.0001	0.0000
67	Propane	105.2320	0.0200	4640.4164	0.0141	9.1585
68	i-Butane	1539.5932	0.2926	89487.3135	0.2726	159.2397

1	 CURTIN UNIV OF TECH Calgary, Alberta CANADA	Case Name:	D:\1FONNY'S DOCUMENTS\OPTIMIZED FLOWSHEET\CO2 80S PPM
2		Unit Set:	SI
3		Date/Time:	Sat Dec 05 20:37:17 2009
4			
5			

Material Stream: C3+REC (continued)

Fluid Package: Basis-1
 Property Package: Peng-Robinson

COMPOSITION

Liquid Phase (continued)

Phase Fraction 1.000

13	COMPONENTS	MOLAR FLOW (kgmole/h)	MOLE FRACTION	MASS FLOW (kg/h)	MASS FRACTION	LIQUID VOLUME FLOW (m3/h)	LIQUID VOLUME FRACTION
15	n-Butane	1907.7410	0.3626	110885.5384	0.3377	190.1254	0.3418
16	i-Pentane	1709.1582	0.3248	123317.4738	0.3756	197.8010	0.3555
17	n-Pentane	0.0000	0.0000	0.0000	0.0000	0.0000	0.0000
18	n-Hexane	0.0000	0.0000	0.0000	0.0000	0.0000	0.0000
19	CO2	0.0000	0.0000	0.0000	0.0000	0.0000	0.0000
20	Nitrogen	0.0000	0.0000	0.0000	0.0000	0.0000	0.0000
21	H2O	0.0000	0.0000	0.0000	0.0000	0.0000	0.0000
22	H2S	0.0000	0.0000	0.0002	0.0000	0.0000	0.0000
23	Oxygen	0.0000	0.0000	0.0000	0.0000	0.0000	0.0000
24	SO2	0.0000	0.0000	0.0000	0.0000	0.0000	0.0000
25	Ethylene	0.0000	0.0000	0.0000	0.0000	0.0000	0.0000
26	DTRM-G	0.0000	0.0000	0.0000	0.0000	0.0000	0.0000
27	Total	5261.7255	1.0000	328330.7762	1.0000	556.3248	1.0000

Material Stream: C4+


Fluid Package: Basis-1
 Property Package: Peng-Robinson

CONDITIONS

33		Overall	Liquid Phase
34	Vapour / Phase Fraction	0.0000	1.0000
35	Temperature: (C)	-8.333 *	-8.333
36	Pressure: (kPa)	4275 *	4275
37	Molar Flow (kgmole/h)	1.315e+004 *	1.315e+004
38	Mass Flow (kg/h)	8.208e+005	8.208e+005
39	Std Ideal Liq Vol Flow (m3/h)	1391	1391
40	Molar Enthalpy (kJ/kgmole)	-1.639e+005	-1.639e+005
41	Molar Entropy (kJ/kgmole-C)	48.90	48.90
42	Heat Flow (kJ/h)	-2.157e+009	-2.157e+009
43	Liq Vol Flow @Std Cond (m3/h)	1385 *	1384

PROPERTIES

46		Overall	Liquid Phase
47	Molecular Weight	62.40	62.40
48	Molar Density (kgmole/m3)	10.02	10.02
49	Mass Density (kg/m3)	625.3	625.3
50	Act. Volume Flow (m3/h)	1313	1313
51	Mass Enthalpy (kJ/kg)	-2627	-2627
52	Mass Entropy (kJ/kg-C)	0.7837	0.7837
53	Heat Capacity (kJ/kgmole-C)	130.3	130.3
54	Mass Heat Capacity (kJ/kg-C)	2.089	2.089
55	Lower Heating Value (kJ/kgmole)	2.842e+006	2.842e+006
56	Mass Lower Heating Value (kJ/kg)	4.555e+004	4.555e+004
57	Phase Fraction [Vol. Basis]	---	1.000
58	Phase Fraction [Mass Basis]	2.122e-314	1.000
59	Partial Pressure of CO2 (kPa)	0.0000	---
60	Cost Based on Flow (Cost/s)	0.0000	0.0000
61	Act. Gas Flow (ACT_m3/h)	---	---
62	Avg. Liq. Density (kgmole/m3)	9.458	9.458
63	Specific Heat (kJ/kgmole-C)	130.3	130.3
64	Std. Gas Flow (STD_m3/h)	3.110e+005	3.110e+005
65	Std. Ideal Liq. Mass Density (kg/m3)	590.2	590.2
66	Act. Liq. Flow (m3/s)	0.3646	0.3646
67	Z Factor	0.1937	0.1937
68	Watson K	13.43	13.43

1	 CURTIN UNIV OF TECH Calgary, Alberta CANADA	Case Name:	D:\1FONNY'S DOCUMENTS\OPTIMIZED FLOWSHEET\CO2 80S PPM
2		Unit Set:	SI
3		Date/Time:	Sat Dec 05 20:37:17 2009
4			
5			

Material Stream: C4+ (continued)

Fluid Package: Basis-1

Property Package: Peng-Robinson

PROPERTIES

	Overall	Liquid Phase		
12	User Property	---	---	
13	Cp/(Cp - R)	1.068	1.068	
14	Cp/Cv	1.258	1.258	
15	Heat of Vap. (kJ/kgmole)	---	---	
16	Kinematic Viscosity (cSt)	0.4051	0.4051	
17	Liq. Mass Density (Std. Cond) (kg/m3)	593.2	593.2	
18	Liq. Vol. Flow (Std. Cond) (m3/h)	1385	1384	
19	Liquid Fraction	1.000	1.000	
20	Molar Volume (m3/kgmole)	9.979e-002	9.979e-002	
21	Mass Heat of Vap. (kJ/kg)	---	---	
22	Phase Fraction [Molar Basis]	0.0000	1.0000	
23	Surface Tension (dyne/cm)	15.76	15.76	
24	Thermal Conductivity (W/m-K)	0.1042	0.1042	
25	Viscosity (cP)	0.2533	0.2533	
26	Cv (Semi-Ideal) (kJ/kgmole-C)	122.0	122.0	
27	Mass Cv (Semi-Ideal) (kJ/kg-C)	1.956	1.956	
28	Cv (kJ/kgmole-C)	103.6	103.6	
29	Mass Cv (kJ/kg-C)	1.660	1.660	
30	Cv (Ent. Method) (kJ/kgmole-C)	---	---	
31	Mass Cv (Ent. Method) (kJ/kg-C)	---	---	
32	Cp/Cv (Ent. Method)	---	---	
33	Reid VP at 37.8 C (kPa)	334.7	334.7	
34	True VP at 37.8 C (kPa)	340.1	340.1	
35	Liq. Vol. Flow - Sum(Std. Cond) (m3/h)	1384	1384	

COMPOSITION

Overall Phase


Vapour Fraction 0.0000

COMPONENTS	MOLAR FLOW (kgmole/h)	MOLE FRACTION	MASS FLOW (kg/h)	MASS FRACTION	LIQUID VOLUME FLOW (m3/h)	LIQUID VOLUME FRACTION
42	Methane	0.0000 *	0.0000 *	0.0000 *	0.0000 *	0.0000 *
43	Ethane	0.0028 *	0.0000 *	0.0847 *	0.0002 *	0.0000 *
44	Propane	263.0909 *	0.0200 *	11601.5192 *	22.8972 *	0.0165 *
45	i-Butane	3847.1921 *	0.2925 *	223614.1974 *	397.9141 *	0.2861 *
46	n-Butane	4769.9833 *	0.3626 *	277250.5139 *	475.3765 *	0.3418 *
47	i-Pentane	4274.0445 *	0.3249 *	308376.5904 *	494.6356 *	0.3556 *
48	n-Pentane	0.0000 *	0.0000 *	0.0000 *	0.0000 *	0.0000 *
49	n-Hexane	0.0000 *	0.0000 *	0.0000 *	0.0000 *	0.0000 *
50	CO2	0.0000 *	0.0000 *	0.0000 *	0.0000 *	0.0000 *
51	Nitrogen	0.0000 *	0.0000 *	0.0000 *	0.0000 *	0.0000 *
52	H2O	0.0000 *	0.0000 *	0.0000 *	0.0000 *	0.0000 *
53	H2S	0.0000 *	0.0000 *	0.0004 *	0.0000 *	0.0000 *
54	Oxygen	0.0000 *	0.0000 *	0.0000 *	0.0000 *	0.0000 *
55	SO2	0.0000 *	0.0000 *	0.0000 *	0.0000 *	0.0000 *
56	Ethylene	0.0000 *	0.0000 *	0.0000 *	0.0000 *	0.0000 *
57	DTRM-G	0.0000 *	0.0000 *	0.0000 *	0.0000 *	0.0000 *
58	Total	13154.3137	1.0000	820842.9061	1390.8236	1.0000

Liquid Phase

Phase Fraction 1.000

COMPONENTS	MOLAR FLOW (kgmole/h)	MOLE FRACTION	MASS FLOW (kg/h)	MASS FRACTION	LIQUID VOLUME FLOW (m3/h)	LIQUID VOLUME FRACTION
63	Methane	0.0000	0.0000	0.0000	0.0000	0.0000
64	Ethane	0.0028	0.0000	0.0847	0.0002	0.0000
65	Propane	263.0909	0.0200	11601.5192	22.8972	0.0165
66	i-Butane	3847.1921	0.2925	223614.1974	397.9141	0.2861
67	n-Butane	4769.9833	0.3626	277250.5139	475.3765	0.3418
68	i-Pentane	4274.0445	0.3249	308376.5904	494.6356	0.3556

1	 CURTIN UNIV OF TECH Calgary, Alberta CANADA	Case Name:	D:\1FONNY'S DOCUMENTS\OPTIMIZED FLOWSHEET\CO2 80S PPM
2		Unit Set:	SI
3		Date/Time:	Sat Dec 05 20:37:17 2009
4			
5			

Material Stream: C4+ (continued)

Fluid Package: Basis-1
Property Package: Peng-Robinson

COMPOSITION

Liquid Phase (continued)

Phase Fraction 1.000

13	COMPONENTS	MOLAR FLOW (kgmole/h)	MOLE FRACTION	MASS FLOW (kg/h)	MASS FRACTION	LIQUID VOLUME FLOW (m3/h)	LIQUID VOLUME FRACTION
15	n-Pentane	0.0000	0.0000	0.0000	0.0000	0.0000	0.0000
16	n-Hexane	0.0000	0.0000	0.0000	0.0000	0.0000	0.0000
17	CO2	0.0000	0.0000	0.0000	0.0000	0.0000	0.0000
18	Nitrogen	0.0000	0.0000	0.0000	0.0000	0.0000	0.0000
19	H2O	0.0000	0.0000	0.0000	0.0000	0.0000	0.0000
20	H2S	0.0000	0.0000	0.0004	0.0000	0.0000	0.0000
21	Oxygen	0.0000	0.0000	0.0000	0.0000	0.0000	0.0000
22	SO2	0.0000	0.0000	0.0000	0.0000	0.0000	0.0000
23	Ethylene	0.0000	0.0000	0.0000	0.0000	0.0000	0.0000
24	DTRM-G	0.0000	0.0000	0.0000	0.0000	0.0000	0.0000
25	Total	13154.3137	1.0000	820842.9061	1.0000	1390.8236	1.0000

Material Stream: LNG


Fluid Package: Basis-1
Property Package: Peng-Robinson

CONDITIONS

31		Overall	Liquid Phase
32	Vapour / Phase Fraction	0.0000	1.0000
33	Temperature: (C)	-162.6	-162.6
34	Pressure: (kPa)	310.3 *	310.3
35	Molar Flow (kgmole/h)	4.141e+004	4.141e+004
36	Mass Flow (kg/h)	7.146e+005	7.146e+005
37	Std Ideal Liq Vol Flow (m3/h)	2296	2296
38	Molar Enthalpy (kJ/kgmole)	-9.088e+004	-9.088e+004
39	Molar Entropy (kJ/kgmole-C)	76.05	76.05
40	Heat Flow (kJ/h)	-3.763e+009	-3.763e+009
41	Liq Vol Flow @Std Cond (m3/h)	---	---

PROPERTIES

44		Overall	Liquid Phase
45	Molecular Weight	17.26	17.26
46	Molar Density (kgmole/m3)	26.05	26.05
47	Mass Density (kg/m3)	449.7	449.7
48	Act. Volume Flow (m3/h)	1589	1589
49	Mass Enthalpy (kJ/kg)	-5265	-5265
50	Mass Entropy (kJ/kg-C)	4.407	4.407
51	Heat Capacity (kJ/kgmole-C)	55.59	55.59
52	Mass Heat Capacity (kJ/kg-C)	3.221	3.221
53	Lower Heating Value (kJ/kgmole)	8.480e+005	8.480e+005
54	Mass Lower Heating Value (kJ/kg)	4.913e+004	4.913e+004
55	Phase Fraction [Vol. Basis]	---	1.000
56	Phase Fraction [Mass Basis]	2.122e-314	1.000
57	Partial Pressure of CO2 (kPa)	0.0000	---
58	Cost Based on Flow (Cost/s)	0.0000	0.0000
59	Act. Gas Flow (ACT_m3/h)	---	---
60	Avg. Liq. Density (kgmole/m3)	18.03	18.03
61	Specific Heat (kJ/kgmole-C)	55.59	55.59
62	Std. Gas Flow (STD_m3/h)	9.790e+005	9.790e+005
63	Std. Ideal Liq. Mass Density (kg/m3)	311.2	311.2
64	Act. Liq. Flow (m3/s)	0.4414	0.4414
65	Z Factor	1.296e-002	1.296e-002
66	Watson K	19.11	19.11
67	User Property	---	---
68	Cp/(Cp - R)	1.176	1.176

1	 CURTIN UNIV OF TECH Calgary, Alberta CANADA	Case Name:	D:\1FONNY'S DOCUMENTS\OPTIMIZED FLOWSHEET\CO2 80S PPM
2		Unit Set:	SI
3		Date/Time:	Sat Dec 05 20:37:17 2009
4			
5			

Material Stream: LNG (continued)

Fluid Package: Basis-1

Property Package: Peng-Robinson

PROPERTIES

	Overall	Liquid Phase		
12	Cp/Cv	1.626	1.626	
13	Heat of Vap. (kJ/kgmole)	1.096e+004	---	
14	Kinematic Viscosity (cSt)	0.3019	0.3019	
15	Liq. Mass Density (Std. Cond) (kg/m3)	---	---	
16	Liq. Vol. Flow (Std. Cond) (m3/h)	---	---	
17	Liquid Fraction	1.000	1.000	
18	Molar Volume (m3/kgmole)	3.838e-002	3.838e-002	
19	Mass Heat of Vap. (kJ/kg)	634.8	---	
20	Phase Fraction [Molar Basis]	0.0000	1.0000	
21	Surface Tension (dyne/cm)	13.56	13.56	
22	Thermal Conductivity (W/m-K)	0.1968	0.1968	
23	Viscosity (cP)	0.1358	0.1358	
24	Cv (Semi-Ideal) (kJ/kgmole-C)	47.28	47.28	
25	Mass Cv (Semi-Ideal) (kJ/kg-C)	2.739	2.739	
26	Cv (kJ/kgmole-C)	34.19	34.19	
27	Mass Cv (kJ/kg-C)	1.981	1.981	
28	Cv (Ent. Method) (kJ/kgmole-C)	---	---	
29	Mass Cv (Ent. Method) (kJ/kg-C)	---	---	
30	Cp/Cv (Ent. Method)	---	---	
31	Reid VP at 37.8 C (kPa)	---	---	
32	True VP at 37.8 C (kPa)	---	---	
33	Liq. Vol. Flow - Sum(Std. Cond) (m3/h)	0.0000	0.0000	

COMPOSITION

Overall Phase


Vapour Fraction 0.0000

COMPONENTS	MOLAR FLOW (kgmole/h)	MOLE FRACTION	MASS FLOW (kg/h)	MASS FRACTION	LIQUID VOLUME FLOW (m3/h)	LIQUID VOLUME FRACTION	
40	Methane	38613.6992	0.9325	619475.7180	0.8668	2069.0986	0.9011
41	Ethane	1872.1779	0.0452	56296.2039	0.0788	158.2763	0.0689
42	Propane	513.3249	0.0124	22636.0889	0.0317	44.6755	0.0195
43	i-Butane	50.8664	0.0012	2956.5596	0.0041	5.2611	0.0023
44	n-Butane	47.3346	0.0011	2751.2760	0.0038	4.7174	0.0021
45	i-Pentane	40.7497	0.0010	2940.1287	0.0041	4.7160	0.0021
46	n-Pentane	0.0000	0.0000	0.0000	0.0000	0.0000	0.0000
47	n-Hexane	0.0000	0.0000	0.0000	0.0000	0.0000	0.0000
48	CO2	3.7280	0.0001	164.0681	0.0002	0.1988	0.0001
49	Nitrogen	264.8124	0.0064	7418.1910	0.0104	9.1994	0.0040
50	H2O	0.0000	0.0000	0.0000	0.0000	0.0000	0.0000
51	H2S	0.0000	0.0000	0.0000	0.0000	0.0000	0.0000
52	Oxygen	0.0000	0.0000	0.0000	0.0000	0.0000	0.0000
53	SO2	0.0000	0.0000	0.0000	0.0000	0.0000	0.0000
54	Ethylene	0.0000	0.0000	0.0000	0.0000	0.0000	0.0000
55	DTRM-G	0.0000	0.0000	0.0000	0.0000	0.0000	0.0000
56	Total	41406.6931	1.0000	714638.2343	1.0000	2296.1430	1.0000

Liquid Phase

Phase Fraction 1.000

COMPONENTS	MOLAR FLOW (kgmole/h)	MOLE FRACTION	MASS FLOW (kg/h)	MASS FRACTION	LIQUID VOLUME FLOW (m3/h)	LIQUID VOLUME FRACTION	
61	Methane	38613.6992	0.9325	619475.7180	0.8668	2069.0986	0.9011
62	Ethane	1872.1779	0.0452	56296.2039	0.0788	158.2763	0.0689
63	Propane	513.3249	0.0124	22636.0889	0.0317	44.6755	0.0195
64	i-Butane	50.8664	0.0012	2956.5596	0.0041	5.2611	0.0023
65	n-Butane	47.3346	0.0011	2751.2760	0.0038	4.7174	0.0021
66	i-Pentane	40.7497	0.0010	2940.1287	0.0041	4.7160	0.0021
67	n-Pentane	0.0000	0.0000	0.0000	0.0000	0.0000	0.0000
68	n-Hexane	0.0000	0.0000	0.0000	0.0000	0.0000	0.0000

1	 CURTIN UNIV OF TECH Calgary, Alberta CANADA	Case Name:	D:\1FONNY'S DOCUMENTS\OPTIMIZED FLOWSHEET\CO2 80S PPM
2		Unit Set:	SI
3		Date/Time:	Sat Dec 05 20:37:17 2009
4			
5			

6	Material Stream: LNG (continued)	Fluid Package:	Basis-1
7		Property Package:	Peng-Robinson

COMPOSITION

Liquid Phase (continued) Phase Fraction 1.000

13	COMPONENTS	MOLAR FLOW (kgmole/h)	MOLE FRACTION	MASS FLOW (kg/h)	MASS FRACTION	LIQUID VOLUME FLOW (m3/h)	LIQUID VOLUME FRACTION
14							
15	CO2	3.7280	0.0001	164.0681	0.0002	0.1988	0.0001
16	Nitrogen	264.8124	0.0064	7418.1910	0.0104	9.1994	0.0040
17	H2O	0.0000	0.0000	0.0000	0.0000	0.0000	0.0000
18	H2S	0.0000	0.0000	0.0000	0.0000	0.0000	0.0000
19	Oxygen	0.0000	0.0000	0.0000	0.0000	0.0000	0.0000
20	SO2	0.0000	0.0000	0.0000	0.0000	0.0000	0.0000
21	Ethylene	0.0000	0.0000	0.0000	0.0000	0.0000	0.0000
22	DTRM-G	0.0000	0.0000	0.0000	0.0000	0.0000	0.0000
23	Total	41406.6931	1.0000	714638.2343	1.0000	2296.1430	1.0000

24	Energy Stream: EECOND	Fluid Package:	Basis-1
25		Property Package:	Peng-Robinson

CONDITIONS

29	Duty Type:	Utility Fluid	Duty Calculation Operation:	Condenser @COL1	Duty SP:	2.017e+008 kJ/h
30	Available UA:	3.600e+005 kJ/C-h	Utility Fluid Holdup:	100.0 kgmole	Fluid Heat Capacity:	75.00 kJ/kgmole-C
31	Actual Fluid Flow:	---	Minimum Fluid Flow:	---	Maximum Fluid Flow:	---
32	Fluid Inlet Temperature:	15.00 C	Fluid Outlet Temperature:	15.00 C	Temperature Approach:	10.00 C

COMPOSITION

(Not a material stream - No compositions exist)

36	Energy Stream: EEREB	Fluid Package:	Basis-1
37		Property Package:	Peng-Robinson

CONDITIONS

41	Duty Type:	Direct Q	Duty Calculation Operation:	Reboiler @COL1		
42	Duty SP:	1.407e+008 kJ/h	Minimum Available Duty:	---	Maximum Available Duty:	---

COMPOSITION

(Not a material stream - No compositions exist)

46
47
48
49
50
51
52
53
54
55
56
57
58
59
60
61
62
63
64
65
66
67
68

Appendix E. Calculation of Equivalent Fuel

A. RH Process

1. Compression HP

a. Compression HP = $5.291e5$ HP $\approx 1.346e9$ Btu/hr

b. Fuel Data:

Net Heating Value (LHV) = $2.888e5$ Btu/lbm

Fuel Flow = $2.066e4$ lbmole/hr ~ 188.1 MMSCFD

c. Estimate the efficiency of compressor driver:

- GE Frame 7 heat rate = 9795 Btu/shp-hr
- Formula to calculate the compressor efficiency (η):

$$\eta = \frac{2544.43 \text{ Btu} / h}{9795 \text{ Btu} / \text{shp} - h} = 0.26$$

d. Calculate Equivalent Fuel required for compressor duties:

- Equivalent Fuel (lbmole/h):

$$= \frac{\text{Compressor HP} \times 2544.43 \text{ Btu} / h}{\text{LHV} \times \eta} = \frac{5.291e5 \times 2544.43}{2.888e5 \times 0.26} = 1.793e4 \quad \text{lbmole} / h$$

- Equivalent Fuel (MMSCFD):

$$= \frac{1.793e4 \text{ lbmole} / h}{2.066e4 \text{ lbmole} / h} \times 188.1 \text{ MMSCFD} = 163.3 \quad \text{MMSCFD}$$

2. Heating Medium Oil (Heat supply to the dehydration regeneration process and reboilers of distillation columns)

a. Heating Medium Oil = $5.688e8$ Btu/hr

b. Fuel Data:

Net Heating Value (LHV) = $2.888e5$ Btu/lbm

Fuel Flow = $2.066e4$ lbmole/hr ~ 188.1 MMSCFD

c. Calculate Equivalent Fuel required for compressor duties:

80% regeneration gas efficiency

Thus, energy supplied by Fuel = $5.688e8 / 2.888e5 / 0.8 = 2,462$ lbmole/hr

d. Equivalent Fuel:

$$= \frac{2462}{2.066e4} \times 188.1 \text{MMSCFD} = 22.42 \text{MMSCFD}$$

3. Pumps

a. Total Pump HP = 4809 HP ~ 1.224e7 Btu/hr

b. Fuel Data:

Net Heating Value (LHV) = 2.888e5 Btu/lbm

Fuel Flow = 2.066e4 lbmole/hr ~ 188.1 MMSCFD

c. Calculate Equivalent Fuel required for compressor duties:

26% compressor driver efficiency

Thus energy supplied by Fuel = $1.224e7 / 2.888e5 / 0.26 = 162.9$ lbmole/hr

d. Equivalent Fuel:

$$= \frac{162.9}{2.066e4} \times 188.1 \text{MMSCFD} = 1.48 \text{MMSCFD}$$

4. Dehydration

a. Compression HP = 37.48 ~ 9.536e4 Btu/hr

b. Regeneration Gas = 1.112e7 Btu/hr

c. Fuel Data:

Net Heating Value (LHV) = 2.888e5 Btu/lbm

Fuel Flow = 2.066e4 lbmole/hr ~ 188.1 MMSCFD

d. Calculate Equivalent Fuel required for compressor duties:

26% compressor driver efficiency

80% regeneration gas efficiency

Then energy supplied by Fuel =

$(9.536e4 / 2.888e5 / 0.26) + (1.112e7 / 2.888e5 / 0.8) = 49.40$ lbmole/hr

e. Equivalent Fuel:

$$= \frac{49.40}{2.066e4} \times 188.1 \text{MMSCFD} = 0.4498 \text{MMSCFD}$$

5. **Total Equivalent Fuel** = 163.3 + 22.42 + 1.48 + 0.4498 = 187.6 MMSCFD Fuel.

B. Amine Process

The same calculation was performed for amine with the data as follow:

- a. Compressor HP = 4.771 e5 ~ 147.1 MMSCFD
- b. Heating Medium Oil = 4.326e8 ~ 34.06 MMSCFD
- c. Pumps = 1.644e4 HP ~ 5.07 MMSCFD
- d. Dehydration Process = 8.354e7 Btu/hr and 618.4 HP pumps ~ 3.48 MMSCFD
- e. Fuel Data:

Net Heating Value (LHV) = 2.891e5 Btu/lbm

Fuel Flow = 2.079e4 lbmole/hr ~ 189.3 MMSCFD

- f. Off Gas from the amine flash tank:

Off gas Mass Lower Heating Value = 2163 Btu/lb.

Off gas Mass Flow Rate = 4.093e4 lb/h.

Off gas Standard Gas Flow = 20.36 MMSCFD.

Off gas contribution to the fuel demand:

$$= \frac{2163 \times 4.093e4}{2.891e5 \times 2.079e4} \times 20.36 = 0.3 \text{ MMSCFD}$$

- g. Total Equivalent Fuel = 147.1+34.06+5.07+3.48-0.3 = 189.4 MMSCFD.

Appendix F. List of Equipment

	Amine1	RH1	HRH1	Amine2	RH2	HRH2
Amine Absorber	2			2		
Amine Regenerator	2			2		
Amine Reg Reboiler	2			2		
Amine Reg Stripper	2			2		
Amine Reg Reflux Pump	2			2		
Amine Reg Reflux Drum	2			2		
Amine Flash Tank	2			2		
Lean/Rich Heat Exchanger	2			2		
Amine Air Cooler	2			2		
Amine Booster Pump	4			4		
Amine Charge Pump	12			12		
Amine Storage Tank	1			1		
DEC1						
Column		1	1	1	1	1
Condenser		1	1	1	1	1
Reboiler		1	1	1	1	1
Reflux Pump		1	1	1	1	1
Reflux Drum		1	1	1	1	1
Azeo						
Column		1	1		1	1
Condenser		1	1		1	1
Reboiler		1	1		1	1
Reflux Pump		1	1		1	1
Reflux Drum		1	1		1	1
SR						
Column		1	1			
Condenser		1	1			
Reboiler		1	1			
Reflux Pump		1	1			
Reflux Drum		1	1			
DEC2						
Column				1	1	
Condenser				1	1	
Reboiler				1	1	
Reflux Pump				1	1	
Reflux Drum				1	1	
DEC3						
Column				1	1	1
Condenser				1	1	1
Reboiler				1	1	1
Reflux Pump				1	1	1
Reflux Drum				1	1	1

	Amine1	RH1	HRH1	Amine2	RH2	HRH2
DEC4						
Column	1			1	1	1
Condenser	1			1	1	1
Reboiler	1			1	1	1
Reflux Pump	1			1	1	1
Reflux Drum	1			1	1	1
Stripper						
Column				1	1	1
Reboiler				1	1	1
Heat Exchangers						
Process/Liquefaction	7	15	15	8	19	19
Refrigeration	5	5	5	4	4	4
Reboiler/Hot Oil Syst.	1	3	3	1	3	3
Amine Pre-Heater	1	0	0	1	0	0
Air Cooler	5	5	6	9	9	10
Tank/Vessel						
Refrigeration system	4	4	5	5	5	4
CO ₂ compression	3	0	0	3	0	0
LNG-Fuel	1	1	1	1	1	1
3-Phase Separator				1	1	1
Compressor						
Refrigeration	7	7	8	8	9	9
CO ₂	4	2	3	4	2	4
Fuel	1	1	1	1	1	1
Feed Recompression				1	1	1
Expander	1	1	1	1	1	1
Pump						
Operating	2	4	4	5	6	5
Spare pump	2	4	4	5	6	5
Dehydration system						
Columns	6	6	6	6	6	6
Regenerator gas heater	1	1	1	1	1	1
Water Knock Out	1	1	1	1	1	1
Regenerator gas cooler	1	1	1	1	1	1
Regenerator gas compressor	1	1	1	1	1	1
Piping	X	X	X	X	X	X

	Amine1	RH1	HRH1	Amine2	RH2	HRH2
Membrane system						
Membrane Module			28			24
C2 Recovery Column			1			1
C2 Rec Condenser			1			1
C2 Rec Reboiler			1			1
C2 Rec Reflux Pump			1			1
C2 Rec Reflux Drum			1			1
Heat Exchanger			1			1
Air Cooler			1			1
Compressors			3			4
C2 Product Pump						
LNG Tank	1	1	1	1	1	1
Solvent Tank	0	1	1	0	1	1
Gas Turbine	5	5	5	5	5	5
Generator	X	X	X	X	X	X

Appendix G. DCF Calculation (RH1 Process)

Year		0	1	2	3	...	9	10	11	...	20
	Equipment Installed Cost (\$)	-6.780E+08									
	Turbine+Generator Cost (\$)	-3.502E+08									
A	Total Investment Cost (\$)	-6.854E+09									
	UTILITIES										
	Initial Utility Capacity, minutes	20									
	a. Propane Refrigerant										
	Std Volumetric Flow, b/d	1.729E+06									
	Price, \$/barrel	40									
	Cost (\$)	9.607E+05									
	b. Ethylene Refrigerant										
	Mass Flow, lb/h	5.083E+06									
	Price, cents/kg*	70.5									
	Cost (\$)	5.417E+05									
	c. Methane Refrigerant										
	Mass Flow, lb/h	3.239E+06									
	Lower Heating Value, Btu/lb	2.131E+04									
	Price, \$/MMBtu	5									
	Purchase (\$)	1.151E+05									
	d. Hot Oil										
	Std Volumetric Flow, b/d	9.632E+05									
	Price, \$/gallon [#]	21.92									
	Purchase (\$)	1.232E+07									
	e. Initial Fuel Demand										
	Mass Flow, lb/h	3.718E+05									
	Mass Lower Heating Value	1.605E+04									
	Price, \$/MMBtu	5									
	Purchase (\$)	9945									
B	Total Initial Utility Cost (\$)	-1.394E+07									
	Feed flow rate, lb/h	2.822E+06									
	Lower Heating Value, Btu/lb	1.407E+04									
	Feed stock price, \$/MMBtu	0.5									
	Production Days	337.3									
	Production Rate		0.8	0.9	1		1	1	1		1
C	Production Cost		1.285E+08	1.446E+08	1.607E+08		1.607E+08	1.607E+08	1.607E+08		1.607E+08
	a. LNG product										
	Sales volume, lb/hr	1.575E+06									
	Lower Heating Value, Btu/lb	2.112E+04									
	Sales price, \$/MMBtu	5									
	Sales/y, \$		1.078E+09	1.212E+09	1.347E+09		1.347E+09	1.347E+09	1.347E+09		1.347E+09
	b. Condensate product										
	Std Volumetric Flow, b/d	1.907E+03									
	Price, \$/barrel	43									
	Sales/y, \$		2.212E+07	2.489E+07	2.765E+07		2.765E+07	2.765E+07	2.765E+07		2.765E+07
D	Total Revenue		1.100E+09	1.237E+09	1.375E+09		1.375E+09	1.375E+09	1.375E+09		1.375E+09
E	Gross Income (D-C)		9.713E+08	1.093E+09	1.214E+09		1.214E+09	1.214E+09	1.214E+09		1.214E+09
F	Depreciation		6.854E+08	6.854E+08	6.854E+08		6.854E+08	6.854E+08	0		0
G	Taxable Income (E-F)		2.858E+08	4.072E+08	5.286E+08		5.286E+08	5.286E+08	1.214E+09		1.214E+09
H	Income Tax	40%									
I	Cash Flow		-6.868E+09	8.569E+08	9.298E+08	1.003E+09	1.003E+09	1.003E+09	7.284E+08		7.284E+08
F	DCF (Discounted Cash Factor)	11.19%									
G	Discount Factor Value	$e^{-(DCF \times \text{year } n)}$	1	0.8942	0.7995	0.7149	0.3654	0.3267	0.2921		0.1067
H	Discounted Cash Flow		-6.868E+09	7.662E+08	7.434E+08	7.168E+08	3.663E+08	3.276E+08	2.128E+08		7.775E+07
I	Sum of Discounted Cash Flow		0								

* Source of ethylene price: <http://www.yarnsandfibers.com/textile-pricewatch/ethylene-price-trends-reports.html>, <http://www.the-innovation-group.com/ChemProfiles/Ethylene.htm>

Source of Dowtherm G Hot Oil price : <http://search.cpan.org/src/KWILLIAMS/reuters-21578/test/17563>

^ Price information for feed2 and amine system:

Ethane = \$22.00/BBL
 LPG (C3) = \$37.00/BBL
 LPG (C4) = \$40.00/BBL
 Condensate (C5+) = \$55.50/BBL
 Amine solvent = \$1.25/lb

Appendix H. H₂S Removal Facility Calculation

1. Determine the column diameter of the molecular sieve.

- Flow rate of C2/C3 product stream (overhead of SR column) = 5213 m³/day = 128 ft³/min.
- Liquid superficial velocity in a molecular sieve = 5 ft/min (Kidnay and Parrish 2006)
- Thus, section area required = 128/5 = 25.6 ft² → D = 5.7 ft = 1.75 m.

2. Determine the height of the molecular sieve.

a. Determine the amount of sieve required

- Adsorption temperature
Stream temperature = 24°F = -4.6°C → closest adsorption temperature = 0°C.
- H₂S partial pressure
Mole fraction H₂S = 7.11e-4.
Pressure = 42.2 atm = 620 psia.
H₂S partial pressure = 7.11e-4 x 42.2 x 760 = 23 mmHg.
Amount of H₂S = 134.7 lb/h
- Figure H-1 shows the amount of sieve required at the adsorption condition.

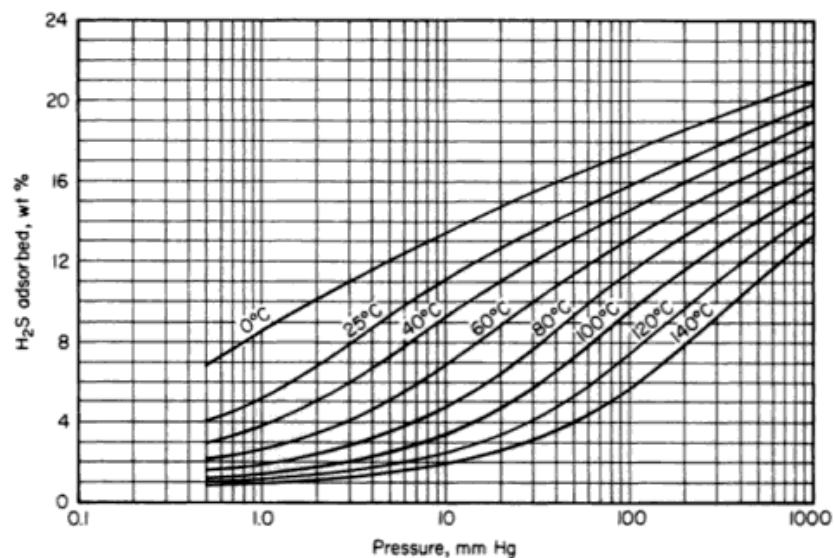


Figure H-1. Hydrogen sulphide adsorption isotherms on 13X molecular sieve (Schweitzer 1997)

- The amount of H₂S adsorbed = 15 wt%, 15 lb H₂S/100 lb adsorbent.
- Estimate adsorption time = 48 hours.
- Amount of H₂S to be removed = 134.7 lb/h x 48 h = 6465 lb H₂S.
- Amount of sieve = 6465 lb H₂S/0.15 = 43100 lb sieve.

b. Calculate the height of the sieve

- Bulk density of 13X molecular sieve (1/8-in pellets) = 38 lb/ft³.
- Volume sieve = 43100/38 = 1134 ft³.
- Length of sieve = Volume sieve/section area = 1134/25.6 = 44.4 ft.

c. Total column height:

- Additional height of 6 ft for above and below sieve bed to provide space to remove the desiccant and refill (Arnold and Stewart 1999).
- = 44.4 + 6 = 50 ft = 15 m.

3. Check the pressure drop in the column

Data:

- Liquid stream viscosity = $\mu = 0.09$ cP (centiPoise).
- Density = $\rho = 29.60$ lb/ft³.
- $\Delta P/L$ for 1/8-in. extrudate:

$$\frac{\Delta P}{L} = 0.0722\mu V + 0.000124\rho V^2$$

- $\Delta P/L = 0.124/\text{ft} \sim (\text{x bed length}) = 5.5$ psi.
- The recommended pressure drop range = 5-8 psi.

4. Regeneration duty calculation (identical with dehydration calculation).

a. Estimate heat of desorption

- Heat of adsorption can be calculated from adsorption isosteres (Schweitzer 1997).

$$\ln p = -\frac{Q}{R}\left(\frac{1}{T}\right) + C$$

- For a same amount of H₂S adsorbed (adsorption isosteres), plot ln p vs 1/T.
- The slope of the equation corresponds to the heat of adsorption Q.
- For 15% wt H₂S, the heat of adsorption = 894.5 J/g = 1869 Btu/lb.

b. Calculate the total heat requirement for the regeneration

- Regeneration temperature = 284°F = 140°C (maximum temperature in Figure H-1).
- Heat of desorption = 1869 Btu/lb x 6465 lb = 1.209e7 Btu.
- Heating sieve = 43100 lb x 0.24 x (284 – 24)°F = 2.693e6 Btu.
- Column thickness =

$$t(\text{inches}) = \frac{12D_{bed}P_{design}}{(2 \times 18,800) - 1.2P_{design}} = \frac{12 * 5.7 * (620 * 1.1 - 14.7) \text{psig}}{(2 * 18800) - ((1.2 * (620 * 1.1) - 14.7))} = 1.24 \text{inches}$$

- Weight of steel:

$$\text{Weight}(lb) = 155(t + 0.125) * (L_{TOTAL} + 0.75D_{bed})D_{bed} = 6.601e4lb$$

- Heating steel = 6.601e4 x 0.12 x (284-24)°F = 2.062e6 Btu.
- Heat Loss = (1.209e7 + 2.693e6 + 2.062e6) x 0.1 = 1.684e6 Btu..
- Q total = 1.209e7 + 2.693e6 + 2.062e6 + 1.684e6 = 4.631e7 Btu.

5. Mass flow rate of regeneration gas.

- Estimate regeneration time: 48 hours.
- Heating time = 60% of total heating time (GPSA 2004)
- Calculate average Cp of CO₂ gas as the regenerating gas (at average temperature of 24°F and 284°F).
- Regeneration gas rate = Q total / (Cp x ΔT x regeneration time) = 9651 lb/h.

6. Check the pressure drop:

- Density of CO₂ regenerating gas = 6.54 lb/ft³.
- Volumetric flow = Regeneration gas rate/density = 1052 ft³/min.
- Superficial velocity = Volumetric flow/section area = V = 41 ft/min.
- CO₂ gas stream viscosity = μ = 2.33e-2 cP (centiPoise).
- Calculate ΔP/L:

$$\frac{\Delta P}{L} = 0.0722\mu V + 0.000124\rho V^2 = 1.44 \text{psi} / \text{ft}$$

- The minimum value of 0.01 psi/ft is needed to prevent channelling (GPSA 2004).